Investigating Aberrant Signalling in Enzalutamide-Resistant Prostate Cancer

A Thesis submitted in part requirement for the degree of Doctor of Philosophy

Massar Ibrahim Alsamraae

Solid Tumour Target Discovery Group

Northern Institute of Cancer Research

Newcastle University

August 2017

Abstract

Prostate cancer is usually androgen-dependent and consequently, initial therapy for many patients, particularly with advanced disease, is androgen withdrawal, via anti-androgen therapeutics. Most patients respond to anti-androgen therapy in the early stages of their disease but many will develop resistance, entering a "castrate-resistant" disease state. Enzalutamide and ARN-509 have shown promise in the treatment of castration resistant prostate cancer (CRPC) patients, however response rates are just 50% and there is the inevitable development of resistance and subsequent disease progression. The aims of this study are to investigate the role of HER2/HER3 in CRPC models (Casodex-, Enzalutamide- and ARN509-resistant cell lines) and the signalling pathway(s) that can be stimulated through HER2/HER3 activation in these models. In addition, the project focusses on drug-resistant disease models, investigating the genes upregulated in a cell-line model of enzalutamide-resistance. The data showed that HER2/HER3 has a crucial role in the CRPC model cell lines, seen in the activation of both MAP kinase and PI3K/Akt pathways, which are responsible for tumour growth and metastasis. This activity is more pronounced in enzalutamide resistant- LNCaP cells. For that reason, this study aimed to interrogate the global gene expression consequences in this enzalutamide resistant- LNCaP cell model. These aims were approached using Illumina Human HT-12 arrays to detect significantly up-regulated genes and therefore could have a vital role in proliferation, migration and cell cycle. SGK1 and TROP-2 were selected from this microarray to study in more details.

The data showed an increase in the expression of SGK1 in Casodex-, enzalutamide- and ARN509-resistant cell lines, compared with parental LNCaP cells. AR regulates SGK1 in both LNCaP and enzalutamide resistant- LNCaP cells. However, GR regulates SGK1 and AR target genes in enzalutamide resistant- LNCaP cells. This study indicated that GR has no effect on the AR target genes in parental LNCaP cells. SGK1 has a vital role in the proliferation, migration and cell cycle of the enzalutamide resistant- LNCaP cell line.

In addition, the data from this study showed an increase in the expression of TROP-2 in enzalutamide resistant- LNCaP cells, compared with LNCaP parental cells. The results obtained from this study suggested that TROP-2 might regulates pAkt, pERK1, c-MYC and p27 signalling that are important in proliferation and cell cycle of enzalutamide resistant- LNCaP cells. In addition, TROP-2 potentially regulates the migration of

enzalutamide resistant- LNCaP cells by its effect on the EMT process that is important in metastases.

SGK1 and TROP-2 demonstrated higher protein expression in patients' tissue samples who had relapsed after androgen withdrawal, compared to naïve patients. In conclusion, SGK1 and TROP-2 could represent either potential biomarkers of enzalutamide-resistance, or potential therapeutic targets in advanced disease.

Acknowledgements

First, I would like to thank my supervisors, Prof. Craig N. Robson and Dr. Stuart McCracken, for their continuous help, guidance and support over the last three years. I am very grateful for the opportunity they have given me to become one of their laboratory members. My thanks also extend to all members of the Solid Tumour Discovery Laboratory, both present and past members for their assistance, advice and support, especially Dr. Luke Gaughan, Dr. Kelly Coffey, Dr. Kasturi Rao, Dr. Scott Walker, Dr. Mahsa Azizyan, Laura Wilson, Dr. Mark Wade Dr. Dominic Jones and Dr. James Grey.

I would also like to give special thanks to my country Iraq and my sponsor The Higher Committee for Education Development in Iraq, for awarding me this scholarship to study for my PhD in the UK.

My deep gratitude for my parents Dr. Ibrahim Shekhan Alsamraae and Mrs. Batool Ghani for their unlimited love, help, support and prayers. You have always been the light at the end of the tunnel for me and your love is my biggest achievement ever.

My love and thanks to my only brother for being in my life and for his unconditional love and support.

At the beginning and the end my greatest appreciations for my lovely wife Dr. Zainab Alebady and my kids Sohaib and Yazin for their patience, love and support throughout my PhD journey, without you it would not have been possible.

Finally, thanks to all members of staff at the Northern Institute for Cancer Research for creating such an amazing welcoming atmosphere within the institute and for their continuous help.

List of abbreviations

ADT	Androgen deprivation therapy
AF	Activation function
APS	Ammonium persulphate
AR	Androgen receptor
ARE	Androgen response element
ATP	Adenosine-5'-triphosphate
BM	Basal medium
BPH	Benign prostate hyperplasia
BSA	Bovine serum albumin
PC	Prostate cancer
CAFs	Cancer-associated fibroblast
Cdk	Cyclin dependent kinase
cDNA	Complementary DNA
ChIP	Chromatin immunoprecipitation
CRPC	Castration resistant prostate cancer
CTD	C-terminal domain
DBD	DNA binding domain
DCC	Dextran coated charcoal
DDR	DNA damage response
DEPC	Diethylpyrocarbonate
DHT	5 α-dihydrotestosterone

DMSO	Dimethyl sulfoxide
DNA	Deoxyribonucleic acid
dNTP	Deoxyribo nucleoside triphosphate
DRE	Digital Rectal Examination
DSBs	Double strand breaks
ECL	Enhanced Chemi luminescence
EDTA	Ethylene diaminetetra acetic acid
EGF	Epidermal growth factor
EMT	Epithelial-mesenchymal transition
ERK	Extracellular-signal regulated kinases
FCS	Foetal calf serum
FM	Full medium
FOXM1	Forkhead box protein M1
GADD	Growth arrest and DNA-damage-inducible
G-phase	Gap phase
GPCR	G-protein coupled receptor
GR	Glucocorticoid receptor
H	Histone
HAT	Histone acetyltransferase
HBD	Histone binding domain
HDAC	Histone deacetylase
HER2	Receptor tyrosine-protein kinase2

HER3	Receptor tyrosine-protein kinase3
HEG	Heregulin
HGPIN	High-grade prostatic intraepithelial neoplasia
HMT	Histone methyl transferase
HPRT-1	Hypoxanthine phosphoribosyl transferase 1
HR	Hinge region
HSPs	Heat shock proteins
HTS	High throughput screening
IHC	Immunohistochemistry
IL	Interleukin
IP	Immunoprecipitation
K	Lysine
kDa	Kilo Dalton
KLK2	Kallikrein-related peptidase 2
KMT	Lysine methyltransferase
LBD	Ligand binding domain
LEF-1	Lymphoid enhancer-binding factor 1
LH-RH	Luteinizing hormone –releasing hormone
MAPK	Mitogen activated protein kinase
Me	Methyl group
miRNA	microRNA
M-phase	Mitosis phase

mRNA	Messenger RNA
mTOR	Mechanistic Target of Rapamycin
mTORC	mTOR complex
NR3C4	Nuclear receptor subfamily 3, group C, member 4
N/S	Non silencing
NTD	N-terminal domain
Oligo	Oligonucleotide
p53	Protein 53
PBS	Phosphate buffered saline
PCNA	Proliferating cell nuclear antigen
PGS	Protein G sepharose
PI	Propidium iodide
PIN	Prostatic intraepithelial neoplasia
PI3K	Phosphatidylinositol 3-kinase
PIP2	Phosphatidylinositol 4,5-bisphosphate
PIP3	Phosphatidylinositol (3, 4, 5)-triphosphate
PMSF	Phenyl methane sulfonyl fluoride
PSA	Prostate specific antigen
QRT-PCR	Quantitative real time polymerase chain reaction
RLN1	Relaxin 1
RNA	Ribonucleic acid
RTK	Receptor tyrosine kinase

S	Serine
SDM	Steroid depleted medium
SDS-PAGE	Sodium dodecyl-sulphate polyacrylamide gel electrophoresis
shRNA	Short hairpin RNA
siRNA	Small interfering RNA
SGK1	Serine/threonine-protein kinase
SPA	Scintillation proximity imaging assay
S-phase	Synthesis phase
SPR	Surface plasmon resonance
SRC	Steroid receptor coactivator
SYT4	Synaptotagmin-4
TACSTD	Tumor-associated calcium signal transducer 2
TBS	Tris buffered saline
TCF-4	Transcription factor-4
TEMED	Tetramethylethylenediamine
TMA	Tissue Microarray
TMPRSS2	Transmembrane protease serine 2
TNM	Tumour, Node and Metastasis
TRUS	Trans-rectal ultrasonography

TTBS	TBS Tween20
TURP	Transurethral resection of prostate
Ub	Ubiquitination
VEGF	Vascular endothelial growth factor
WT	Wild type

Table of Contents

List of Figures

List of Tables

Chapter 1. Introduction

1.1 Introduction to cancer

Cancer is a disease that results from uncontrolled cell proliferation. It initiates when normal cells evolve into neoplastic phenotypes by the acquisition of certain traits that promote them to become tumourigenic and eventually malignant. These traits have been reported as the 'hallmarks of cancer". It has been suggested (Hanahan and Weinberg, 2000) that cancers share six hallmarks: insensitivity to growth inhibitory signals; limitless replicative potential; the ability to evade apoptosis; self-sufficiency to growth signals; the ability to sustain angiogenesis; the ability to invade tissues and metastasize. The list of hallmarks was extended to ten (Hanahan and Weinberg, 2011), who added four more: the presence of inflammation; the tendency towards genomic instability; evade the immune system and a dysregulated metabolism (Figure 1-1). These ten hallmarks suggest theoretical frameworks for chemotherapy and research. However, additional hallmarks can be added to the list, such as aberrant alternative splicing, which in turn causes the inappropriate expression of multiple oncogenic splice isoforms (Ladomery, 2013).

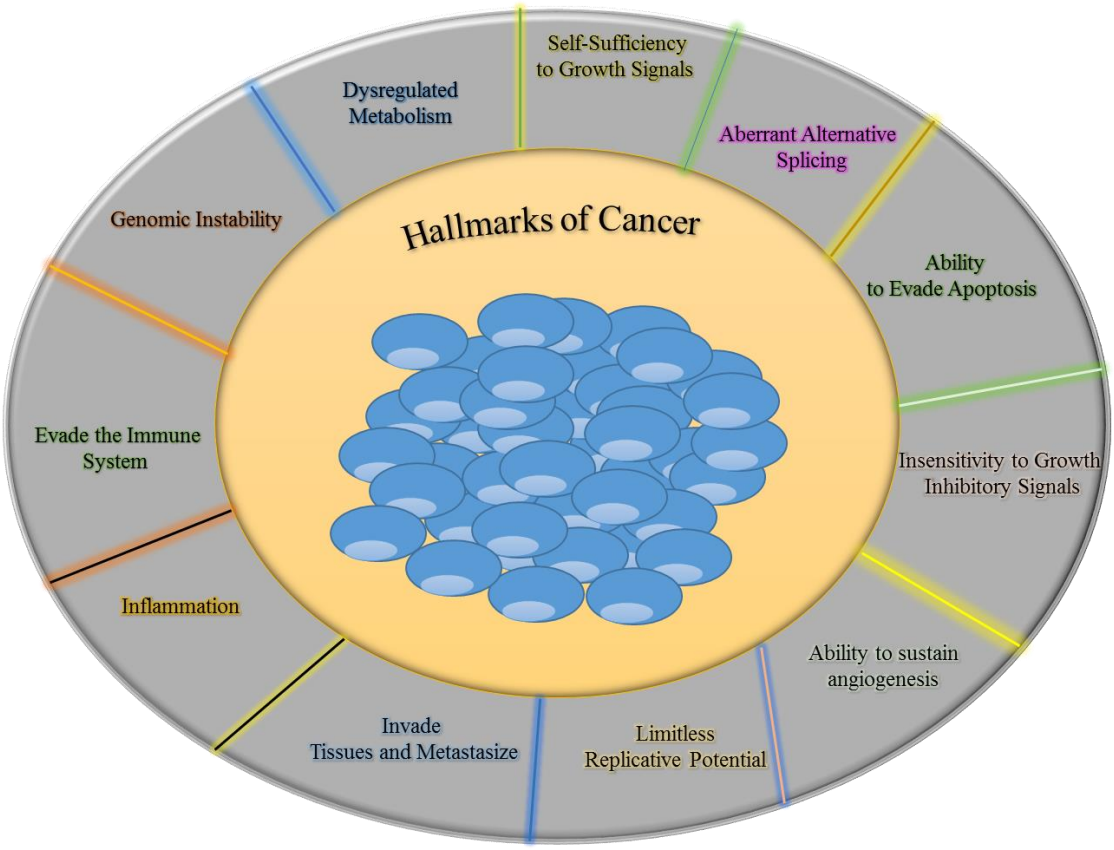

Figure 1-1 Hallmarks of Cancer, adapted from (Hanahan and Weinberg, 2011)

1.2 Prostate gland

1.2.1 Function of prostate gland

The prostate gland is an organ belonging to the male reproductive system and is responsible for secreting a milky, alkaline fluid, which contains nutrient materials for the spermatozoa and also maintains their viability and motility. This fluid contains prostate specific antigen (PSA) which aids the motility of sperm by maintaining the liquid texture of the semen (Lilja *et al.*, 1987; Rosenberg, 1989).

1.3 Zonal anatomy of the prostate

The prostate gland is an exocrine gland and is an acorn-shaped organ weighing 30-40 g, about the size of a walnut. It is located below the bladder, behind the pubic bone and in front of the rectum. The prostate gland consists of three major glandular zones: the peripheral, the central and the transition zones (Figure 1-2) (McNeal, 1988; Abate-Shen and Shen, 2000).

• **The peripheral zone**: this forms about 70% of the prostate gland. The peripheral zone is rich in acini and it is widely known that acinar cells produce PSA (Robinson *et al.*, 2017). A study based on biopsies taken from patients who had prostate cancer showed that more than 75% of all prostate cancer originates from the peripheral zone (Chang *et al.*, 1998).

• **The transition zone:** this is the smallest zone of the prostate gland, forming about 5-10% of the prostate and it surrounds the urethra between the bladder neck and verumontanum. A detectable increase in this zone's volume occurs in benign prostatic hyperplasia (BPH), often accompanied by lower urinary tract symptoms (LUTS). 10-20% of prostatic cancer originates from this zone (McNeal, 1988; Villers *et al.*, 1991; Amin *et al.*, 2010).

• **The central zone:** this forms about 25% of the prostate and is a funnel (sagittal section) or ring-like (horizontal) zone that contains the ejaculatory ducts. Only around 5-10% of cancers originate from the central zone and it is relatively low frequency to carcinoma and other disease (McNeal, 1988; Schulz *et al.*, 2003).

Anterior fibromuscular stroma – The anterior fibromuscular stroma forms about 5% of the prostate and is located anterior to the urethra and extends into the transition zone (McNeal, 1988). This region separates the transition zone from the central and peripheral zones. This region is mainly composed of striated and smooth muscle. The distal and proximal regions of the stroma are important for voluntary and involuntary sphincter functions, respectively (Amin *et al.*, 2010).

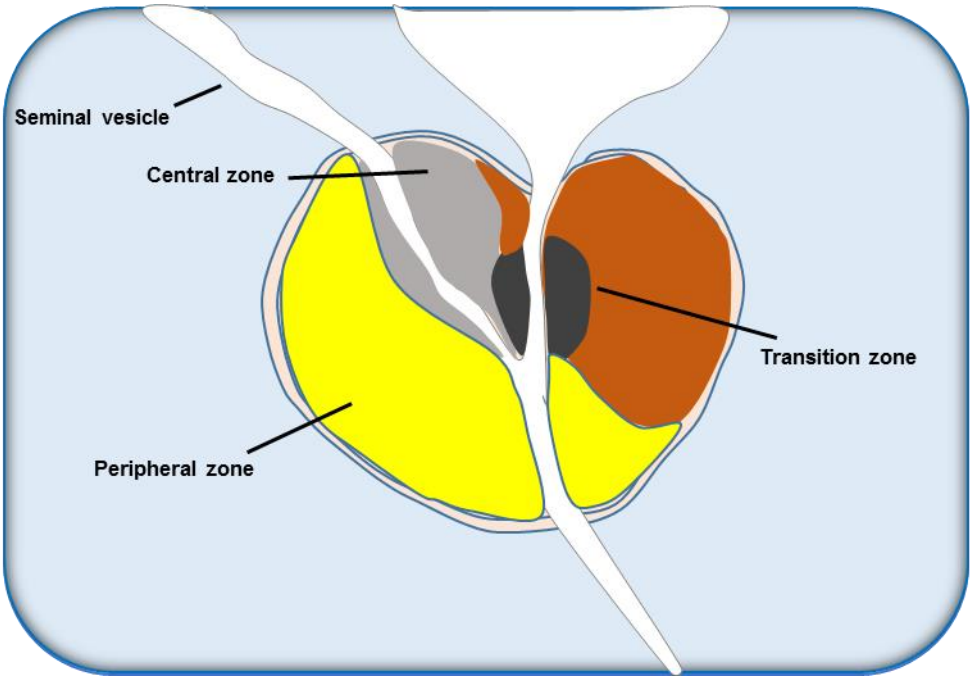

Figure 1-2 Prostate gland zones, adapted from (McLaughlin *et al.*, 2005)

1.4 Histology of the prostate

The prostate gland consists of epithelial and stromal cells and these cells are bound together by connective tissue. Hormones and growth factors such as testosterone, which is primarily secreted from Leydig cell of the testes, control and regulate the growth and maintenance of the prostate gland (Thiruchelvam, 2014). The prostate epithelium is composed of prostatic ducts comprised of four types of cell: basal, secretory luminal, neuroendocrine and stem cells. The stromal part of the prostate contains smooth muscle,

vascular endothelial cells, nerve cells, fibroblasts, inflammatory cells, soluble factors and an insoluble matrix (Josson *et al.*, 2010) (Figure 1-3). The prostate epithelia mainly consists of luminal cells that produce prostatic secretory proteins. These cells are controlled by androgen receptors (AR) and therefore androgen-dependent. Another type of epithelial cell known as basal cells are located between the luminal cells and the basement membrane. These cells express a low level of AR. Neuroendocrine cells are another type of epithelial cell distributed throughout the basal layer. These cells are androgen-independent and provide paracrine signalling to assist the growth of the luminal cells (Liu *et al.*, 1997; Abrahamsson, 1999; Abate-Shen and Shen, 2000).

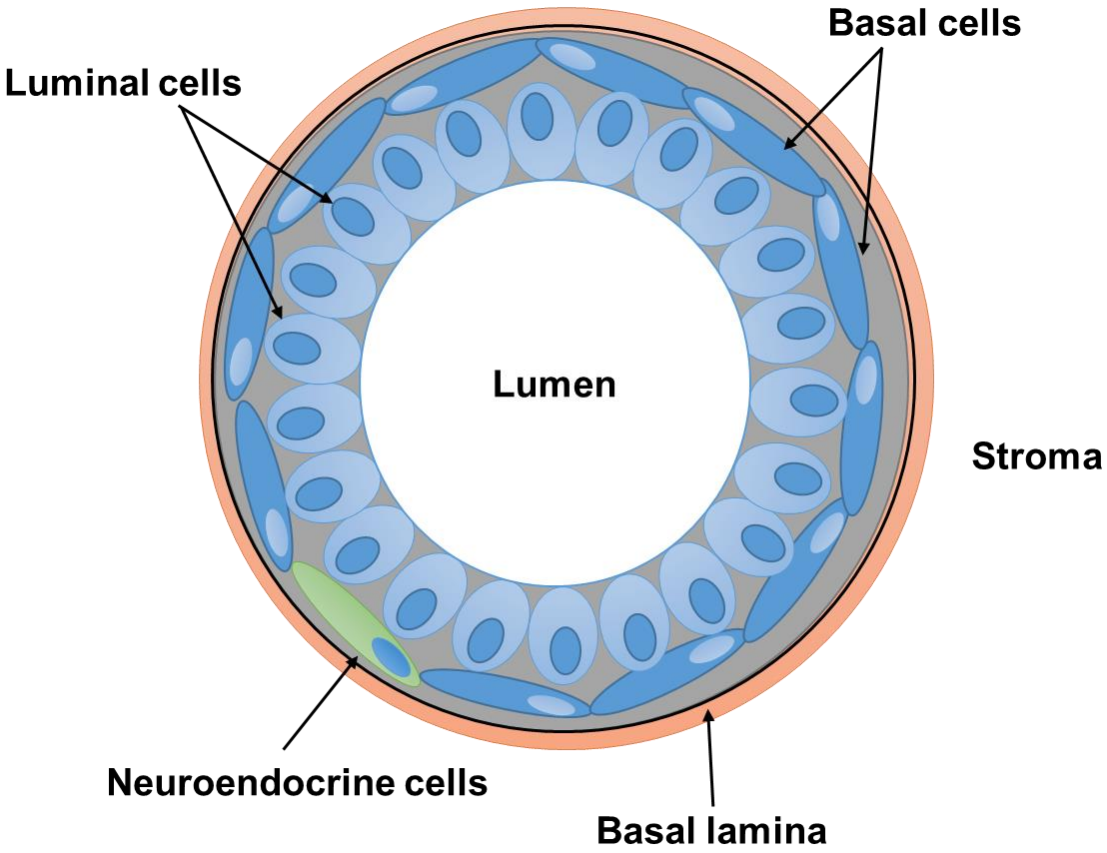

Figure 1-3 Schematic overview of cells in the prostate epithelium, adapted from (Montano and Djamgoz, 2004)

1.5 Prostatic abnormalities

1.5.1 Benign prostatic hyperplasia

BPH results from an increased number of epithelial and stromal cells within the periurethral region of the prostate gland, but not an increase in their size. It is characterized by increased cellular proliferation and/or reduced cell death. Numerous factors regulate this biological process, including androgen, growth factors, oestrogen and inflammatory and autoimmune mediators. BPH develops in the transition zone, located around the urethra and the periurethral zone. BPH often develops from around the age of 40 and increases with age. It has been reported that 90% of men aged over 80 suffer from BPH. A quarter of the cases of prostate cancer arise in the transition zone and the majority (around 60-70%) arise in the peripheral zone. However, BPH arises in the periurethral tissue, suggesting that BPH does not lead to prostate cancer (Coyne *et al.*, 2009; Thiruchelvam, 2014). Lower urinary tract symptoms, common in elderly patients, are associated with BPH causing bladder outflow obstruction (BOO). Although there is no specific, predictive biomarker, the majority of patients' symptoms are often alleviated with surgery (Kirby and Gilling, 2011). A reduction in prostate size and bladder outflow obstruction resulting from BPH can be improved using the 5a-reductase inhibitors, e.g. finasteride and dutasteride. These work by reducing the levels of DHT (by inhibition of type 1 and type 2 5a-reductase, thereby blocking the enzymatic conversion of testosterone to DHT) (Thiruchelvam, 2014).

1.5.2 Prostatic intraepithelial neoplasia (PIN)

It was shown before that high-grade PIN is a pre-invasive stage of adenocarcinoma and a predictive biomarker of adenocarcinoma, which was more appear in transgenic mouse model of prostate cancer (TRAMP) (Bostwick and Qian, 2004). Biopsy is currently the only method to detect PIN. Serum prostate-specific antigen (PSA) concentration is not elevated significantly at the PIN stage and cannot be detected by ultrasound. Most studies have indicated that patients who are diagnosed with high-grade PIN will be likely to develop carcinoma within ten years. Similar to cancer, PIN is associated with phenotype and genotype abnormalities. Androgen depletion therapy decreases the incidence of PIN, suggesting that this form of treatment may play a role in chemoprevention (Bostwick, 2000). PIN under microscopy is characterized by cellular proliferation within ducts and

acini, with an enlargement of the nuclear and nucleolus. Unlike cancer, which lacks a basal cell layer, PIN has an intact basal cell layer (Bostwick and Brawer, 1987). PIN directly invades through the ductal or acinar wall, disrupting the basal cells layer. However, early stromal invasion is associated with carcinoma (Bostwick *et al*., 1993). Furthermore, similar to prostate cancer, high-grade PIN exhibits chromosomal instability, including the loss of heterozygosity and the gaining of chromosomes, strongly suggesting that high-grade PIN may precede prostate cancer (Qian *et al*., 1999) (Figure 1-4).

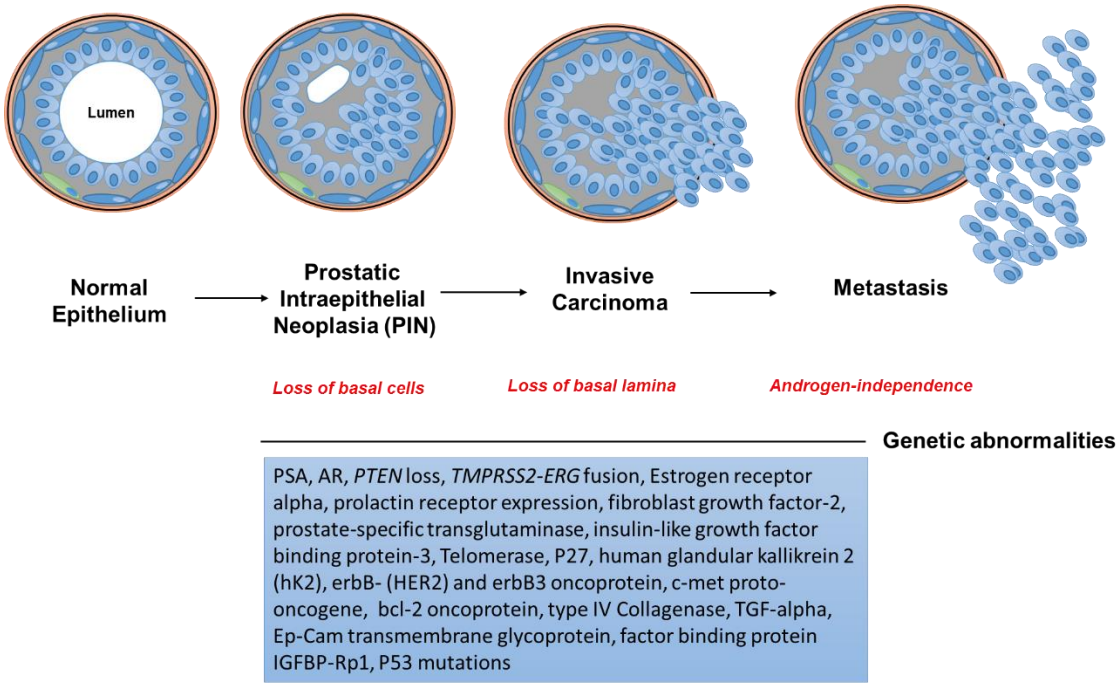

Figure 1-4 Schematic representation of the development and progression of prostate cancer, adapted from (Baker and Reddy, 2013)

1.6 Prostate cancer

Prostate cancer is the most frequently diagnosed cancer among males in 87 countries in North and South America and Northern, Western and Southern Europe. The highest incidence rates are in the U.S., followed by France and Australia and the lowest incidence and mortality rates are in Asia. A large part of the variation in incidence rates is because of the use of PSA testing. However, genetic and/or dietary differences might play a crucial role in the high rates in some populations (Torre *et al.*, 2016).

1.6.1 The etiology of prostate cancer

Race: Despite the prostate cancer incidence rate tending to be highest in more developed countries, Afro-Caribbean and sub-Saharan African (SSA) men experience the highest prostate cancer mortality in the world. In contrast, Asian men have the lowest mortality rates of prostate cancer (Rebbeck, 2017). The underlying mechanisms behind this are unclear. Trinucleotide repeat sequences occur throughout human DNA, where they contract and expand during the replication of DNA, giving rise to increased or decreased length (length polymorphisms). Although the majority of trinucleotide repeats are located in non-coding regions and thus have no effect, those located in coding region of the DNA can affect gene expression, modulate the stability of mRNA and alter the function of proteins.

The most studied polymorphism in the human *AR* is the CAG trinucleotide repeat, encoding a polyglutamine tract within the N-terminal transactivation domain (NTD), which is located in the coding region within exon 1 of AR. It has been shown that African males tend to have the shortest repeats (10-20) compared with Asian men, who tend to have the longest tracts (23-30), while Caucasian males have tracts of a length in between these two (Buchanan *et al.*, 2004; Albertelli *et al.*, 2008).

Age: The most prominent risk factor of prostate cancer is ageing, with approximately 75% of all cases diagnosed between 50-70 years of age. Despite prostate cancer being considered a disease of old men, young patients' prostates are rarely examined, in part due to the smaller numbers of cases (Zhou *et al.*, 2016).

According to Cancer Research UK, (last updated 07/05/16), the overall incidence of PC is strongly linked to age, in that the incidence begins to increase in males over the age of 40 and sharply rises from the age of 50, with a peak observed between 70-74 years (Figure 1-5)(UK data collated by Cancer Research UK).

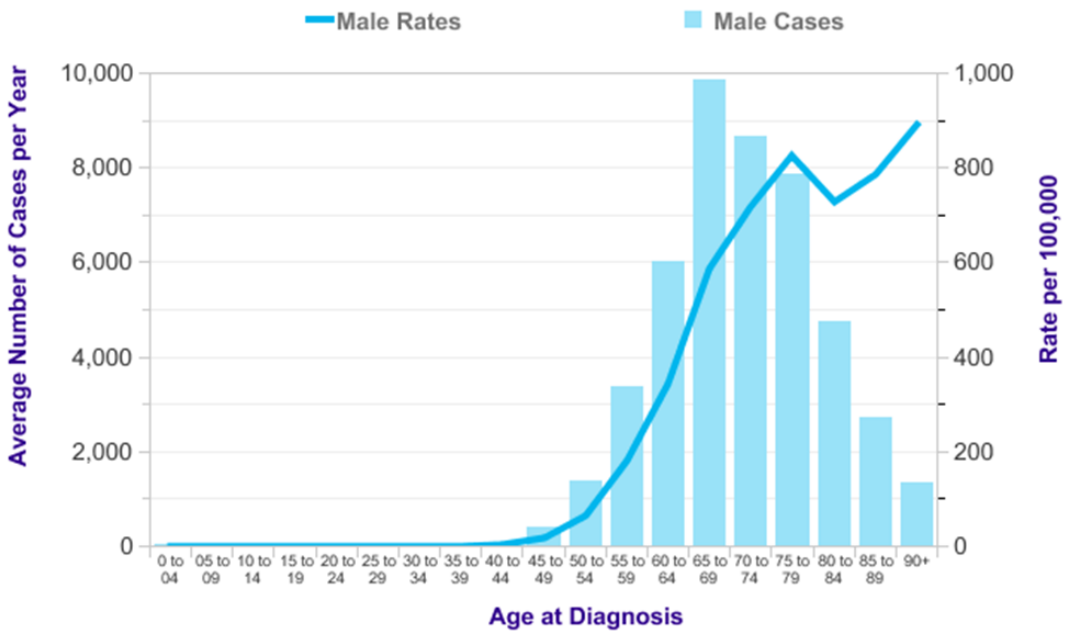

Figure 1-5 Average number of new cases per year and age-specific incidence rates per 100,000 population, males, in the UK (UK data collated by Cancer Research UK)

Family history: A family history of prostate cancer is associated with an increased risk of the disease. The risk factor for prostate cancer is also correlated with a family history of prostate cancer and/or breast cancer. According to a study of 4,258 patients with prostate cancer, followed up between 1996 to 2012, it was reported that the risk of lethal prostate cancer was also significantly increased for men with a positive family history of prostate cancer, as well as for men with a family history of breast cancer (Barber *et al.*, 2016).

Meta-analysis studies have shown that there are many possible factors associated with the development of potentially lethal prostate cancer, such as obesity. Same study suggested that vigorous activity that causes sweating and an increased heart and respiratory rate is might associated with a reduced risk of lethal prostate cancer. Moreover, smokers consistently have a higher risk of prostate cancer progression (Peisch *et al.*, 2016).

1.6.2 Diagnosis of prostate cancer

Prostate cancer is initially suspected by the combination of clinical examination of the prostate with the determination of the protein level of prostate specific antigen (PSA) in the serum of the patients. The diagnosis is then confirmed in patients felt to be at risk by histological analysis of trans-rectal ultrasonography (TRUS)-guided biopsy samples. Histopathological analysis is used to determine the aggressiveness of the disease by applying Gleason's score to the patient's tissue (Sciarra *et al*., 2012).

Prostate specific antigen:

PSA is a glycoprotein, also known as human kallikrein-3 and is a serine protease that belongs to the human kallikrein family of proteases, produced primarily by epithelial cells that line the ducts and acini of the prostate gland. The PSA levels are normally present in the blood at very low levels. However, a greater amount of PSA enters the circulation and increases the serum levels in prostate disease processes such as infection, inflammation, trauma and cancer. It can be used to assess prostate cancer progression, during and after treatment (e.g. chemotherapy). However, despite the early detection of prostate cancer using PSA being controversial, due to over-diagnosis and over-treatment, a gradual decrease in prostate cancer mortality in the USA of approximately 30% has been reported since the introduction of PSA testing (Greene *et al.,* 2009). While measuring the level of serum PSA is currently the best blood test for early prostate cancer detection, digital rectal examination (DRE) can also identify the disease in the men. Evidence suggests that using both tests improves the rate of prostate cancer diagnosis. On the other hand, using DRE alone did not improve prostate cancer detection over a PSA test alone (Gosselaar *et al.*, 2006).

The most common methods of diagnosing prostate tissue with cancer is trans-rectal, ultrasound-guided prostate biopsy, which targets the peripheral zone at the apex, mid gland and base, as well as laterally directed cores on each side of the prostate gland. This technique is used with patients with persistently elevated PSA levels +/- suspicious findings on DRE (Greene *et al.,* 2009).

Histopathology:

Only histopathological examination of trans-rectal ultrasonography (TRUS)-guided biopsy can confirm prostate cancer, which is then evaluated, based on the Gleason grading

system. This is performed by staining the biopsied tissue section with haematoxylin & eosin stain and observing the architecture arrangement of the cancerous cells (Gleason and Mellinger, 1974). The Gleason grading system was updated at a 2005 consensus conference of the International Society of Urological Pathology. This meeting was suggested to update the grading system in to the 6 score as a first grade which is usually 3+3, and for 7 grade is usually (3+4 or 4+3), for 8 grade is (4+4), for grade 9 is (4+5 or 5+4) and for grade 10 is (5+5) (Epstein *et al.*, 2005). Many other techniques were also introduced here to diagnose prostate cancer, including prostate specific antigen testing, trans-rectal ultrasound guided prostate needle biopsy and immunohistochemistry for basal cells (Epstein, 2010).

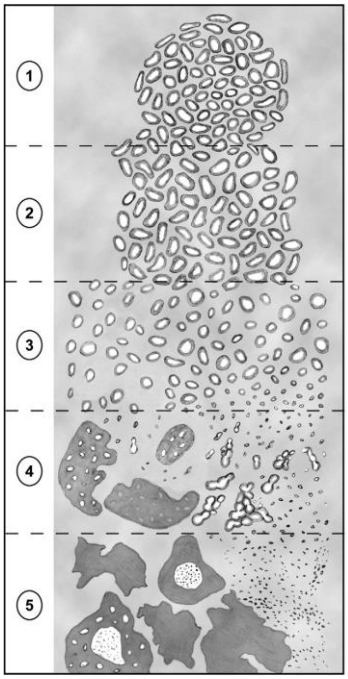

Figure 1-6 Modified Gleason system (Epstein, 2010)

The above diagram describes how the Gleason system is used to establish a Gleason score. Grade 1 consists of well-differentiated and closely packed glands and occurs quite rarely. Grade 2 can be identified by a slightly less well-defined mass and tumour-stromal boundary of the gland. The size and shape of the gland also varies. Grade 3 is the most common pattern observed in prostate carcinoma and consists of moderately differentiated glands of various sizes, with the most prominent feature being the presence of invasive stroma. Grade 4 is considered a high grade and poorly differentiated carcinoma and is characterised by the presence of ill-defined glands and chains of malignant epithelial cells. Grade 5 is the most undifferentiated pattern and can resemble other undifferentiated cancers of other organs. The highest Gleason sum scores are associated with metastatic disease and have poor prognosis (Epstein, 2010).

1.7 Prostate cancer treatment

Treatment of prostate cancer is based on assessing the risk of the disease, progression and spread, which are established by evaluating life expectancy, biopsy grade (Gleason score), serum PSA levels of patients and a TMN staging system (Sobin and Fleming, 1997; Carter *et al.*, 2007). The TMN staging system is used to evaluate the progression of the disease: T refers to gaining an indication of the size and extent of the tumour, N indicates regional lymph node involvement and M is the metastases of the disease (DeSantis *et al.*, 2014). Recurrence after localized treatment of prostate cancer can be classified into low, intermediate and high risk, based on the PSA, DRE and Gleason grade (D'amico *et al.*, 2000). These classifications are based upon the following (Table 1-1):

	PSA	**Gleason**	**Clinical stage**
Low-risk	<10ng/mL	≤6	T1-T2a
Intermediate-risk	10-20ng/mL	7	T2b
High-risk	>20ng/mL	8-10	T2c-T3a

Table 1-1 prostate cancer stratification

Low risk: this occur in patients with stage T1-T2a and the level of PSA is <10ng/mL with a Gleason score of ≤6. Patients with low risk cancer are not candidates for androgen depletion therapy. As above, Active Surveillance is considered the recommended option, though curative treatments, such as radical prostatectomy (RP) or external beam radiotherapy (EBRT) can also be considered for localized disease (Kuban *et al.*, 2008).

Intermediate risk: this happens in patients with clinical stage T2b, Gleason score 7 and the level of serum PSA 10-20ng/mL. Treatment in this stage is either observation, surgery, or radiation therapy. Administering androgen-depleting treatment (ADT) before, during and after radiation prolongs survival in patients (Bolla *et al.*, 2002; Merrick *et al.*, 2004).

High risk: this occur in patients with Clinical stage T2c-T3a, Gleason score 8-10, PSA >20 ng/mL (Heidenreich *et al.*, 2014). ADT is used in men with locally advanced T3-4, disease with PSA >50 ng/ml and Gleason score 8-10. ADT is reported to be highly effective if started at the initial time of metastases (van den Bergh *et al.*, 2016).

Luteinising hormone-releasing hormone (LHRH): This is a peptide hormone that binds to receptors on gonadotropic cells in the anterior pituitary. This stimulates the hypothalamic signalling axis, leading to the release of luteinizing hormone (LH) and subsequent androgen biosynthesis in the testes (Tammela, 2004).

ADT and LHRH agonists have somewhat replaced surgical castration because these agents are able to avoid physical and psychological discomfort and the risk associated with orchiectomy. LHRH antagonists are also available. These antagonists bind and compete LHRH receptors, leading to a decrease in LH and testosterone levels, which may be useful for patients with locally advanced or metastatic disease (Crawford *et al.*, 2014; Heidenreich *et al.*, 2014).

Antiandrogens: there are two kind of anti-androgen, steroid antiandrogen and nonsteroidal antiandrogens (NSAAs). It has shown that the synthetic steroid cyproterone acetate is a potent anti-androgen, which is lead to inhibition of testosterone action on seminal vesicle and prostate tissue (Whalen and Edwards, 1969). However, a study showed that Flutamide (Nonsteroidal antiandrogens) is approximately 2-fold more potent than cyproterone acetate in reversing the stimulatory effect of DHT (Poyet and Labrie, 1985). Nonsteroidal antiandrogens (NSAAs) do not decrease the testosterone level but are basically used to improve the clinical effect (Cornford *et al.*, 2016). These antiandrogens bind to the ligand-binding domain of the AR and prevent DHT from activating AR (Figure 1-10 A, B). The first antiandrogen, approved in the late 1970s/early 1980s, was called flutamide and then later bicalutamide was developed by the middle of 1990s (Figure 1-10 D). This was found to be more potent than flutamide (Anantharaman and Friedlander, 2016). The CYP17 inhibitor abiraterone and the anti-androgen, enzalutamide were approved by the US Food and Drug Administration (FDA) in April 2011 and August 2012, respectively, for men with castration-resistant prostate cancer (CRPC), after docetaxel chemotherapy. Abiraterone is a potent inhibitor of CYP17, a key enzyme for the extra gonadal synthesis of androgens and oestrogens, which can improve the survival prognosis by around 4.6 months (De Bono *et al.*, 2011). Enzalutamide is a

next generation non-steroidal anti-androgen and demonstrated a 4.8 month improvement in median overall survival (Bianchini *et al.*, 2014) (Figure 1-7). Enzalutamide is a high affinity antagonist, with an 5-8 fold higher binding affinity for AR than bicalutamide (Casodex) (Tran *et al.*, 2009).

ARN509 is another nonsteroidal anti-androgen, differing from enzalutamide by one atom (Figure 1-7). The mechanism of action of both compounds is binding to the ligand-binding domain (LBD) of AR, which leads to the prevention of nuclear localisation and recruitment to AR-regulated gene promoters. This results in the inhibition of AR-target gene expression. Furthermore, both compounds were shown to differ from the action of bicalutamide in that enzalutamide and ARN-509 were able to specifically inhibit AR binding to DNA (Tran *et al.*, 2009; Clegg *et al.*, 2012). A study of 396 men with non-metastatic or metastatic prostate cancer showed that enzalutamide significantly reduced the risk of disease progression or death by 76% compared with bicalutamide (Penson *et al.*, 2016). A study of patients with high-grade prostate cancer demonstrated that enzalutamide reduced tumour size and down staging was also noted with histological changes (Van der Roest *et al.*, 2016). However, the majority of patients treated with ARN509 or enzalutamide who exhibit a decrease in serum PSA level, eventually develop progressive disease (Joseph *et al.*, 2013).

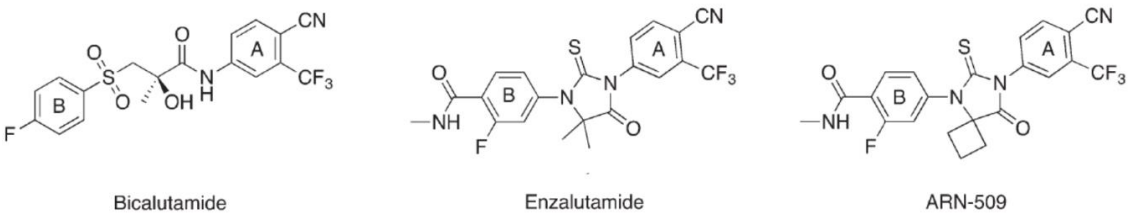

Figure 1-7 Structure of anti-androgen small molecules approved by FDA. (Bassetto *et al.*, 2017)

1.8 Androgen Receptor

1.8.1 Structure of the androgen receptor

Androgens play a crucial role in male reproductive system development and physiological processes. The effect of androgens is mediated by the activity of the nuclear androgen receptor (AR). AR is a ligand-inducible transcription factor and acts as a

regulator of the downstream androgen-dependent signalling pathway. This transcription factor regulates gene expression through the various co-regulator complexes, histone modifications and the induction of chromatin reorganization. Dysregulation of AR signalling disturbs normal reproductive development and affects a wide variety of biological conditions, such as androgen-insensitive syndrome and prostate cancer (Matsumoto *et al.*, 2013).

AR is a member of the nuclear receptor (NR) superfamily and shares structural similarities with other NRs. Its gene is located on chromosome X q (11-12) and is comprised of eight exons; its protein is 919 amino acids in length and 110 kDa in mass. The AR transcription factor consists of N-terminal transactivation domain (NTD) (activation function 1(AF1)) that is encoded by exon 1, a C-terminal ligand-binding domain (LBD) that is associated with a second transcriptional regulatory function (AF2), which is encoded by exons 4-8 and a central DNA-binding domain (DBD) encoded by exons 2-3. There is also a hinge region between the DNA-binding domain and LBD that contributes to nuclear localization and degradation (Figure 1-8) (Koryakina *et al.*, 2014; Yuan *et al.*, 2014; Wadosky and Koochekpour, 2017).

AF1 activity is ligand independent, while AF2 requires a ligand for its activity. Moreover, AF1 and AF2 activity are modulated by posttranslational modifications of the AR protein, such as phosphorylation, acetylation and sumoylation. The effect of AF2 on AR transactivation appears to be lower than AF1. However, a ligand-dependent functional interaction between the N-terminal and C-terminal regions suggests that AF-1 and AF-2 synergize to achieve full AR transactivation (Matsumoto *et al.*, 2013).

It has shown that N-terminal transactivation domain has several subdomains which play a role in transcription of AR. various proteins binds to the NTD such as P160 family, TATA-box binding protein, IIF transcriptional factor, which have a role in prostate cancer growth. An interaction between N- and C-terminals occur where NTD binds with LBD, and the hormone dependent interaction between NTD and LBD are essential for AR stabilization (Sakkiah *et al.*, 2016).

DNA-binding domain contains a number of basic amino acids as well as a nine of cysteine residues. DBD is divided into three substructures: two zinc finger motifs and one carboxyl-terminal extension (Jakób *et al.*, 2007). These zinc finger motifs are crucial for direct binding to DNA responsive elements in target genomic sections. The N-terminal

of α-helix in the zinc finger motif directly interacts with DNA responsive elements at the groove of DNA. Once the DBD binds to DNA this lead to stimulate the transcription of AR-regulated genes by activating NTD and LBD (Sakkiah *et al.*, 2016).

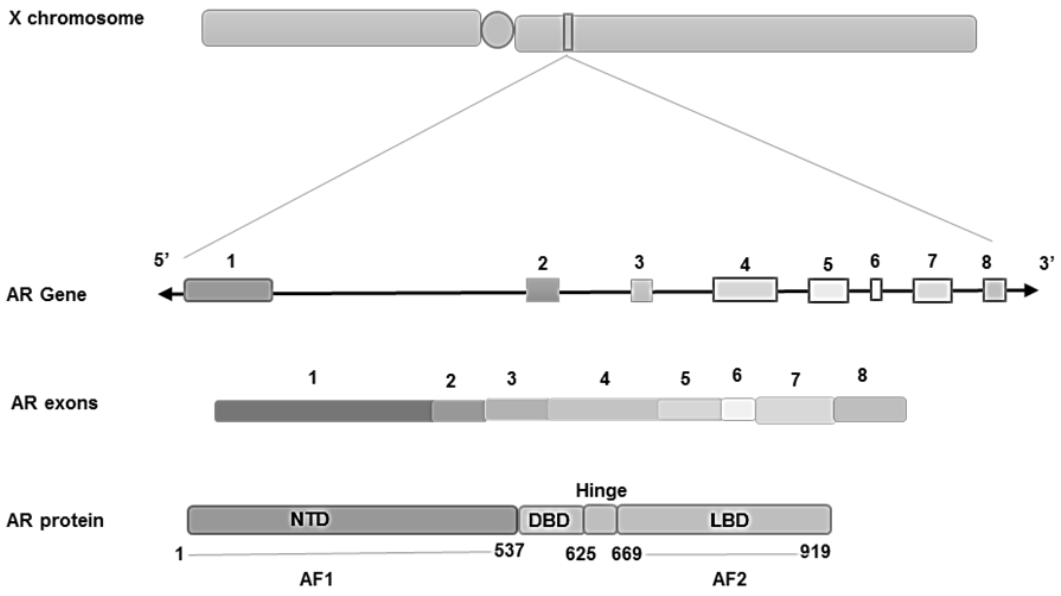

Figure 1-8 Schematic representation of the androgen receptor gene and protein, with indications of its specific domains, adapted from (Lonergan and Tindall, 2011)

1.8.2 Mechanism of action

Androgens are the main regulator of prostate growth by both stimulating proliferation and inhibiting apoptosis. Testosterone is a circulating androgen and is secreted mainly by the testes, but also by the adrenal gland. It appears in blood bound to albumin and sex hormone binding globulin (SHBG). When free testosterone enters the cell, 90% is converted to dihydrotestosterone (DHT), a more active form, by the enzyme 5α-reductase. The active hormone DHT has a greater affinity to bind with AR than the less active form testosterone. In the basal state, AR is bound to heat shock proteins, which prevents DNA binding. Once androgen binding to AR occurs induces conformational changes, this leads to dissociation from the heat shock proteins and receptor phosphorylation. When ligand binding to the AR occurs (Figure 1-10 C), this facilitates the formation of an AR homodimer and then leads to translocation to the nucleus and binding to Androgen Response Elements (ARE) generally in the promotor region of targets genes. AR homodimer complex recruits co-activators or co-repressors to the AR complex. The co-regulators interact with AR complex to stimulate or inhibit target gene

transcription. Activation or repression of target genes leads to biological responses, including growth, survival and the production of prostate-specific antigen (PSA) (Figure 1-9) (Feldman and Feldman, 2001a; Yuan *et al.*, 2014).

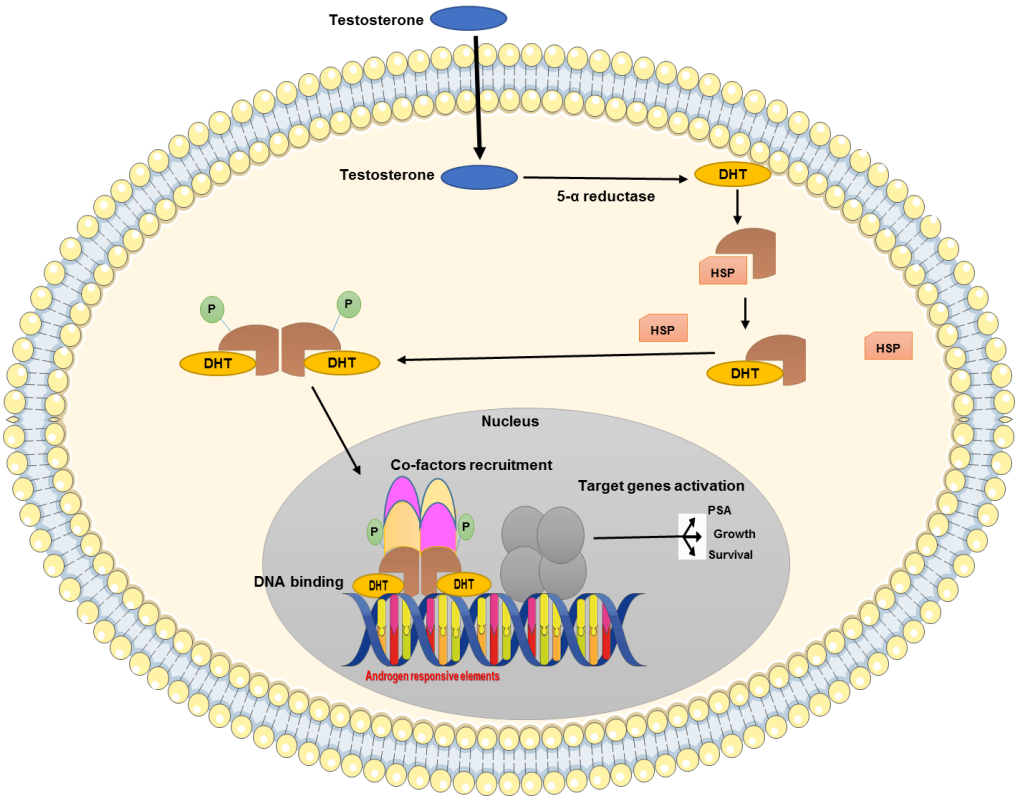

Figure 1-9 Mechanism of androgen receptor action, adapted from (Feldman and Feldman, 2001b). Testosterone is converted to DHT by 5-alpha reductase in the membrane of the cell. DHT then binds to the AR, HSPs dissociate and conformational changes take place to allow homo-dimerization, phosphorylation and translocation into the nucleus. Then, AR binds to sequences in the DNA, termed androgen response elements, to activate transcription. Adapted from (Li and Al-Azzawi, 2009).

Under normal conditions, only half of the cellular AR protein is believed to be occupied by the ligand for mediating genomic androgen action. The remaining half of unbound AR is thought to regulate other biological events, such as cell cycle (Matsumoto *et al.*, 2013).

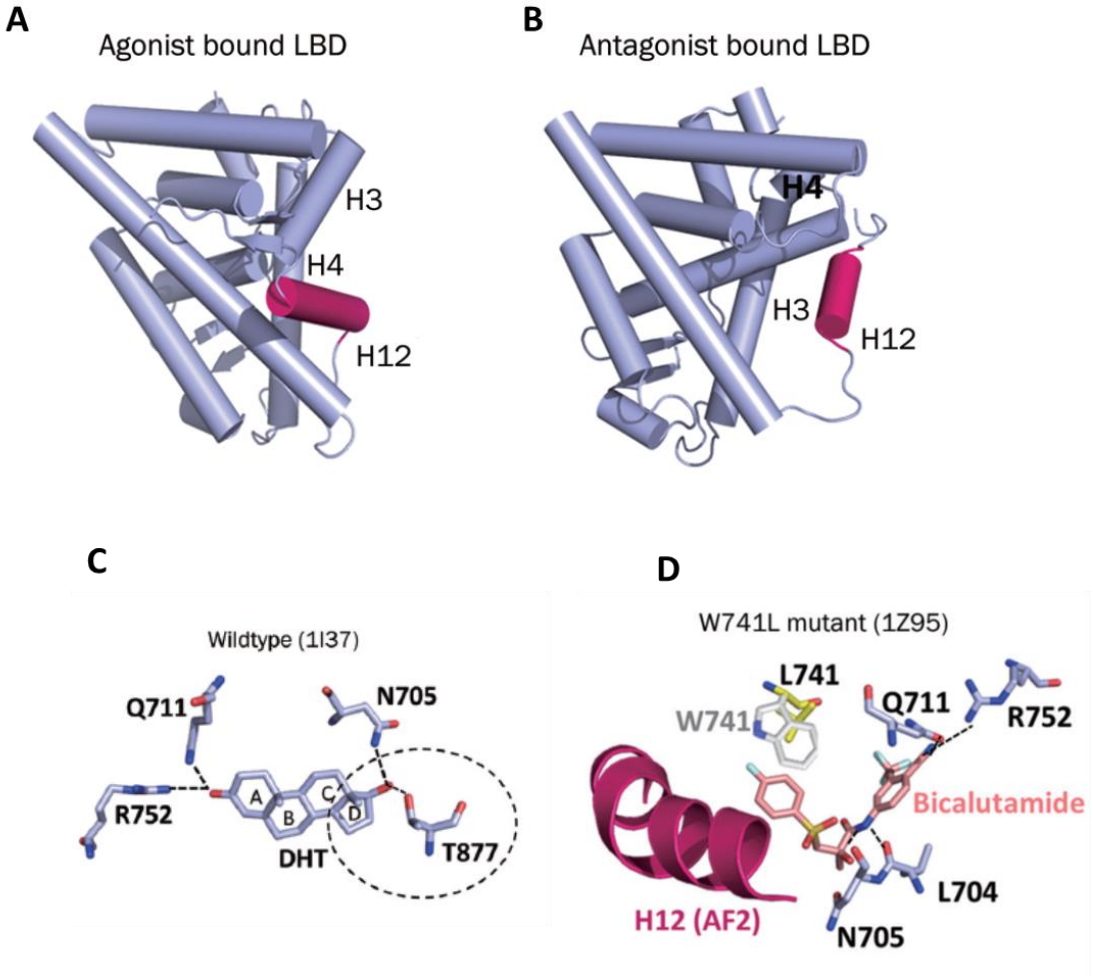

Figure 1-10 Structural understanding of AR. A. Nuclear receptor H12 helices can adopt different conformations. In an agonist state, the H12 of DHT-bound AR (PDB: 1I37 or 2AMA) is held near H3, H4, and H11, which form groove for coactivator binding. **B.** In an antagonist state, H12 rotates clockwise toward H3 and blocks the coactivator binding site. **C.** Structural composition of wild-type AR LBDs in complex with dihydrotestosterone. **D.** Structure of AR LBD W741L complexed with bicalutamide (PDB: 1Z95). Residues L704, N705, Q711, and R752 form hydrogen bonds with bicalutamide (indicated by dotted lines). Also shown is the wild-type W741 residue (white) to illustrate a possible steric clash between tryptophan and the B-ring of bicalutamide.

1.9 Androgen receptor signaling in castrate-resistant prostate cancer

Since the 1940s, the typical treatment of advanced prostate cancer is androgen deprivation therapy (surgical or chemical castration) to downregulate AR transcriptional activity. Unfortunately, the majority of patients relapse within a few years with more aggressive and incurable cancer, no longer responsive to standard hormonal treatments, referred to

as castrate-resistant prostate cancer (CRPC). It is widely accepted that the AR is still active and can stimulate the growth of these cancers that relapse, despite low levels of androgen testosterone and dihydrotestosterone. A study demonstrated that AR was reactivated in CRPC, which is driven by low residual steroid hormones from the adrenal gland (Yuan *et al.*, 2014). Surgical and chemical castration were later joined by other medical therapies, such as prednisone and ketoconazole, which decrease adrenal androgen synthesis and subsequently decrease the PSA serum level (Small *et al.*, 2004; Taplin *et al.*, 2009). This is based on the hypothesis that residual androgens are still able to activate AR after castration. There are many possible mechanisms of AR activity in CRPC, as listed below.

1.9.1 AR gene amplification in CRPC

For the majority of men with CRPC, AR signalling remains the main oncogenic driver for uncontrolled PCa growth, despite the low level of testosterone. Increased signalling of AR is thought to be due to increased AR expression as a result of AR gene amplification and AR copy number, which has been found to be increased in up to 80% of CRPC patients (Koivisto *et al.*, 1996; Waltering *et al.*, 2012; Anantharaman and Friedlander, 2016). This elevation in AR copy number may help increase AR sensitivity to the low level of androgen in CRPC patients and sustain the AR signalling. A possible proposal for this evolution is that most of the primary tumour cells respond to surgical and chemical ADT. However, a small population of cells with AR gene amplification are selected according to their ability to grow in a castration environment, resulting in a clonal population of tumour cells that are able to sustain AR signalling in a Darwinian-like manner (Anantharaman and Friedlander, 2016). In a study of genome-wide screens for genetic aberration, in nine recurrent prostate cancer patients undergoing androgen-depleting treatment, it was reported that *AR* amplification in relapsed prostate cancer occurred as a result of ADT. This is based on elevated *AR* copy number that facilitates tumour cell growth in the low level of serum androgens. According to the fact that AR mediates prostate cell growth, the amplification of the *AR* gene and subsequently the AR protein is likely to enhance cell growth in an environment with a reduced concentration of androgen. In the same study, it was shown that *AR* amplification was not noticed in untreated primary prostate cancer and thus *AR* amplification is exclusively related with regrowth of cancer during androgen depletion (Visakorpi *et al.*, 1995). It has been found that 5α-reductase is overexpressed in CRPC, suggesting that the tumour attempts to

increase sensitivity to androgens by converting testosterone to its more potent form of DHT (Montgomery *et al.*, 2008) (Figure 1-11).

1.9.2 AR gain of function mutations in CRPC

Although patients with prostate cancer initially respond to the anti-androgen, the majority of men eventually relapse with an androgen-independent tumour. One of the mechanisms is through mutation, which has been identified in some androgen-independent cancers. Like other receptors, AR activity can be enhanced or diminished by mutations within the *AR* gene, allowing weaker androgens to activate AR receptors, such as dehydroepiandrosterone, oestrogens/progesterone, or even cortisol. It has been reported that mutations within AR are more prominent in CRPC compared to primary tumours, enabling these cells to survive in any environment. This mutation has the ability to switch AR antagonists (e.g. bicalutamide, nilutamide and flutamide) to agonists (Anantharaman and Friedlander, 2016).

Genomic DNA sequencing data showed a mutation was found in 5 of 16 patients who received anti-androgen treatment with the AR antagonist flutamide and these mutant ARs were strongly associated by flutamide. In addition, these patients with flutamide-stimulated AR mutations responded to treatment with bicalutamide, another AR antagonist that blocks AR, suggest that mutation may be related to flutamide treatment (Taplin *et al.*, 1999).

Another study showed that prolonged treatment with bicalutamide and flutamide might select thee cells with $AR_{W741L/C}$ and AR_{H874Y}/AR_{T877A} mutations which could promote the androgenic signalling and tumour cell growth (Sridhar *et al.*, 2014). Using a bicalutamide-activated $AR_{W741L/C}$ mutation model, one study demonstrated that this mutation prompts an androgenic-like signalling programme and growth promoting phenotype in the presence of bicalutamide(O'Neill *et al.*, 2015).

Second generation antiandrogens such as abiraterone, enzalutamide and ARN509, are potential drugs to treat CRPC, however response rates of just 50% and the development of resistance have limited their success in the clinic. The use of an enzalutamide-resistant model (Korpal *et al.*, 2013) identified a novel F_{876L} mutation in AR that drives genetic and phenotype resistance to enzalutamide. Moreover, this mutation can use enzalutamide as an agonist, promoting the tumour phenotype (Figure 1-11).

1.9.3 Expression of AR splice variants in CRPC

One postulated mechanism of resistance to the conventional and next generation ADT is modified AR mRNA and synthesis of truncated AR variant (AR-V) protein, which lacks AR ligand binding domain (LBD). The presence of an N-terminal domain (NTD) and central DNA binding domain only is sufficient for AR-V to function as ligand independent transcription factors, reported to be upregulated in CRPC and related with poor prognosis. Despite AR-V being able to promote CRPC growth phenotype, inducible expression of AR-V has been demonstrated to remain dependent on the activity of full length AR. Therefore, overcoming AR-V activity could be achieved by targeting full length AR (Watson *et al.*, 2010). ARv7, is formed by splicing inclusion of a cryptic exon called CE3 located within intron 3. AR CE3 is a terminal exon, meaning that splicing inclusion is linked to the selection of a new poly (A) site, thus creating a truncated AR mRNA that lacks coding information for the Ligand-Binding Domain. ARv567es mRNA is formed by skipping of exons 5–7 of the AR pre-mRNA. In addition, The ARv567es protein isoform regulates the transcription of genes involved in cell cycle control. Transcriptional activation by the ARv567es AR isoform occurs via a DNA looping mechanism (Munkley *et al.*, 2017).

The variants AR-V1, AR-V7/AR3, AR-12/ AR_{v567es} and AR-V9 were found to have putative clinical relevance. The mRNA expression of AR-V1 and AR-V7 were found to be significantly higher in CRPC compared with that in hormone-naive PC. The mRNA levels of AR-V1, AR-V7 and AR_{v567es} were also found to be significantly higher in analyses of CRPC bone metastases compared with those of hormone-naive tumours (Lallous *et al.*, 2013; Anantharaman and Friedlander, 2016).

A study aimed at understanding enzalutamide resistance in prostate cancer cell lines stated that cells with AR-V can act in an androgen-independent manner and are resistant to enzalutamide. AR-Vs are key mediators of AR signalling and resistance to next generation antiandrogens. These AR-Vs could be therapeutic targets in advanced disease (Li *et al.*, 2013b). A clinical study of 31 enzalutamide-treated patients and 31 abiraterone-treated patients showed an increase of androgen receptor splice variant 7 mRNA (AR-V7) in their circulating tumour cells. This suggests that the detection of AR-V7 in circulating tumour cells from patients with castration-resistant prostate cancer may be associated with resistance to enzalutamide and abiraterone (Lallous *et al.*, 2013). It has been established that AR splice variants can cooperate with full length AR to potentiate

AR signalling, even in the presence of a potent anti-androgen, such as enzalutamide (Anantharaman and Friedlander, 2016) (Figure 1-11).

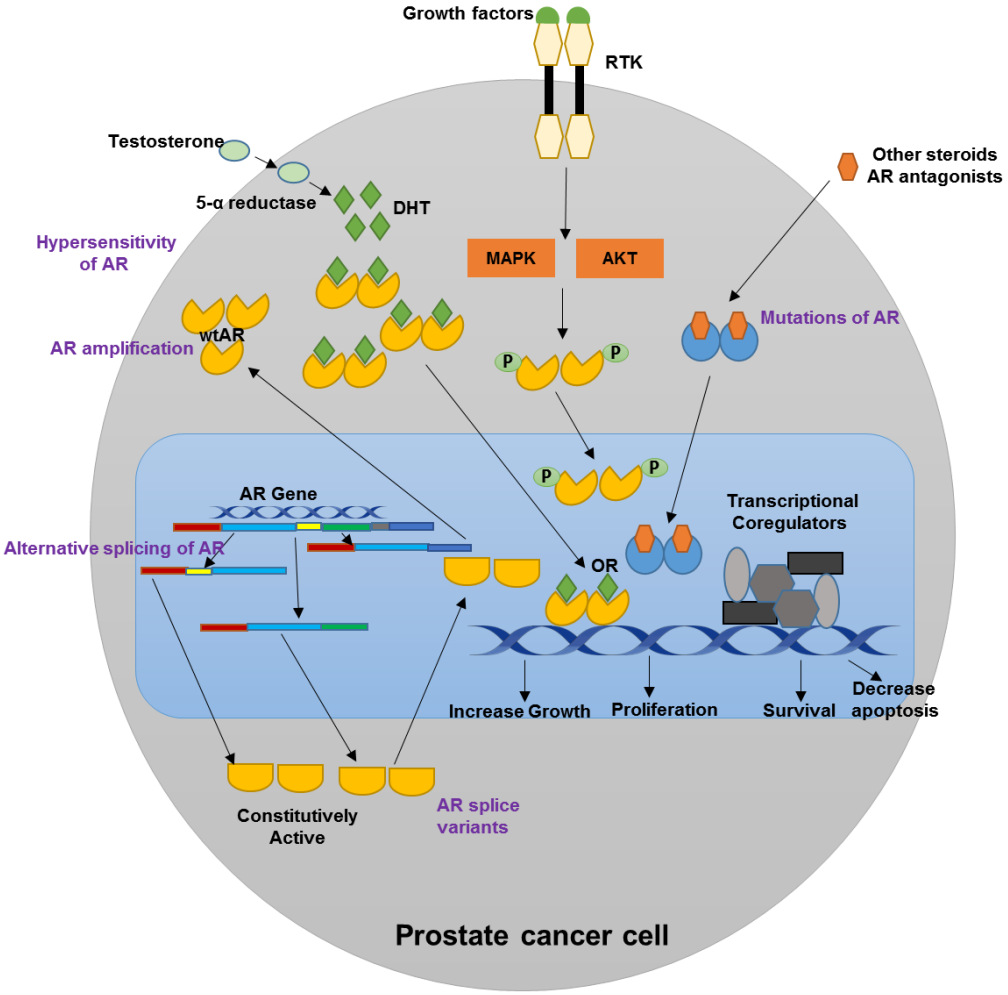

Figure 1-11 Mechanisms of resistance to androgen deprivation therapy, adapted from (Anantharaman and Friedlander, 2016)

1.9.4 AR activation by interaction with co-regulators

AR activation by interaction with co-activator or co-repressor proteins leads to sustained AR signalling in CRPC. This can be achieved by increasing AR stability, increasing the interaction of AR with co-activators, decreasing AR co-repressor interactions, chromatin remodelling and post-translational modification of AR. AR functions could be enhanced by interaction with co-activators, resulting in the regulation of cellular events. Several co-activators have been reported to increase their expression in cancer tissue. AR co-activators bind to one or more regions of the AR and their expression may change during different stages of prostate cancer, suggesting that detection of these co-activators in tumour tissue may have prognostic and diagnostic importance (Culig, 2016).

Steroid receptor co-activators (SRC1, SRC2 and SRC3) are co-factors that mediate transcriptional functions of nuclear receptors and have a role in various cancers. These proteins are the most frequently studied of all co-activators. All SRCs show structural similarity. They mediate protein-protein interaction, including with other transcriptional factors. SRCs also regulate transcription factors such as nuclear factor kappa B, signal transducers and activators of transcription (STAT), or hypoxia inducible factor. AR complex recruits SRC, which is facilitated by the transcription factor GATA2-binding protein, which in turn sustains the activity of wild type and truncated AR (He *et al.*, 2014). GATA2 expression is elevated in patient samples with cancer compared to benign samples. In addition, GATA2 expression associated with tumour stage and grade and inhibition of GATA2 with the small molecular inhibitor K7174, decreased the expression of AR and growth of prostate cancer. Importantly, GATA2 expression was elevated in prostate cancer cells treated with enzalutamide, suggesting that GATA2 be considered a mediator of enzalutamide resistance (He *et al.*, 2014; Culig, 2016).

SRC2 is an important transcriptional co-activator associated with the anti-apoptotic and proliferation pathways of PI3K/Akt and MAP kinase. SRC2 expression is increased in androgen deprivation conditions, which might indicate that it is correlated with prostate cancer progression (Qin *et al.*, 2014).

AR is required to bind for the androgen-responsive elements (AREs) to function. However, this will not happen unless the chromatin is opened and accessible and this can be achieved by FOXa1, a transcription factor, which opens the chromatin locally so AR can access the ARE. These sites are marked by H3K4me2-containing nucleosomes. A co-activator, LSD1, functions as an androgen-stimulated gene and correlated with the demethylation of H3K9me2 (Yuan *et al.*, 2014). In addition to transcriptional activation, it has been established that the expression of multiple genes is decreased in response to androgen, which is likely to be secondary to transcriptional effects on other genes.

AR can act as a repressor to several genes more directly by interacting with other transcriptional activators or by functioning as a transcriptional repressor (Yuan *et al.*, 2014). It has been reported that E74-like factor 3 (ELF3), a member of the ETS family of transcription factors, is a repressor of AR activity (Shatnawi *et al.*, 2014), who found that endogenous expression of ELF3 represses the AR transcriptional level. In addition, ELF3 knockdown increases AR transcriptional activity and promotes LNCaP cells to migrate,

whereas an increase in ELF3 expression inhibits cells growth, suggesting that interaction between ELF3 and AR inhibits the recruitment of AR to specific androgen response elements within target gene promoters.

The initiation of cancer and its development and progression, can be determined by epigenetic markers such as histone methylation and histone acetylation, which have a crucial role in AR regulation in prostate cancer. One method of controlling transcription is histone methylation, which is mediated by histone methyltransferase (HMT) and histone demethylase (HDM) enzymes. Methylation changes the local chromatin to increase or decrease transcription, depending on the site of modification (Peterson and Laniel, 2004; Cucchiara *et al.*, 2017).

Protein arginine methyltransferase (PRMT) family members such as PRMT6 and co-activator-associated arginine methyltransferase 1 (CARM1) are the enzymes responsible for histone methylation. Evidence indicates that histone methylation of AR regulates its transcription activity. SET9 is one HMT enzyme that has a role in prostate cancer and its level is elevated in malignant epithelial cells from PC patients (Cucchiara *et al.*, 2017). One study identified SET9 as an AR co-regulator by directly methylating lysine 632, located in the hinge domain of the receptor, to enhance AR transcription. This activation signal facilitates both inter-domain communication between the N and C-terminal of the receptor and AR promoter association. This study also indicates that SET9 regulates the proliferation and apoptosis of the LNCaP, suggesting the significant role of SET9 in prostate cancer as a therapeutic target (Gaughan *et al.*, 2011). The histone acetyltransferases (HAT) and deacetylases (HDAC) are enzymes responsible for acetylation and deacetylation. In general, active chromatin is hyper-acetylated while inactive chromatin is hypo-acetylated. An acetylation motif is located in the hinge region of AR with short sequences (KLKK). Placing and removing acetyl groups can improve or reduce AR transcriptional activity respectively (Cucchiara *et al.*, 2017). TIP60, an AR factor acetyl transferase, is responsible for the acetylation of the LBD of the AR and it can interact with HDACs at the PSA promoter region. This interaction can lead to activation or suppression of AR transcription. It has been indicated that overexpression of TIP60 facilitates the acetylated form of AR and AR localization in the nucleus, in the absence of androgen (Brady *et al.*, 1999; Gaughan *et al.*, 2005; Shiota *et al.*, 2010).

As mentioned above, acetylation enhances AR activity at specific residues and this opposite process leads to the inhibition of the AR transcriptional activity. For example, HDAC1 interacts with the PSA promoter to inhibit AR signalling, while HDAC6 regulates AR activity via modelling heat shock protein 90 (HSP90) acetylation. The acetylation of HSP90 leads to destabilization of AR and subsequently degradation by the proteasome (Ai *et al.*, 2009; Cucchiara *et al.*, 2017).

1.9.5 Androgen receptor bypass signaling

Recent work revealed a novel resistant mechanism of the AR pathway, known as "bypass signalling" (Arora *et al.*, 2013). The term bypass refers to a mechanism in which downstream signalling of the AR is controlled by another cellular receptor. This was shown in an LNCaP xenograft model with exogenous AR overexpression (LNCaP-AR). The model demonstrated acquired resistance to enzalutamide, or ARN-509, associated with the upregulation of the glucocorticoid receptor (GR). In addition, the LNCaP-AR subline tends to be GR-dependent for enzalutamide-resistant growth. According to ChIP-seq analyses data, GR can bind over half of all AR binding sites in enzalutamide-resistant cells and can occupy a large number of sites not bound by AR. This gives the possibility that GR transcriptional activity could contribute to resistance. Moreover, it has indicated that GR regulates AR target genes such as *PSA* and *TMPRSS2,* which may suggest that GR enables cells to become resistant to enzalutamide (Arora *et al.*, 2013; Watson *et al.*, 2015). Similar to the AR, GR is a transcription factor belonging to the superfamily of nuclear hormone receptors and can be activated through steroid ligands. GR also dissociates from cytoplasmic chaperone proteins and translocates to the nucleus. The homodimers bind to the hormone response elements (Epstein *et al.*) to recruit gene expression. Therefore, the dual target of GR and AR could be suggested as a therapeutic target for prostate cancer. Two studies have considered non-steroid phyto-chemical compound A (CpdA), which an AR/GR modulator is acting as an anti-inflammatory anti-androgen. This suppresses prostate cell growth and survival and induces endoplasmic reticulum stress (ERS) (Yemelyanov *et al.*, 2008; Yemelyanov *et al.*, 2012).

Despite the hypothesis that GR can confer resistance, this seems inconsistent with patient data suggesting that glucocorticoids can be effective in some patients with CRPC. However, this can be explained by the fact that glucocorticoids (GCs) decrease adrenocorticotropic hormone (ACTH) production by the pituitary gland, which results in

decreased androgen levels (Figure 1-12 A). This androgen reduction explains the decline of serum PSA levels noticed in men taking prednisone alone, which was reported in the comparator arm of the Phase III clinical trial that led to the approval of abiraterone for chemotherapy-naive CRPC (Tannock *et al.*, 1989; Ryan *et al.*, 2013). However, evidence indicates that GCs stimulate tumour proliferation by the regulation of AR target genes. One proposed mechanism is that GCs compete with enzalutamide to bind with the AR target gene in those tumours carrying an AR_{L702H} mutation, which is stimulated by GCs. Another suggested mechanism is that GCs activate GR expression in tumours carrying GR overexpression, thereby bypassing the blockade of AR target gene expression by enzalutamide (Figure 1-12 B) (Watson *et al.*, 2015).

Upregulated of GR protein expression was detected in CRPC and it is associated with an acquired resistance to enzalutamide and it has been validated in pre-clinical studies. A study aimed to determine the expression of GR in circulating tumor cells (CTCs) from patients with progressing metastatic CRPC, showed higher expression of GR detected in (CTCs). This suggested that detection of GR in patient-derived CTCs may be a useful biomarker (Wise *et al.*, 2016). Recently, a study showed that enzalutamide inhibits the inactivation of cortisol to cortisone which lead to GR stimulation and enzalutamide resistance. This happens by way a decrease in the expression of 11β-HSD2, which converts cortisol to cortisone, in response of enzalutamide in the prostate cancer model, reveling a surprising metabolic activity of enzalutamide resistance that could be targeted with a strategy that circumvents a condition for systemic GR ablation (Sharifi *et al.*, 2017).

In addition to AR, GR, the progesterone receptor (PGR) and the mineralocorticoid receptor (MR) are all steroid hormone nuclear receptor family members and that share substantial homology within the DNA-binding domain. It is suggested that PGR or MR may perhaps transcriptionally regulate a number of AR target genes in prostate cancer model by bypass AR (Watson *et al.*, 2015).

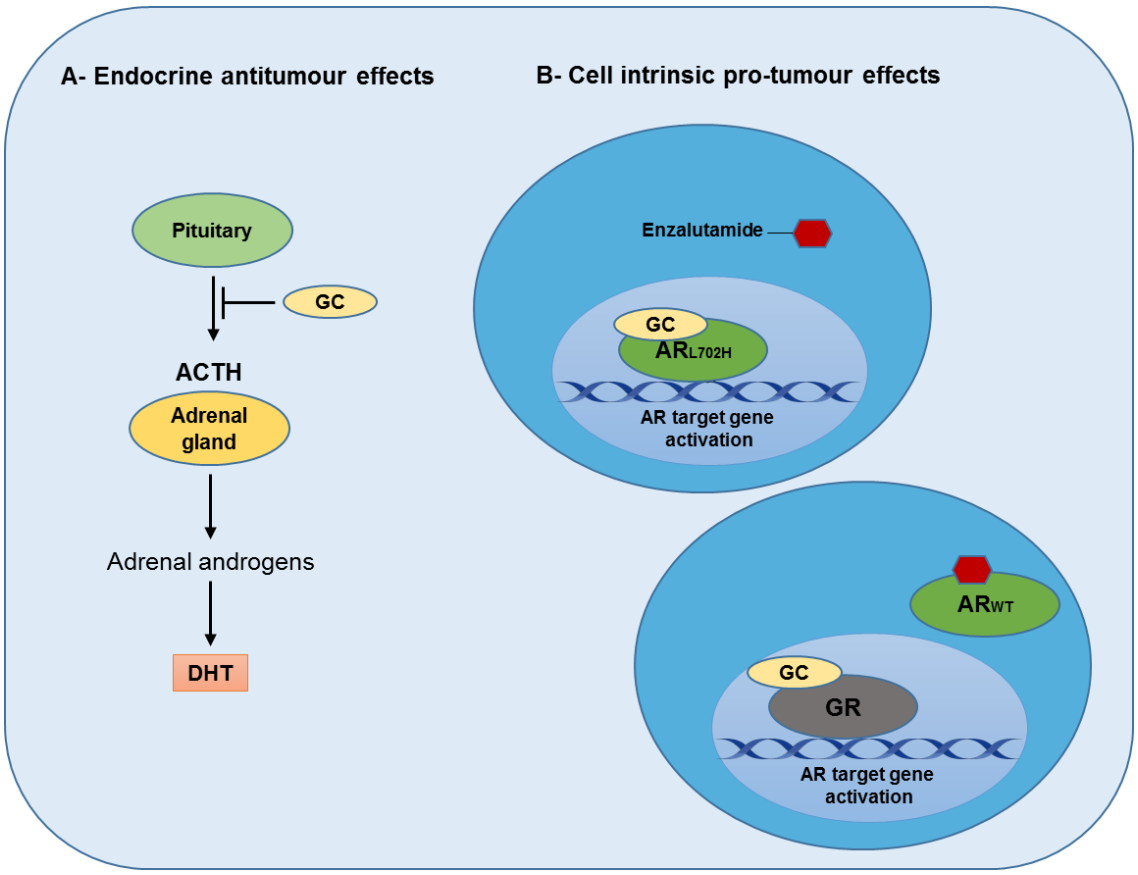

Figure 1-12 The roles of glucocorticoids in prostate cancer, adapted from (Watson *et al.*, 2015)

1.9.6 Kinase signalling pathways regulating AR

There are two possible pathways that regulate AR activity in prostate cancer and this is discussed in the following section.

The phosphatidylinositol-3-kinase/Akt/mammalian target of rapamycin (PI3K/Akt/mTOR) pathway:

This pathway is the most frequently dysregulated pathway in prostate cancer and several other cancers. It is responsible for proliferation, survival, apoptosis and therapeutic resistance, potentially due to its role in the regulation of cell growth, malignant transformation and progression of the cancer. Dysregulation of this pathway often occurs because of mutation, deletion, amplification and post-translation modification (Chang *et al.*, 2015). Structurally, this pathway is composed of the PI3K family, split into Class I, Class II and Class III. Class I PI3K are heterodimeric molecules that are further divided

into two subclasses: subclass IA (PI3Kα, β and δ), which is activated through receptor tyrosine kinases (RTK) and subclass IB (PI3K γ), which is activated by G-protein-coupled receptors and rat sarcoma (RAS) oncogene. Class II and Class III are different from Class I PI3K in their structure and function (Leevers *et al.*, 1999).

A number of down-stream signals are activated by PI3K, including serine/threonine kinase Akt, which activates mTOR. Akt is divided into three structurally similar isoforms; Akt1, Akt2 and Akt3. They consist of three domains; an N-terminal domain, a central kinase domain and a C-terminal domain. Once Akt is phosphorylated, it phosphorylates many downstream proteins such as mTOR, GSK3 and IRS-1. Akt plays a crucial role in numerous biological process, such as cell proliferation, apoptosis, cell migration, transcription and therapeutic resistance (Manning and Cantley, 2007; Porta *et al.*, 2014). As an Akt substrate, mTOR is a serine/threonine protein kinase that plays a vital role in the regulation of cell growth, proliferation, motility, survival, protein synthesis and transcription. mTOR has two complexes, mTORC1 and mTORC2, which both localise at different subcellular compartments, thus affecting their activation and function. mTOR activation results in an increased level of multiple proteins, such as cyclin D1 and vascular endothelial growth factor (VEGF), leading to up-regulated tumourigenesis (Chang *et al.*, 2015). The PI3K/Akt/mTOR pathway is negatively regulated by phosphatase and tensin homolog (PTEN), which is considered a tumour suppresser gene. However, it is frequently mutated and deleted in various human cancers including prostate cancer.

One study found that aberrant PI3K/Akt/mTOR signal proteins were identified in prostate cancer cell lines, xenografts and between 30-50% of patients with prostate cancer (Morgan *et al.*, 2009). Another study demonstrated that alterations in the PI3K/Akt/mTOR pathway were detected in 42% of early stage prostate tumours and 100% in the metastatic stage (Taylor *et al.*, 2010). Clinical data from patients also revealed that an increase in the signalling of PI3K/Akt/mTOR was accompanied with AR phosphorylation in CRPC (McCall *et al.*, 2008). Another study reported that 42% of prostate cancer patients had abnormal PTEN and Akt up-regulation (Teng *et al.*, 1997). It has been suggested that activation of PI3K can lead to the development of chemo-resistance in prostate cancer cells, through multidrug resistance protein1 (MRP-1) overexpression (Lee *et al.*, 2004). Another clinical study based on patients with prostate cancer showed that more than 90% had up-regulated expression and/or phosphorylation of PI3K/Akt in malignant tissue, compared to benign tissue. Phosphorylation increased

in patients with Gleason scores of ≥6 (100%) compared with those with Gleason scores of 4-5 and this increased PI3K/Akt phosphorylation was correlated with loss or inactivation of PTEN (Jendrossek *et al.*, 2008).

The binding of growth factors to receptor tyrosine kinases also recruits and activates PI3K. Activated PI3K alters PIP2 to PIP3, which subsequently phosphorylates Akt through PDK1. Phosphorylated Akt activates the most important target, which is mTOR and this in turn regulates proliferation, cell growth and survival. The active form of Akt also regulates AR in an androgen-independent manner, resulting in over-activation of the AR signalling in CRPC. PTEN negatively inhibits this pathway by removing the 3-phosphate from PIP3, converting it back to PIP2. Loss of PTEN leads to over-activation of Akt, leading to uncontrolled cell proliferation, decreased apoptosis and enhanced tumour angiogenesis (Phin *et al.*, 2013) (Figure 1-13).

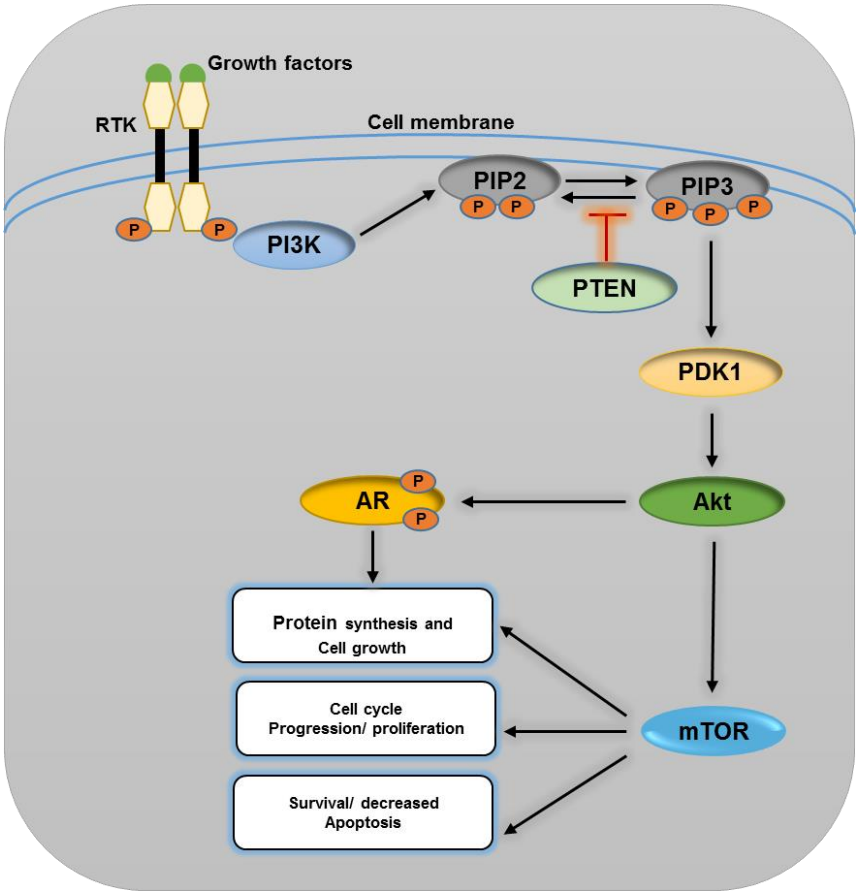

Figure 1-13 The interaction between PI3K/PTEN/Akt pathway and AR signalling, adapted from (Phin *et al.*, 2013).

Recently, it has been shown that the PI3K/Akt/mTOR pathway regulates AR through complex reciprocal feedback mechanisms. Deregulation of PI3K/Akt/mTOR results from *PTEN* loss associated with androgen independence to develop CRPC. PTEN loss was observed in prostate epithelial cells and leads to a decrease in the AR target genes through de-repression of EGR1 and c‑Jun, which is known as a negative regulator of AR (Figure 1-14 A). This might suggest that the PI3K/Akt/mTOR pathway reactivates AR signalling in the presence of low level endogenous androgen, which can contribute to CRPC (Edlind and Hsieh, 2014). Additionally, it has been demonstrated that inhibition of either the PI3K/Akt/mTOR or AR signalling pathways drives the reciprocal activation of the other pathway. Moreover, genetic ablation of AR, or using the AR anti-androgen enzalutamide, in a prostate cancer mouse model driven by *PTEN* loss, enhances Akt signalling through downregulation of FKBP5. In turn, this leads to a reduction in levels of PHLPP, a negative regulator of Akt signalling (Figure 1-14 B). Another study indicated that inhibition of AR transcription or activity reciprocally enhances Akt signalling through down-regulation of PHLPP. Moreover, mTOR inhibition accompanied by *PTEN* loss leads to an increase in AR levels through upregulation of HER3, which increases AR stability (Figure 1-14 C). This leads to the proposal that the PI3K/Akt/mTOR pathway and AR signalling can compensate for each other if there is inhibition of either pathway in prostate cancer (Carver *et al.*, 2011; Bitting and Armstrong, 2013; Edlind and Hsieh, 2014).

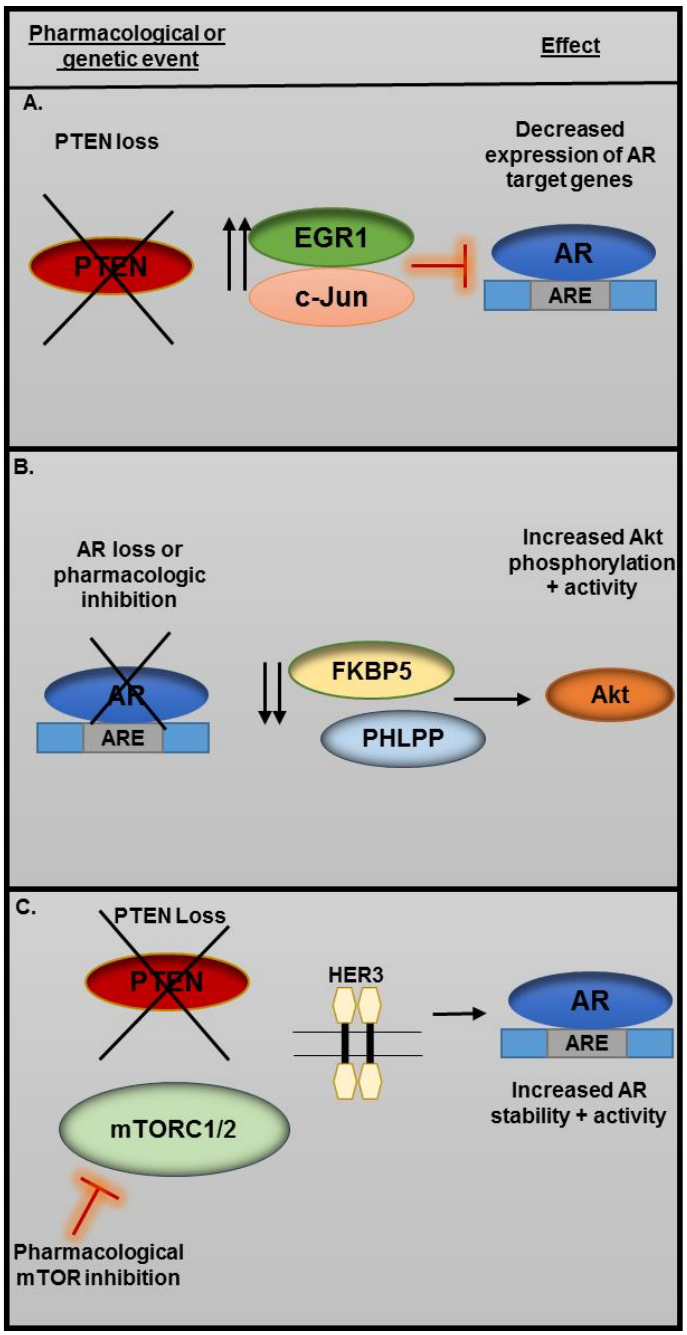

Figure 1-14 Reciprocal feedback mechanisms between PI3K/Akt/mTOR pathway and AR signalling, adapted from (Edlind and Hsieh, 2014)

Aberrant Raf/MEK/ERK signalling pathway in prostate cancer

The Raf/MEK/ERK pathway can be activated in response to the signals from receptor tyrosine kinases and other cell membrane receptors. Activating this pathway can regulate differentiation, cell cycle, cell survival and its deregulation is a central signature of many epithelial cancers, including prostate cancer (Imada *et al.*, 2013; Park, 2014). However,

although mitogenic signals activate this pathway to mediate cell growth, they also mediate growth inhibitory signalling such as cell cycle arrest and cell death in response to several signals.

The classic Raf/MEK/ERK pathway consists of the Ser/Thr kinase Raf (i.e., A-Raf, B-Raf, or C-Raf), MEK1/2 and ERK1/2. All three Raf proteins have properties which allow them to control cellular transformation as well as growth inhibition and also activate downstream proteins such as MEK/ERK (Woods *et al.*, 1997; Park, 2014).

MEK1 and MEK2 are activated by Raf phosphorylation (i.e., Ser217/221 for MEK1 and Ser222/226 for MEK2). In contrast to Raf, MEK is abundant in the cells. Therefore, activation of the Raf/MEK/ERK pathway can occur at the Raf/MEK step due to the greater abundant ratio between Raf/MEK than between MEK/ERK (Ferrell, 1996).

ERK1 and ERK2 are activated by MEK1/2 phosphorylation of Tyr and Thr residues and can also auto-phosphorylate at the Tyr residue. All effects of ERK1/2 are mediated by MEK1/2. This interaction between MEK1/2 and ERK1/2 is a typical characteristic of the MAPK pathway due to the high affinity between them. Activation of ERK1/2 can activate 160 substrates, including kinases, transcription factors, cytoskeletal proteins, receptors and other molecular switches (Park, 2014).

It has been demonstrated that increased signalling in the MAPK pathway is associated with prostate cancer and activation of this pathway leads to increased prostate cancer cell growth. However, activation of MAPK signalling reduced but did not replace the requirement of LNCaP cells for androgen (Bakin *et al.*, 2003). Activation of Raf/MEK/ERK has been shown to increase AR target genes, independently of androgen, by phosphorylation of AR or its co-factors (Mukherjee *et al.*, 2011). Mutation of Ras and gene expression deregulation of Raf are correlated with tumour progression (Mukherjee *et al.*, 2011). In addition, Raf and MEK are both thought to be overexpressed in non-metastatic and metastatic prostate cancer cells (Weinstein-Oppenheimer *et al.*, 2000). It has been shown that increased activity of MAPK is elevated in CRPC (Abreu-Martin *et al.*, 1999). Activation of MAPK is believed to stimulate prostate cancer cell growth independent of AR by activating several transcription factors such as AP-1 (a homo-heterodimer of phosphorylated c-jun and c-fos) and c-myc. Moreover, increased expression of Raf-1 is associated with CRPC development (Weinstein-Oppenheimer *et al.*, 2000; Mukherjee *et al.*, 2011).

A study showed that activation of prostate cancer cells with DHT leads to ERK1/2 phosphorylation within 1-2 minutes and the peak level of phosphorylation occurs within 5-10 minutes (Liao *et al.*, 2013). The same study demonstrated that activation of ERK1/2 by DHT leads to translocation of ERK1/2 from cytoplasm to the nucleus. ERK1/2 directly interacts and phosphorylates transcription factors, such as nuclear ETS, which is involved in cell proliferation. However, a study observed that introduction of activated Raf genes (Raf-1 and B-Raf) did not increase the resistance to the chemotherapy, while the introduction of activated Akt genes did increase the resistance to the chemotherapy (Lee *et al.*, 2005). Another study claimed that some prostate cancer cell lines, such as LNCaP and PC3, which have PTEN mutation and express a high level of Akt, expressed a low level of active Raf/MEK/ERK pathway members (McCubrey *et al.*, 2007).

Although the role of Raf/MEK/ERK pathway in prostate cancer is still controversial, a gene microarray screen between a non-metastatic prostate cancer cell and its metastatic derivative line revealed a decrease in the expression of Raf kinase inhibitor protein (RKIP) in the metastatic cell line. This suggests increased Raf activity, by inhibition of RKIP, which is related with metastasis in prostate cancer (Keller *et al.*, 2004).

The Raf/MEK/ERK pathway is also involved in cross talk with the PI3K/Akt/mTOR pathway in the regulation of AR in prostate cancer and activation of this pathway has been reported to decrease the sensitivity to the PI3K/Akt/mTOR pathway blockers. Furthermore, using the MEK inhibitor (PD325901) to inhibit the Raf/MEK/ERK pathway showed significantly decreased metastatic progression with PTEN loss models (Ihle *et al.*, 2009; Mulholland *et al.*, 2011). A study showed that inhibition of both PI3K kinase and MAP kinase signalling by using dual PI3K/mTOR inhibitor GSK2126458 and AZD6244, respectively, decreased both phospho-Akt and phospho-ERK effectively as well as prostate cancer tumour growth, both *in vitro* and *in vivo*. This suggests that a combination treatment targeting both the PI3K and MAPK pathways is an effective treatment strategy for CRPC (Park *et al.*, 2015).

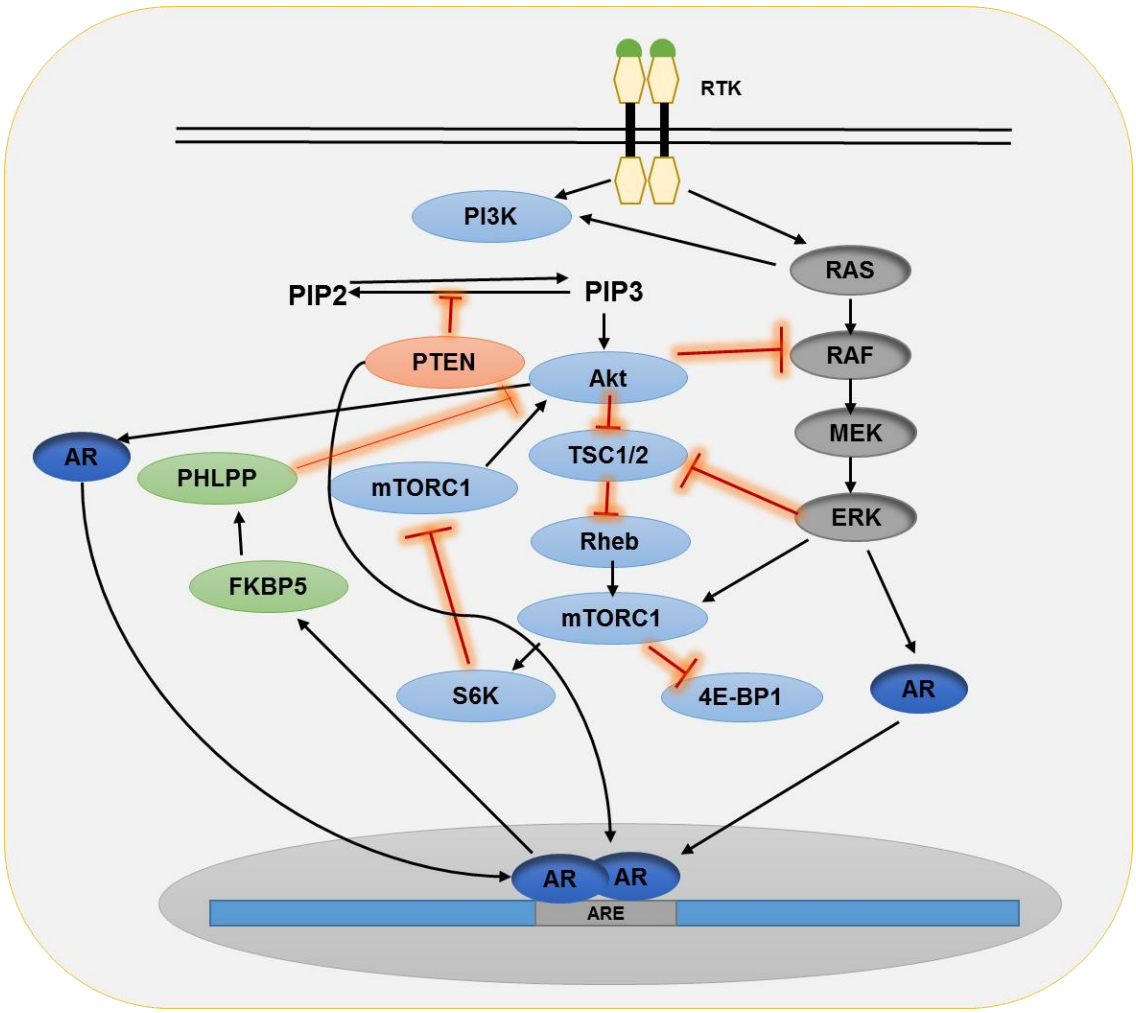

Figure 1-15 The PI3K/Akt/mTOR pathway and cross talk with the AR signalling and RAS/RAF/MEK pathways, adapted from (Bitting and Armstrong, 2013)

4E-BP1, eukaryotic initiation factor 4E-binding protein 1; **ERK**, extracellular signal-related kinase; **FKBP5**, FK506-binding protein 5; **MEK**, mitogen-activated protein/ERK kinase; **PHLPP**, PH and leucine-rich repeat phosphatase; **PI3K**, phosphatidylinositol 3-kinase; **PTEN**, phosphatase and tensin homolog; **RAS**, rat sarcoma oncogene; **Rheb**, RAS homolog enriched in the brain; **S6K**, S6 kinase; **TSC**, tuberous sclerosis protein; **mTORC**, target of rapamycin complex; C/K. Akt activity can both enhance and suppress AR signalling. Possible mechanisms of Akt-mediated regulation of AR activity include direct phosphorylation of AR, Akt-mediated regulation of a variety of transcription factors, including FOXO3a and NF-kb; and Akt-mediated regulation of b-catenin via GSK3b (Bitting and Armstrong, 2013).

Receptor tyrosine kinases regulate both the PI3K/Akt/mTOR and the RAS/RAF/MEK pathways. EGFR is family of the receptor tyrosine kinase which regulates proliferation and survival in prostate cancer (Robinson *et al.*, 1996).

1.10 EGFR family

This family consists of type 1 tyrosine kinases ErbB1/HER1/epidermal growth factor receptor (EGFR), ErbB2/HER2/neu, ErbB3/HER3 and ErbB4/HER4. Prostate cancer cells express EGFR, HER2 and ErbB3, but not ErbB4 (Figure 1-16) (Chen *et al.*, 2010). According to a previous study in our lab, cytoplasmic and nuclear expression of HER2 and HER3 increases within cancer stage and grade of the patients with prostate cancer. In addition, over-expression models of HER2 and HER3 cause an increase in cell migration, proliferation, invasion and activation of both PI3K/Akt/mTOR and RAS/RAF/MEK pathways (Rao, 2015). For this reason, this study will focus on the role of HER2/HER3 in castrate resistant prostate cancer models.

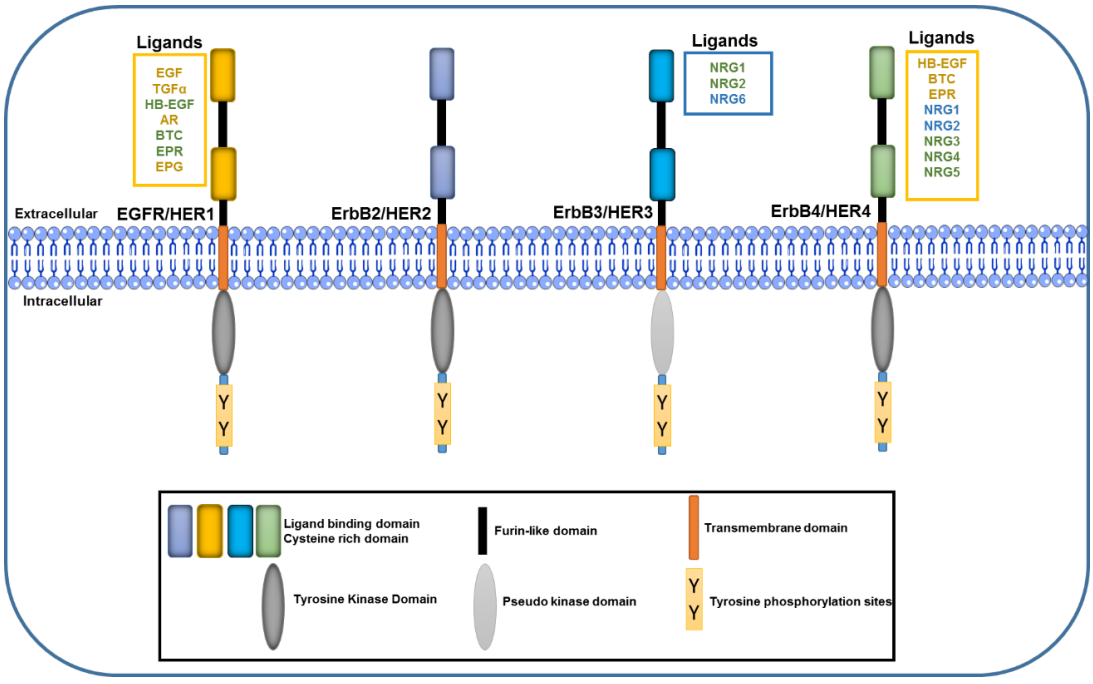

Figure 1-16 ErbB/HER receptors and their ligands, adapted from (Iwakura and Nawa, 2013)

EGFR/HER1

EGFR signalling regulates a variety of cellular functions such as cell survival, cell growth and proliferation. The downstream signalling pathways from EGFR are linked to many solid tumours, including prostate cancer (Iwakura and Nawa, 2013). The ligands mediate EFGR activity by a conformational change in the extracellular domain of the receptor, resulting in dimerization of the EGFR receptor to activate the downstream signalling pathways. The active form of EGFR undergoes auto-phosphorylation of its tyrosine residues in the cytoplasmic tail of the receptor, resulting in the activation of multiple signal transduction pathways, including PI3K/Akt/mTOR and RAS/RAF/MEK (Tomas *et al.*, 2014). One study found that EGFR is required for primary and secondary prostate cancer. EGFR expression was noticed in circulating tumour cells (CTC) during prostate cancer metastasis and dual inhibition of HER2 and EFGR resulted in a decrease in tumour xenograft growth (Day *et al.*, 2017).

It is known that EGFR overexpression is associated with the development of CRPC in patients. However, EGFR expression is not significantly associated with tumour differentiation or preoperative prostate-specific antigen (PSA), suggesting that EGFR expression only increases during disease progression and in the development of castration-resistant disease (Shah *et al.*, 2006).

ErbB2/HER2/neu

Aberrant activity of HER2 has been correlated with the development of CRPC. It has been reported that HER2 expression is elevated in bone metastases of prostate cancer and inhibiting its expression reduced the proliferation of bone tumour xenografts (Day *et al.*, 2017). Similar to other HER family members, HER2 is a type I transmembrane growth factor receptor that functions to activate intracellular signalling pathways in response to extracellular signals. The structure of HER2 protein consists of an extracellular ligand-binding domain, a transmembrane domain and an intracellular tyrosine kinase domain (Figure 1-16). In contrast to other HER members, HER2 has no known ligand and therefore its signal cannot function unless there is heterodimer with other HER members (Moasser, 2007). Among all the HER family proteins, HER2 has the strongest catalytic kinase activity and acts as the most active signalling complex after heterodimerization with other HER family members. Overexpression of HER2 leads to increased

homodimerization (HER2:HER2) and heterodimerization with HER3 (HER2:HER3), which initiates tumourigenic signalling cascades and malignancy (Yan *et al.*, 2015).

It has been noticed that dysregulation of RTK signalling, such as EGFR and HER2, can regulate the PI3K/Akt/mTOR signalling pathway, which is shown to be correlated with progression of prostate cancer (Di Lorenzo *et al.*, 2002). A study demonstrated that in the inducible overexpression HER2 cell line, ERK1/2 appears to be activated with increased PSA level and androgen leads to HER2 phosphorylation at Tyr1221/2 but not Tyr1248. In addition, under androgen depletion conditions and in the presence of HER2 inhibitor AG879, the growth of LNCaP cells was attenuated (Muniyan *et al.*, 2015). Furthermore, an HER2 inhibitor effectively caused AR degradation and decreased AR phosphorylation at Ser81 (Hsu *et al.*, 2011).

According to a differential gene expression study on androgen-dependent and androgen-independent sublines, it was noticed that an increase in HER2 protein level is associated with the progression to androgen-independence. Additionally, forced overexpression of HER2 was sufficient to confer androgen-independent growth *in vitro* and accelerate progression to androgen-independence in castrate animals, suggesting that overexpression of HER2 mediates androgen independence (Craft *et al.*, 1999). However, by using the FISH technique to identify HER2 gene amplification, a study indicated that, from a total of 86 cases, only 8 (9.3%) were found to be amplified (Mark *et al.*, 1999). Another study demonstrated HER2 amplifications were not detected at any stage of prostate cancer progression (Bubendorf *et al.*, 1999). On the other hand, it has been shown that activation of HER2 by heregulin leads to HER2 phosphorylation and enhances the cell proliferation of the androgen-independent prostate cancer cell line. Heregulin is known to be the ligand of HER3, indicating that both HER2 and HER3 have a role in prostate cancer (Hsu *et al.*, 2011). Inhibition of HER2 shows reduced AR transcriptional activity and the AR function is mediated by the HER2/HER3 pathway, but not by EGFR. HER2/HER3 signalling stabilizes AR protein levels and optimizes binding of AR to the promoter/enhancer regions of androgen-regulated genes. This indicates that the HER2/HER3 pathway is an important target in CRPC patients (Mellinghoff *et al.*, 2004).

A study showed that prostate cancer patient with low levels of PTEN and high level of HER2/HER3 have poor prognosis. Same study showed that activation of HER2 in PTEN loss murine model led to increase prostate cancer progression significantly. This can by

explained by HER2 activation led to with activation of the MAPK pathway abrogation of the PTEN loss-induced cellular senescence program and inhibits MEK activity strongly suppressed proliferation within these tumours by restoring the PTEN loss-induced cellular senescence program (Ahmad *et al.*, 2011)

ERBB3/HER3

HER3 belongs to the ErbB (HER) receptor family of type I receptor tyrosine kinases (RTKs). The HER3 gene is located on chromosome 12q13 and expressed in normal epithelial tissues. HER3 has 40-50% sequence homology with HER1 and 40-45% homology with HER2. The structure of HER3 is typical of the receptor tyrosine kinase family, which includes an extracellular domain (ECD) with 612 amino acid residues, a transmembrane helix domain with 32 hydrophobic amino acids and an intracellular tyrosine kinase domain (TKD) with 677 amino acids (Figure 1-16) (Li *et al.*, 2013a).

HER3 is one of the most important receptors with a crucial role in tumourigenesis. It has been reported that HER3 is overexpressed in both the primary cancer and cell lines of many cancers, including pancreatic, colonic, breast, ovarian and prostate. Overexpression of HER3 is considered a hallmark of prostate cancer and could be a biomarker for its clinical progression (Zhang *et al.*, 2016).

Similar to other HER family members, dimerization of HER3 receptors is an essential step for its function and, as a consequence of dimerization, a signal transfers from extracellular to intracellular compartment and leads to activation of the downstream signalling pathways, which induces biologic responses, including cell proliferation, maturation, survival, apoptosis and angiogenesis. Heregulin is a binding ligand that causes dimerization through the extracellular domain of HER3 and promotes receptor-receptor interactions. HER3 has been considered a “kinase-dead” receptor, because it lacks significant intrinsic kinase activity. Therefore, in order for HER3 to induce cell signalling, it needs to be phosphorylated by its partners; of these, HER2 is the most important (Ma *et al.*, 2014). Moreover, the activation of HER3 by heregulin is dependent on HER2 expression (Li *et al.*, 2013a). HER3 also interacts with other members of the HER family, such as HER1. It has been reported that EGF can activate both HER1 and HER3 at the same time and tyrosine kinase inhibitors are able to block HER1 as well as HER3 and their downstream signalling pathways (Carrasco-García *et al.*, 2011).

Two downstream signalling pathways are activated by HER3. The first is PI3K/Akt/mTOR and activation of PI3K is mediated by heterodimerization between HER3 and HER1/2. PI3K is a protein kinase composed of a P110 catalytic subunit and P85 regulatory subunit. It has been shown that HER3 binds to this P85 regulatory subunit. When PI3K is activated this leads to the accumulation and activation of PDK1/Akt in the cell membrane. Once this pathway is activated by HER3 heterodimerization, this stimulates the downstream signalling responsible for cell growth, cell apoptosis, tumour cell invasion and metastasis and chemotherapy resistance. The second pathway is the Ras/Raf/MEK/mitogen-activated protein kinase (MAPK) pathway that can be activated by HER3. Phosphorylation of HER3 can activate Grb2-SOS, complex leading to activation of Raf, MEK and MAPK. The activation of RAS/RAF/MEK promotes migration and proliferation of the cells as well as the regulation of transcription factors in the nucleus (Vivanco and Sawyers, 2002; Li *et al.*, 2013a).

A study to examine the expression of heregulin and HER3 in prostate cancer using immunohistochemistry found that 72% of cases showed high expression of heregulin, while high expression of HER3 was noticed in 54% of cases. In addition, the high expression of heregulin appears to be related to a high grade of the cancer. However, no correlation between the high expression of HER3 and the grade of cancer was noticed in this study (Leung *et al.*, 1997).

Another study explained how androgen withdrawal might lead to the development of castrate resistance. This study identified HER3 as mediator of increased proliferation during CRPC progression, leading to the release of these cells from cell cycle arrest, which happens because of androgen withdrawal. In addition, this study showed that HER3 is increased in the androgen withdrawal condition and this is caused by negative regulation of HER3 by AR, noticed in androgen dependent cells. This can be explained by the fact that despite AR regulating androgen dependent cell proliferation, it also resists the activation of the androgen independent pathway that mediates cell growth. Androgen withdrawal relieves this suppression by causing an increase in HER3 levels, promoting proliferation and therapy resistance. This suggests that the inability of the AR to downregulate HER3 expression is one cause of CRPC (Chen *et al.*, 2010).

This negative mechanism is explained by the theory that AR can mediate HER3 degradation by regulating the neuregulin receptor degradation protein-1 (Nrdp1). This is

an E3 ubiquitin ligase that targets HER3 and AR, which transcriptionally regulates Nrdp1 expression in the androgen dependent but not CRPC. Nrdp1 is known as a RING finger domain protein that binds to the cytoplasmic tail of HER3 and mediates its degradation (Qiu and Goldberg, 2002; Chen *et al.*, 2010).

Another study has found that HER3 and HER2 have a role in recurrent prostate cancer and heregulin can activate both HER2 and HER3 and downstream pathways, including PI3K/Akt pathways, while also increasing androgen-dependent AR transactivation in this cell line. Furthermore, the dual tyrosine kinase inhibitor GW572016 (Lapatinib) was able to inhibit the phosphorylation of HER2 and HER3, AR transactivation and cell proliferation induced by heregulin (Gregory *et al.*, 2005; Perner *et al.*, 2015).

It has been shown that HER2/HER3 heterodimers lead to aberrant activation of AR, contributing to the development of hormone resistant prostate cancer. Moreover, it was demonstrated that EBP1, a HER3 binding protein acting as a co-repressor of AR, is decreased in hormone refractory prostate cancer (Mujoo *et al.*, 2014).

Data has suggested that combination therapies directed toward both HER2/
HER3 and the PI3K pathway could have efficacy in prostate malignancy more than targeting individual members of this family, such as EGFR or HER2, which has resulted in limited success in clinical trials (Poovassery *et al.*, 2015).

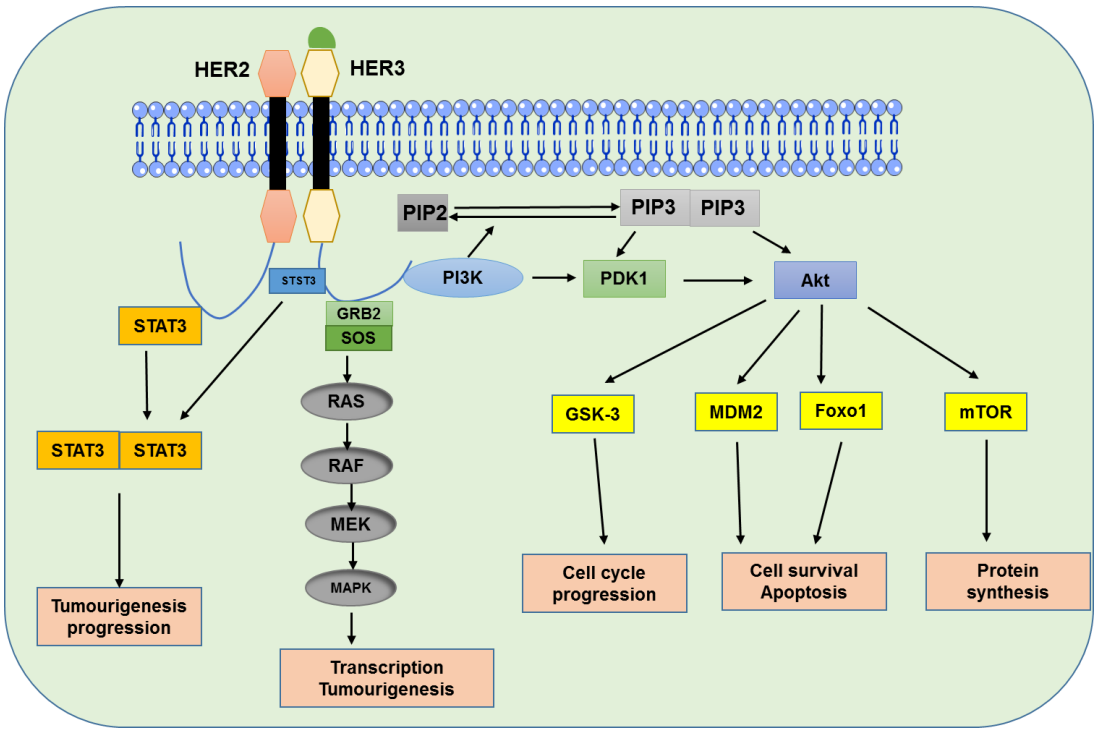

Figure 1-17 HER3 and its downstream signalling pathways, adapted from (Li *et al.*, 2013a)

The downstream signalling pathways include the PI3K/PDK1/AKT and the Ras/Raf/MEK/MAPK pathways. HER3, human epidermal growth factor receptor-3; MAPK, mitogen-activated protein kinase.

Erbb4/HER4

ErbB4 is mainly related to the Ras-MAPK and PI3K-Akt pathways, with ErbB4 phosphorylation promoting activation of the Ras-MAPK pathway, leading to cell cycle arrest and differentiation. Similarly to other members of the HER family, when HER4 is phosphorylated with a HER partner, the signal is translocated into the nucleus and acts as a transcriptional factor (Iwakura and Nawa, 2013).

HER4 is expressed in 20% of breast cancer; however, a few studies have investigated the role of HER4 in prostate cancer. One study reported that levels of HER4 do not change in the transition from hormone-sensitive to hormone-refractory prostate cells. However, high levels of HER4 in hormone-refractory tumours have been linked to improved patient survival (Edwards *et al.*, 2006).

1.11 Targeting the EGFR family in prostate cancer

Trastuzumab was the first drug used to target the HER2 receptor in breast cancer. The mechanism of action of this monoclonal immunoglobulin G antibody is its binding specificity to the extracellular domain of HER2 receptor and subsequent inhibition of its activity. It has been shown that the administration of Trastuzumab alone and in combination with Paclitaxel, significantly inhibits the growth of breast cancer that showed overexpressing of the HER2 gene (Goldenberg, 1999).

Cetuximab (C225) is another HER family inhibitor that shows promising results in prostate cancer. Cetuximab is an anti-EGFR monoclonal antibody that blocks the ligand binding to EGFR, resulting in the prevention of EGFR transfer and tyrosine kinase activation. It has been shown that Cetuximab inhibits prostate cancer cell proliferation and induces cell apoptosis. However, these results were noticed only in a cell line with high EFGR expression (Du145 and A431 cells), but no effect was noticed in a cell line with a low level of EGFR (PC3) (Dhupkar *et al.*, 2010).

Gefitinib and Erlotinib have shown some efficiency in clinical trials in patients with CRPC. Pertuzumab, a monoclonal antibody is used to prevent HER2 heterodimerization with other HER family members, rather than obstructing the HER2 ligand binding domain itself. According to a preclinical study, the growth of CRPC xenografts was inhibited by the use of Pertuzumab, while Trastuzumab used in the same study showed minimal effectiveness in preventing CRPC xenograft growth (K Jathal *et al.*, 2011).

The HER3 antibody MM-121 was tested in a variety of cancer and xenograft models (lung, renal, gastric, breast and ovarian) and showed effective results. MM-121 was used to block ligand binding to HER3, or the activation induced by EGFR and HER2. However, this antibody yielded poor results in prostate cancer cell lines with amplified HER2 gene, perhaps because these cells are ligand-independent, not ligand-dependent (Schoeberl *et al.*, 2010).

Recently, AZD8931 has been identified as a novel small molecule inhibitor of EGFR, HER2 and HER3 signalling, showing significant inhibition with apoptosis induction in overexpressed EGFR and HER2 breast cancer cell models (Mu *et al.*, 2014).

The effect of AZD8931 on the prostate cancer was identified by Rao (2015), who reported that AZD8931 was able to reduce cellular proliferation and colony forming of the studied prostate cancer cell lines. In addition, AZD8931 reduces HER2 and HER3 translocation to the nucleus and reduces their activity in the cellular and nuclear compartments. Moreover, knockdown of HER2 and HER3 using siRNA showed a similar effect to that of AZD8931 on the prostate cancer cells. Also, AZD8931 reduced AR activity in a cloned HER3 overexpressing cell line.

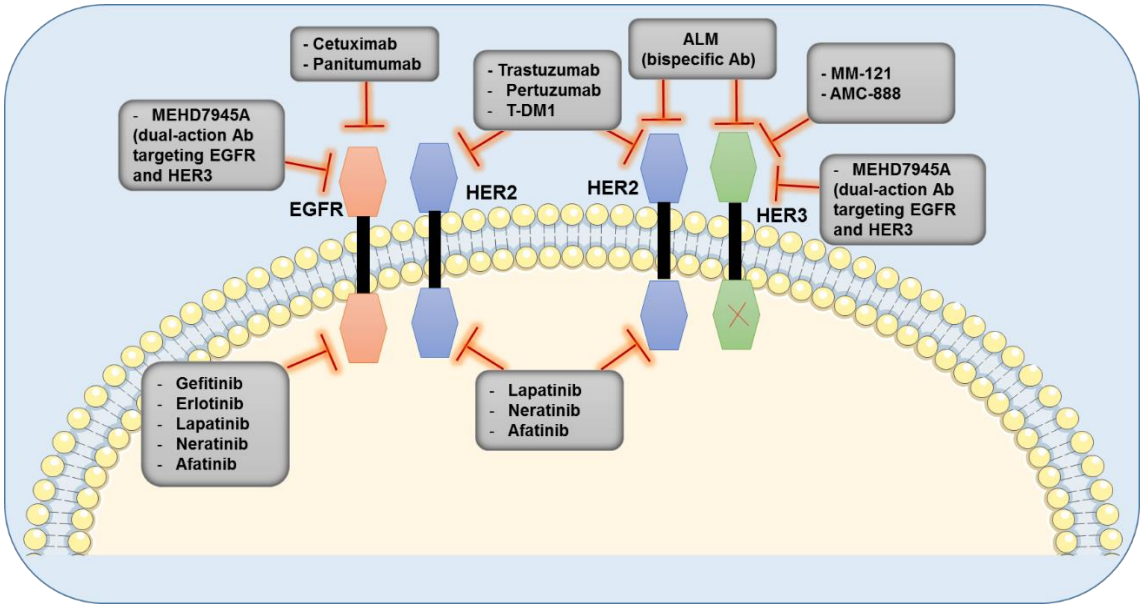

Figure 1-18 Antibodies and small molecules interfering with HER family signalling, adapted from (Yarden and Pines, 2012)

Erlotinib and Gefitinib are tyrosine kinase inhibitors (TKIs) which target the epidermal growth factor receptor (EGFR). **Lapatinib, Neratinib and Afatinib** are dual-specificity inhibitors, which target both EGFR and HER2. **Trastuzumab, T-DM1 and Panitumumab** are monoclonal antibodies that are able to bind HER2. **MM-121 and AMG-888** are antibodies that target HER3. **ALM** is a dual-action antibody able to bind HER3 in combination with HER2. **MEHD7945A** is dual action antibody able to bind HER3 in combination with either HER2, or EGFR.

1.12 Aims of this study

- Identify the role of the HER2 and HER3 in CRPC models.
- Explore novel signalling pathways activated through HER2 and HER3, in CRPC models
- Study the phenotypic and genotypic differences between the LNCaP-enzalutamide resistant cell line and the parental LNCaP cell line
- Investigate the role of SGK1, a target identified from microarray data, comparing LNCaP-enzalutamide resistant cell line and LNCaP parental line
- Investigate the role of TROP-2, a target identified from microarray data, comparing LNCaP-enzalutamide resistant cell line and LNCaP parental line.

Chapter 2. Materials & Methods

2.1 Materials and Reagents

Chemicals that are used in the lab were either analytical or molecular biology grade, unless stated otherwise. These chemicals were purchased from Merck Biosciences (Nottingham, UK), VWR International (Leicestershire, UK) and Sigma-Aldrich (Dorset, UK). Oligonucleotide primers were designed by National Centre for Biotechnology Information NCBI (http://www.ncbi.nlm.nih.gov/), purchased from Sigma-Aldrich (Dorset, UK) and diluted with sterile distilled water to 1µg/µl as a final stock concentration. Plastic-ware used in tissue culture was purchased from Corning (Surrey, UK) and Becton Dickinson (BD, Oxford, UK).

2.1.1 Compounds

Heregulin-β1

Heregulin was purchased from (R&D Systems). The stock concentration was 1µg/ml in sterile PBS and aliquots were stored at -80ºC. Working concentration was 20ng/ml.

Dihydrotestosterone (DHT)

DHT (Sigma Aldrich) stock concentration was 10mM in ethanol and aliquots were stored at -80ºC. Working stock was diluted to 1:1000 in basal medium, to achieve a 10µM stock.

Dexamethasone (DEX)

DEX was purchased from (Sigma Aldrich) at 1mg/ml stock concentration, dissolved in ethanol and was stored at -80ºC.

Lapatinib

N-{3-Chloro-4-[(3-fluoro benzyloxy]phenyl}-6-[5-({[2-methylsulfonyl)ethyl]amino}methyl)-2-furyl]-4-chinazolinamin (Lapatinib) was purchased from Selleck Chemicals. Stocks of 30mM concentration were made in DMSO and stored at -20 ºC.

AZD8931

The pan-HER inhibitor, AZD8931, was supplied by AstraZeneca. Endotoxin free DMSO was used to make 30mM working stocks and stored at -80ºC.

Casodex

N-[4-cyano-3-(trifluoromethyl) phenyl]-3-[(4-fluorophenyl) sulfonyl]-2-hydroxy-2-methylpropanamide (bicalutamide) or Casodex was supplied by AstraZeneca. Endotoxin free DMSO was used to make 20mM working stocks and stored at -80ºC.

ARN509

Benzamide,4-[7-[6-cyano-5-(trifluoromethyl)-3-pyridinyl]-8-oxo-6-thioxo-5, 7-diazaspiro [3.4]oct-5-yl]-2-fluoro-N-methyl (ARN509) is an AR antagonist which was purchased from Selleck Chemicals. DMSO was used to make stock at 30mM concentration and stored at -20ºC.

Enzalutamide

4-(3-(4-Cyano-3-(trifluoromethyl) phenyl)-5, 5-dimethyl-4-oxo-2-thioxoimidazolidin-1-yl)-2-fluoro-N-methylbenzamide (enzalutamide) was purchased from Selleck Chemicals. Endotoxin free DMSO was used to make 30mM stock concentration and stored at -80ºC.

GSK650395

GSK650395 was kindly obtained from Dr. Luke Gaughan (Newcastle University). GSK650395 was purchased from Selleck Chemicals. Stocks of 20mM concentration were made in DMSO and stored at -20ºC.

2.2 General Methodology

2.2.1 Mammalian Cell Culture

2.2.1.1 Cell lines

All cell lines used in this study were purchased from the American Type Culture Collection (Manassas, VA, USA). Parental LNCaP cell line used in the project was authenticated by RNAseq and cell morphology.

LNCaP: The androgen sensitive LNCaP cell line (Lymph Node Carcinoma of the Prostate) is a model of androgen dependent prostate cancer, derived from a left supraclavicular lymph node prostate carcinoma metastasis from a 50 years old patient, in 1977 (Horoszewicz *et al.*, 1980).

LNCaP-CDX-R: LNCaP-Casodex resistant (LNCaP-CDX-R) is a subclone of LNCaP that was derived by serial passage in the presence of an escalating dose of Casodex. LNCaP-CDX-R were maintained in full media + 10μM Casodex. LNCaP-CDX-R cells are used as a model of resistance to the first generation of anti-androgen.

LNCaP-ENZ-R: LNCaP- enzalutamide (MDV3100) resistant (LNCaP-ENZ-R), is a subclone of LNCaP that was derived by serial passage in the presence of an escalating dose of enzalutamide. LNCaP-ENZ-R cells were maintained in full media + 10μM enzalutamide. LNCaP-ENZ-R cells are used as a model of resistance for this next generation anti-androgen.

LNCaP-ARN-R: LNCaP-ARN509 resistant (LNCaP-ARN-R) is a subclone of LNCaP that was derived by serial passage in the presence of an escalating dose of ARN509. LNCaP-ARN-R cells were maintained in full media + 10μM ARN509. LNCaP-ARN-R cells are used as a model of resistance for this next generation anti-androgen.

LNCaP-7B7: This cell line was kindly obtained from Jan Trapman (Erasmus Medical Centre, Netherlands). The LNCaP-7B7 cell line was established by transfecting the LNCaP cell line with a pPSA luciferase reporter. In this cell line, AR transcriptional activity can be detected in an androgen-dependent manner by utilising luciferase assay.

LNCaP-AI-7B7: This cell line was a kindly made available by Dr. Scott Walker. The LNCaP-AI-7B7 cell line was established by transfecting the LNCaP-AI cell line with a pPSA luciferase reporter. In this cell line, AR transcriptional activity can be detected in an androgen-independent manner by utilising luciferase assay.

2.2.1.2 Cell Passaging

LNCaP cells were maintained in full medium (Huffman *et al.*, 2005) (RPMI 1640 medium containing HEPES buffer (25mM)), 10% foetal calf serum (FCS) and L-Glutamine (20mM), at 37°C in a humidified atmosphere of 5% CO_2.

LNCaP-CDX-R cells were maintained in full medium (Huffman *et al.*, 2005) (RPMI 1640 medium containing HEPES buffer (25mM)), 10% foetal calf serum (FCS) and L-Glutamine (20mM) and 10μM of Casodex, at 37°C in a humidified atmosphere of 5% CO_2.

LNCaP-ENZ-R cells were maintained in full medium (Huffman *et al.*, 2005) (RPMI 1640 medium containing HEPES buffer (25mM)), 10% foetal calf serum (FCS) and L-Glutamine (20mM) and10μM of enzalutamide, at 37°C in a humidified atmosphere of 5% CO_2.

LNCaP-ARN-R cells were maintained in full medium (Huffman *et al.*, 2005) (RPMI 1640 medium containing HEPES buffer (25mM)), 10% foetal calf serum (FCS) and L-Glutamine (20mM) and 10μM of ARN509, at 37°C in a humidified atmosphere of 5% CO_2.

LNCaP-7B7 cells were maintained in full medium (Huffman *et al.*, 2005) (RPMI 1640 medium containing HEPES buffer (25mM)), 10% foetal calf serum (FCS) and L-Glutamine (20mM), at 37°C in a humidified atmosphere of 5% CO_2.

LNCaP-AI-7B7 cells were grown in steroid depleted medium (SDM) (RPMI 1640 10% charcoal treated FCS and L-Glutamine (20mM), at 37°C in a humidified atmosphere of 5% CO_2.

All cell lines were passaged every 3-5 days. Medium was aspirated under sterile conditions and the cells were then washed with sterile phosphate buffered saline (PBS). Cells were then trypsinised (1X trypsin/ EDTA) for 3-5 minutes at 37°C, followed by

neutralisation by the addition of the appropriate medium (FM, SDM), according to the cell line. Cells were then transferred to a new flask and incubated at 37°C in a humidified atmosphere of 5% CO_2.

2.2.1.3 Cryopreservation of cell lines

Cell lines were routinely cryopreserved for storage. After trypsinisation, the cells were pelleted by centrifugation at 400g for 5 min, followed by aspiration of all the supernatant. The cell pellet was re-suspended with 1ml of freezing medium (80% FM, 10% FCS, 10% dimethyl sulfoxide (DMSO)) at 2-5 x 10^6 cells/ml. Cells were then frozen at -80°C in cryovials. For re-culturing, the cells were defrosted at 37 °C and transferred gently into fresh 10ml of respective growth medium, followed by centrifugation at 400g for 5 minutes to create a cell pellet. The supernatant containing the remaining DMSO was then aspirated and the pellet was re-suspended in 10 ml of the respective medium, transferred to a new flask and incubated at 37°C.

2.2.1.4 Cell growth

An IncuCyte ZOOM live-cell imager (Essen Bioscience) was used to assess cell growth by cell counting. The IncuCyte® live-cell imaging and analysis system permits real-time, automated cell proliferation assays within a tissue culture incubator. Cell proliferation was observed by analysing the percentage of confluence of cells over time. For this assay, cells were grown in 96-well plates (2000 cell/well for LNCaP and LNCaP-ENZ-R cells) with 6 replicates /plate and incubated in the IncuCyte for 168 hours, with 2 hours interval scan. Data were presented as the average fold difference in confluence relative to the control from three independent experiments.

2.2.1.5 Cell counts

Cells were seeded at the required density in a 6-well plate and treated with appropriate drugs, depending on the experiment. After 72 hours, the cells were pelleted and re-suspended in 1ml of medium. 10µl of the suspension was stained with Trypan blue and the number of cells were counted by a haemocytometer. Only cells that were not stained were counted, as Trypan blue interacts only with dead cells, giving a blue stain.

2.2.2 Wound healing assay

Wound healing assay is one technique used to study cell direction and migration. This method is based on creating a wound on a cell monolayer and cell direction was observed

by capturing images at the beginning and at regular intervals during cell migration. Cells were seeded out on a 6-well plate and the wound was created manually by using a 20µl pipette tip. The cells were then washed with PBS to remove detached cells and replaced with fresh medium. Three images were taken for each well by using microscopy at 0, 6, 24 and 48 hours. The images were analysed using ImageJ software by grading each image between 20 lines and calculating the width between the wound edges. The data was analysed by taking the average of each image and comparing it to different time points within the same condition. The data was normalized to the zero-time point.

2.2.3 Gene expression analysis

2.2.3.1 RNA isolation

All techniques were carried out under RNase free conditions using filter tips (Axygen) and by using Diethylpyrocarbonate (DEPC) treated water in all the required solutions. Trizol® reagent (Invitrogen) is a monophasic solution of phenol and guanidine isothiocyanate, which maintains RNA integrity whilst lysing cells and was used to isolate RNA from cells. Adherent cells were washed with 1X PBS and then Trizol® (500µl) was added and incubated at room temperature for 5 minutes following the manufacturer's protocol. Chloroform (200µl) was then added followed by centrifugation at 12000g for 15 minutes to separate the aqueous phase, which exclusively contains the RNA. The aqueous phase was collected and Isopropanol (500µl) was added to precipitate the RNA, during a 10 minute incubation at room temperature. The precipitated RNA was then pelleted by centrifugation at 12000g for 15 minutes at 4 °C. Following a washing step with 500µl of 75 % ethanol and centrifugation at 7500g for 5 minutes, the RNA pellet was re-suspended in an appropriate volume of DEPC treated water. Another method for RNA isolation was also performed by using RNeasy Mini Kit QIAGEN® for purification of total RNA from animal cells, animal tissues and bacteria. RNeasy's procedure represents a well-established technology for RNA purification. This technology combines the selective binding properties of a silica-based membrane with the speed of microspin technology. A specialized high-salt buffer system allows up to 100µg of RNA longer than 200 bases to bind to the RNeasy silica membrane. After cells were trypsinized and collected, 350µl of RLT buffer (supplied) was added to lyse the cells. The lysate was then transferred into a QIAshredder spin column (supplied) placed in a 2ml collection tube (supplied) and centrifuged for 2 minutes ≥8000g. One volume of 70% ethanol was

added to the homogenized lysate, mixed well by pipetting, then immediately transferred to an RNeasy spin column placed in a 2 ml collection tube (supplied) and centrifuged for 15 second at ≥8000g. 700µl Buffer RW1 (supplied) was added to the RNeasy spin column and centrifuged for 15 second at ≥8000g to wash the spin column membrane. 500µl Buffer RPE (supplied) was added to the RNeasy spin column and centrifuged for 15 second at ≥8000g to wash the spin column membrane. Again, 500µl Buffer RPE was added to the RNeasy spin column and centrifuged for 2 minutes at ≥8000g to wash the spin column membrane. Finally, the RNeasy spin column was placed in a new 1.5 ml collection tube (supplied) and 30µl RNase-free water (supplied) was added directly to the spin column membrane and centrifuged for 1 minute at ≥8000 x g to elute the RNA. The concentration and purity of RNA was measured using a NanoDrop® ND-1000 UV-Vis Spectrophotometer (Labtech, East Sussex, UK). The concentration of the sample is calculated by the program using Beer's law and the integrity of the sample was assessed by the 260/280 ratio (the ratio of absorbance at 260 nm and 280 nm). Optimal 260/280 ratio for RNA is 2.0.

2.2.4 Reverse transcription

A Moloney Murine Leukaemia virus (MMLV) reverse transcriptase system (Promega, Madison, USA) was used for cDNA preparation. Complementary DNA (cDNA) was prepared by diluting 1µg of RNA in the required volume of DEPC water to a final volume of 12.7µl. RNA was incubated at 65°C for 5 minutes to denature the secondary structure of RNA. A master mix of MMLV was prepared, containing 4µl of 5 X reverse transcriptase (RT) MMLV Buffer, 2µl of 4mM dNTPs (dGTP, dATP, dCTP and dTTP) (Bioline, London, UK), 1µl of 5µM oligo $(dT)_{16}$ and 0.3µl of MMLV reverse transcriptase enzyme. MMLV master mix was added to each sample to make up a final volume of 20µl and mixed well by vortex. Samples were incubated at 37°C for 1 hour, followed by incubation at 100°C for 5 minutes and then transferred immediately to ice to inactivate the MMLV-RT enzyme. The cDNA was then stored at -20°C until required.

2.2.5 Quantitative real time polymerase chain reaction (QRT-PCR)

Following reverse transcription, standard cDNA, known to express the transcript of interest, was used to quantify relative amounts of cDNA produced in the PCR reactions. A fluorescent reporter (SyBr Green) was used to detect the amount of DNA template in

the samples. SyBr Green intercalates with the DNA by binding to the minor groove of the double helix. Upon binding, SyBr Green fluorescence is enhanced significantly, which makes it easier to be detected by real time PCR thermocycling. A 5µl reaction master mix was prepared (2µl of diluted cDNA, 2.5µl of Platinum® SYBR® Green qPCR SuperMix-UDG plus ROX (Invitrogen, New York, USA), 0.2µl forward and 0.2µl reverse primer and 0.1µl sterile distilled water) and loaded into a 384-well plate.

For the standard curve, sample cDNAs were diluted in sterile H_2O prior to use. Seven dilutions ranging from 1- 0.0005 were used. The same sterile H_2O used for cDNA dilution was loaded first on the plate as non-template control, followed by master mix loading, standard curve dilutions and finally the tested samples. Samples were run in triplicate on each plate. The plate was then sealed with a clear plastic cover and ran under the following PCR conditions: denaturation of 40 cycles at 95 °C for 15 seconds followed by annealing at 60°C for 1 minute and finally dissociation at 95 °C for 15 seconds, 60°C for 15 seconds and 95°C for 15 seconds. Hypoxanthine phosphoribosyl transferase 1 (HPRT1) was used as a housekeeping gene to normalise expression levels. HPRT1 was validated with standard curve in different concentration ranging from 1- 0.0005. Also our research group validate it in response to different treatment and it showed consistence results. The absolute quantification method was used on an ABI 7900 sequence detection system (Applied Biosystems, UK) according to the manufacturers' instructions. A single peak in the resultant dissociation curve indicates the production of single product. Results were analysed using SDS 2.2 software (Applied Biosystems, Warrington).

Genes	Forward Primer (5'-3')	Reverse Primer (5'-3')
PSA	TCGGCACAGCCTGTTTCAT	TGGCTGACCTGAAATACCTGG
KLK2	AGCATCGAACCAGAGGAGTTCT	TGGAGGCTCACACACTGAAGA
HPRT1	TTGCTTTCCTTGGTCAGGCA	AGCTTGCGACCTTGACCATCT
HER2	CACCACCATGGAGCTGGCGG	CATTGGCACGTCCAGACC
HER3	CACCGTCATGGGGGCGAA	CGTTCTCTGGGCATTA
RLN1	AGAGGCAACCATCATTACCAGA	AAACAGTGCCACGTAGGGTC
TACSTD2	CATCAAGGGCGAGTCTCTATTC	CCCGACTTTCTCCGGTTGG
SYT4	ATGGGATACCCTACACCCAAAT	TCCCGAGAGAGGAATTAGAACTT
RLN2	ATTGCCATTTGCGGCATGAG	CACAATTTGGAAAGGGCACCA
SGK1	GAGATTGGCCGTATCCCACC	GATGGAGAATCTAGCGGGGC
GRα	CTATGCATGAAGTGGTTGAAAA	TTTCAGCTAACATCTCGGG
FKBP5	GCAACCAGAAATCCACCTG	CTCCAGAGCTTTTG
TMPRSS2	CTGCTGGATTTCCGGGTG	TTCTGAGGTCTTCCCTTTCTCCT
c-Myc	CACAGCAAACCTCCTCACAGC	GGAGACGTGGCACCTCTTGA

Table 2-2-1 Primers used for QRT-PC

2.2.6 Agilent Bio-analyzer 2100

Total RNA was extracted from parental LNCaP and LNCaP-ENZ-R with or without enzalutamide for 48 hours cells using RNeasy Mini Kit detailed in Chapter 2.2.1. The integrity and purity of total RNA were assessed using Agilent Bioanalyzer 2100.

2.2.7 Illumina Human HT-12 arrays

The Human HT-12 v4.0 Expression BeadChip has 47,312 probes. The array reports probe intensity levels which represents the level of expression of a gene against which a particular probe is targeted. Array processing, normalization and quality control checks were performed using the R package 'Lumi'. Probe intensity values were converted to VSD (variance-stabilized data) using variance-stabilizing transformation. The robust spline normalization (RSN) was used as the array normalization method. Outlier samples, poor quality probes (detection threshold < 0.01) and probes that were not detected at all were removed prior to downstream analysis. The remaining probes (21,111) normalized intensities, VSD were used in the differential expression analysis. Differential expression analysis was performed using the R package 'Limma' and p values were adjusted to control the false discovery rate (FDR) using the Benjamini–Hochberg method.

2.2.8 Protein Expression Analysis

2.2.8.1 Sodium dodecyl sulphate-polyacrylamide gel electrophoresis (SDS-PAGE)

Cell lysates were generated with the addition of RIPA buffer (150mM NaCl pH 7.5; 50mM Tris-HCl pH 7.5 (Fisher Scientific); 1% NP40 (BDH Chemicals); 1mM EDTA; 0.25% sodium deoxycholate. Cells were washed with chilled PBS and lysed in RIPA buffer for 30 minutes at 4ºC, after which the samples were sonicated for 5 minutes and cell debris was pelleted by centrifugation at 12,000g at 4ºC for 10 minutes. The supernatant (whole cell lysate) was then used for further analysis. Protein concentration was estimated by using Qubit™ protein assay Kits for use with the Qubit™ 3.0 Fluorometer (Thermo Fisher Scientific). The kits provide concentrated assay reagent (200X concentrate in 1, 2-propanediol) and dilution buffer. Qubit™ working solution was made by diluting Qubit™ protein reagent 1:200 in Qubit™ protein buffer by using a clean plastic tube. 1µl of protein sample + 199µl of working solution were mixed in the

Qubit™ assay tubes (Cat. no. Q32856) and incubated for 15 minutes in a dark place. The samples were placed in to Qubit™ 3.0 Fluorometer (Thermo Fisher Scientific) to give the protein concentration in mg/ml. Equal amounts of protein were added to appropriate amounts of 5X SDS sample buffer (250mM Tris-HCl pH6.8; 10% SDS; 30% glycerol (Fisher Scientific), 5% β-mercaptoethanol, 0.02% bromophenol blue (Sigma Aldrich) and analysed using western blotting.

Polyacrylamide gels were prepared by pouring a 12% resolving gel (0.375M Tris-HCl, pH 8.8, 0.1% SDS, 12% acrylamide:bisacrylamide mix, 1% ammonium persulfate (APS) and 0.1% N,N,N′,N′-Tetramethylethylenediamine (TEMED)) under a 6% stacking gel (0.125M Tris-HCL, pH 6.8, 0.1% SDS, 6% acrylamide:bisacrylamide mix, 1% APS and 0.1% TEMED) Protein lysates (10-15µl) were loaded alongside the Spectra™ Multicolour Broad Range Protein Ladder (Thermo Fisher Scientific) as a molecular weight reference. Samples were then resolved in reservoir buffer (25mM Tris-HCl, 190mM glycine, 0.1% SDS) at 200 V for 45-60 minutes.

2.2.8.2 Western blotting

Following SDS-PAGE electrophoresis, the protein was then transferred onto a Hybond C membrane (GE Healthcare, Wisconsin, USA) by electrophoresis in transfer buffer (25mM Tris-HCl, pH 8.3; 0.15M glycine, 10% methanol) for 1 hour at 200 volts, or overnight at 30 volts. Membranes were blocked in 5% non-fat powdered Marvel™ milk in Tris- buffered saline (TBS-20mM Tris-HCl, 500mM NaCl) to block nonspecific antibody binding for an hour, followed by washing with 0.001% Tween TBS (TTBS) for 10 minutes. The membrane was probed with the appropriate primary antibody overnight at 4°C then washed with TTBS twice for 5 minutes and probed with the horseradish peroxidase HRP-conjugated secondary antibody at room temperature, for 1 hour (Table 2.1). The antibodies were diluted according to optimized conditions in 1% (w/v) Marvel™ diluent. α tubulin was used as a loading control. ECL reagents (1:1 from reagent 1 and 2) were then spread over the membrane and incubated for 1 minute (GE Healthcare), before being exposed to X-ray film (Fuji Film) for an appropriate length of time, before development using an automated MediPhot 937 developer.

Antibody Target	**Species**	**Company/Cat No**	**Ig Type**	**Dilution**	**Incubation time**
HER2	Rabbit	Cell Signalling (D8F12)/#4290	Monoclonal	1:1000	Overnight at 4ºC
Phospho-HER2	Rabbit	Cell Signalling Tyr 1221/1222(6B12)/#2243	Monoclonal	1:1000	Overnight at 4ºC
HER3	Rabbit	Cell Signalling (D22C5)/#12708	Monoclonal	1:1000	Overnight at 4ºC
Phospho-HER3	Rabbit	Cell Signalling (Tyr1289) (21D3)/# 4791	Monoclonal	1:1000	Overnight at 4ºC
Phospho-HER3	Rabbit	Cell Signalling (Tyr1289) (21D3)/# 4791	Monoclonal	1:1000	Overnight at 4ºC
AKT 1/2	Rabbit	Santa Cruz sc-1619	Polyclonal	1:1000	Overnight at 4ºC
Phospho- AKT 1/2/3 (Ser 473)	Rabbit	Santa Cruz sc-7985	Polyclonal	1:1000	Overnight at 4ºC
ERK 1/2	Mouse	Santa Cruz sc-135900	Monoclonal	1:500	Overnight at 4ºC
α – tubulin	Mouse	Sigma Aldrich T 9026	Monoclonal	1:2000	Overnight at 4ºC

ERK5	Rabbit	Cell Signalling #3372S	Polyclonal	1:1000	Overnight at 4ºC
Phospho – ERK5 (Thr218/ Tyr220)	Rabbit	Cell Signalling #3371S	Monoclonal	1:1000	Overnight at 4ºC
SGK1	Rabbit	Sigma Aldrich # S 5188	Polyclonal	1:1000	Overnight at 4ºC
Phosph-SGK1 (Ser422)	Rabbit	Santa Cruz sc-16745	Polyclonal	1:1000	Overnight at 4ºC
GRα	Rabbit	Santa Cruz sc-1002	Polyclonal	1:1000	Overnight at 4ºC
TROP-2	Goat	R&D Systems Bio-techne Brand # AF650	Polyclonal	1:1000	Overnight at 4ºC
P27	Rabbit	Santa Cruz # sc-528	Polyclonal	1:1000	Overnight at 4ºC
Myc	Mouse	Cell Signalling #2276	monoclonal	1:1000	Overnight at 4ºC

Table 2-2-2 Primary antibodies used for Western Blotting

Antibody	Species	Company/Cat No
HRP-conjugated Rabbit anti-mouse	Mouse polyclonal	DakoCytomation (P0260)
HRP- conjugated Swine anti-Rabbit	Rabbit polyclonal	DakoCytomation (P0217)

Table 2-2-3 Secondary antibodies used for Western Blotting

2.2.9 siRNA oligo design to mediated gene knockdown

siRNA oligos were generated using Tuschl's rules of design and cross-checked using Invitrogen Block-iT RNAi designer. siRNA sequences were also blasted against EST libraries (NCBI database) to ensure specificity. siRNA oligos were ordered dry from Sigma Aldrich and resuspended in sterile dH_2O upon arrival to a concentration of 50μM. Aliquots were made (20-50μl, depending on yield) and stored at -20^{o}C. As a negative control, non-targeting siRNA, termed scrambled siRNA, was used (catalogue number 1022076, Qiagen). siRNA sense and anti-sense strand sequences:

siRNA	Sense sequence	Anti-sense sequence
Non-silencing (N/S) (1022076) (Qiagen)	UUCUCCGAACGUGUCACGU	ACGUGACACGUUCGGAGAA
TROP2 #1	CGUGGACAACGAUGGCCUCUA	UAGAGGCCAUCGUUGUCCACG
TROP2 #2	GCACGCUCAUCUAUUACCU	AGGUAAUAGAUGAGCGUGC
TROP2 #3	GCCUGAACGCAGUUUGGAU	AUCCAAACUGCGUUCAGGC
GR #1	GAGUAUGGUUGGAGCCUAAUU	AAUUAGGCUCCAACCAUACUC
GR #2	CGUGUGAAGAUGAGUGAAAUU	AAUUUCACUCAUCUUCACACG

Table 2-2-4 siRNA sequences used for mRNA knockdown

Reverse transfection with siRNAs against TROP2 or GR and /or non-silencing were used to knockdown these proteins. siRNA, basal medium and lipofectamine RNAi Max (Life Technologies) were mixed into 1.7ml Eppendorf tubes (Axygen) to give a final concentration of 25nM/well. The cocktail was added to the 6 well plate after gentle mixing and incubated for 30 minutes. This was followed by seeding out 150,000 cell/ml of LNCaP and LNCaP-ENZ-R cells in full media into each well, then the cells along with the siRNA were incubated for 72 hours.

2.2.10 Immunohistochemistry

2.2.10.1 Human tissue samples

A database of patients diagnosed with prostate cancer was generated from the Freeman Hospital, Newcastle upon Tyne, database. An anonymized database was used which included the following sample information: clinic-pathological data (e.g. age at diagnosis, PSA values, TNM stage, Gleason grade), plus hormone manipulation, demographic data and other treatment modalities. Gleason grade, presence of HGPIN and BPH was confirmed by Dr. Mathers, Uropathologist, RVI, Newcastle upon Tyne.

2.2.10.2 Methodology

Tissue microarrays (TMAs) were generated within the STTD laboratory and were used in immunohistochemical analysis of protein expression in different patient samples that includes BPH and different grades of prostate cancer (Gnanapragasam *et al.*, 2006).

The TMA samples were deparaffinised in xylene for 5 minutes and rehydrated through a series of ethanol concentrations (99%, 99%, 95%, 70% and 50%) followed by washing in distilled water. Antigen retrieval was performed by incubating the TMA slides in 0.01M sodium citrate buffer pH 6 using a decloaker (Menapath). To block endogenous peroxide activity, the TMA slide was treated with 3% hydrogen peroxide for 10 minutes, followed by washing under running tap water for 5 minutes. The area around the cores were determined by using a hydrophobic PAP pen (Dako) and unspecific binding was blocked using 0.5% of BSA for 1-20 minutes depending on the antibody. The TMA slides were incubated in primary antibody overnight at 4ºC. The TMA slides were then washed twice with TTBS (Tris buffered saline – Tween 20) for 5 minutes, followed by incubation in secondary antibody for 30 minutes (Table 2-5) and Washed under running water for 5 minutes. The TMA slides were then incubated in DAB (Diaminobenzidine tetrahydrochloride) for 5 minutes, followed by a wash in tap water for 5 minutes. The slides were then stained with Harris Haematoxylin for 15 seconds, immediately washed with tap water and treated with Scott's tap water for 30 seconds. Finally, the TMA slides were dehydrated in a series of ethanol concentration (50%, 70%, 95%, 99% and 99%) followed by 5 minute xylene treatment and mounted in DPX.

Target	Primary Antibody	Secondary Antibody
TROP-2	1:150 in 0.5% BSA in PBS as diluent overnight incubation R&D System Bio-Techne Brand # AF650 Polyclonal Goat IgG	1:250 0.5% BSA in PBS as diluent of HRP-conjugated Swine anti-Goat DakoCytomation
SGK1	1:60000 in 0.5% BSA in PBS as diluent overnight incubation Rabbit poly clonal Sigma Aldrich # S 5188	ImmPRESS™ HRP Anti-Rabbit IgG (Peroxidase) Polymer Detection Kit

Table 2-2-5 Primary and secondary antibodies used in IHC

2.2.10.3 Scoring

After TMA staining, all slides were scanned using the online digital scanner Aperio® and scored by two independent observers for nuclear and cytoplasmic staining, using a histoscore method, also known as H-score. This method considers the intensity of the stained proteins and the percentage of cells with the same intensity of staining across the sample.

The score is calculated by using the formula:

$Histoscore$= (1 x % $cells\ with\ weak\ staining$) + (2 x % $cells\ with\ moderate\ staining$) + (3 x % $cells\ with\ strong\ staining$).

This method has been well established (Kirkegaard *et al.*, 2006; Ahmad *et al.*, 2011) and is useful for scoring heterogeneous staining of samples. It provides a maximum score of 300 (100% cells with strong staining) and a minimum of 0 (100% cells with no staining), which makes the data quantifiable.

2.2.11 Flow cytometry

Flow cytometry can be used to measure multiple features of individual cells that are flowing in a single file in a stream of fluid through an illumination and light detection system. Light scattering at different angles can distinguish differences in size and internal complexity, whereas light emitted from fluorescently labelled antibodies can identify a wide array of cell surface and cytoplasmic antigens (Brown and Wittwer, 2000).

2.2.12 Cell harvesting for fluorescence-activated cell sorting (FACS) analysis

Cells were harvested for DNA staining. Firstly, media from the wells was collected in a FACS tube (BD biosciences). Cells were then washed with 500µl PBS (which was also retained for analysis) then detached from the well with 500µl 1 X trypsin/EDTA. Trypsin was neutralised by adding media to the collected cells and PBS. Cells were then pelleted by centrifugation at 2000 rpm for 5 minutes and re-suspended in 100µl citrate buffer (0.25M sucrose, 40mM sodium citrate, pH 7.6). Cell permeabilization was achieved by using 0.74% TritonX-100, cells were stained with 2.5mg/ml propidium iodide and 100µg/ml RNase. FACScan (BD Biosciences, California, USA) was used to analyse the samples which measures 10,000 events per sample.

Data analysis: Cyflogic software was used for data acquisition and analysis. PI attaching was measured using a BD FACsCalibur, capturing 10,000 events per tube. Cells were gated on Forward Scatter versus Side Scatter to exclude cell debris and FL2-Width versus FL2-Area dot-blot was used to discriminate doublets and to ensure only single cells were examined for cell cycle analysis. Only single cells representing subG1, G1, S and G2/M in a FL2-W vs FL2-A plot.

2.2.13 Luciferase assay

When LNCaP-7B7 cells were used, the cells were starved in SDM for 72 hours prior to heregulin stimulation. However, in LNCaP-AI-7B7 (grown continuously in steroid-depleted media), the cells were not starved. The cells were seeded out in quadruplets per experimental arm, using a 24-well plate and the experiment was carried out accordingly. Once the experiment was completed, the cells were washed with PBS and lysed using 50µl of 1X reporter lysis buffer (Promega) /well. 10µl of lysate from each well was transferred onto an opaque flat-bottomed 96-well plate. The plate was then placed in the automated FLUOstar Omega (BMG Labtech) plate reader where 50µl of Steady-Glo luciferase substrate (Promega) was injected per well, shaken for 5 seconds and the emitted luciferase counts per second was recorded. The data was then normalised to the proliferation data obtained per well using IncuCyte. The average values were then used to interpret the results.

2.2.14 General statistical analysis

Statistical analysis was performed for the obtained data. To overcome the inter-experimental variation, fold changes of individual experimental repeats were compared rather than raw data and for the intra experimental variation, 3 independent experiments were done for each data set. Student's t-test was used for data analysis and p value ≤ 0.05 was significant. For non-parametric data and matched samples, Wilcoxon signed-rank test were used to compare two related samples and p value ≤ 0.05 was considered significant.

Chapter 3. The expression of HER2, HER3 and androgen receptor in parental LNCaP versus castration resistant derivative prostate cancer cell lines

3.1 Introduction

The androgen receptor (AR) is a transcription factor that plays a crucial role in male sexual development and growth of the prostate gland. In addition, AR plays a dominant role in the progression of human prostate cancer. Androgen ablation therapy is primarily used to inhibit tumour cell growth in patients with advanced disease. However, despite chemical or surgical castration, tumour regrowth and symptoms recurrence usually occur following a period of treatment response. A hormone refractory stage of the disease is characterised by an increase in the expression of AR and AR target genes, such as *PSA*, suggesting that the AR pathway remains active during this stage (Isaacs and Isaacs, 2004). A study of differential gene expression between androgen-dependent and androgen-independent PC cell lines found a consistent increase in HER2 protein level in an androgen-independent cell line, compared with an androgen-dependent cell line and further that the forced expression of HER2 in a PC cell line enhanced AR function and activated the AR signalling pathway (Craft *et al.*, 1999).

Neuregulins (HRG) are a family of ligands that activate HER3 to heterodimerize with its partner HER2 to regulate a number of signalling pathways that are associated with maintenance of cell division, proliferation and differentiation (Sithanandam and Anderson, 2008). It was previously suggested that androgen deprivation can promote castration resistant prostate cancer (CRPC) progression by increasing the level of HER3 in androgen-dependent cells, resulting in increased AR transcriptional activity. Additionally, downregulation of HER3 was demonstrated to inhibit the growth of a CRPC cell line (Chen *et al.*, 2010). A study conducted in our group using PC patient tissue samples found an increase in the expression of both HER2 and HER3 in advanced PC and further that the expression level was associated with poor prognosis. Moreover, forced overexpression of HER2 and HER3 led to increased cell proliferation, migration and invasion in the PC3 cell line. AR stability and activity can also be increased through HER2 and HER3 activation (Rao, 2015). However, the role of HER2 and HER3 in CRPC models that have been generated in our lab is unknown and the pathway(s) that can be stimulated through activated HER2 and HER3 in these CRPC models is therefore also unknown.

The aims of this chapter are:

1. To investigate the relationship between AR and HER2 and HER3.
2. To investigate the role of HER2 and HER3 in CRPC models.

3. To investigate the signalling pathway(s) that can be stimulated through HER2 and HER3 activation in CRPC models.

3.2 Results

3.2.1 Validating the activity of HER3 and Akt by heregulin stimulation

A previous study in our laboratory (Rao, 2015) showed an increase in the expression of HER3 in a LNCaP and LNCaP-AI cell lines in response to heregulin stimulation. To validate these results the androgen-dependent LNCaP cell line was used and activated using heregulin at different time points (0, 5, 15, 30 and 60 minutes). The results showed an increase in the level of both pHER3 and pAkt after 5 minutes with maximum activation achieved following 15 minutes stimulation with heregulin (Figure 3-1).

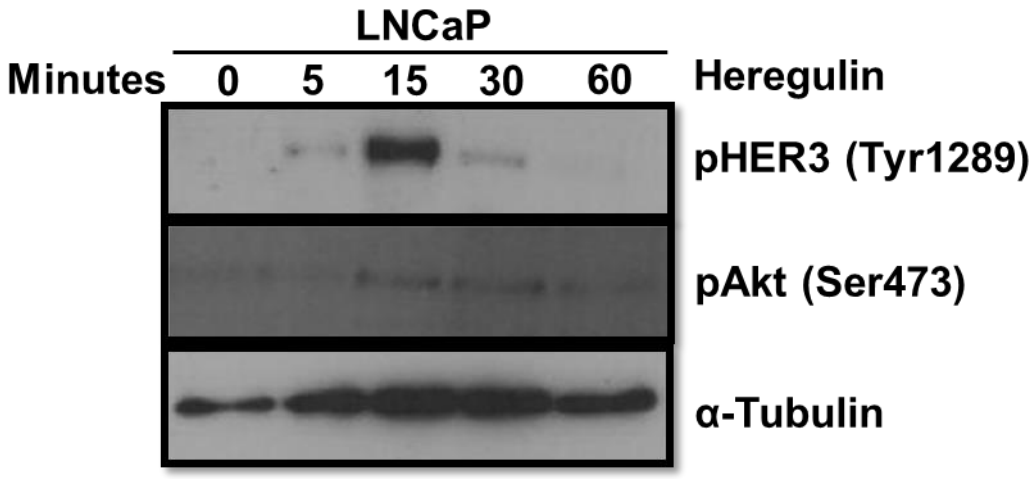

Figure 3-1 Heregulin activates the phosphorylation of HER3 and Akt

LNCaP cell lines was seeded out in 6-well plates in normal growth medium for 24 hours. This was followed by an overnight starvation in basal medium, then cells were activated with 20ng/ml of heregulin for 0, 5, 15, 30 and 60 minutes. DMSO was used as a vehicle control. Lysates were collected in a RIPA buffer and pHER3, pAkt protein level were detected by western blotting. Alpha-tubulin was used as a loading control (representative blot).

3.2.2 Anti-androgen treatment increases the expression of HER2/3 in the LNCaP cell line

It has been previously suggested that HER2/HER3 signalling increases AR stability and enhances its binding to the promoter region of AR target genes; an important step for proliferation and survival (Mellinghoff *et al.*, 2004). To examine the role of AR on the expression of HER2 and HER3, LNCaP cells were treated with the anti-androgen drugs enzalutamide, ARN509 and Casodex for 24 hours. RNA was isolated and HER2 and HER3 expression were assessed by QRT-PCR using specific primers. The data was normalised to the DMSO vehicle control. No significant change in the expression of HER2 or HER3 mRNA was observed in response to anti-androgen treatment compared to the DMSO control (Figure 3-2 A, B). However, both HER2 and HER3 increased at the protein level in response to the anti-androgen drugs enzalutamide, ARN509 and Casodex compared with DMSO vehicle untreated control (Figure 3-2 C).

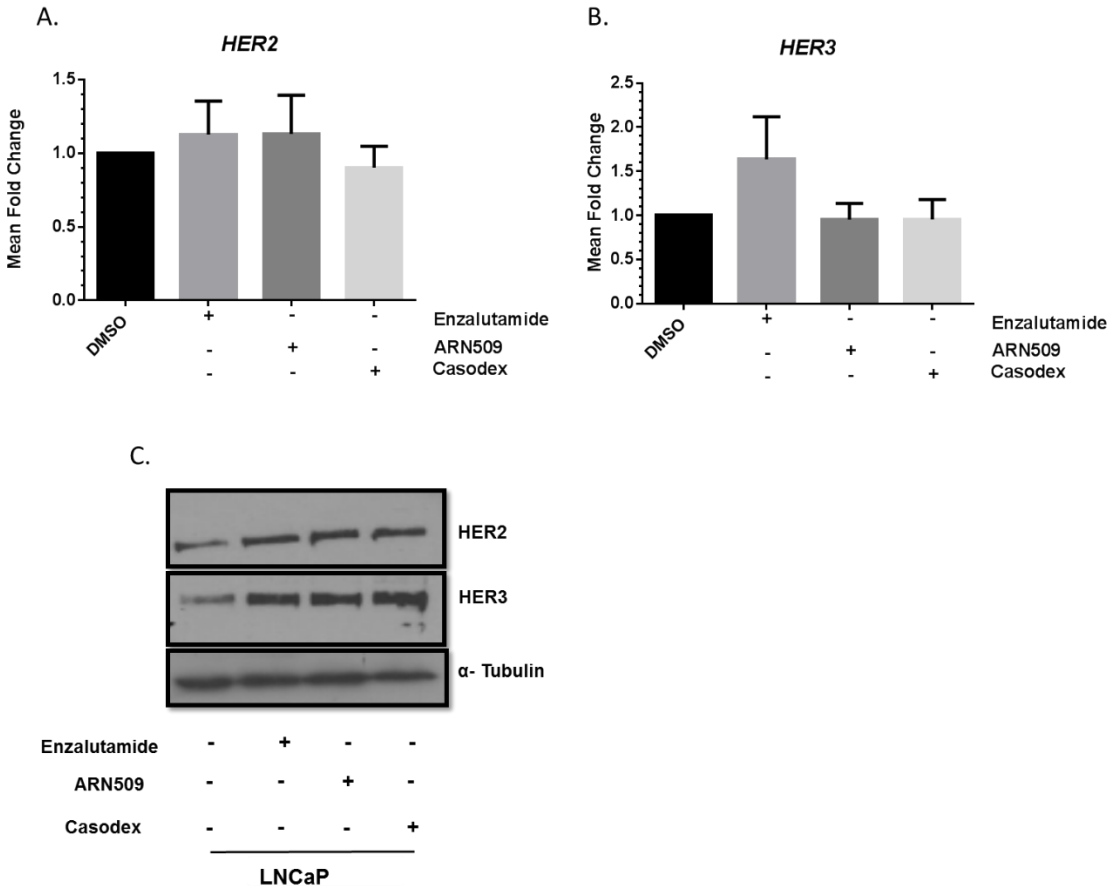

Figure 3-2 Anti-androgens increase total HER2 and HER3 level in LNCaP cell line

LNCaP cells were seeded out in normal growth medium for 24 hours. This was followed by treatment with 10μM of Casodex, enzalutamide or ARN509 for 24 hours. DMSO was used as control. Cells were then lysed in RIPA buffer for protein samples or Trizol for RNA extraction. **A**. HER2 expression was determined by QRT- PCR. **B**. HER3 expression was determined by QRT- PCR. **C**. Total HER2 and HER3 protein level was detected by western blotting. Alpha-tubulin was used as a loading control. Error bars represent the mean ± SD for triplicate independent experiments (representative blot).

3.2.3 Higher level of HER2 and HER3 in Casodex, enzalutamide and ARN509 Resistant cell lines compared to parental LNCaP cells

Despite initial good response rates to ADT, nearly all men eventually develop the castration-resistant prostate cancer (CRPC) phenotype, where low levels of androgen can stimulate tumour growth (Snoek *et al.*, 2009). It has been shown that increased HER2 expression is seen in enzalutamide-resistant prostate cancer models (Shiota *et al.*, 2015). In our laboratory, cell lines models have been generated that represent the CRPC phenotype. These lines have all been generated from the LNCaP parental cell line and are resistant to Casodex (LNCaP-CDX-R), enzalutamide (MDV1300) (LNCaP-ENZ-R) or ARN509 (LNCaP-ARN-R). LNCaP-CDX-R, LNCaP-ENZ-R and LNCaP-ARN-R are LNCaP sub-clones that were generated by growing LNCaP in serial passage of escalating dose of Casodex, enzalutamide and ARN509, respectively. These resistant cell lines are routinely maintained in full medium supplemented with either 10μM Casodex, 10μM enzalutamide or 10μM ARN509 (O'Neill, 2014). To investigate the role of HER2 and HER3 in CRPC models parental LNCaP, LNCaP-CDX-R, LNCaP-ENZ-R and LNCaP-ARN-R cell lines were grown in full medium containing DMSO vehicle, 10μM casodex, 10μM enzalutamide and 10μM ARN509, respectively for 24 hours. As expected, high expression of HER2 was apparent in LNCaP-CDX-R cells which showed a ~5 fold significant increase in mRNA expression ($p < 0.05$) when compared with LNCaP cells. Similarly, LNCaP-ENZ-R cells showed a ~13 fold significant increase in HER2 mRNA expression ($p < 0.05$) when compared with LNCaP cells. The same trend was also noticed with LNCaP-ARN-R cells which showed an increase in mRNA expression of HER2 of ~2 fold (Figure 3-3A).

For HER3, the results demonstrated a significant increase in mRNA expression of HER3 ($p < 0.05$) for the LNCaP-CDX-R cells of ~14 fold compared with LNCaP cells. In LNCP-ENZ-R cells the highest expression of HER3 mRNA was observed with a ~20 fold increase in expression ($p < 0.05$) compared to LNCaP cells. The LNCaP-ARN-R cells showed a significant increase in the mRNA expression of HER3 ($p < 0.05$) of ~12 fold (Figure 3-3B).

To confirm the results of QRT-PCR, HER2 and HER3 protein level were further examined using western blotting and the results showed an apparent increase in the level of HER2 and HER3 total protein in LNCaP-CDX-R, LNCaP-Enz-R and LNCaP-ARN-R cell lines compared with LNCaP cells that (Figure 3-3C).

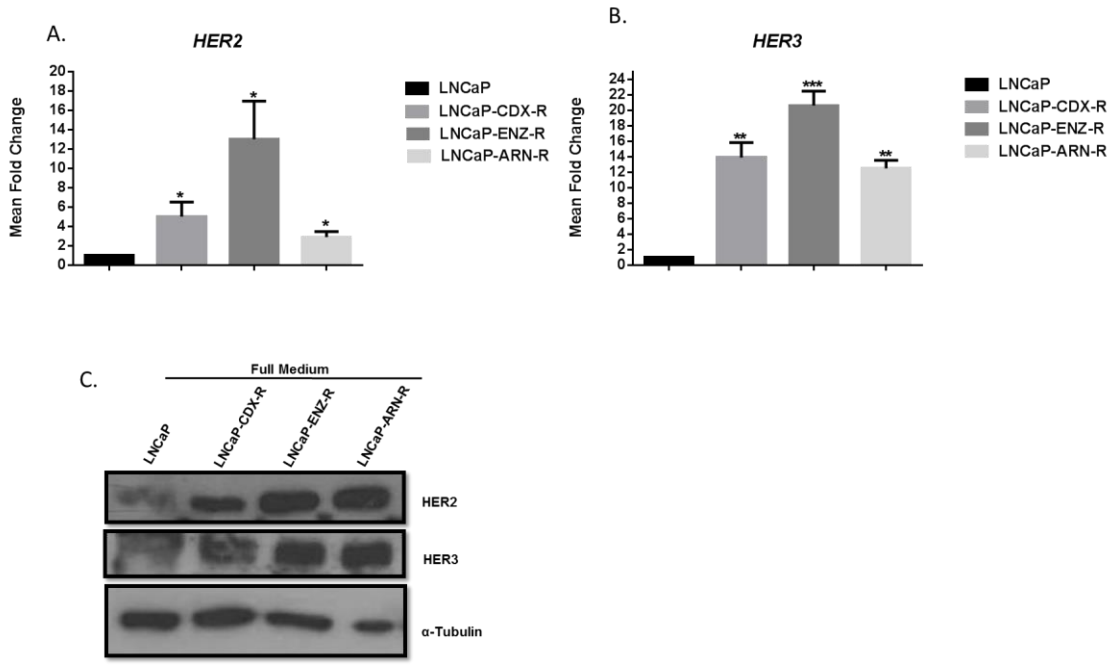

Figure 3-3 Elevated expression of HER2 and HER3 in Casodex, enzalutamide and ARN509 resistant cell lines

Parental LNCaP and Casodex, enzalutamide and ARN509 resistant cell lines were seeded out in in their respective growth medium for 24 hours. The cells were then lysed in RIPA buffer for protein samples and Trizol reagent was used for RNA extraction. **A**. HER2 expression was determined by QRT- PCR. **B**. HER3 expression was determined by QRT-PCR. **C**. Total HER2 and HER3 protein level. Alpha-tubulin was used as a loading control. Error bars represent mean ± SD for triplicate independent experiments. p-values were determined by using student t-test (* p-value <0.05, ** p-value <0.01m and *** p-value <0.001) (representative blot).

3.2.4 Higher level of HER2/HER3 in Casodex-, enzalutamide- and ARN509-resistant cell lines stimulated with heregulin

The previous experiment (Figure 3-3) showed a high level of HER2/HER3 in Casodex, enzalutamide and ARN509 resistant cell lines compared with LNCaP cells. To test the role of HER2/HER3 activity in PC resistant cell lines; LNCaP, Casodex, enzalutamide and ARN509 resistant cell lines were grown in full medium, followed by an overnight starvation in basal medium to reduce any possible activation through FBS. Cells were then activated with heregulin for 15 minutes. RNA was isolated and HER2 and HER3 expression were assessed by QRT-PCR using oligonucleotide primers. The results observed an increase in the expression of HER2 at mRNA level in response to heregulin stimulation in parental LNCaP and in all tested resistant cell line (Figure 3-4A). The results also noticed a significant increase in the HER3 expression at mRNA level in response to heregulin stimulation. However, it was not significant in parental LNCaP that activated with heregulin (Figure 3-4 B). To confirm the results of QRT-PCR, HER2 and HER3 protein level were examined with western blotting and the results showed an increase in the level of the HER2 and HER3 total protein level in LNCaP-CDX-R, LNCaP-ENZ-R and LNCaP-ARN-R cell lines compared with LNCaP cells grown in basal medium and with heregulin stimulation (Figure 3-4 C).

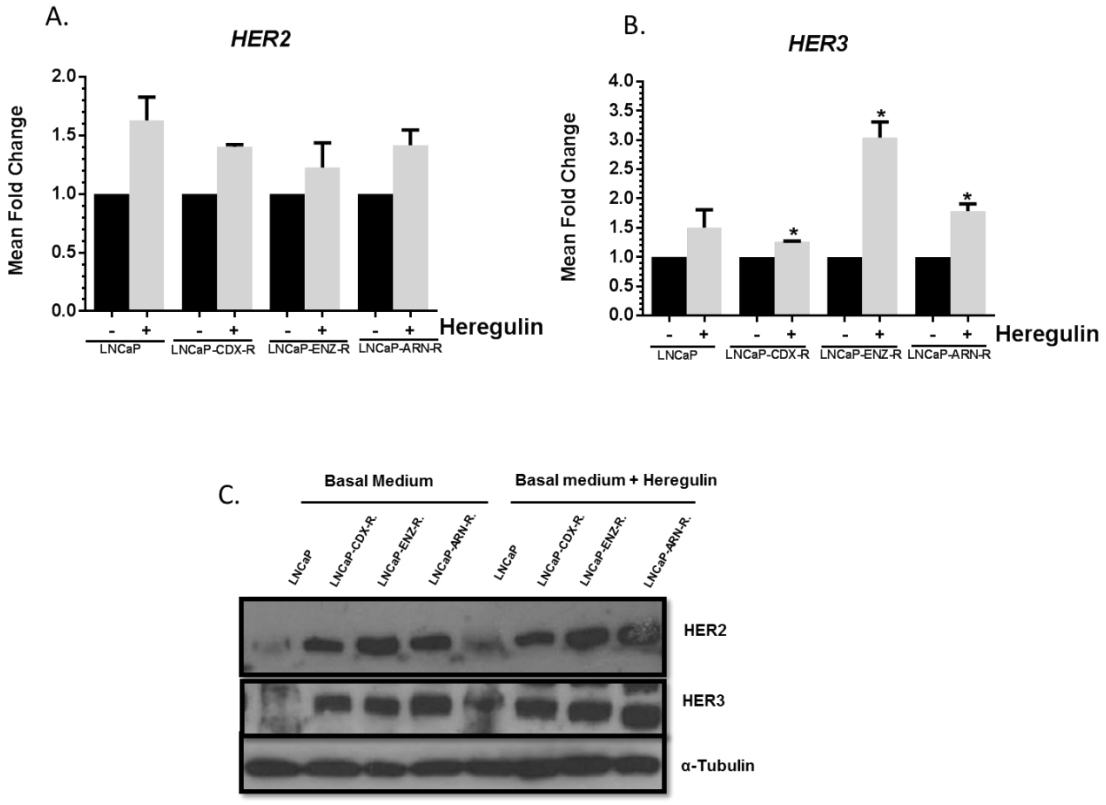

Figure 3-4 Higher level of HER2 and HER3 in PC resistant cell lines

Parental LNCaP and Casodex, enzalutamide and ARN509 resistant cell lines were seeded out in 6-well plates in full medium for 24 hours. This was followed by an overnight starvation in basal medium, then the cells were activated with 20ng/ml of heregulin for 15 minutes. The cells were then lysed in RIPA buffer for protein samples and Trizol kits were used for RNA extraction. **A**. HER2 expression was determined by QRT-PCR. **B**. HER3 expression was determined by QRT-PCR. **C**. HER2 and HER3 protein level in parental LNCaP cells, Casodex-resistant cell line, enzalutamide-resistant cell line and ARN509-resistant cell line. Alpha-tubulin was used as loading control. Error bars represent the mean ± SD for triplicate independent experiments. p-values were determined by using student t-test (* p-value <0.05)

3.2.5 Higher level of pHER2, pHER3, pAkt and pERK1/2 in LNCaP-CDX-R, LNCaP-ENZ-R and LNCaP-ARN-R cell lines compared with parental LNCaP in basal medium

A previous microarray study of PC tissue revealed that the RAS/RAF/MEK signalling pathway is up-regulated in both primary and metastatic cancer (Mulholland *et al.*, 2012). Another study showed that the PI3K/Akt/mTOR signalling pathway is important for the development and progression of CRPC (Bitting and Armstrong, 2013). To test which pathways are activated in resistant cell line models, LNCaP, Casodex-resistant, enzalutamide-resistant and ARN509-resistant cell lines were grown in full medium, then starved for 24 hours to eliminate any possible activation from FBS. Western blots were then probed for the phospho-species of HER2, HER3, Akt and ERK1/2. The data might demonstrates high level of pHER2, pHER3, pAkt and pERK1/2 in Casodex-, enzalutamide- and ARN509-resistant cell lines compared to the parental LNCaP cells in basal medium (Figure 3-5A).

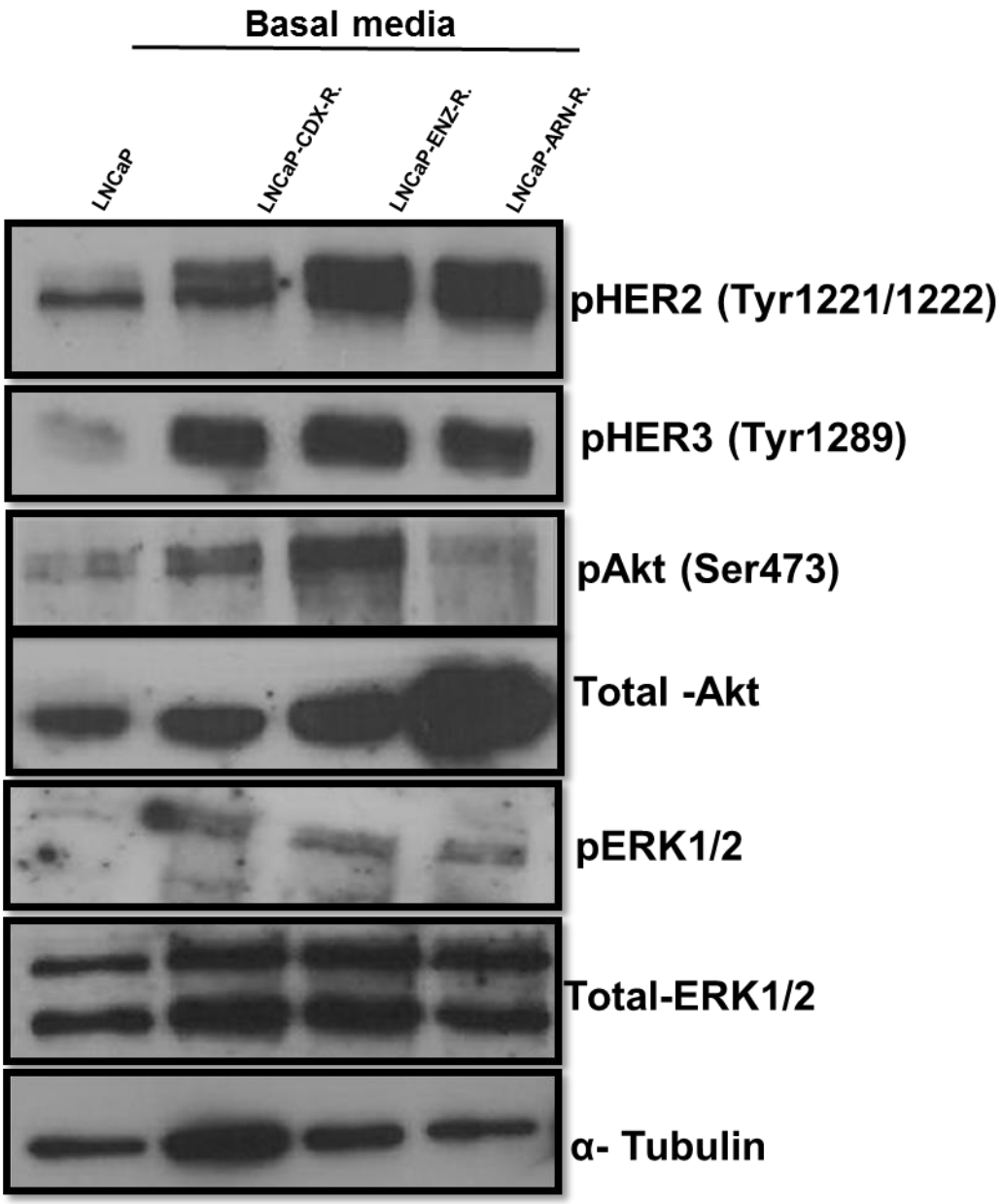

Figure 3-5 High level of phosphorylated HER2, HER3, Akt and ERK1/2 in resistant cell lines compared to parental LNCaP cells

LNCaP and resistant cell lines were seeded out in 6-well plates in full medium for 24 hours and followed by an overnight starvation in basal medium. The cells were then lysed in RIPA buffer for protein samples. pHER2, pHER3, pAkt, total Akt, total ERK1/2, pERK1/2 protein level in parental LNCaP, Casodex-resistant cell line, enzalutamide-resistant cell line and ARN509-resistant cell line were detected. Alpha-tubulin was used as a loading control (representative blot).

3.2.6 Increased level of pHER2, pHER3, pAkt and pERK1/2 in LNCaP-ENZ-R and LNCaP-ARN-R cells in response to the heregulin stimulation

To investigate the pathways that might be stimulated through HER2/HER3 activity in PC resistant cell line models, LNCaP, Casodex-resistant, enzalutamide-resistant and ARN509-resistant cell lines were grown in full medium, then starved for 24 hours to eliminate any possible activation from FBS. The cells were then activated with heregulin for 15 minutes. The LNCaP-CDX-R cell line showed no change in the protein level of pHER2 in response to the heregulin, while high level of pHER3, pAkt and pERK1/2 was noticed in response to heregulin stimulation. The LNCaP-ENZ-R cell line showed an increase in the protein level of the pHER2, pHER3, pAkt and pERK1/2 in response to the heregulin stimulation, which was observed to be more pronounced than the other resistant cell lines. The results also demonstrated a possible increase in the protein level of the pHER2, pHER3, pAkt and pERK1/2 in response to the heregulin stimulation in LNCaP-ARN-R cell line (Figure 3-6).

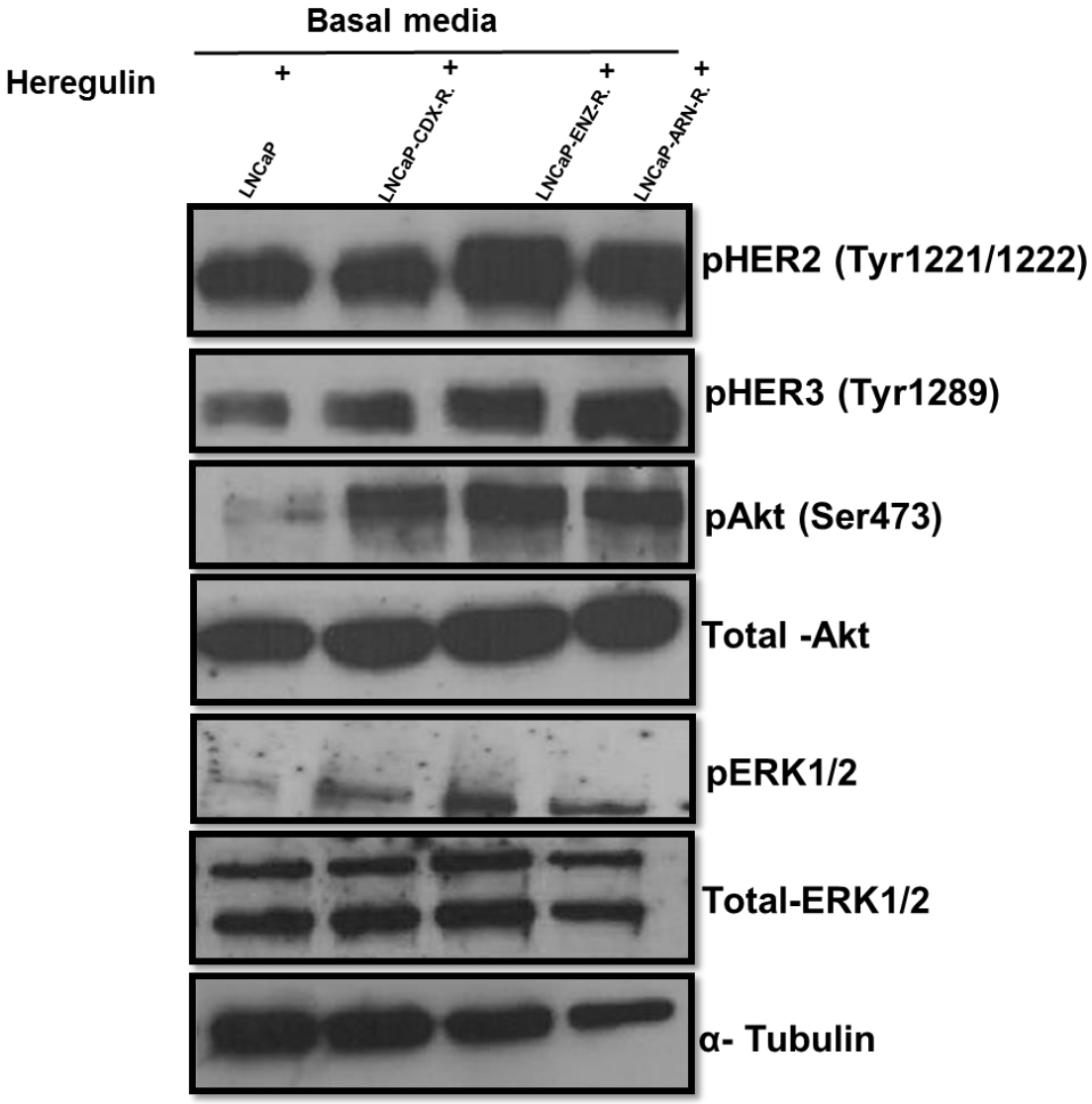

Figure 3-6 Increase in the activity of pHER2, pHER3, pAkt and pERK1/2 in response to heregulin stimulation

LNCaP and resistant cells were seeded out in 6-well plates in full medium for 24 hours, followed by overnight starvation in basal medium. The cells then were activated with 20ng/ml of heregulin for 15 minutes. The cells were then lysed in RIPA buffer for protein samples. pHER2, pHER3, pAkt, total Akt, total ERK1/2, pERK1/2 protein level in parental LNCaP, Casodex-resistant cell line, enzalutamide-resistant cell line and ARN509-resistant cell line were detected. Alpha-tubulin was used as a loading control (representative blot).

3.2.7 AZD8931 and Lapatinib abrogates the activity of HER2/ HER3 and downstream signaling pathways

A previous study in our lab indicated that a transient over-expression of HER2 and HER3 increases downstream signalling of PI3 kinase pathways. Also AZD8931 which inhibits EGFR, HER2 and HER3 reduces HER2 and HER3 activity in the cellular and nuclear compartments as expected (Rao, 2015). Akt can activate AR in a ligand independent manner (Feldman and Feldman, 2001a). To understand which downstream signalling pathways could be effected by the inhibition of HER2 and HER3, AZD8931 and Lapatinib were used. Lapatinib inhibits both EGFR and HER2 activity but not HER3. LNCaP cells were grown in full medium then starved overnight in basal medium and treated with AZD8931 or Lapatinib, then activated with heregulin for 15 minutes. It was observed that the AZD8931 might decrease pHER2 and HER3 level apparently in the presence of heregulin and also decreases pAkt protein expression. The results also suggested that Lapatinib was able to reduce pHER2 and HER3 dramatically in the presence of heregulin and also decrease pAkt protein level (Figure 3-7).

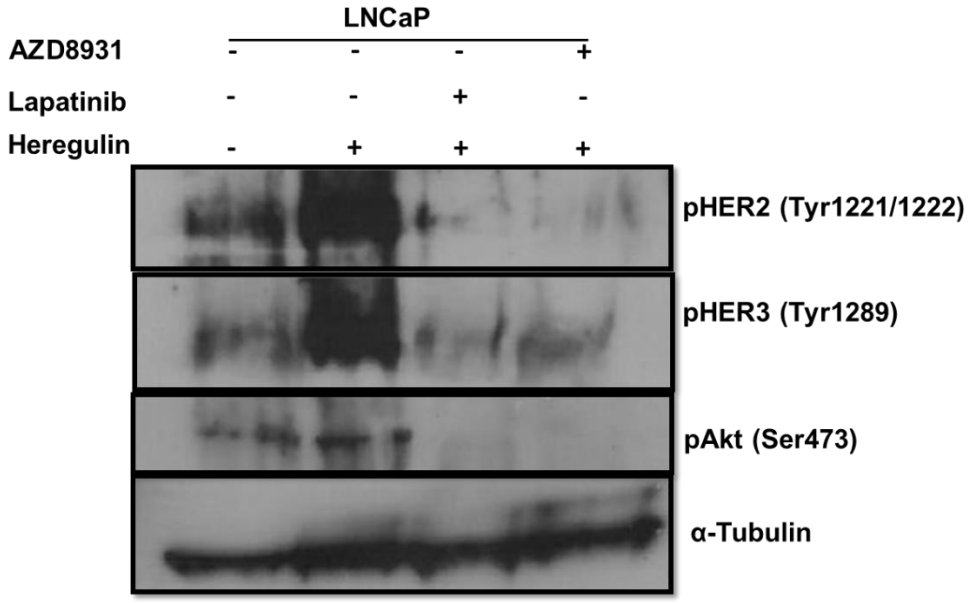

Figure 3-7 AZD8931 and Lapatinib abrogates HER2/HER3 and Akt phosphorylation

LNCaP cells were seeded out in 6-well plates in full medium for 24 hours, followed by overnight starvation in basal medium containing 3μM AZD8931 or 5μM of Lapatinib. The cells were then stimulated with 20ng/ml of heregulin for 15 minutes. Next, the cells were lysed in RIPA buffer to obtain protein samples. pHER2, pHER3 and pAkt protein level in parental LNCaP cells were determined. Alpha-tubulin was used as a loading control (representative blot).

3.2.8 Heregulin significantly increases AR promoter activity, while AZD8931, MK2206 and PD325901 abrogate heregulin stimulation of AR promotor activity in an androgen dependent cell line

To further understand which pathways are able to influence AR activity, a cloned LNCaP-7B7 cell line was used which has a chromosomally integrated PSA-luciferase promoter, thus enabling the analysis of AR activity. LNCaP-7B7 cells line were validated in our group by adding enzalutamide which show decreased in the activity of PSA promoter, while increased in the PSA promoter's activity was noticed in the full medium condition compared to SDM (Rao, 2015). LNCaP-7B7 cells were starved in SDM medium then stimulated with heregulin to activate the HER2/HER3 pathways. AR activity increased significantly ($p < 0.05$) with at least ~1.5 fold increase compared with DMSO control (Figure 3-8). Cells were treated with AZD8931 (HER family inhibitor), MK2206 (inhibitor of the serine/threonine protein kinase Akt) or PD325901 (MEK1/MEK2 inhibitor). DMSO was used as a control. This study observed that AZD8931 might decrease AR activity in the androgen-dependent cloned cell line stimulated with heregulin. The results also showed that MK2206 Akt inhibitor was able to significantly decrease AR activity ($p < 0.05$). Although a similar trend was noticed, it was also detected that PD325901 (MEK1/MEK2 inhibitor) had no significant effect on the AR activity in androgen dependent cloned cell line (Figure 3-8 C).

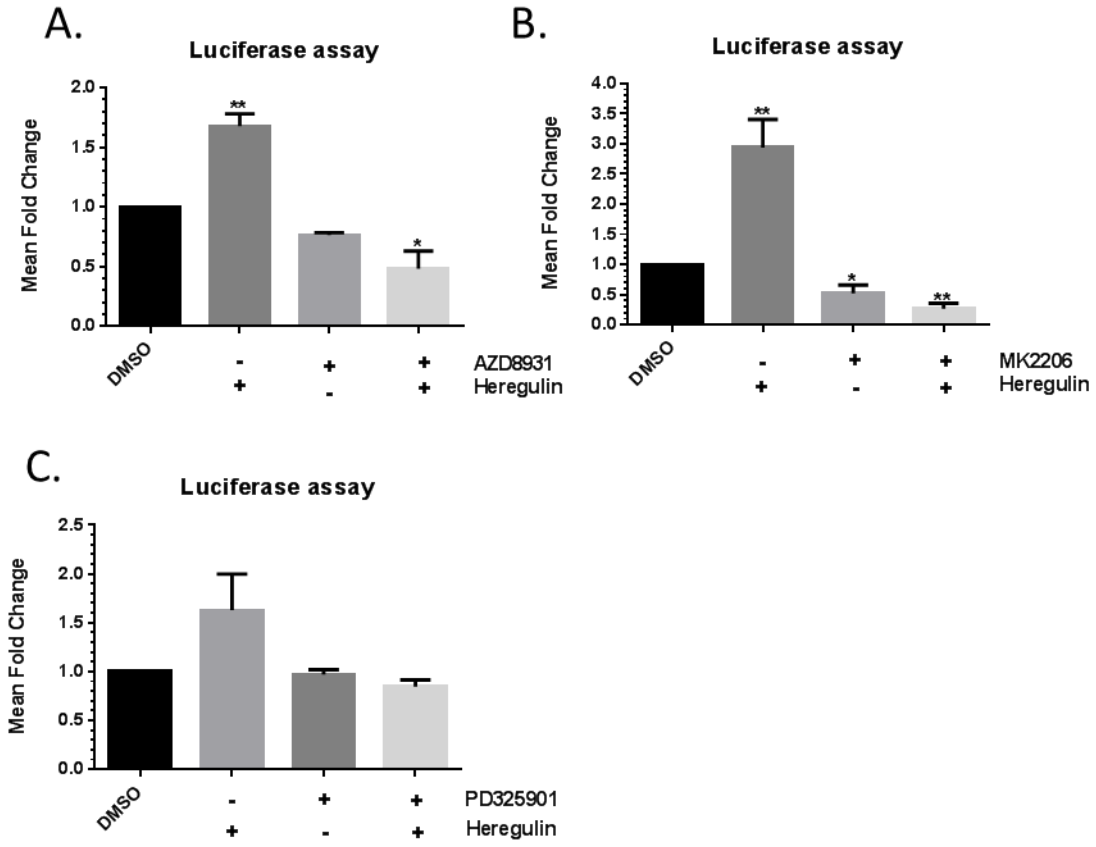

Figure 3-8 AZD8931, MK2206 and PD325901 inhibit AR promoter activity, while heregulin increases AR promoter activity in an androgen-dependent cell line

LNCaP-7B7 cells were seeded out in quadruplets per experimental arm using a 24-well plate. The cells were then starved in SDM for 72 hours. 16 hours prior to the starvation period, the cells were treated with either DMSO or AZD8931, MK2206 or PD3225901 after which the cells were treated with heregulin 20ng/ml for another 16 hours. The cells were then lysed in reporter lysis buffer and luciferase substrate was added to measure the luciferase activity. The luciferase counts per second were measured and the data was normalised to the number of the cells per well by utilising an IncuCyte machine. **A**. LNCaP-7B7 treated with AZD8931. **B**. LNCaP-7B7 treated with MK2206. **C**. LNCaP-7B7 treated with PD325901. Error bars represent the mean ± SD for triplicate independent experiments. p-values were determined by using student t-test (* p-value <0.05, ** p-value <0.01).

3.2.9 AZD8931, MK2206 and PD325901 inhibit AR promoter activity, while heregulin significantly increases AR promoter activity in an androgen-independent cloned cell line

An investigation of the effects of HER2 and HER3 plus downstream partners Akt and MEK on androgen receptor activity was continued in the cloned androgen-independent cell line LNCaP-AI-7B7. This cell line has a chromosomally integrated PSA-luciferase promoter, thus enabling the analysis of AR activity in an androgen-independent model. To prove that these changes are occurring through the activity of the androgen receptor, a previous study in our lab validated these cell line by treating the cells with the anti-androgen drug enzalutamide, and it was observed that PSA transcriptional activity was inhibited (Rao, 2015). LNCaP-AI-7B7 cells were grown in SDM medium, then stimulated with heregulin to activate the HER2/HER3 pathways. AR activity increased significantly ($p < 0.05$) with at least ~2.5 fold increase compared with DMSO control (Figure 3-9 A). Cells were treated with AZD8931 (HER family inhibitor), MK2206 (inhibitor of the serine/threonine protein kinase Akt) or PD325901 (MEK1/MEK2 inhibitor). DMSO was used as a control. It was observed that AZD8931 decreases AR activity in the androgen-independent cloned cell line, seen on stimulation with heregulin. It was also observed that PD325901 (MEK1/MEK2 inhibitor) had no significant effect on the AR activity in this androgen-independent cloned cell line.

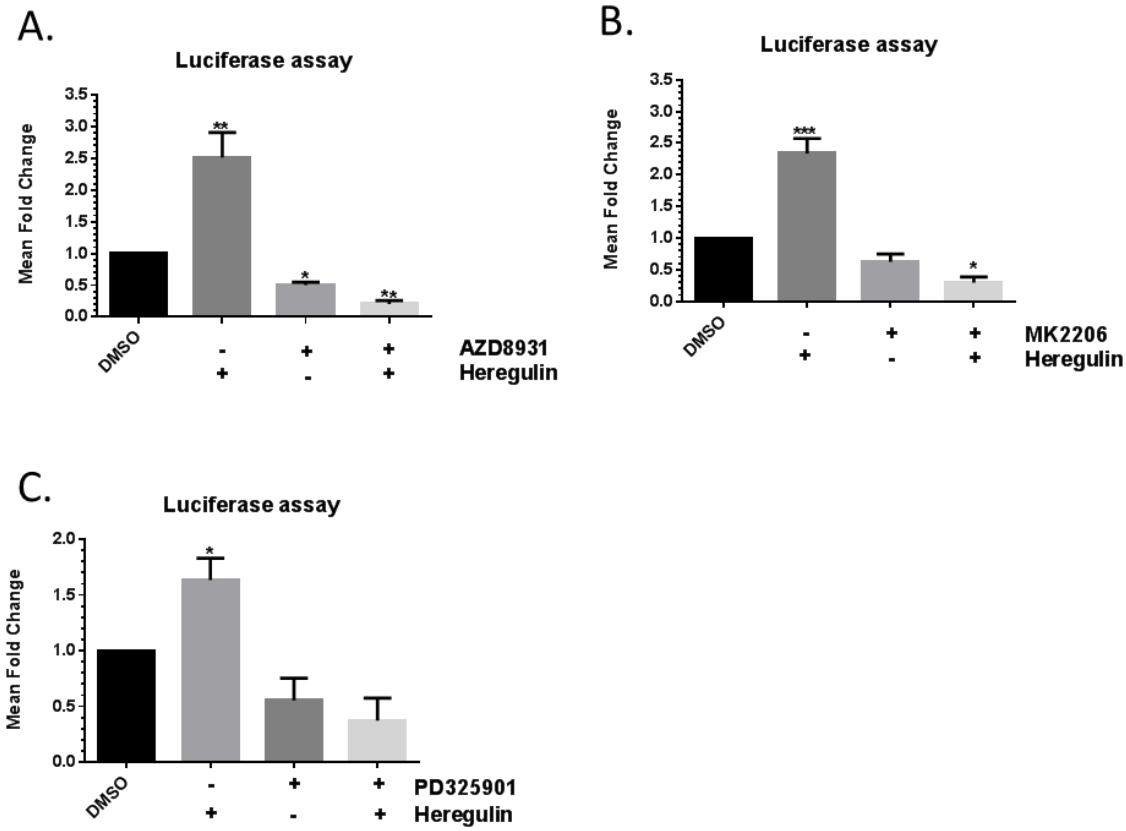

Figure 3-9 AZD8931, MK2206 and PD325901 inhibits AR promoter activity, while heregulin increase AR promoter activity significantly in androgen independent cell line

LNCaP-AI-7B7 cells were seeded out in their normal growth medium (SDM).The cells were pre-treated with DMSO control, AZD8931, MK2206 or PD3225901 followed by 16 hours of 20ng/ml heregulin stimulation. The cells were then lysed and luciferase activity was measured. The luciferase counts per second were measured and the data was normalised to the number of the cells per well by utilising an IncuCyte machine. **A**. LNCaP-AI-7B7 treated with AZD8931. **B**. LNCaP-AI-7B7 treated with MK2206. **C**. LNCaP-AI-7B7 treated with PD325901. Error bars represent the mean ± SD for triplicate independent experiments. p-values were determined by using student t-test (* p-value <0.05, ** p-value <0.01, *** p-value <0.001).

3.3 Discussion:

It has previously been shown that HER2/HER3 signalling enhances the stability of AR protein and optimizes binding of the AR to the promoter region of androgen receptor target genes (Mellinghoff *et al.*, 2004). Additionally, the HER2/HER3 pathway is directly upstream of the PI3K-Akt pathway, as well as many other known pathways, including the MAP Kinase pathway, suggesting that the HER2/HER3 pathway represents a critical target of prostate cancer (Mellinghoff *et al.*, 2004). A previous study in our research group demonstrated that stable overexpression of HER2 and HER3 in PC3 cells leads to increased PI3 Kinase (pAkt) and MAP Kinase (pERK1/2) pathway activity. In addition, this cell line showed an increase in migration and invasion, compared to empty vector control. Furthermore, the use of the pan-EGFR family inhibitor, AZD8931 (an inhibitor of EFGR, HER2 and HER3), caused a reduction of AR activity (Rao, 2015).

The stimulation of HER2/3 by heregulin was validated and it showed that heregulin activates HER2/3 and Akt after 15 minutes stimulation (Figure 3-1). The limitation of this experiment is not investigate the total HER3 and Akt at the protein level, which might be useful if this study detect these proteins in response of heregulin stimulation.

The role of the HER2/HER3 pathway in the regulation of AR has been investigated in several studies (Agus *et al.*, 2002; Mellinghoff *et al.*, 2004). In order to investigate the possible feedback mechanism between AR and HER2/HER3, LNCaP cells were treated with the anti-androgen drugs Casodex, enzalutamide and ARN509. The data showed no possible feedback mechanism between AR and HER2/HER3 at the transcription level (Figure 3-2). However, an upregulation of HER3/HER2 at the protein level has been detected in cells treated with Casodex, enzalutamide and ARN509 which might suggest a possible negative feedback mechanism between AR and HER3. Similarly, another group Chen *et al.* (2010) has shown that on knockdown of the AR by two different RNAi in both experimental arms there were higher HER3 levels, and AR activation promotes HER3 degradation through Nrdp-1, an E3 ubiquitin ligase that targets HER3 for degradation. This study suggested that inhibits AR with antiandrogen Casodex, enzalutamide and ARN509, cause upregulate of HER3/HER2 which might leads to increase the signalling of LNCaP in AR independent manner. This could happens by reduced the level of Nrdp-1 and increase HER3 level in response to Casodex, enzalutamide and ARN509 treatment. This study investigated the role of HER2/HER3 in our in-house generated CRPC models of drug-resistance compared to parental LNCaP cells.

Expression of HER2/HER3 were tested in LNCaP, LNCaP-Casodex-resistant, LNCaP-enzalutamide-resistant and LNCaP-ARN509-resistant cells. The data showed that expression of HER2 and HER3 were significantly higher in all tested resistant cell lines compared to parental LNCaP cells at the protein and at the mRNA levels. HER3 has previously been described to be over expressed in widely available cell line models of CRPC (DU145, PC3 and LNCaP-AI) (Chen *et al.*, 2010), which agreed with obtained data (Figure 3-4). Similar results were observed in cells grown in basal medium (Figure 3-5). Also, these results showed that stimulation of cells with heregulin leads to higher expression of HER2/HER3 at the mRNA level, which was more pronounced in the LNCaP-enzalutamide resistant cell line (Figure 3-4 A, B). This was also similarly reflected at the total protein level (Figure 3-4 C).

Heregulin is known to activate the HER2/HER3 pathway at tyrosine residues (Gregory *et al.*, 2005). Therefore, the same experiment as in Figure 3-4 was repeated looking at the phosphorylated forms of HER2 and HER3. The effect of heregulin stimulation on the phosphorylation of HER2/HER3 and the possible pathways that could be activated through this activation of the HER2/HER3 pathway was assessed in resistant cell line models compared to the parental LNCaP cells (Figure 3.5) (Figure 3.6). The most interesting finding was higher levels of pHER2, pHER3, pAkt and pERK1/2 detected in the LNCaP-Casodex-resistant, LNCaP-enzalutamide-resistant and LNCaP-ARN509-resistant cells compared with parental LNCaP cells in basal medium condition. However, no change was detected in total Akt and total ERK1/2 among the studied cell lines which acted as an additional loading control (Figure 3-5). Another important finding was that activation of the HER2/HER3 pathway in LNCaP-enzalutamide resistant cells, LNCaP-Casodex resistant and LNCaP-ARN509 resistant cells led to an activation of both PI3 Kinase (pAkt) and MAP Kinase (pERK1/2) signalling pathways compared to parental LNCaP, which was most apparent in LNCaP-enzalutamide resistant cells (Figure 3-6). HER2 was previously suggested to induce PSA through the MAP kinase pathway (Yeh *et al.*, 1999). Another study indicated that the loss of HER3 results in a reduction of ~50% in Akt phosphorylation and rapid tumour regression (Hsieh and Moasser, 2007). The limitation of this experiment is not investigate the total HER3 and Akt at the protein level. However, this study suggested that heregulin might only able to phosphorylate HER3 at tyrosine residues, which was observed in experiment (Figure 3-5). And no change in the total HER2/HER3 protein level was noticed in response to heregulin stimulation (Figure 3-4).

To confirm that Akt is activated through the HER2/HER3 pathway in the studied PC cell lines, cells were treated with AZD8931 (EGFR, HER2 and HER3 inhibitor) and Lapatinib (EGFR and HER2 inhibitor) (Medina and Goodin, 2008). The results showed that both inhibitors were might capable of reducing the activity of pHER3, pHER2 and pAkt in the presence of heregulin (Figure 3-7). This experiment has limitation of not investigate the total HER2/HER3 and Akt, which might be useful if this study detect these proteins in response of AZD8931 and Lapatinib treatment.

To investigate the effect of the HER2/HER3 pathway and downstream partners (PI3 Kinase and MAP Kinase pathways) on AR activity, AZD8931 (EGFR, HER2 and HER3 inhibitor), MK2206 (inhibitor of the serine/threonine protein kinase Akt) and PD325901 (MEK1/MEK2 inhibitor) were used. In androgen-responsive LNCaP7B7 cells (Figure 3-8) heregulin increased AR activity, while AZD8931 abrogated this activity (Figure 3-8A). The LNCaP7B7 cells were validated in our group by grown these cells in present enzalutamide, which showed decrease in AR activity (Rao, 2015).

An interesting question was whether the increased AR activity was mediated through PI3K or MAPK pathways downstream of the activated HER2/HER3 heterodimer? MK2206 (inhibitor of the serine/threonine protein kinase Akt) reduced AR activity seen with heregulin stimulation (Figure 3-8 B). However, no significant effect of PD325901 (MEK1/MEK2 inhibitor) was seen on AR activity (although a similar trend was seen). Gioeli *et al.* (2011) Suggested the use of a combination of PD325901 with any PI3/Akt Kinase pathway inhibitor to provide a greater growth inhibition than the individual drug alone in PC (Figure 3-8 C). Similarly, heregulin increases AR activity in LNCaP-AI-7B7 cells (a model of androgen-independent disease). While AZD8931 and MK2206 significantly reduce this activity and abrogate heregulin induced AR activity, PD325901 does reduce AR activity and appears to abolish the effects of heregulin stimulation, however, again this was not seen to reach significance (Figure 3-9).

The LNCaP-AI 7B7 cells were validated in our group by grown these cells in present enzalutamide, which showed decrease in AR activity (Rao, 2015).

In summary, these results show that the HER2/HER3 pathway has a crucial role in the CRPC model cell lines. These two members of the EFGR family can activate both MAP kinase and PI3K/Akt pathways, which are responsible for tumour growth and metastasis. This activity is seen to be more pronounced in the LNCaP-enzalutamide resistant cell. Therefore this clinically relevant model was selected for further investigation, comparing all results to the parental LNCaP cells.

Chapter 4. Phenotypic and transcriptomic comparison between parental LNCaP and enzalutamide resistant LNCaP-ENZ-R cell lines

4.1 Introduction

Targeting AR signalling by androgen deprivation is the primary option for clinical intervention in prostate cancer. Although initially response to the treatment, the majority of patients will experience only temporary benefit and relapse with CRPC. Enzalutamide a second generation antiandrogen is currently used for the treatment of CRPC. Despite transient benefit, resistance to enzalutamide occurs frequently, however the mechanisms of resistance are still not fully defined (Liu *et al*., 2015). Several mechanisms of enzalutamide resistance have been described including AR variant expression, which promotes the translation of an active truncated AR splice variants lacking the AR ligand binding domain. It has been demonstrated that PC cells which express full length AR and AR splice variants are androgen independent and enzalutamide resistant (Li *et al.*, 2013b).

An alternative mechanism of enzalutamide resistance is accomplished through production of the F876L mutation in the AR gene. This mutation was originally identified as a novel mutation in the AR gene in the LNCaP cell line following long-term culture in the presence of enzalutamide (Korpal *et al*., 2013).

Over-expression of the glucocorticoid receptor (GR) is another mechanism of resistance to enzalutamide. Same study was indicated that the GR is able to substitute for the AR to activate AR target genes and the maintenance of the enzalutamide resistant phenotype (Arora *et al*., 2013).

Previously, the LNCaP-ENZ-R cell line was demonstrated to express a high level of HER2 and HER3 proteins (Figure 3.4). In addition, an increase in the activity of both PI3 kinase (pAkt) and MAP kinase (pERK1/2) signalling pathway in response to HER2 or HER3 stimulation was also noticed (Figure 3.5). Based on these observations the LNCaP-ENZ-R cell line was used to investigate the biological and genetic changes occurring in response to enzalutamide treatment and compared with the responses observed in the parental LNCaP cell line.

The aims of this chapter are to:

1. Investigate the phenotypic differences between LNCaP-ENZ-R and parental LNCaP cell lines

2. Examine the transcriptomic differences between LNCaP-ENZ-R and parental LNCaP cell lines

4.2 Results

4.2.1 Heregulin stimulation increases the proliferation rate of LNCaP-ENZ-R and LNCaP cell lines

From the data obtained in Chapter 3, heregulin stimulation was shown to activate the RAS/RAF/MEK and PI3K/Akt/mTOR signalling pathways in the LNCaP-ENZ-R cell line (Figure 3-6). To understand the effect of stimulation of HER2/HER3 on the proliferation of LNCaP-ENZ-R cell line compared to the parental LNCaP, both cell lines were cultured in SDM with or without heregulin for the whole experiment. The results showed the proliferation of the parental LNCaP in SDM was much reduced compared to the proliferation of LNCaP-ENZ-R under these conditions. Stimulation with heregulin showed an increase in the proliferation rate of both cell lines compared to the SDM-treated controls (Figure 4-1). The greatest heregulin-induced change was observed in the LNCaP-ENZ-R cell line.

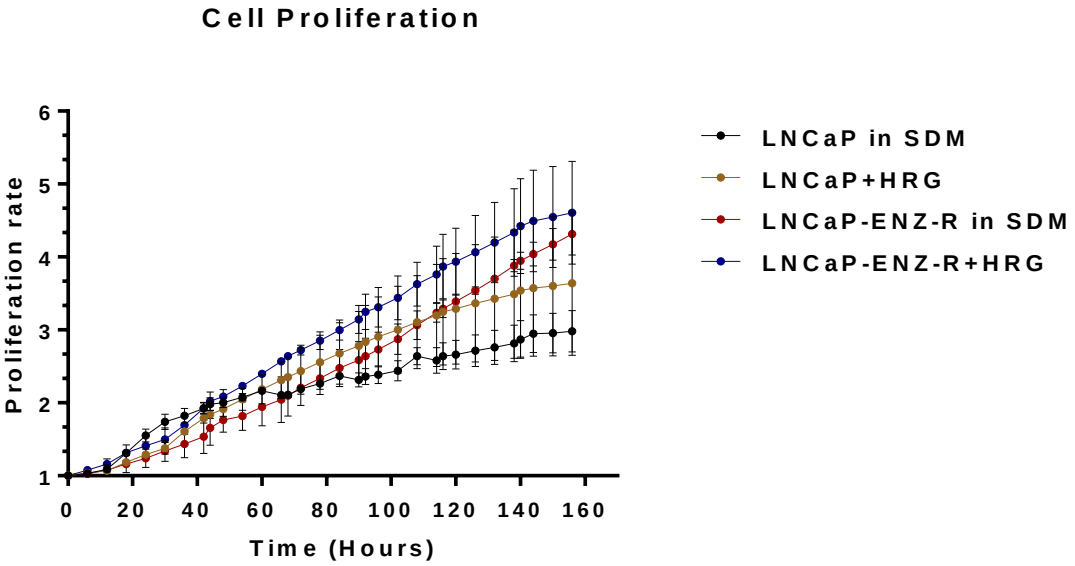

Figure 4-1 Heregulin increases proliferation rate of LNCaP and LNCaP-ENZ-R cell lines

LNCaP and LNCaP-ENZ-R cells were seeded out in a 96-well plate. The cells were grown in SDM with or without 20ng/ml heregulin (HRG). The proliferation was determined by using the IncuCyte® ZOOM System. The data were normalized to the zero hours for each condition. Error bars represent the mean ± SD for triplicate independent experiments.

4.2.2 Expression of phosphorylated HER2, HER3 and Akt in LNCaP and LNCaP-ENZ-R cell lines

To study the consequences of the enzalutamide treatment on the expression of pHER2/pHER3 and the pathways that could be affected, both cell lines LNCaP and LNCaP-ENZ-R were grown in full medium in the absence or presence of enzalutamide for 48 hours. The results showed that LNCaP-ENZ-R cell line had a higher endogenous expression of pHER2, pHER3 and pAkt when compared with parental LNCaP cells (Figure 4-2). Furthermore, the addition of enzalutamide to the LNCaP cell line appeared to have a small effect in reducing the expression of pHER2, pHER and pAkt. In contrast, the expression of these three phospho-proteins was similar in the absence or presence of enzalutamide in the LNCaP-ENZ-R cell line. Also the results might suggested that no effect of enzalutamide on the expression of pERK5 in LNCaP-ENZ-R. While a decreased in the level of pERK5 was noticed in response to the enzalutamide treatment in the LNCaP cell line.

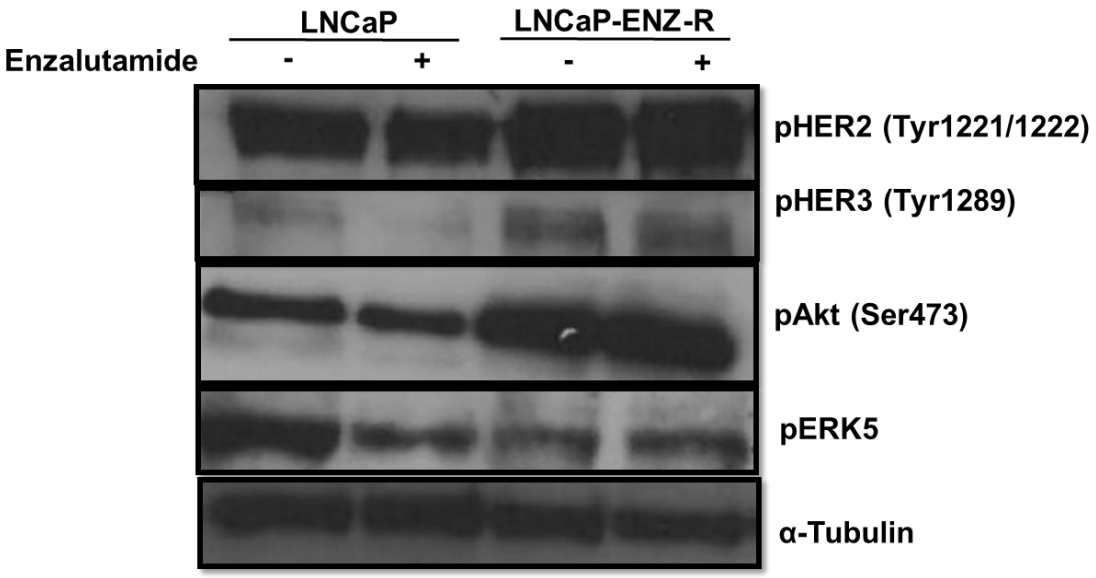

Figure 4-2 Elevated level of phosphorylated HER2, HER3 and AKT in the LNCaP-ENZ-R cell line

LNCaP and LNCaP-ENZ-R cells were seeded out in 6-well plate. The cells were grown in full medium in the absence or presence of 10μM enzalutamide for 48 hours. The cells were lysed in RIPA buffer. pHER2, pHER3, pAkt and pERK5 protein level in parental LNCaP and LNCaP-ENZ-R cell lines were detected by western blotting. Alpha-tubulin was used as a loading control (representative blot).

4.2.3 Enzalutamide reduces the proliferation rate of LNCaP and LNCaP-ENZ-R cell lines

To study the effect of the enzalutamide on the proliferation of LNCaP-ENZ-R cell line compared to LNCaP cells. Both cell lines were grown in full medium in the absence or presence of enzalutamide and the IncuCyte® ZOOM System was used to monitor changes in cell phenotype over time. The data showed that enzalutamide treatment significantly reduced parental LNCaP cells proliferation ($p < 0.05$) compared to DMSO vehicle control. The LNCaP-ENZ-R cell line demonstrated a slightly faster growth rate in the absence of enzalutamide but its growth was similarly inhibited by the inclusion of 10µM enzalutamide in the growth medium (Figure 4-3). These results suggest that extended treatment with enzalutamide is necessary to distinguish the degree of sensitivity of the LNCaP and LNCaP-ENZ-R cell lines to enzalutamide.

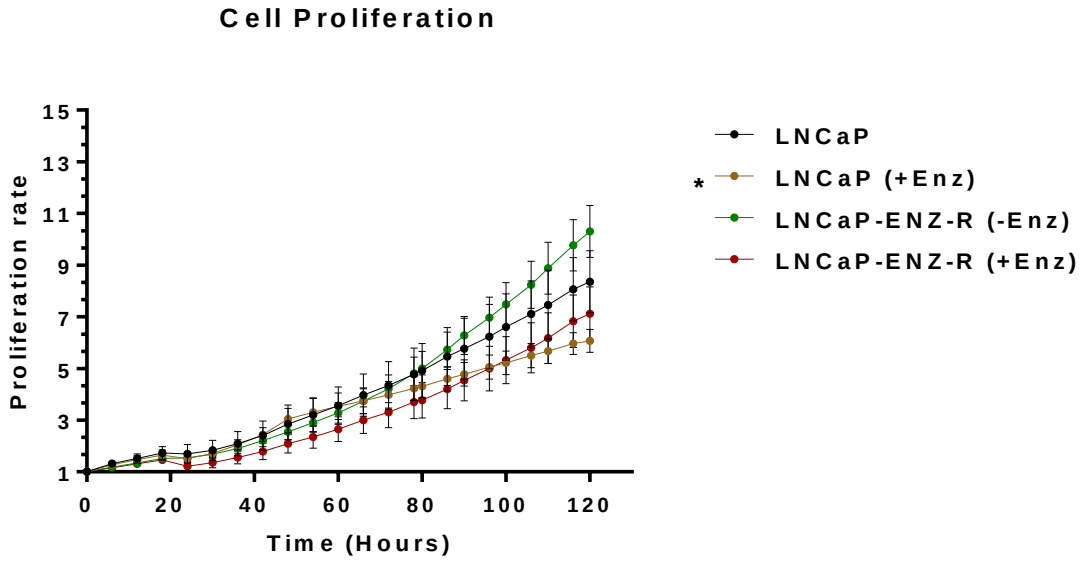

Figure 4-3 Enzalutamide decrease the proliferation of LNCaP and LNCaP-ENZ-R cell lines

LNCaP and LNCaP-ENZ-R cells were seeded out in 96-well plates in full medium. After overnight incubation, the cells were treated with 10µM enzalutamide or DMSO vehicle as a control. The plate was placed in the IncuCyte® ZOOM System and changes in cell confluency were monitored over time. Error bars represent the mean ± SD for triplicate independent experiments. p-values were determined by using student t-test (* p-value <0.05).

4.2.4 Enzalutamide causes LNCaP cells to accumulate in the G1 phase of the cell cycle

The effect of enzalutamide on cell cycle progression of the LNCaP-ENZ-R cell line compared to the parental LNCaP cells was examined as a part of the study of the phenotypic comparison between the two cell lines in response to enzalutamide. To do so, parental LNCaP and LNCaP-ENZ-R cell lines were grown in FM in the absence or presence of enzalutamide for 48 hours. The data showed that enzalutamide significantly arrested the LNCaP in the G1 phase ($p \leq 0.05$), increasing the percentage of G1 phase cells from 67.4% to 77.5% when compared with LNCaP cells cultured in DMSO control (Figure 4-4 A). No possible effect on cell cycle distribution was noticed for enzalutamide treatment of LNCaP-ENZ-R cells (Figure 4-4 B).

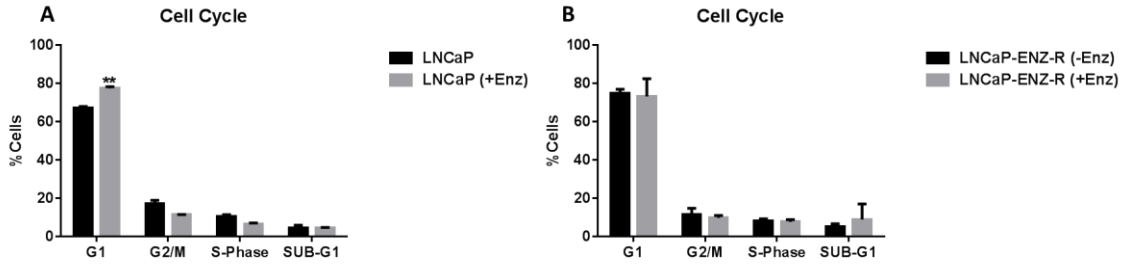

Figure 4-4 Enzalutamide arrests LNCaP cells in the G1 phase of the cell cycle

LNCaP and LNCaP-ENZ-R were seeded out in 6-well plates in FM and then the cells were treated with 10µM enzalutamide for 48 hours or DMSO vehicle as a control. **A**, LNCaP cell cycle analysis. **B**, LNCaP-ENZ-R cell cycle analysis. Error bars represent the mean ± SD for triplicate independent experiments. p-values were determined by using student t-test (** p-value <0.01).

4.2.5 Enzalutamide decreases the migration rate of LNCaP cells without affecting the migration of LNCaP-ENZ-R cells

To study the effect of enzalutamide on the migration of the parental LNCaP cell line. The cells were grown in FM then treated with or without enzalutamide for 48 hours. Migratory behaviour was monitored by using wound healing assays which measure the cells directional movement into the area of the wound. The cellular motility was measured at 0, 6, 24 and 48 hours. The results suggested that enzalutamide treatment significantly decreased the overall migration between the two edges of the wound when compared with LNCaP cell motility cultured in DMSO vehicle (Figure 4-5).

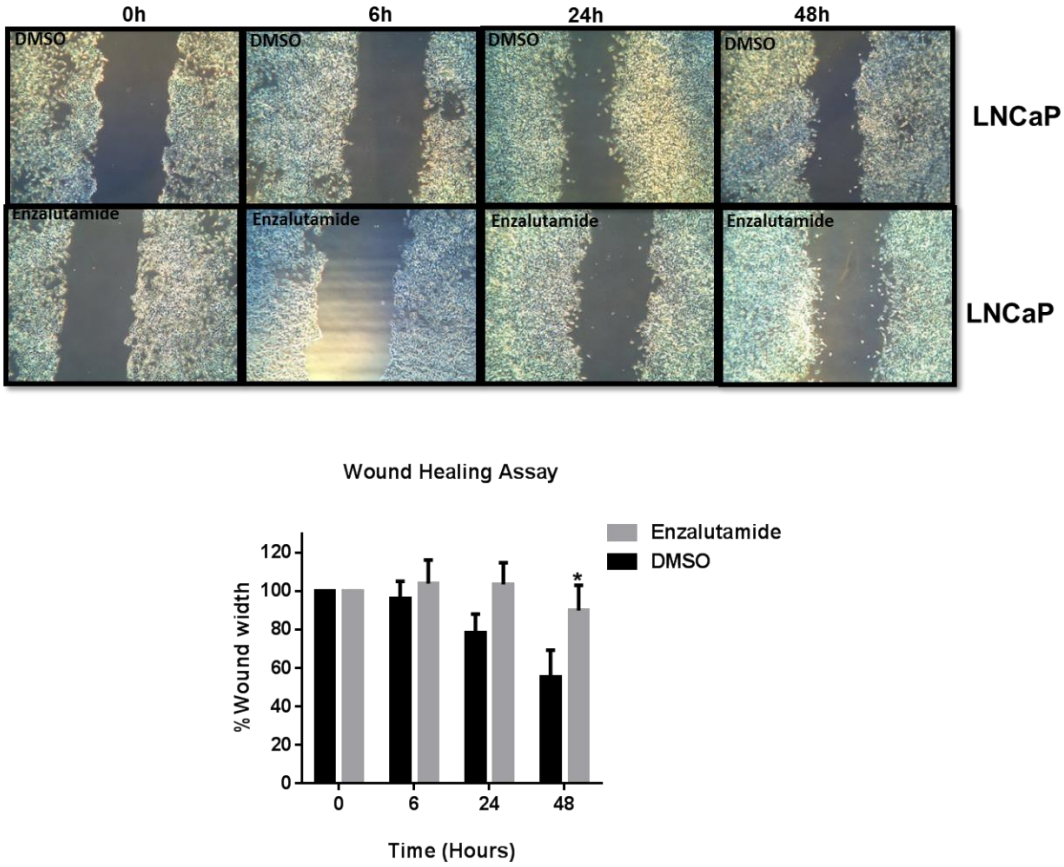

Figure 4-5 Enzalutamide decreases the migration of LNCaP cells

LNCaP cells were seeded out into 6-well plates in FM and the cells were grown to 100% confluency. Perpendicular scratches were then generated using p20 filter tips. The media was replaced with fresh media with either DMSO vehicle or with 10µM enzalutamide. Images were taken of three separate fields for each well at 0h, 6h, 24h and 48h. The width of the "wound" was measured using ImageJ software. This was achieved by overlaying a 20 square grid over each image taking an average and normalising to the 0 hour control. Error bars represent the mean ± SD for triplicate independent experiments. p-values were determined by using student t-test (* p-value <0.05).

The experiment was similarly performed with the LNCaP-ENZ-R cell line using identical treatment conditions. The results showed that there was no effect of the enzalutamide on the migration of the LNCaP-ENZ-R cell line when compared to cells grown in the absence of enzalutamide (Figure 4-6).

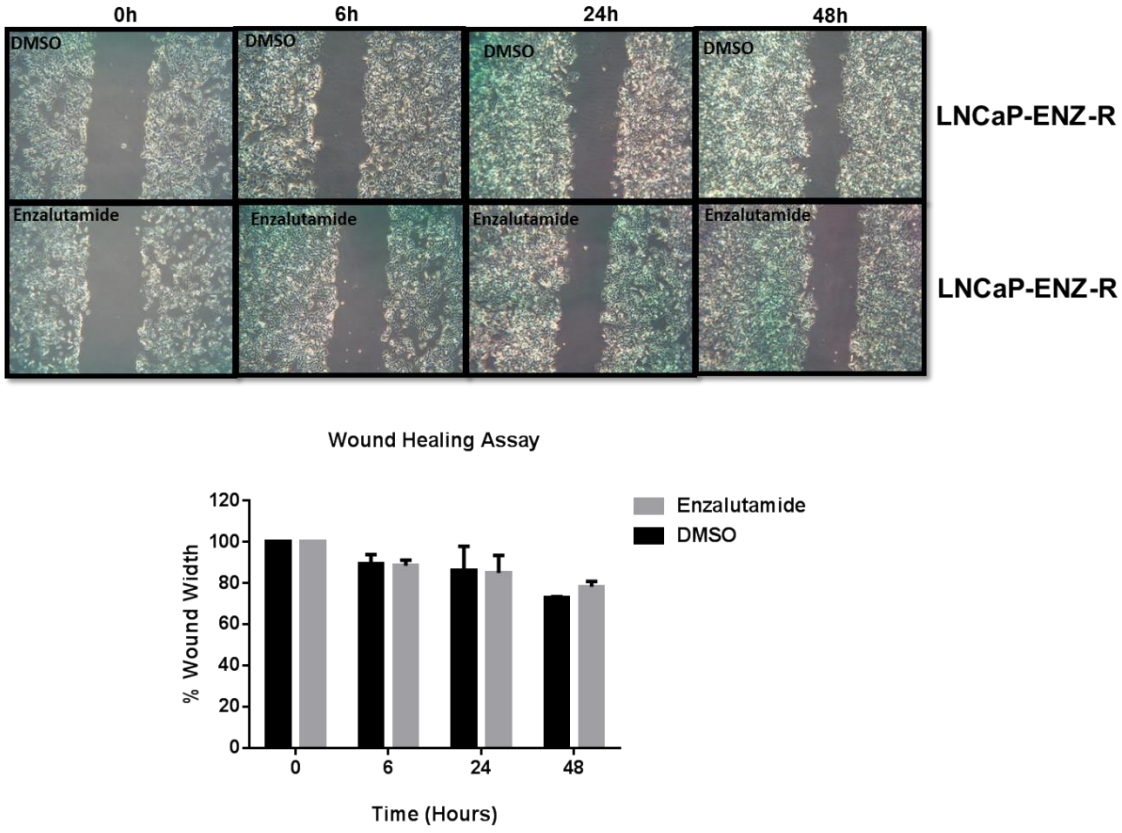

Figure 4-6 Migration of LNCaP-ENZ-R cell line is not affected by enzalutamide treatment

LNCaP-ENZ-R cells were seeded out into 6-well plates in FM and the cells were grown to 100% confluency. Perpendicular scratches were then generated using p20 filter tips. The media was replaced with fresh media with either DMSO vehicle or with 10μM enzalutamide. Images were taken of three separate fields for each well at 0h, 6h, 24h and 48h. The width of the "wound" was measured, using ImageJ software. This was achieved by overlaying a 20 square grid over each image taking an average and normalising to the 0 hour control. Error bars represent the mean ± SD for triplicate independent experiments.

4.2.6 Microarray experiment

In the previous chapter, it was observed that the LNCaP-ENZ-R cell line displayed higher expression of HER2 and HER3 compared with parental LNCaP cells at both the protein and mRNA level. Furthermore, activation of pHER2 and pHER3 led to the activation of both RAS/RAF/MEK and PI3K/Akt/mTOR signalling pathways when compared to the parental LNCaP cells (Figure 3-6). A microarray experiment was designed to study the global relative gene expression pattern of LNCaP-ENZ-R cells compared with parental LNCaP cells and also to investigate the consequence of enzalutamide resistance in this prostate cancer model. To do this, four conditions were selected as shown in (Table 4-1). Parental LNCaP and LNCaP-ENZ-R cell lines were treated with or without 10μM enzalutamide for 48 hours. Three biological repeats were performed for each condition and all samples were validated using QRT-PCR prior to microarray analysis using Illumina Human HT-12 arrays.

Cell line	**Condition**	
	DMSO (48 hours)	Enzalutamide (48 hours)
LNCaP	+	+
Enzalutamide Resistant cell (LNCaP-ENZ-R)	+	+

Table 4-1 Microarray experimental conditions

4.2.7 RNA integrity number (RIN) of the microarray samples

RNA quality of each sample was examined by determining the RNA integrity number (RIN) which represents the integrity and quality of the RNA samples using a 2100 Bio-analyzer system. The RIN provides sizing, quantitation and quality of RNA on a single platform providing high quality digital data. The RIN value was calculated using a software tool designed to estimate the integrity of total RNA for each sample. RIN values of 8 to 10 were considered to represent high quality RNA with little or no degradation of the RNA (Figure 4-7).

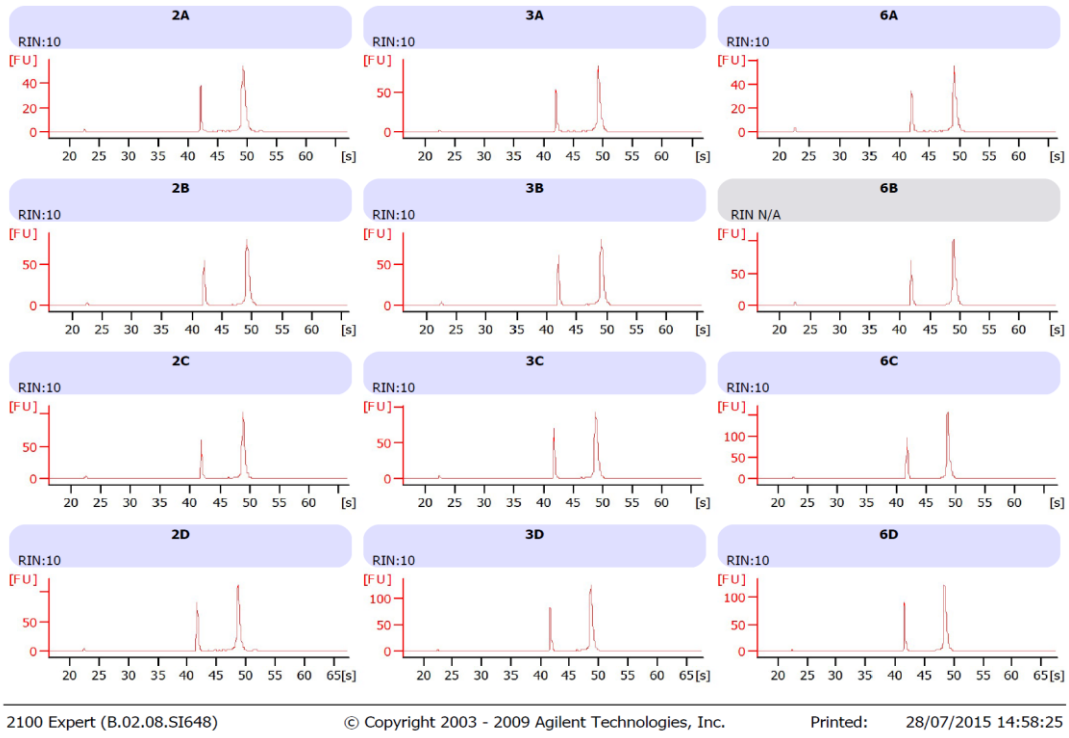

Figure 4-7 High RNA integrity number (RIN) of the microarray samples

LNCaP and LNCaP-ENZ-R cells were seeded out in 6-well plates. The cells were grown in FM with 10µM enzalutamide or DMSO vehicle for 48 hours. The cells were collected for RNA extraction by using RNA mini kits QIAGEN®. 2A, 3A and 6A are the three biological repeats of LNCaP cells without enzalutamide condition. 2B, 3B and 6B the three biological repeats of LNCaP cells with 10µM enzalutamide condition. 2C, 3C and 6C are the three biological repeats of LNCaP-ENZ-R cells without enzalutamide condition. 2D, 3D and 6D are the three biological repeats of LNCaP-ENZ-R cells with 10µM enzalutamide condition.

4.2.8 AR target genes expression in parental LNCaP and LNCaP-ENZ-R cell lines: validation of experimental conditions in each sample prepared for the microarray experiment

LNCaP and LNCaP-ENZ-R cell lines were grown in FM in the absence or presence of enzalutamide for 48 hours. RNA was isolated and then *KLK3, KLK2* and *TMPRSS2* expression were assessed by QRT-PCR using specific primers. The data was normalized to the DMSO control. Only samples that showed consistency in the expected expression of AR target genes in each experimental arm were selected for microarray analysis (Figure 4-8).

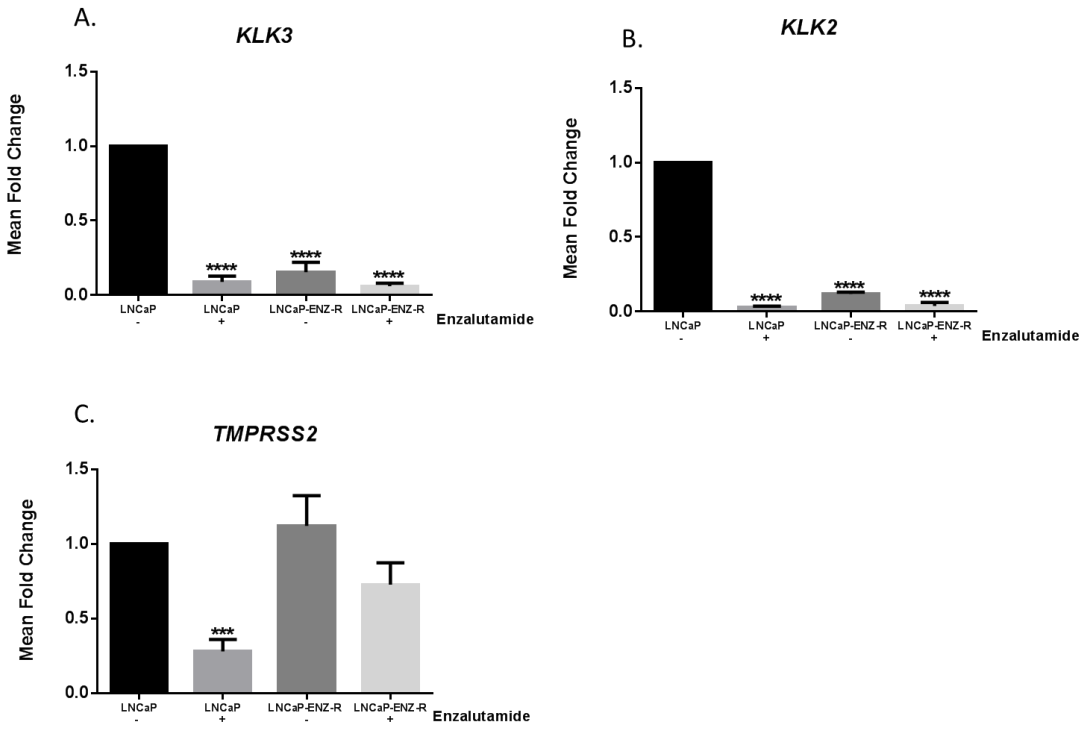

Figure 4-8 AR target genes expression in parental LNCaP and LNCaP-ENZ-R cell lines: validation of samples used for the microarray experiment

LNCaP and LNCaP-ENZ-R cells were seeded out in 6-well plates. The cells were grown in FM with or without 10μM enzalutamide for 48 hours or DMSO vehicle control. The cells were collected to extract RNA. **A,** *KLK3*; **B**, *KLK2* and **C**, *TMPRSS2* expression was determined by QRT-PCR. The relative expression of each gene measured was normalized to the LNCaP cells cultured in DMSO vehicle control. Error bars represent the mean ± SD for triplicate independent experiments. p-values were determined by using student t-test *** p-value <0.001 and **** p- value < 0.0001).

4.2.9 Microarray data analysis

Differential expression analysis was performed as outlined in Chapter 2. High quality data was obtained overall. Relative global gene expression for the LNCaP-ENZ-R cell line with enzalutamide condition was selected to compare with the parental LNCaP cell line grown without enzalutamide. The microarray data analysis of LNCaP-ENZ-R cell line with the enzalutamide condition revealed that 280 genes were significantly up-regulated ($p<0.05$) and 501 genes were significantly down-regulated ($p<0.05$) (Figure 4-9 A) when comparing with parental LNCaP cultured without enzalutamide treatment. The top 10 genes from the microarray data which showed the most significant up- or down-regulation in their expression ($p<0.05$) are highlighted (Figure 4-9 B). 1.2 fold change with was selected as a cut off for a significant genes.

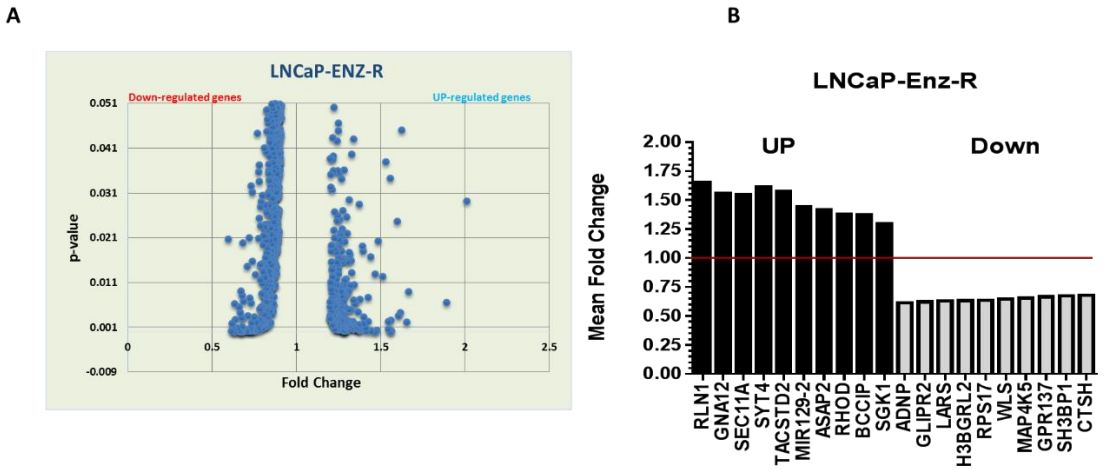

Figure 4-9 Genes most highly up-regulated or down-regulated in LNCaP-ENZ-R cells grown with enzalutamide when compared to LNCaP cells grown in the absence of enzalutamide

A. Volcano graph showing the most up-regulated genes or down-regulated genes significantly altered in LNCaP-ENZ-R cells grown with enzalutamide compared to LNCaP cells. **B.** The top 10 genes from the microarray data which showed the most significant up- or down-regulation in their expression.

4.2.10 Validation of microarray in different sets of RNA

To validate the results from (Figure 4-8), three independent RNA sets from the ones sent from the microarray were generated to validate the microarray data. RNA were extracted using Trizol kits and *KLK3*, *KLK2* and *TMPRSS2* expression at mRNA level were investigated by using QRT-PCR using specific primers and the data were normalized to the DMSO control. The same trend of *KLK3*, *KLK2* and *TMPRSS2* expression as that obtained from the microarray data was detected (Figure 4-8).

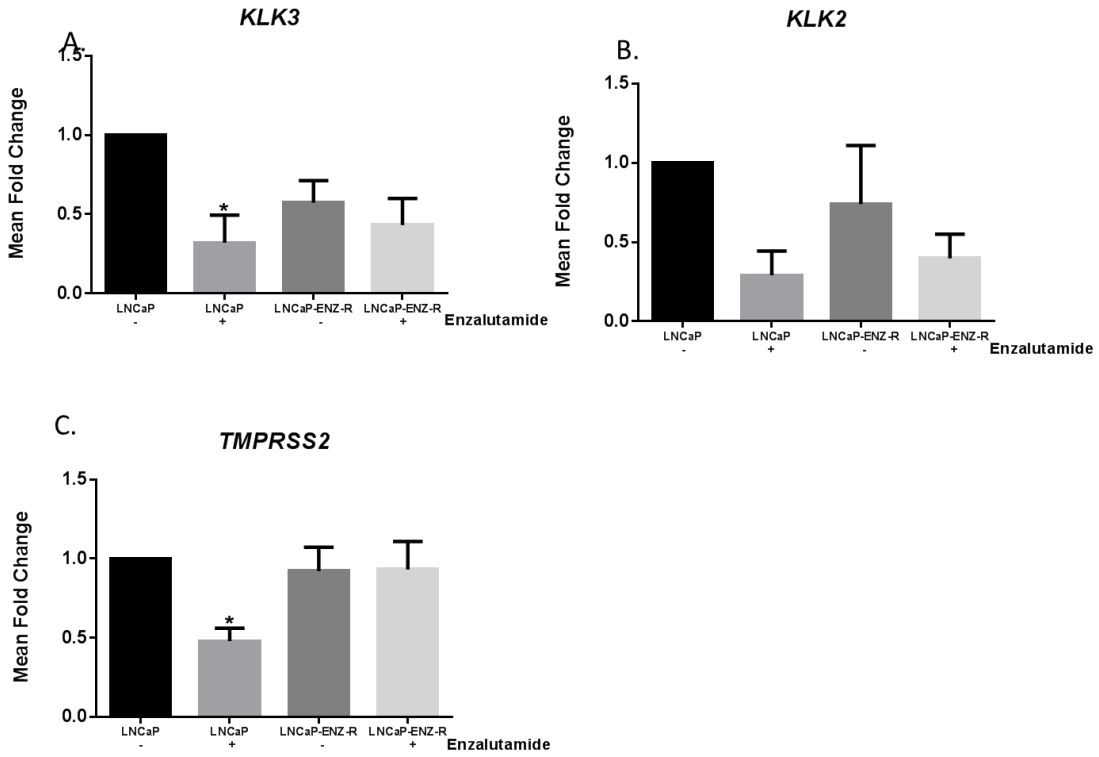

Figure 4-10 Validating the consistency of the microarray results in different sets of RNA

LNCaP and LNCaP-ENZ-R cells were seeded out in 6-well plates. The cells were grown in FM with or without 10µM enzalutamide for 48 hours or DMSO vehicle control. The cells were collected to extract RNA by using Trizol kits. **A**, *KLK3*; **B**, *KLK2* and **C**, *TMPRSS2* expression was determined by QRT-PCR. The relative expression of each gene measured was normalized to the LNCaP cells cultured in DMSO vehicle control. Error bars represent the mean ± SD for triplicate independent experiments. p-values were determined by using student t-test * p-value <0.05.

4.2.11 Validation of selected genes that showed an up-regulation in the microarray analysis

A number of genes were selected from the microarray data which showed a statistically significant upregulation in their expression ($p<0.05$) in the LNCaP-ENZ-R cell line grown in the presence of enzalutamide when compared to LNCaP cell line cultured in the absence of enzalutamide. The selected genes have previously been demonstrated to be involved in pathways that are crucial for cell proliferation, cell growth and cell signalling. These genes could be considered as potential biomarkers for enzalutamide resistance and include *SGK1, TACSTD2, RLN1, RLN2* and *SYT4.*

***SGK1*:**

Serum- and glucocorticoid-induced protein kinase-1 (SGK1) is one of the downstream substrates of the PI3K/Akt pathway, which plays a crucial role in cell growth, stress response and in the regulation of ion channels. Deregulation of SGK1 expression has been identified in different diseases such as cardiac fibrosis, hypertension, inflammatory bowel disease and cancer. Significant expression of SGK1 was identified in 50% of breast cancer by using immunohistochemistry, whereas SGK1 is barely detected in healthy breast cancer. Understanding the mechanism of SGK1 regulation is important and could lead to a clear insight of cancer (Bogusz *et al.*, 2006). *SGK1* was selected to be validated from the microarray results by using QRT-PCR. Specific primers were used to detect the expression of *SGK1* at the mRNA level. An increase in the expression of SGK1 in the LNCaP-ENZ-R cell line was detected in the presence and absence of enzalutamide (Figure 4-11 A).

***TACSTD2*:**

TROP2 is a transmembrane glycoprotein encoded by the *TACSTD2* gene. It is an intra-cellar calcium signal transducer, important in cell proliferation, self-renewal and invasion. TROP-2 is expressed in many heathy tissues. However, its overexpression has also been detected in many cancers and is suggested as a potential prognostic biomarker. Overexpression of TROP-2 in PC enhanced cancer migration and correlated with cancer cell aggressiveness (Shvartsur and Bonavida, 2015). The *TACSTD2* gene was selected to be validated from the microarray results, by using QRT-PCR. Specific primers were used to detect the expression of *TACSTD2* at the mRNA level. The data showed an increase in the expression of *TACSTD2* in the LNCaP-ENZ-R cell line in the presence and absence

of enzalutamide, which is consistent with the data obtained by the microarray experiment (Figure 4-11 B).

***RLN1* and *RLN2*:**

Relaxin is a short circulating peptide hormone that is encoded by two highly homologous genes (*RLN1* and *RLN2*). Relaxin is secreted from the male prostate gland and has a crucial role in connective tissue remodelling, suppression of fibrosis, dilation of blood vessels and angiogenesis. *RLN1* and *RLN2* mRNA expression has been detected in the prostate gland and suppression of *RLN1* and/or *RLN2* reduces invasion and proliferation and increases apoptosis of prostate cancer cells (Feng *et al.*, 2007). *RLN1* and *RLN2* were both selected for validation from the microarray data by using QRT-PCR. The data showed an increase in the expression of *RLN1* and *RLN2* in the LNCaP-ENZ-R cell line in the presence and absence of enzalutamide (Figure 4-11C, D), which is consistent with the data from the microarray experiment.

***SYT4*:**

Synaptotagmin IV (SYT4) is known to play an important role in neuro-transmitter secretion. Increased cells with a neuro-endocrine phenotype is one of the hallmarks of prostate cancer and correlates with poor prognosis and shortened patient survival. AR plays a negative role in the progression of the differentiation of prostate cancer cells towards the neuro-endocrine phenotype, which may suggest that AR inactivation correlates with increased frequency of neuro-endocrine cells in androgen independent PC. *SYT4* was found to be overexpressed in a bicalutamide resistant PC cell line, suggesting it as a possible CRPC phenotypic biomarker (Vias *et al.*, 2007). *SYT4* was selected from the microarray data for validation, by using QRT-PCR. The data showed an increase in the expression of *SYT4* in the LNCaP-ENZ-R cell line in the presence and absence of enzalutamide (Figure 4-11E), which follows the same trend obtained by the microarray data.

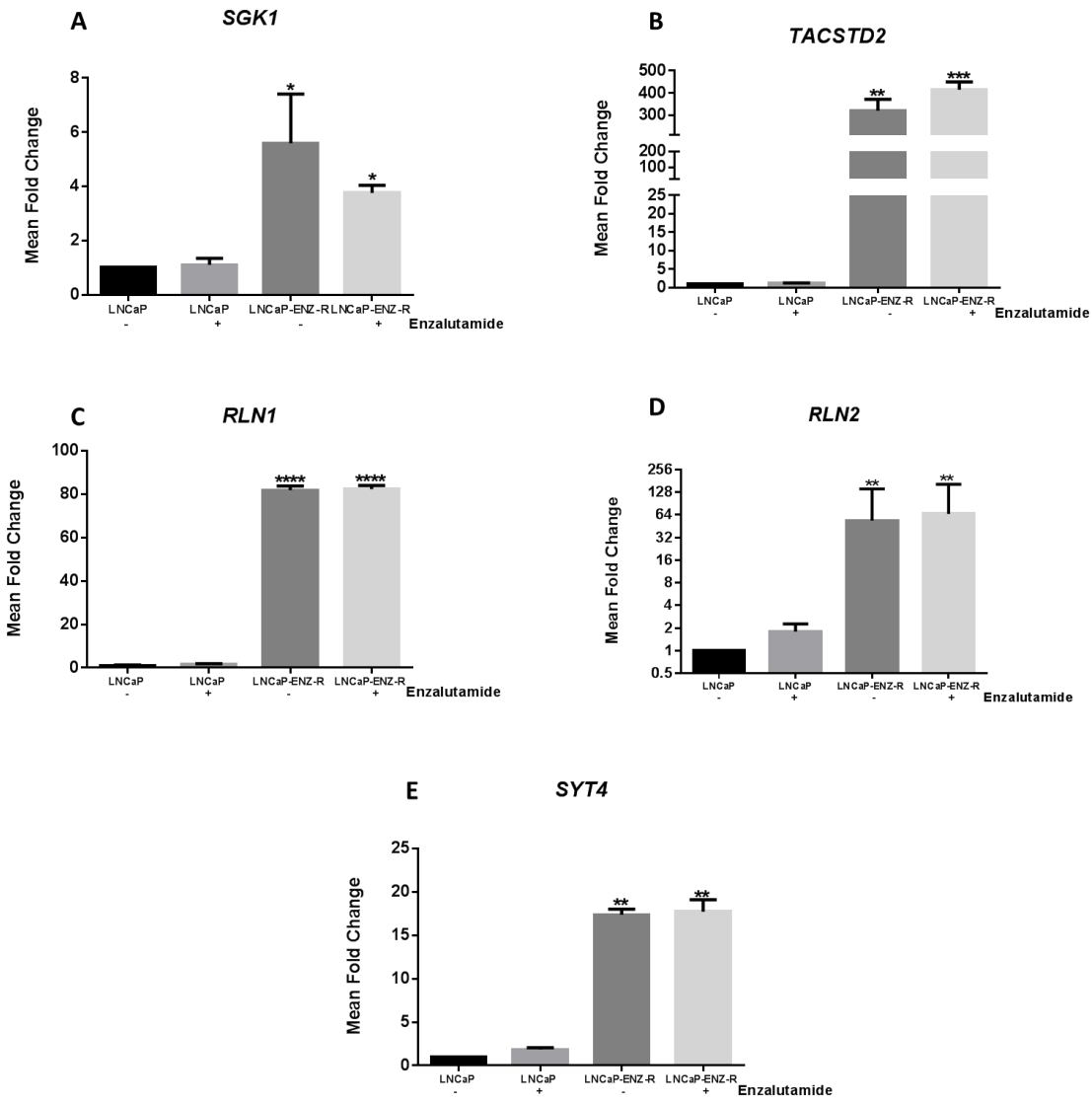

Figure 4-11 Validation of *SGK1, TACSTD2, RLN1, RLN1* and *SYT4* by QRT-PCR

LNCaP and LNCaP-ENZ-R cells were seeded out into 6-well plate. The cells were grown in FM with or without enzalutamide for 48 hours. DMSO were used as vehicle control. Trizol kits were used for RNA extraction. **A.** *SGK1*, **B**. *TACSTD2*, **C**. *RLN1*, **D**. *RLN2* and **E.** *SYT4* expression was determined by QRT- PCR using specific primer sets. The relative expression of each gene was measured by normalizing all samples to the untreated LNCaP cells. Error bars represent the mean ± SD for triplicate independent experiments. p-values were determined by using student t-test (* p-value <0.05, ** p-value <0.01, *** p-value <0.001 and **** p- value < 0.0001).

4.2.12 Increased expression of *SGK1, RLN1, SYT4* and *TACSTD2* in enzalutamide, Casodex and ARN509 resistant cell lines

To further investigate the genes that showed an upregulation in LNCaP-ENZ-R cell line, the expression of *SGK1, RLN1, SYT4* and *TACSTD2* were investigated in other resistant cell lines including cell lines derivatives resistant to Casodex and ARN509. The data showed an increase in the expression of *SGK1 RLN1, SYT4* and *TACSTD2* in both Casodex and ARN509 resistant cell lines (Figure 4-12).

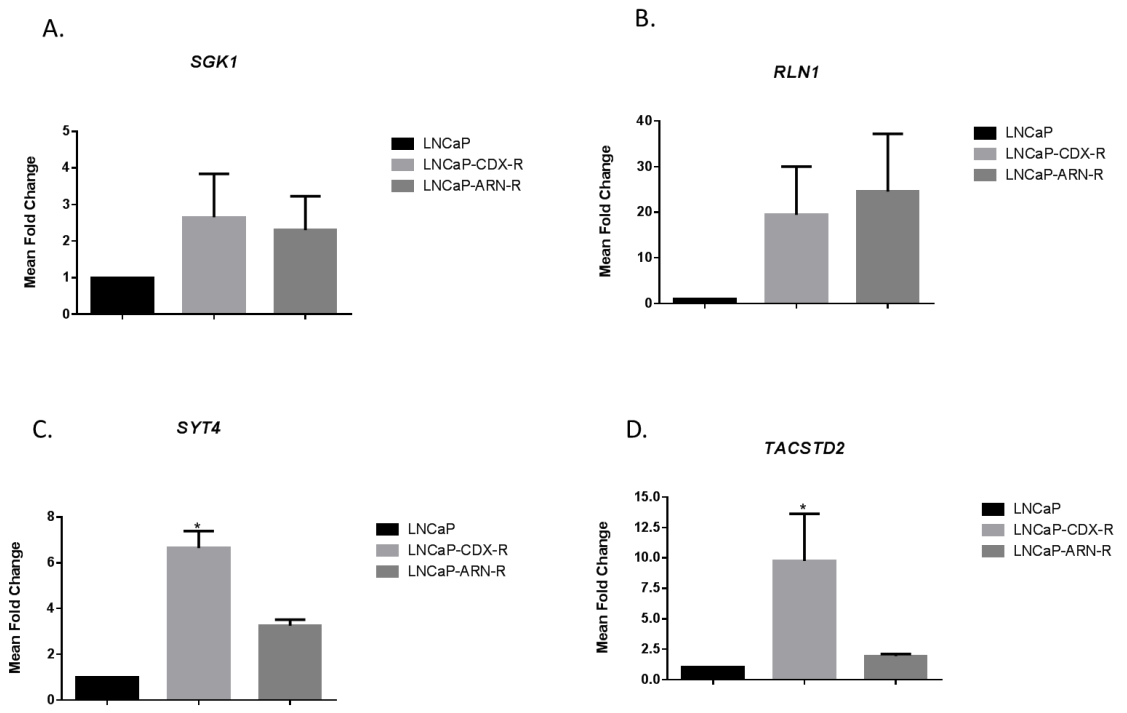

Figure 4-12 Increased expression of SGK1, RLN1, SYT4 and TACSTD2 in Casodex and ARN509 resistant LNCaP derivative cell lines

LNCaP, LNCaP-CDX-R and LNCaP-ARN-R cells were seeded out in 6-well plates. The cells were grown in FM and RNA extracted using Trizol kits. **A**. *SGK1*, **B**. *RLN1*, **C.** *SYT4* and **D**. *TACSTD2* expression was determined by QRT- PCR using specific primers. The relative expression were measured by normalizing all samples to the LNCaP cells. Error bars represent the mean ± SD for triplicate independent experiments. p-values were determined by using student t-test (* p-value <0.05).

4.3 Discussion:

ADT is used to reduce AR activity in PC which achieves a clinical regression in the early stage of the disease. The continued AR signalling in CRPC necessitates development of novel AR inhibitors. Enzalutamide, formally named as MDV3100 is a non-steroidal anti-androgen drug, which was designed to target AR by competitively binding to the ligand binding domain of the AR and inhibiting AR translocation from the cytoplasm to the nucleus and preventing binding to DNA and AR activity. Although patients show initial response to enzalutamide treatment, many patients develop resistance to this second generation anti-androgen. The mechanisms driving resistance are still unclear (Korpal *et al.*, 2013; Beer *et al.*, 2014). An in-house CRPC model (enzalutamide resistant) was developed by growing parental LNCaP cells in escalating doses of enzalutamide. To understand the consequences of the enzalutamide resistance, both parental LNCaP cells and the LNCaP-enzalutamide resistant cell line were tested for phenotypic and biological alterations.

Previously, results showed that both the RAS/RAF/MEK (pERK1/2) and PI3K/Akt/mTOR (pAkt) signalling pathways can be activated through pHER2/pHER3 in LNCaP-ENZ-R cell line (Figure 3-6). To test the effect of pHER2/pHER3 on proliferation, both LNCaP and LNCaP-ENZ-R cell lines were starved in SDM and activated with heregulin. The results from this experiment showed that the parental LNCaP cells proliferation was reduced in SDM and heregulin stimulation increased the proliferation rate as expected. However, proliferation of the LNCaP-ENZ-R cell line was not diminished in SDM and an obvious enhancement in proliferation was apparent following heregulin stimulation (Figure 4-1). This suggests that LNCaP-ENZ-R cells is an androgen independent cell line and that heregulin can enhance proliferation of both cell line. IncuCyte assay has limitation in detecting different morphology of the cells line. However, this was overcome by setting a logarithm are suitable for each cell line.

To study the consequences of enzalutamide resistance on signalling pathways, both LNCaP and LNCaP-ENZ-R cell lines were grown in the presence or absence of enzalutamide for 48 hours. The data from this study showed a possible increase in the expression of pHER2, pHER3 and pAkt in the LNCaP-ENZ-R cell line in the absence or presence of enzalutamide compared to parental LNCaP cells, which confirms the results that were obtained in Chapter 3 (Figure 3-5). Interestingly, pERK5 levels were highest in

the LNCaP line in the absence of enzalutamide and the addition of enzalutamide reduced pERK5 levels. Whereas, in contrast, the lower levels of pERK5 in the LNCaP-ENZ-R cell line were unaffected by the addition of enzalutamide (Figure 4-2). The limitation of this findings is not include total HER2/HER3 and Akt. However, this study showed that higher level of total HER2/HER3 and Akt in last chapter.

To test the enzalutamide effects on the parental LNCaP and LNCaP-ENZ-R cell lines, the proliferation of both cell lines was investigated in the presence and absence of enzalutamide in FM. It can thus be suggested that parental LNCaP cells are more sensitive to enzalutamide treatment. However, enzalutamide did affect proliferation of the LNCaP-ENZ-R cell line but this was not significant (Figure 4-3). This study noticed that LNCaP-ENZ-R cell lines grown faster in medium without enzalutamide this might give two suggestion: either these cells are resistant or they are tolerating the enzalutamide dose. This study suggested that these cells line are resistant as it has been observed previously that enzalutamide half-life was 5.8 days (Gibbons *et al.*, 2015). To prove this suggestion LNCaP and LNCaP-ENZ-R cell lines, cell cycle progression in the presence and absence of enzalutamide was determined. The results showed that in the parental LNCaP cells grown with enzalutamide an accumulation of cells at the G1 phase was noticed compared with LNCaP cells grown in DMSO vehicle control. However, no effect of enzalutamide on the cell cycle progression of LNCaP-ENZ-R was noticed (Figure 4-4). This might suggested that enzalutamide effect on the cell cycle in parental LNCaP. However, the enzalutamide does not effect on the LNCaP-ENZ-R cell cycle, this might put a weight on the hypothesis that LNCaP-ENZ-R are resistant to the enzalutamide rather than tolerating the enzalutamide.

Wound healing assay was applied as another method to study the phenotypic effects of enzalutamide on the LNCaP and LNCaP-ENZ-R cell lines. A long term wound healing assay more than 24 hours cannot distinguish cell proliferation from cell motility. In addition, some cells attached to the edge of the scratch after wounding. This study was tried to measure cell migration using the trans-well assay. The principle of this assay is based on two medium containing chambers separated by 8 μm porous membrane through which cells transmigrate. However, we faced a problem that LNCaP-ENZ-R cell lines was not able to pass through these pores as it was bigger size than parental LNCaP. This study suggested that keep grown the LNCaP-ENZ-R in present of enzalutamide led to change in the morphology of these cells by became bigger in size and more irregular in shape and also slower in the growth than parental LNCaP.

For that reason this study select wound healing assay to measure the cell direction. The results from this assay showed that enzalutamide reduced the migration ability of the parental LNCaP cells. However, no effect was observed for enzalutamide treatment on LNCaP-ENZ-R motility (Figure 4-5). The data above might demonstrates the sensitivity of the parental LNCaP cells and the resistance of the LNCaP-ENZ-R cells to enzalutamide.

The data obtained in this study might suggest that blocking AR is effective in androgen dependent cell lines. However, no effect of AR blocking in androgen resistant cell line was noticed, which might require further in-depth investigation to understand the underling mechanism. Therefore, a gene microarray was applied to investigate the global gene expression differences between the LNCaP-ENZ-R cells compared to parental LNCaP cells in the presence and absence of enzalutamide for 48 hours. Prior to microarray analysis a number of optimisation experiments were performed to ensure that the samples generated for analysis were as consistent and robust as possible in order to ensure that the data generated was of the highest standard. Three consistent experimental replicate were selected for microarray analysis according to AR target genes (*KLK2, KLK3* and *TMPRSS2*) expression in LNCaP-ENZ-R and parental LNCaP cells in the presence or absence of enzalutamide for 48 hours (Figure 4-8). The Illumina Human HT-12 v4.0 Expression Bead Chip technology was used, in order to detect gene expression profiles of LNCaP-ENZ-R cells and parental LNCaP cells in the presence or absence of enzalutamide for 48 hours. To validate the microarray data, another three experimental replicates were generated using the same experimental conditions. The same trends of AR target genes (*KLK2, KLK3* and *TMPRSS2*) expression were obtained in LNCaP and LNCaP-ENZ-R cell lines in the presence and absence of enzalutamide (Figure 4-10). This differences between two experiments could be explain; firstly, this study used different set of RNA than RNA that was used to do the microarray, this to give extra validation of the reproducibility of this experiments. Secondly, this study used different method for RNA extraction. All above might explain the differences were noticed between two validations (Figure 4-8, Figure 4-10).

Only genes that consistently showed an increase in expression in the LNCaP-ENZ-R cells in the presence and absence of enzalutamide compared to LNCaP cells, which have a crucial role in the cell proliferation and growth were selected for further analysis. The activity of these genes was studied in alternative anti-androgen resistant cell lines to try to give a better understanding of the mechanism of enzalutamide resistance.

According to the microarray data, *SGK1* is one of the genes that showed a significant increase in the expression at the mRNA in LNCaP-ENZ-R cells compared to LNCaP cell line. To validate the microarray data for *SGK1* by QRT-PCR, the same experimental condition was applied in the studied cell line and the same trend of microarray results was obtained which is consistent with (Arora *et al.*, 2013) microarray data xenograft derived from enzalutamide resistant tumour which showed an increase in *SGK1* expression (Figure 4-11 A).

TACSTD2 is another gene which showed significant increase in the expression in LNCaP-ENZ-R cells in the presence and absence of enzalutamide for 48 hours compared to LNCaP cells and the validation with QRT-PCR showed the same trends as the microarray data which is in agreement with (Trerotola *et al.*, 2015) who showed that TROP2 is up-regulated in human PC with extracapsular extension as compared to organ-confined (Figure 4-11 B).

RLN1 and *RLN2* are genes which showed a significant increase in their expression in the LNCaP-ENZ-R cells compared to the LNCaP cells according to the microarray data and the validation with QRT-PCR showed the same trends as the microarray results. The data obtained in this study was consistent with what has been suggested as an increase in the expression of the *RLN1* and *RLN2* was observed in recurrent prostate cancer compared to normal prostate tissue (Feng *et al.*, 2007) (Figure 4-11 C, D).

SYT4 another gene which showed a significant increased expression in the LNCaP-ENZ-R cells in the presence and absence of enzalutamide for 48 hours compared to LNCaP cells and the validation with QRT-PCR showed the same trends as the microarray data. *SYT4* was also found to be upregulated in the bicalutamide resistant PC model which is consistent with this study (Vias *et al.*, 2007) (Figure 4-11 E).

From the data above, an increase in the expression of *SGK1*, *TACSTD2, RLN1, RLN2* and *SYT4* was noticed in the LNCaP-ENZ-R cell line. To test if this effect also applied in other PC resistant cell line, the expression of the *SGK1*, *TACSTD2, RLN1, RLN2* and *SYT4* was examined in the LNCaP-CDX-R and LNCaP-ARN-R cell lines, that are resistant to bicalutamide (casodex) and ARN509, respectively. High expression of *SYT4* and *TACSTD2* was noticed in the LNCaP-CDX-R compared to LNCaP-ARN-R cell lines, this finding need extra experiment to prove this results. The results showed an increase in the expression of all 4 genes in these 2 cell lines at mRNA level (Figure 4-12), which might suggest that these genes have a common role in the anti-androgen drug resistance.

Chapter 5. Identification of SGK1 as a potential therapeutic target in castrate resistance prostate cancer

5.1 Introduction

Serum and glucocorticoid regulated kinase 1 (SGK1) is a member of the 16-strong AGC family of serine/threonine protein kinases, which also contains Akt and protein kinase C. There are three isoforms of SGK (SGK1, SGK2 and SGK3). The SGK family controls a variety of ion channels (such as Na^+ ions channels) and the Na^+/K^+-ATPase. They are regulated by several stimuli, including glucocorticoids and serum. The kinase is activated by growth factors and insulin, phosphorylating SGK1, as well as other AGC family members such as Akt and S6K, at a threonine residue, within the T-loop of the kinase domain and a serine residue of the C-terminal hydrophobic motif Ser422. PDK1 (phosphoinositide dependent kinase 1) phosphorylates SGK1 at the T-loop, while mTORC1 (mammalian target of rapamycin complex 1) activates SGK1 at the hydrophobic motif Ser422 (García-Martínez and Alessi, 2008).

Hong *et al.* (2008) demonstrated that SGK1 is an mTORC1 substrate and that an inducible overexpression of mTORC1 can activate both Akt and SGK1. Another study showed that Akt inhibitor-resistant breast cancer cells display markedly elevated SGK1, while an Akt inhibitor-sensitive cell line displayed low levels of SGK1 (Sommer *et al.,* 2013). Furthermore, the group demonstrated that knockdown of SGK1 significantly reduced the proliferation of these resistant cell lines. However, no effect of the knockdown of SGK1 was observed on the Akt inhibitor-sensitive cell line (Sommer *et al.,* 2013). It has also been shown that SGK1 is able to phosphorylate p27, which may suggest a role in cell cycle progression, as demonstrated in a melanoma cancer cell line (Hong *et al.,* 2008).

In prostate cancer, AR regulation of SGK1 has been identified in the LNCaP cells, where upregulation of SGK1 transcript levels was observed in response to androgen treatment and a novel SGK1 inhibitor, GSK650394, which inhibits the enzymatic activity of SGK1 and SGK2, decreased LNCaP cell growth (Sherk *et al.,* 2008).

A study aimed to investigate the acquired resistance mechanisms to ADT, they employed AR-dependent LNCaP/AR (LNAR) mouse xenograft model that previously used to demonstrate the activity of enzalutamide. The method were in this study was injected LNAR subcutaneously into castrate mice and treated with either vehicle or enzalutamide for a long period of time until resistant tumors formed. Same study identified GR upregulation is a driver of enzalutamide resistance. In addition, same research group using

immunohistochemistry (IHC) in five tumor-normal pairs, they found that GR is robustly expressed in both basal and luminal cells in normal prostate tissue, but substantially reduced in primary prostate cancer. finally they have characterized a novel enhancer at the GR locus, demonstrated that this enhancer is required for GR expression, and shown that AR binding at the enhancer is coupled with reduced GR expression (Shah *et al.*, 2017). The glucocorticoid receptor (GR) is another receptor that regulates SGK1 transcription through a GRE region located at the SGK promoter. Existence of this region provides a direct molecular basis for the transcriptional activation of SGK1 by dexamethasone (Maiyar *et al.*, 1997).

A previous study in our lab demonstrated that GR is upregulated in a LNCaP-enzalutamide resistant cell line, compared to parental LNCaP cells (unpublished data). The role of AR and GR in the regulation of SGK1 in enzalutamide-resistant cells remains unclear. For that reason, the aims of this chapter are:

1. To investigate the role of AR in the regulation of SGK1 in LNCaP-ENZ-R cells, compared to that in LNCaP parental cells.

2. To investigate the role of GR in the regulation of SGK1 in LNCaP-ENZ-R cells, compared to that in LNCaP parental cells.

3. To identify the role of SGK1 in the proliferation and migration of LNCaP-ENZ-R cells, compared to that in LNCaP parental cells.

Figure 5-1 Domain structure of SGK1 demonstrating the two essential phosphorylation sites, T256 and Ser422. Adapted from (Bogusz *et al.*, 2006)

5.2 Results

5.2.1 High expression of SGK1 in LNCaP-ENZ-R cells at the mRNA and protein level

In the previous chapter, an increase in the expression of SGK1 in the LNCaP-ENZ-R cell line compared to LNCaP parental cells was detected by microarray data and QRT-PCR (Figure 4-11 B) and (Figure 5-2 A). To elucidate SGK1 expression at the protein level in the same experimental condition as in microarray study, an antibody was used to detect SGK1. The data showed a small increase in the expression of SGK1 in LNCaP-ENZ-R cells at the protein level in the presence and absence of enzalutamide (Figure 5-2 B).

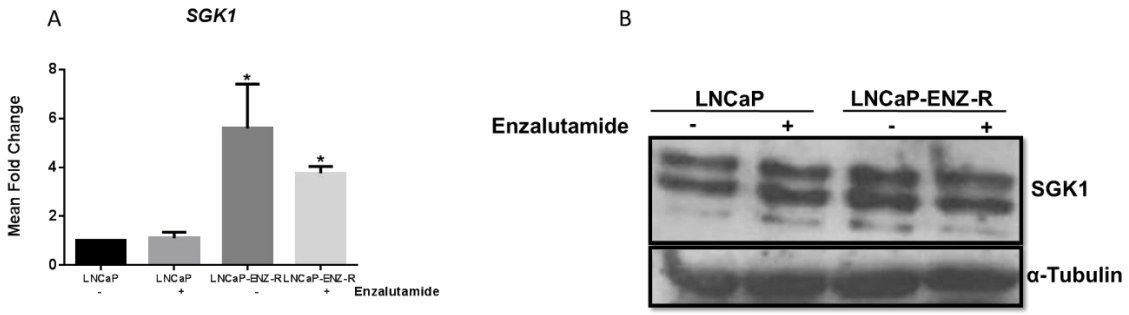

Figure 5-2 High expression of SGK1 in LNCaP-ENZ-R cells at the mRNA and protein level

LNCaP and LNCaP-ENZ-R cells were seeded out in 6-well plate. Cells were grown in FM simultaneously with or without 10µM enzalutamide for 48 hours and DMSO used as a control. **A.** mRNA level of *SGK1* expression was determined by QRT- PCR using specific primers and the relative expression was measured with normalisation of all sample to LNCaP cells. **B.** SGK1 protein expression in parental LNCaP and LNCaP-ENZ-R cells were determined by western blotting. Alpha-tubulin was used as a loading control (representative blot). Error bars represent the mean ± SD for triplicate independent experiments. p-values were determined by using student t-test (* p-value <0.05).

5.2.2 SGK1 expression in parental LNCaP cells in response to DHT stimulation

To investigate SGK1 regulation in androgen-dependent cells, parental LNCaP cells were activated with increasing doses of DHT (0.1nM, 1nM and 10nM) for 24 hours and 48 hours. The mRNA and protein levels of SGK1 were detected using QRT-PCR and western blotting. The results demonstrated an increase in SGK1 expression in response to DHT stimulation at the protein level, which was more pronounced after 48 hours of stimulation (Figure 5-3 C). Similarly, an increase in the expression of *SGK1* was detected at the mRNA level in response to the DHT (Figure 5-3 A, B).

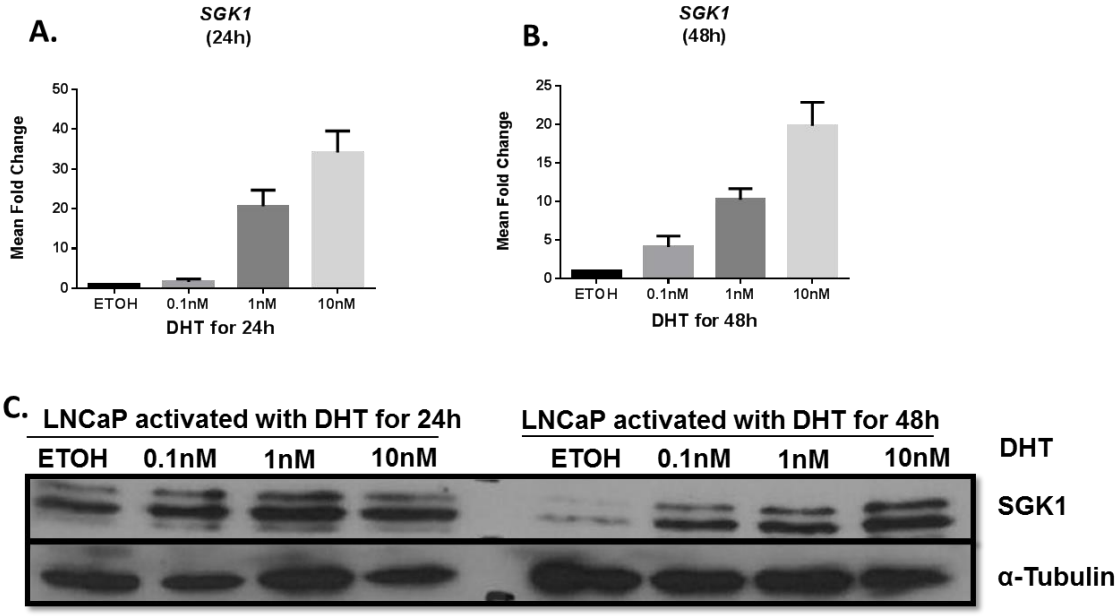

Figure 5-3 Increased expression of SGK1 in parental LNCaP cells in response to DHT stimulation

LNCaP cells were seeded out on 6-well plates. The cells were grown in SDM for 48 hours then activated with 0.1nM, 1nM or 10nM DHT for 24 hours and 48 hours. The cells were then lysed in RIPA buffer for protein samples and Trizol kits were used for RNA extraction. **A.** mRNA level of *SGK1*, which was activated with DHT for 24 hours, then the expression was determined by QRT-PCR using specific primer and the relative expression was measured by normalisation of all samples to LNCaP cells in ethanol. **B.** mRNA level of SGK1, which was activated with DHT for 48 hours, then the expression was determined by QRT-PCR using specific primer and the relative expression was measured by normalisation of all samples to LNCaP cells in ethanol. **C.** SGK1 protein expression in parental LNCaP cells was activated by DHT for 24 hours and 48 hours respectively. Alpha-tubulin was used as a loading control. Error bars represent the mean ± SD for triplicate independent experiments (representative blot).

5.2.3 SGK1 expression in LNCaP-ENZ-R cell line in response to DHT stimulation

To investigate SGK1 regulation in a cell line model of anti-androgen drug-resistance, LNCaP-ENZ-R cells were activated with increasing doses of DHT (0.1nM, 1nM and 10nM) for 24 hours and 48 hours. The mRNA and protein levels of *SGK1* were detected using QRT-PCR and western blotting respectively. The results demonstrated an increase in SGK1 expression in response to DHT stimulation at the protein level, particularly noticeable at 48 hours (Figure 5-4 C). Similarly, an increase in the expression of SGK1 was detected at the mRNA level in response to DHT (Figure 5-4 A, B).

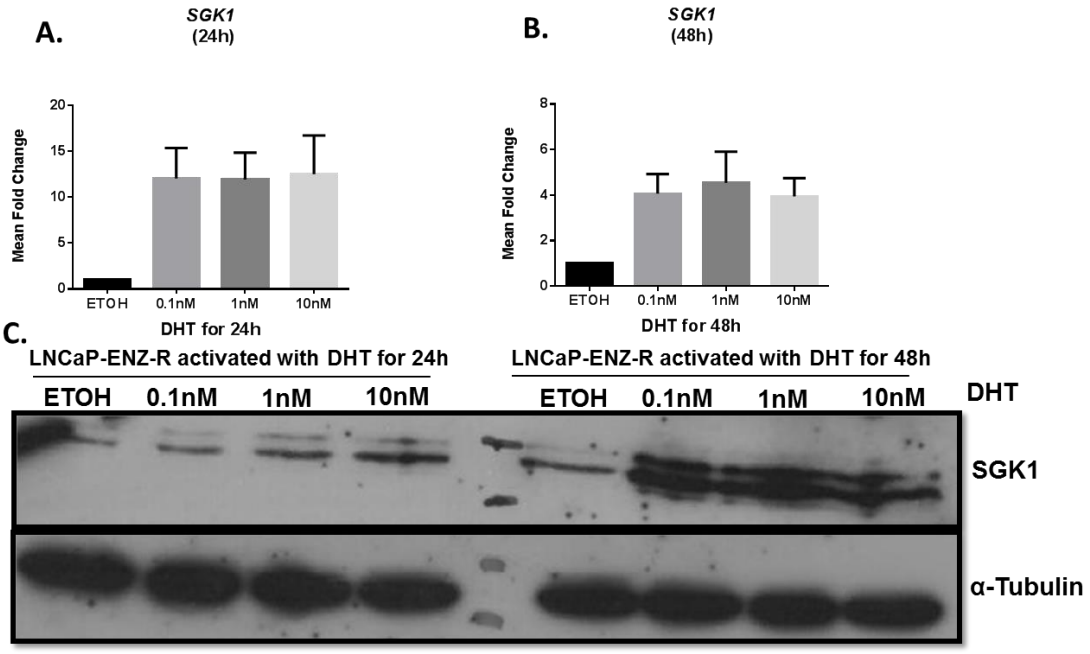

Figure 5-4 Increased expression of SGK1 in LNCaP-ENZ-R cells in response to DHT stimulation

LNCaP-ENZ-R cells were seeded out on 6-well plates. The cells were grown in SDM for 48 hours, then activated with 0.1nM, 1nM or 10nM DHT for 24 hours and 48 hours. The cells were then lysed in a RIPA buffer for protein samples and Trizol kits were used for RNA extraction. **A**. mRNA level of *SGK1*, which was activated with DHT for 24 hours, then the expression was determined by QRT-PCR using specific primer and the relative expression was measured by normalisation of all samples to LNCaP-ENZ-R cells in ethanol. **B**. mRNA level of *SGK1* which was activated with DHT for 48 hours, then the expression was determined by QRT-PCR using specific primer and the relative expression was measured by normalisation of all samples to LNCaP-ENZ-R cells in ethanol. **C**. SGK1 protein expression in LNCaP-ENZ-R cells. Cells were activated by DHT for 24 hours and 48 hours. Alpha-tubulin was used as a loading control. Error bars represent the mean ± SD for triplicate independent experiments (representative blot).

5.2.4 SGK1 expression in parental LNCaP cells in response to dexamethasone stimulation

SGK1 encodes an AGC-family kinase that is known to be transcriptionally upregulated by both AR and GR (Isikbay *et al.*, 2014). To study the role of GR in the regulation of SGK1 in an androgen-dependent cell line, increasing doses of dexamethasone were used to stimulate GR in LNCaP cells for 24 and 48 hours. The results showed an increase in the expression of *SGK1* at the mRNA level (Figure 5-5 A, B). However, no change in SGK1 expression was detected at the protein level (Figure 5-5 C).

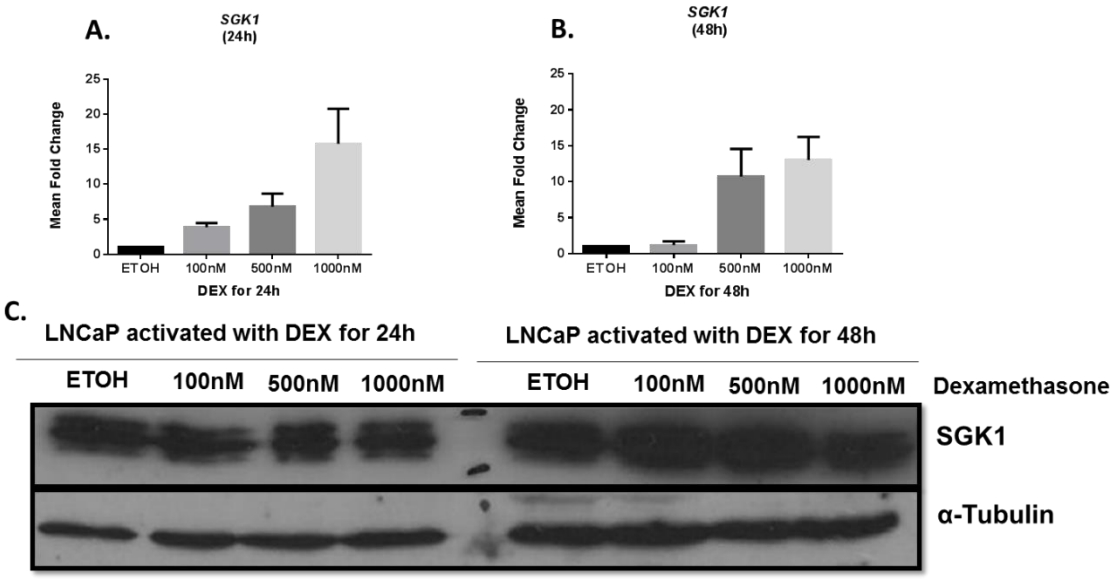

Figure 5-5 Increased mRNA expression of SGK1, but not protein expression in parental LNCaP cells in response to dexamethasone stimulation

LNCaP cells were seeded out on 6-well plates. The cells were grown in SDM for 48 hours, then activated with 100nM, 500nM and 1000nM of dexamethasone for 24 hours and 48 hours. The cells were then lysed in RIPA buffer for protein samples and Trizol kits were used for RNA extraction. **A**. mRNA level of *SGK1*, which was activated with dexamethasone for 24 hours, then the expression was determined by QRT-PCR using specific primer and the relative expression was measured by normalisation of all samples to LNCaP cells in ethanol. **B**. mRNA level of *SGK1*, which was activated with dexamethasone for 48 hours, then the expression was determined by QRT-PCR and the relative expression was measured by normalisation of all samples to LNCaP cells in ethanol. **C**. SGK1 protein expression in parental LNCaP cells. Cells were activated by dexamethasone for 24 hours and 48 hours. Alpha-tubulin was used as a loading control. Error bars represent the mean ± SD for triplicate independent experiments (representative blot).

5.2.5 Increased expression of SGK1 in LNCaP-ENZ-R cells in response to dexamethasone stimulation at mRNA and protein levels

Following the investigation of the role of GR in the regulation of SGK1 in an androgen dependent cell line, the investigation was extended to include the LNCaP-ENZ-R cell line. Increasing doses of dexamethasone were used to stimulate GR activity for 24 and 48 hours. The results showed that GR stimulation by dexamethasone increases the expression of SGK1 at the mRNA and protein level (Figure 5-6).

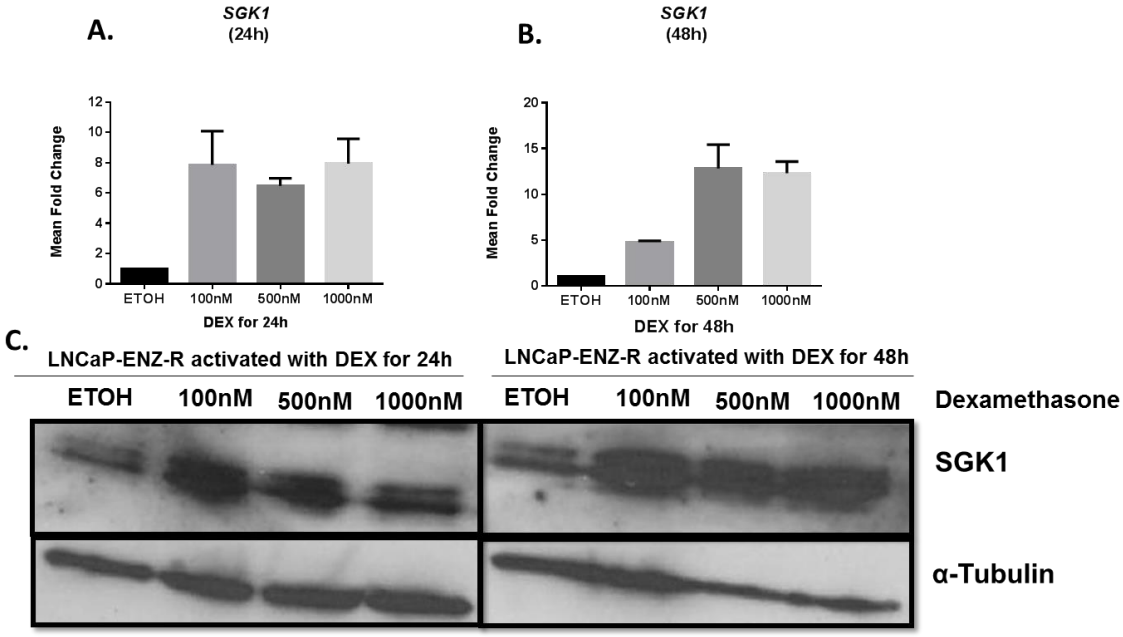

Figure 5-6 Increased expression of SGK1 in LNCaP-ENZ-R at mRNA and protein level in response to dexamethasone stimulation

LNCaP-ENZ-R cells were seeded out on 6-well plates. The cells were grown in SDM for 48 hours, then activated with 100nM, 500nM and 1000nM dexamethasone for 24 hours and 48 hours. The cells were then lysed in a RIPA buffer for protein samples and Trizol kits were used for RNA extraction. **A**. mRNA level of *SGK1*, which was activated with dexamethasone for 24 hours, then the expression was determined by QRT-PCR using specific primers and the relative expression was measured with normalisation of all samples to LNCaP-ENZ-R cells in ethanol. **B**. mRNA level of *SGK1*, which was activated with dexamethasone for 48 hours, then the expression was determined by QRT-PCR and the relative expression was measured with normalisation of all samples to LNCaP-ENZ-R cells in ethanol. **C**. SGK1 protein expression in LNCaP-ENZ-R cells. Cells were activated by dexamethasone for 24 hours and 48 hours. Alpha-tubulin was used as a loading control. Error bars represent the mean ± SD for triplicate independent experiments (representative blot).

5.2.6 Enzalutamide increases GR expression in parental LNCaP and LNCaP-ENZ-R cells

AR and GR are similar in their structure and it has been demonstrated that GR can induce expression of *PSA* upon stimulation with dexamethasone (Cleutjens *et al.*, 1997). AR and GR share several transcriptional targets, including anti-apoptotic genes SGK1 and MAP kinase phosphatase 1 (MKP1) (Isikbay *et al.*, 2014). To identify the role of GR in the resistant cell line model, relative GR mRNA and protein expression was investigated in parental LNCaP and LNCaP-ENZ-R cells. The results showed that treatment with enzalutamide significantly increases the expression of the GR at the protein and mRNA levels in both cell lines ($p < 0.05$) (Figure 5-7).

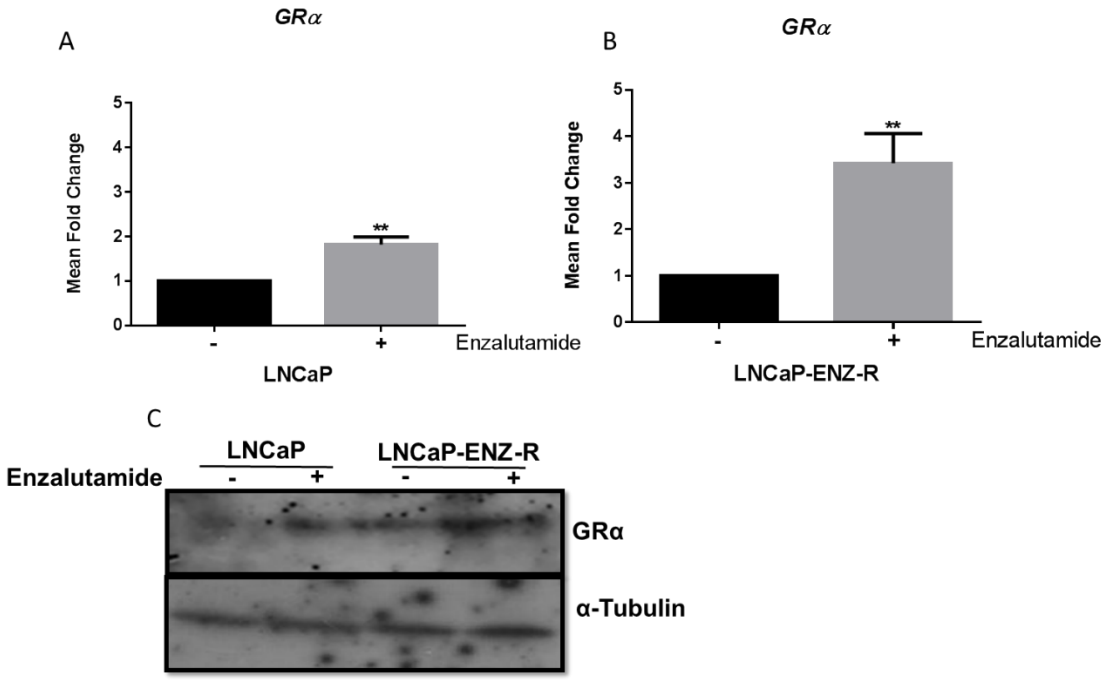

Figure 5-7 Enzalutamide treatment increases GR expression in parental LNCaP and LNCaP-ENZ-R cells

LNCaP and LNCaP-ENZ-R cells were seeded out on 6-well plates. The cells were grown in FM simultaneously with or without 10µM enzalutamide for 48 hours. The cells were lysed in a RIPA buffer. **A**. mRNA expression of *GRα* in LNCaP cells. **B**. mRNA expression of *GRα* in LNCaP-ENZ-R cells. **C**. GRα protein expression in parental LNCaP and LNCaP-ENZ-R cells. Alpha-tubulin was used as a loading control. Error bars represent the mean ± SD for triplicate independent experiments. p-values were determined by using student t-test (* p-value <0.05, ** p-value <0.01m) (representative blot).

5.2.7 Dexamethasone does not lead to upregulation of selected AR target genes in parental LNCaP cells

Previous experiments have demonstrated that blocking AR with enzalutamide led to increasing the expression of GR in LNCaP cells. Higher expression of GR in LNCaP-ENZ-R cells, in the presence and absence of enzalutamide was also noticed at the protein level. To investigate the role of GR in the regulation of selected AR target genes (*KLK3*, *FKBP5*, *KLK2* and *TMPRSS2*), GR was stimulated with dexamethasone and AR target genes were detected using QRT-PCR in parental LNCaP cells. The results showed that GR stimulation does not change the expression of *KLK3*, *FKBP5* and *KLK2*. However, it was noticed a reduction in the expression of *TMPRSS2*, although this did not reach significance (Figure 5-8).

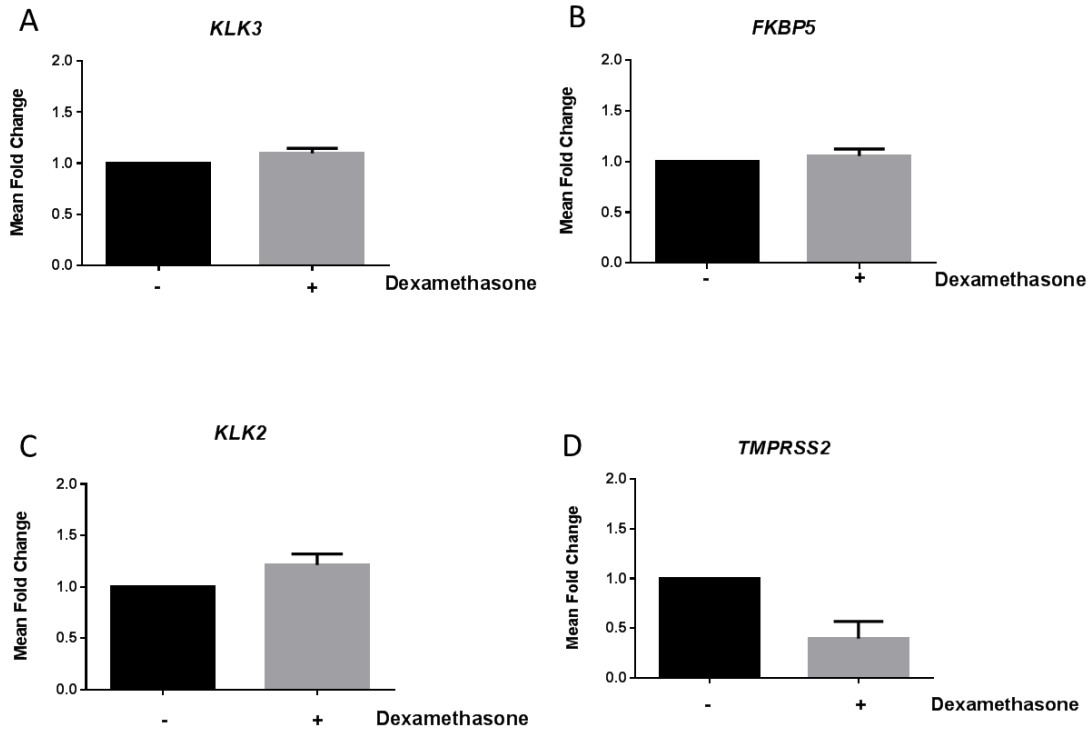

Figure 5-8 Dexamethasone does not lead to upregulation of AR target genes in parental LNCaP cells

LNCaP cells were seeded out in 6-well plates. The cells were grown in SDM for 48 hours then activated with 100nM dexamethasone for 24 hours and ethanol was used as a control. Trizol kits were used for RNA extraction. **A.** *KLK3* **B.** *FKBP5* **C**. *KLK2* **D.** *TMPRSS2* at mRNA level were determined by QRT-PCR. Error bars represent the mean ± SD for triplicate independent.

5.2.8 Dexamethasone activation leads to upregulation of selected AR target genes in LNCaP-ENZ-R cell line

Further validation extended to the LNCaP-ENZ-R cell line to investigate the role of GR in regulation of AR target genes (*KLK3, FKBP5, KLK2* and *TMPRSS2*), GR was stimulated by dexamethasone and AR target genes were detected by using QRT-PCR in the LNCaP-ENZ-R cell line. The results showed that dexamethasone activation led to a significant increase in the expression of *KLK3, FKBP5, KLK2* and *TMPRSS2* ($p < 0.05$) (Figure 5-9).

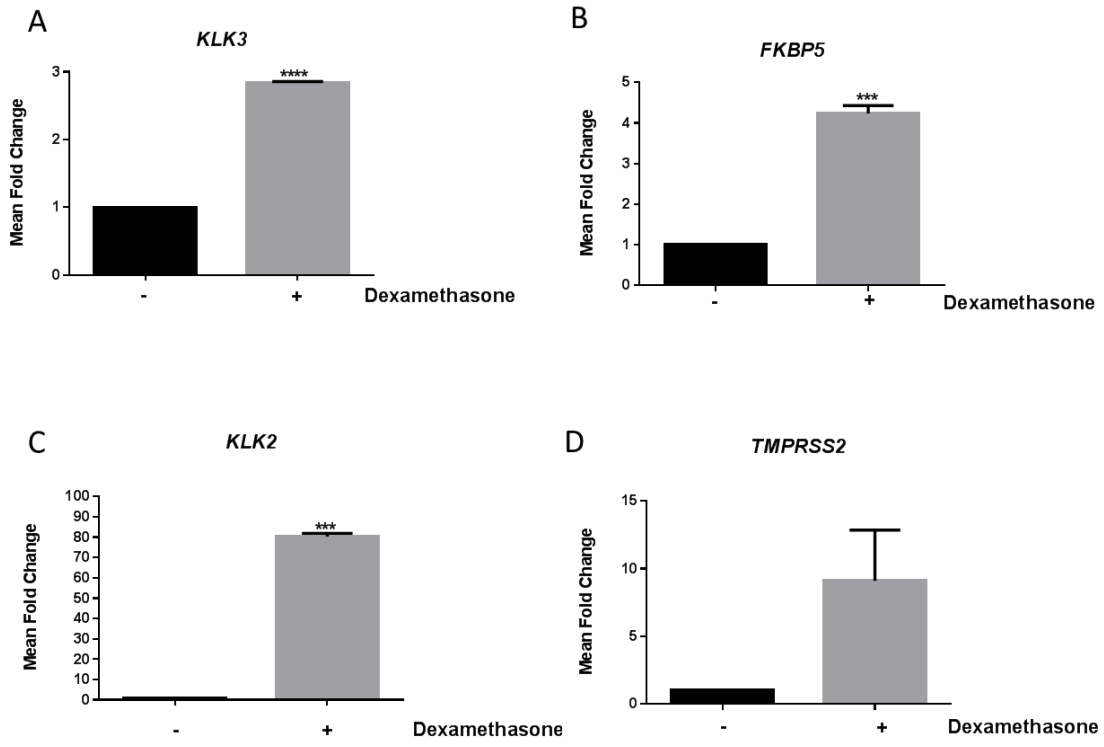

Figure 5-9 Dexamethasone activation leads to the upregulation of selected AR target genes in LNCaP-ENZ-R cells

LNCaP-ENZ-R cells were seeded out in 6-well plates. The cells were grown in SDM for 48 hours then activated with 100nM dexamethasone for 24 hours. Trizol kits were used for RNA extraction. **A.** *KLK3* **B.** *FKBP5* **C**. *KLK2* **D.** *TMPRSS2* at mRNA level were determined by QRT-PCR. Error bars represent the mean ± SD for triplicate independent. p-values were determined by using student t-test (* p-value <0.05, ** p-value <0.01, *** p-value <0.001 and **** p- value < 0.0001).

5.2.9 Knockdown of GR has no effect on the expression of selected AR target genes in parental LNCaP cells

To add further weight to the findings from the previous experiment (Figure 5-8), GR expression was decreased using two specific oligos. The effect on selected AR target genes was investigated using QRT-PCR in LNCaP cells. The result showed that the knockdown of GR increased SGK1 expression. However, no change was detected at the mRNA level of either *KLK3* or *FKBP5* (Figure 5-10).

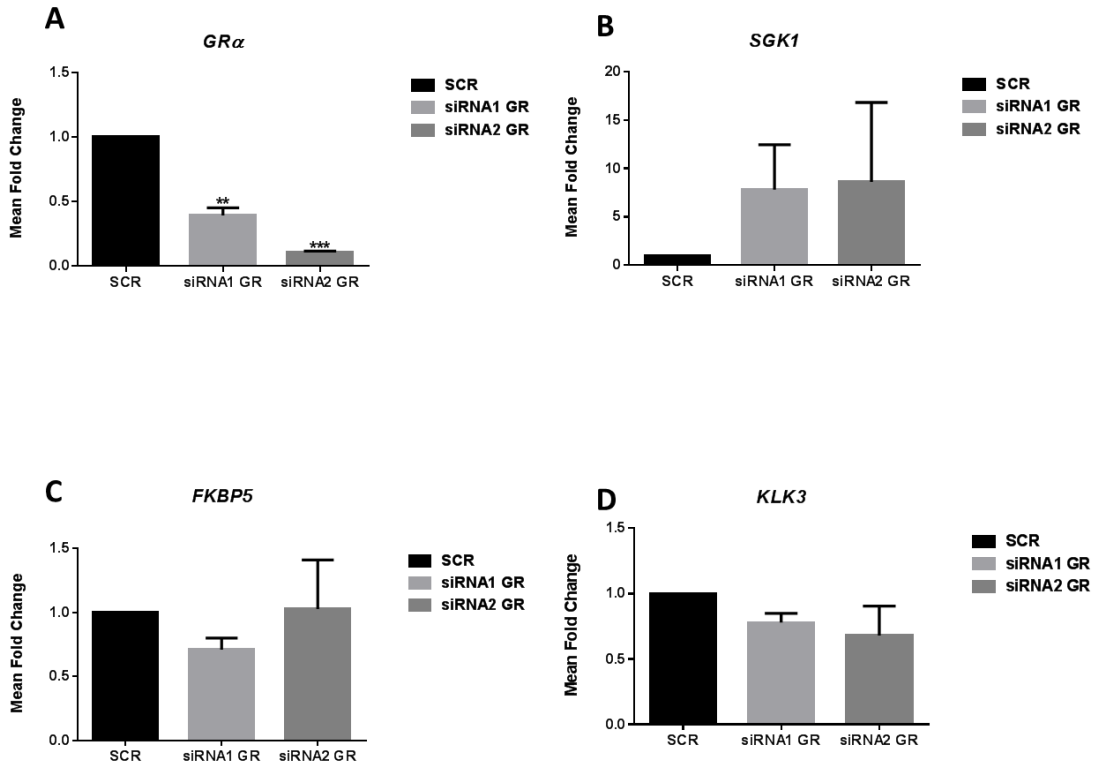

Figure 5-10 Knockdown of GR has no significant effect on the expression of selected AR target genes in parental LNCaP cells

LNCaP cells were reverse transfected with two selected oligos against GR for 72 hours. Non-silencing oligo was used as a control. RNA was extracted and the expression level of **A**. *GR*, **B**. *SGK1*, **C**. *FKBP5* and **D**. *KLK3* at mRNA level were determined by QRT-PCR. Error bars represent the mean ± SD for triplicate independent experiments. p-values were determined by using student t-test (* p-value <0.05, ** p-value <0.01, *** p-value <0.001).

5.2.10 Knockdown of GR decreases the expression of selected AR target genes in LNCaP-ENZ-R cells

Further investigation into potential GR regulation of AR target genes was extended to the LNCaP-ENZ-R cell line. GR was knocked down using two selected oligos and selected AR target gene expression was investigated using QRT-PCR in LNCaP-ENZ-R cells. The results showed that the knockdown of GR decreases SGK1 expression but not significantly. However, the knockdown of GR significantly decreases the mRNA level of *KLK3* and *FKBP5* ($p < 0.05$) (Figure 5-11).

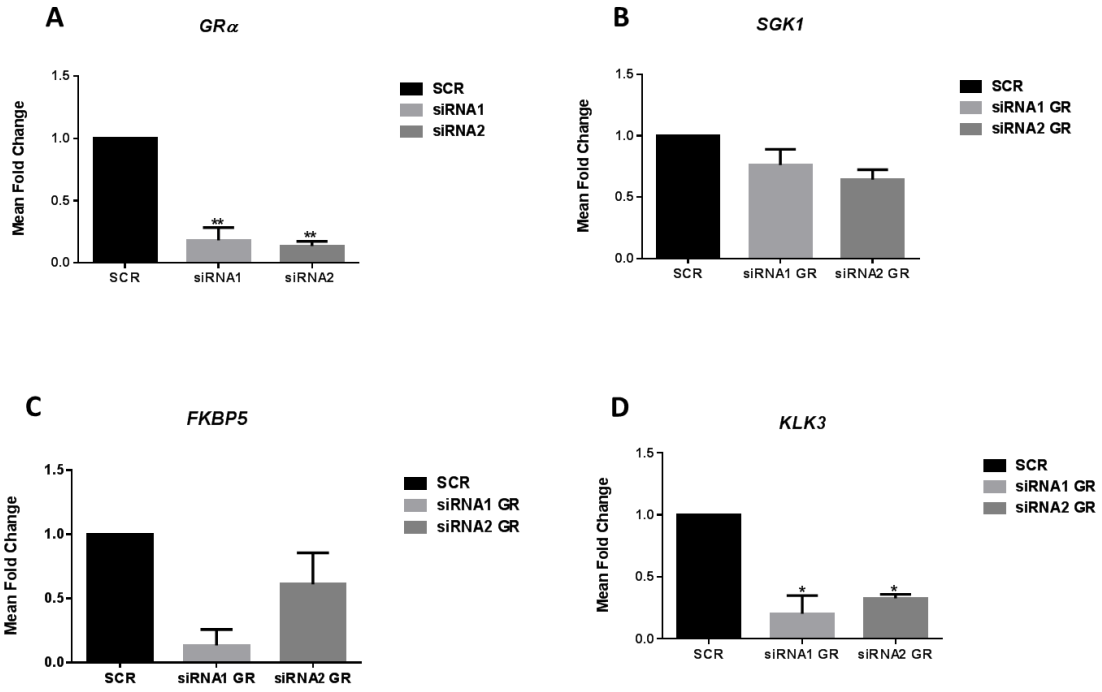

Figure 5-11 Knockdown of GR significantly decreases the expression of selected AR target genes in LNCaP-ENZ-R cells

LNCaP-ENZ-R cells were reverse transfected with two selected oligos against GR for 72 hours. Non-silencing oligo was used as a control. RNA was extracted and the expression level of **A**. *GR*, **B**. *SGK1*, **C**. *FKBP5* and **D**. *KLK3* at mRNA level were determined by QRT-PCR. Error bars represent the mean ± SD for triplicate independent experiments. p-values were determined by using student t-test (* p-value <0.05, ** p-value <0.01).

5.2.11 Blockade of AR activity decreases SGK1, KLK3 and FKBP5 expression while activation of AR increases SGK1, KLK3 and FKBP5 expression in parental LNCaP cells

To confirm the theory that SGK1 may potentially be regulated by AR but not by GR in parental LNCaP cells, LNCaP cells were grown in full media and transfected with siRNA against GR for 72 hours. The cells were cultured simultaneously with and without enzalutamide. SGK1, KLK3 and FKBP5 were detected using QRT-PCR. The results showed that enzalutamide treatment led to a decrease in the expression of SGK1, KLK3 and FKBP5, with no significant effects noticed in the expression of SGK1, KLK3 and FKBP5 in response to GR knockdown (Figure 5-12 A, B, C). To confirm the previous experiment, parental LNCaP cells were transfected with siRNA against GR for 72 hours in SDM, then the cells were stimulated with DHT for 24 hours. The data indicated that the stimulation of LNCaP cells with DHT led to an increase in the expression of SGK1, KLK3 and FKBP5. However no effect of GR knockdown was observed on the expression of the SGK1, KLK3 and FKBP5 in agreement with the results of the previous experiment. Also the data showed that knockdown of GR does not abrogate the effects of DHT on the expression SGK1, KLK3 and FKBP5 (Figure 5-12 D, E, F).

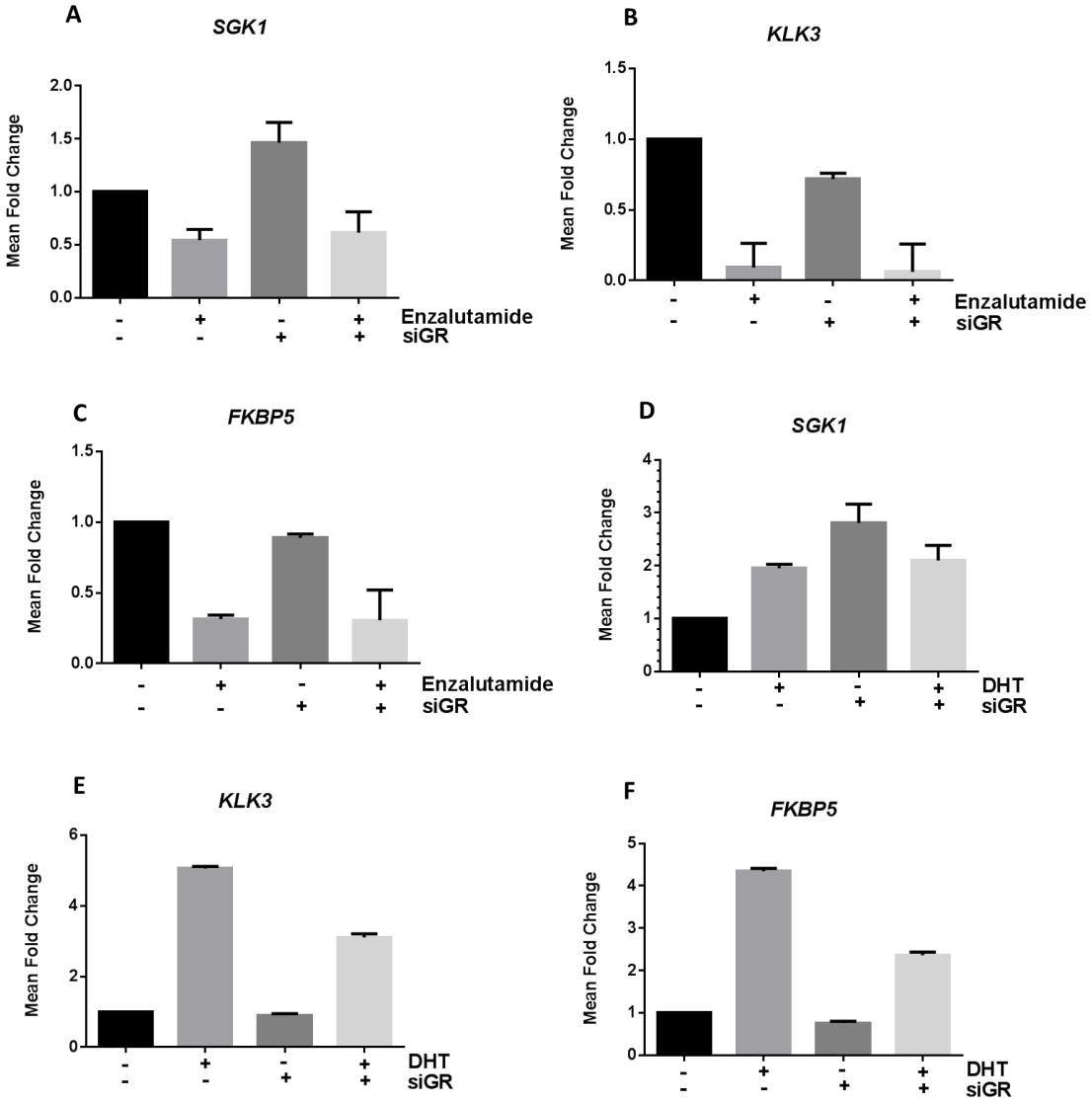

Figure 5-12 Blockade of AR activity decreases the expression of *SGK1, KLK3* and *FKBP5*, while activation of AR increases the expression of *SGK1, KLK3* and *FKBP5* in parental LNCaP cells

LNCaP cells were reverse transfected with one selected oligo against GR for 72 hours, then the cells were cultured with or without 10μM enzalutamide. Non-silencing oligo was used as a control without enzalutamide. RNA was extracted and the expression level of **A**. *SGK1*, **B**. *KLK3*, **C**. *FKBP5* at mRNA level were determined by QRT-PCR. LNCaP cells were reverse transfected with one specific oligo against GR for 72 hours in SDM, then the cells were cultured for 48 hours then treated with 10nM of DHT for 24 hours. Non-silencing oligo was used as a control without DHT. RNA was extracted and the expression level of **D**. *SGK1*, **E**. *KLK3*, **F**. *FKBP5* at mRNA level were determined by QRT-PCR. Error bars represent the mean ± SD for triplicate independent experiments.

5.2.12 Blockade of AR activity increases of selected AR target genes expression, while GR knockdown leads to a decrease in selected AR target genes expression in LNCaP-ENZ-R cells

To add weight to the theory that GR can regulate SGK1 and AR target genes in LNCaP-ENZ-R cells, the LNCaP-ENZ-R cells were grown in full media and transfected with siRNA against GR for 72 hours. The cells were cultured simultaneously with or without enzalutamide. *SGK1, KLK3* and *FKBP5* were detected using QRT-PCR. The results demonstrated that the presence or absence of enzalutamide had no effect on SGK1 expression in LNCaP-ENZ-R cells and GR knockdown leads to a decrease in the expression of SGK1. Enzalutamide treatment led to an increase in the expression of *KLK3* and *FKBP5*. Blocking AR increases the level of AR target genes whereas blocking the AR increases the level of GR, This supports the results obtained from (Figure 5-7).

A decrease in the expression of *KLK3* and *FKBP5* in response to GR knockdown simultaneously with or without enzalutamide was noticed (Figure 5-13 A, B, C). To confirm the previous experiment, LNCaP-ENZ-R was transfected with siRNA against GR for 72 hours in SDM, then the cells were stimulated with DHT for 24 hours. The data indicated that stimulation of LNCaP with DHT led to an increase in the expression of *SGK1, KLK3* and *FKBP5*, which confirm the earlier results (Figure 5-4), indicating that AR might regulate SGK1 in LNCaP-ENZ-R cells. Also the results showed that GR knockdown led to a decrease in the expression of *SGK1, KLK3* and *FKBP5*, which confirms the results of previous experiments. Interestingly, the data demonstrated that knockdown of GR does not abrogate the DHT effect on the expression of SGK1. This confirms the previous results obtained from (Figure 5-4) and (Figure 5-6) which indicated that AR and GR are both able to regulate SGK1. However, knockdown of GR abrogates the effects of DHT on the expression of *KLK3* and *FKBP5* (Figure 5-13 D, E, F).

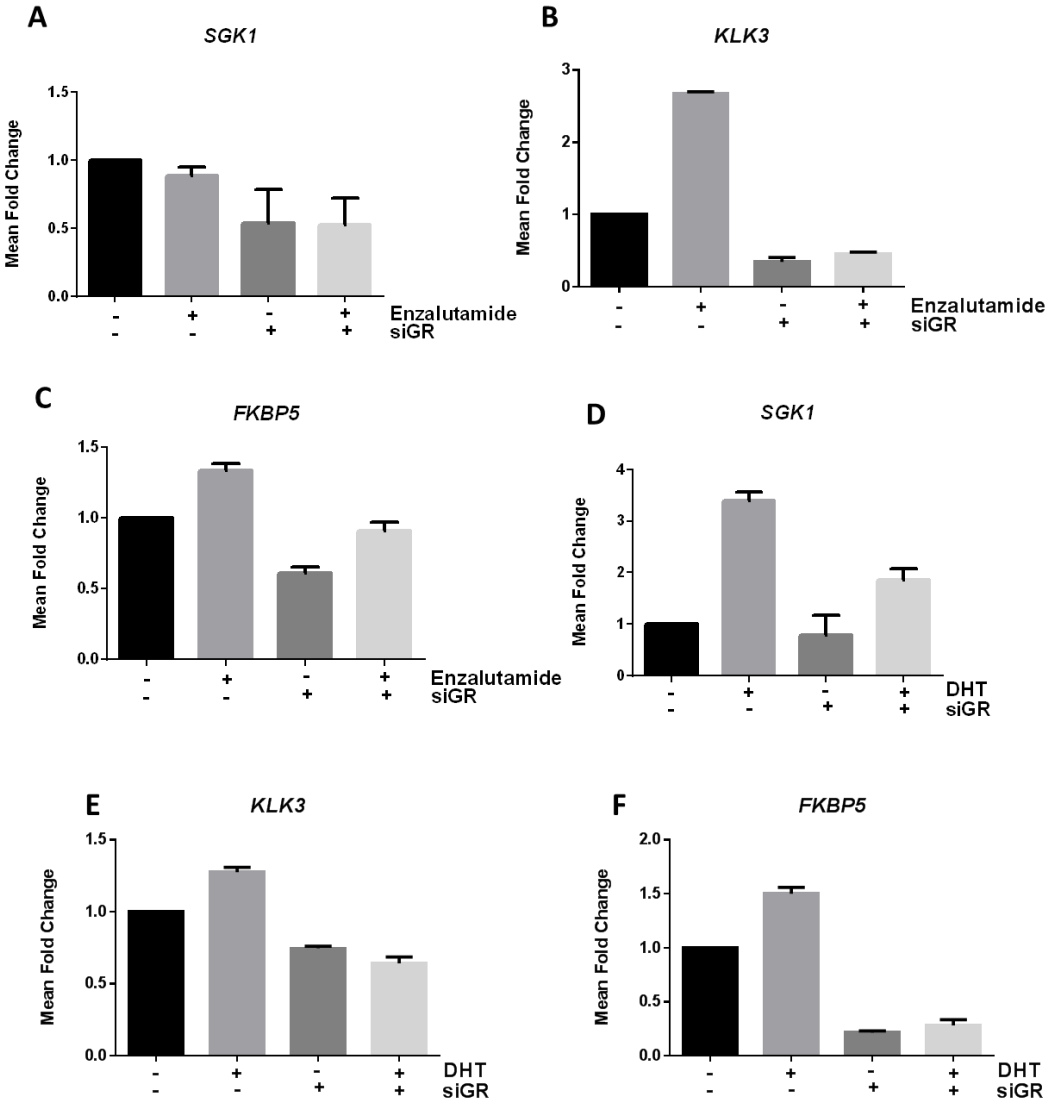

Figure 5-13 Blockade of AR activity increases the expression of AR target genes while GR knockdown leads to a decrease in the expression of AR target genes in LNCaP-ENZ-R cells

LNCaP-ENZ-R cells were reverse transfected with one selected oligo against GR for 72 hours, then the cells were cultured simultaneously with or without 10μM enzalutamide. Non-silencing oligo was used as a control. RNA was extracted and the expression level of **A**. *SGK1*, **B**. *KLK3*, **C**. *FKBP5* at mRNA level was determined by QRT-PCR. LNCaP-ENZ-R cells were reverse transfected with one selected oligo against GR for 72 hours in SDM, then the cells were cultured for 48 hours and treated with 10nM DHT for 24 hours. Non-silencing oligo was used as a control without DHT. RNA was extracted and the expression level of **D**. *SGK1*, **E**. *KLK3*, **F**. *FKBP5* at mRNA level was determined by QRT-PCR. Error bars represent the mean ± SD for triplicate independent experiments.

5.2.13 pSGK1-Ser422 induction by dexamethasone stimulation in LNCaP cells

To investigate the activity of SGK1 in parental LNCaP and LNCaP-ENZ-R cells, pSGK1-S422 protein expression was determined in response to increasing doses of dexamethasone, stimulated for 24 hours, in both cell lines. The results might showed an increase in expression of pSGK1-S422 in response to increasing doses of dexamethasone, for 24 hours, in parental LNCaP. However, no apparent changes were detected in the expression of pSGK1-S422 in LNCaP-ENZ-R cells, in response to increasing doses of dexamethasone (Figure 5-14).

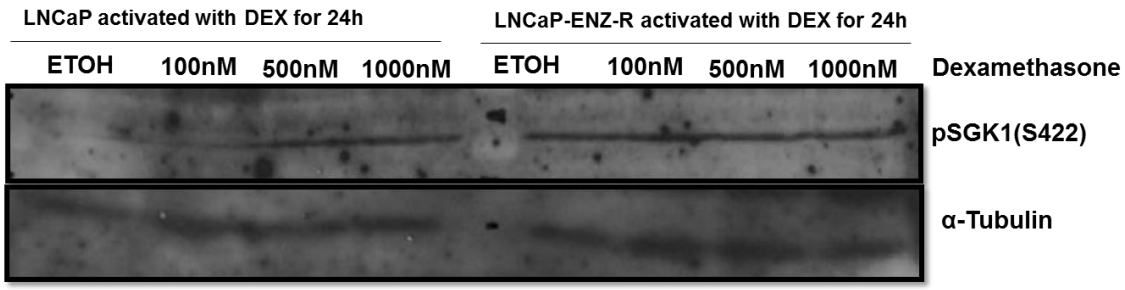

Figure 5-14 pSGK1 (S422) protein expression in response to dexamethasone stimulation in LNCaP and LNCaP-ENZ-R cells

LNCaP and LNCaP-ENZ-R cells were seeded out on 6-well plates. The cells were grown in SDM for 48 hours, then activated with 100nM, 500nM and 1000nM dexamethasone for 24. The cells were then lysed in a RIPA buffer for protein samples. pSGK1 (S422) protein expression in LNCaP and LNCaP-ENZ-R cells was determined. Alpha-tubulin was used as a loading control (representative blot).

5.2.14 GSK650394 decreases the proliferation of parental LNCaP and LNCaP-ENZ-R cells and causes a change in cell morphology

The GI50 of GSK650394 (SGK1 inhibitor) was previously described by our group for (O'Neill *et al.*, 2015) LNCaP cells, as a dose of 5µM. The GI50 dose for GSK650394 was added to LNCaP and LNCaP-ENZ-R cells and IncuCyte live cell imaging used as a measure of proliferation. Increasing doses of GSK650394 (5, 10 and 20µM) were added to the cells for 145 hours in both cell lines. Changes in cell morphology interfered with attempts to detect/validate GI50 using IncuCyte live cell imaging as shown in Figure 5-15 and Figure 5-16.

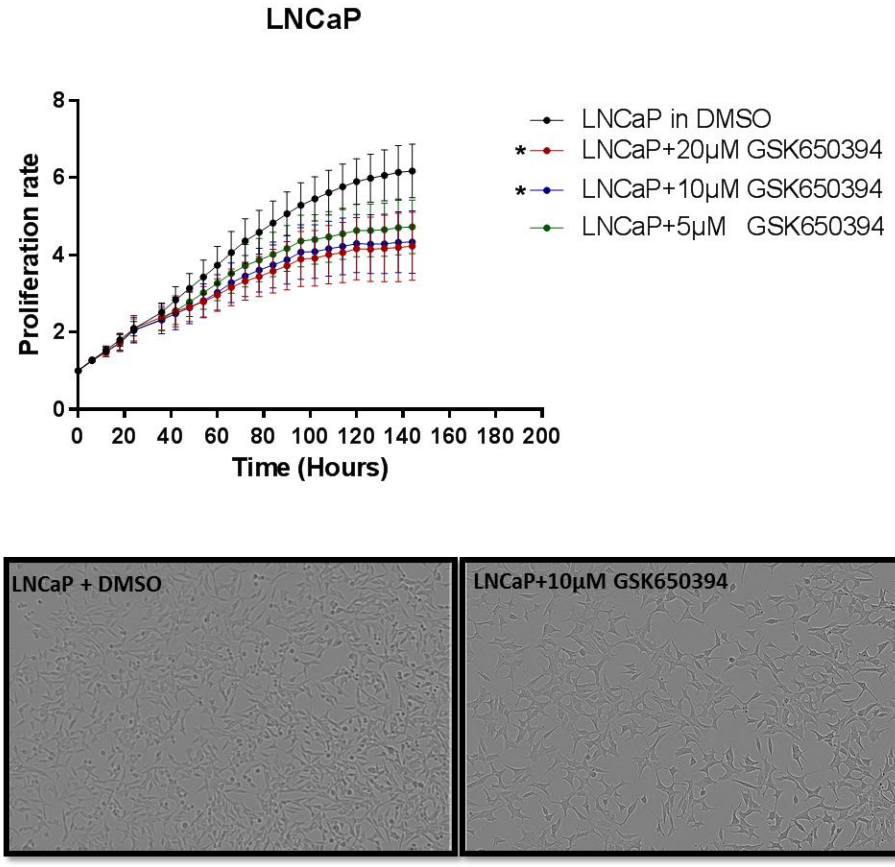

Figure 5-15 GSK650394 decreases the proliferation of LNCaP cells and changes cell morphology

LNCaP cells were seeded out in eight wells per experimental arm, using 96-well plates. The cells were grown in full medium overnight, then the following day the cells were treated with 5µM, 10µM and 20µM of GSK650394. DMSO was used as a control**.** Then the plates were placed in the IncuCyte® ZOOM System. Error bars represent the mean ± SD for triplicate independent experiments. p-values were determined by using student t-test (* p-value <0.05).

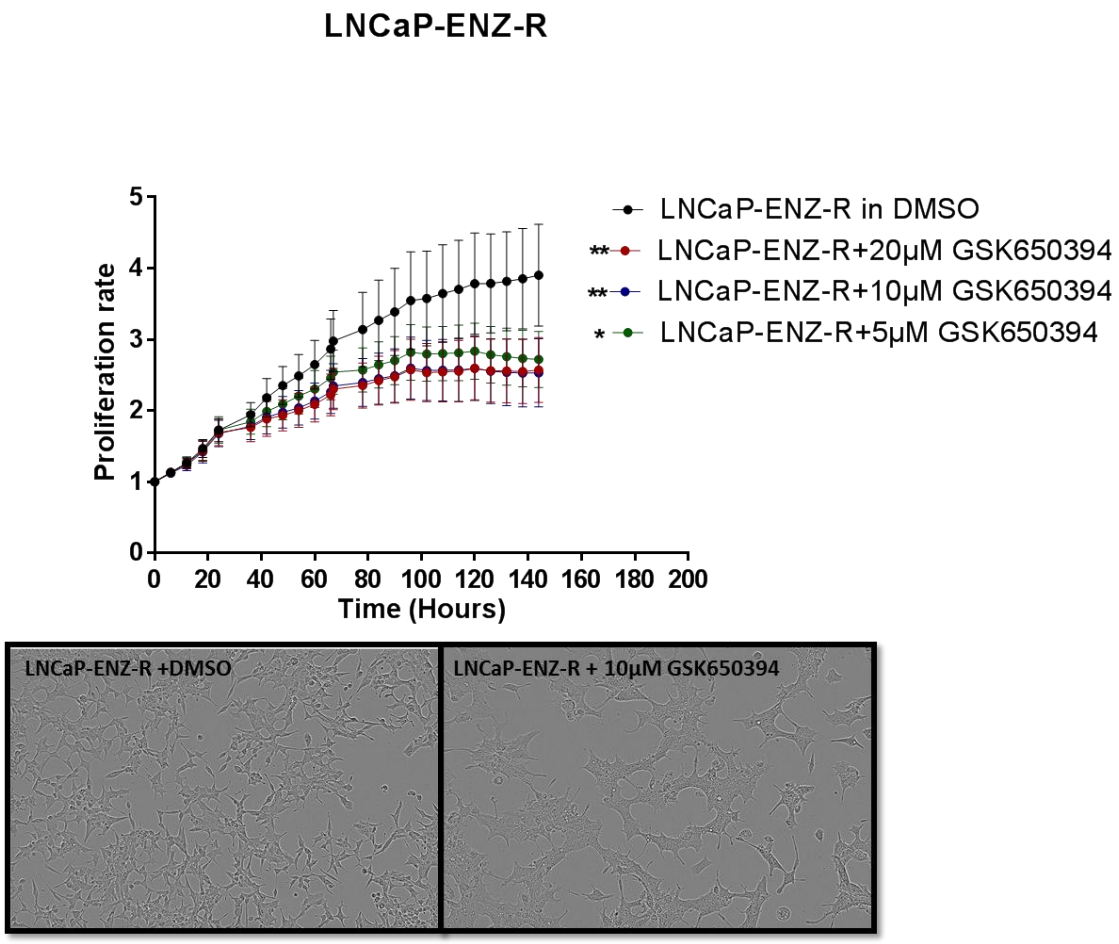

Figure 5-16 GSK650394 decrease the proliferation of LNCaP-ENZ-R cell line and changes cell morphology

LNCaP-ENZ-R cells were seeded out in eight wells per experimental arm using 96-well plates. The cells were grown in full medium overnight, then the following day the cells were treated with 5µM, 10µM and 20µM of GSK650394. DMSO was used as a control**.** Then the plates were placed in the IncuCyte® ZOOM System. Error bars represent the mean ± SD for triplicate independent experiments. p-values were determined by using student t-test (* p-value <0.05,** p-value <0.01).

To overcome the limitations of using IncuCyte live cell imaging to detect the GI50 of GSK650394, cell counts were used to count live cells, as described in Chapter 2. The results showed that the GI50 dose of GSK650394 in parental LNCaP cells was ~ 2.82µM and the GI50 dose of GSK650394 in LNCaP-ENZ-R cells was ~ 2.23µM, as shown in (Figure 5-17).

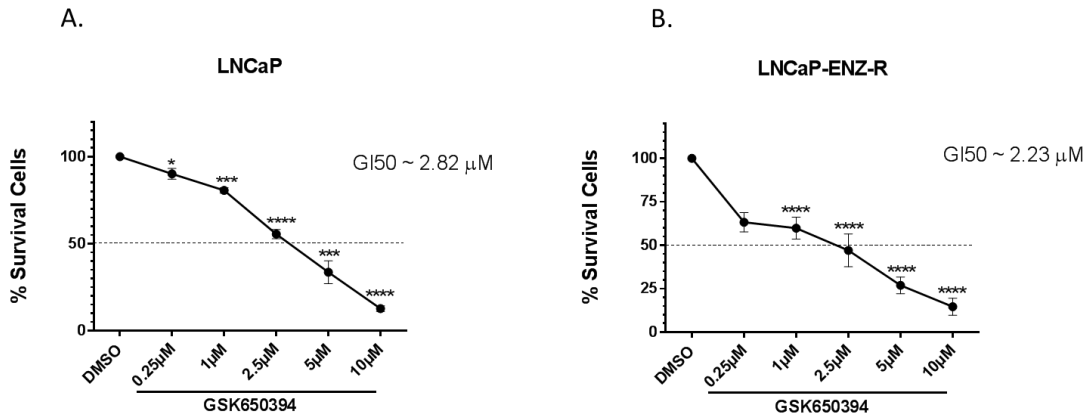

Figure 5-17 GI50 of GSK650394 in LNCaP and LNCaP-ENZ-R cells

LNCaP and LNCaP-ENZ-R cells were seeded out on 6-well plates. The following day the cells were treated with 0.25nM, 1nM, 2.5nM, 5nM and 10nM GSK650394 for 72 hours. The cells were then stained with Trypan blue. Only live cells were counted using the haemocytometer. **A**. Cell number of LNCaP cells treated with different doses of GSK650394 **B**. Cell count of LNCaP-ENZ-R cells treated with different doses of GSK650394. Error bars represent the mean ± SD for triplicate independent experiments. p-values were determined by using student t-test (* p-value <0.05, ** p-value <0.01m, *** p-value <0.001 and **** p- value < 0.0001).

5.2.15 GSK650394 causes an increase in G2/M arrest in LNCaP cells

To investigate the effect of the SGK1 inhibitor on cell phenotype, parental LNCaP cells were treated with SGK1 inhibitor for three days and a cell cycle distribution was used to detect cell cycle progression. The cells were collected and washed with PBS, then fixed with a citrate buffer and later the DNA was stained with propidium iodide (PI). RNase was added for 40 minutes to degrade RNA. PI binding to the DNA was quantified using a BD FACs Calibur, capturing 10,000 events per sample. Only single cells were gated, which represented subG1, G1, S and G2/M in a FL2-W vs FL2-A plot. All data analysis was carried out using FlowJo_V10 software. The results showed that SGK1 inhibition causes an increased number of cells demonstrating arrest at the G2 stage. However, this result was shown not to be statistically significant (Figure 5-18).

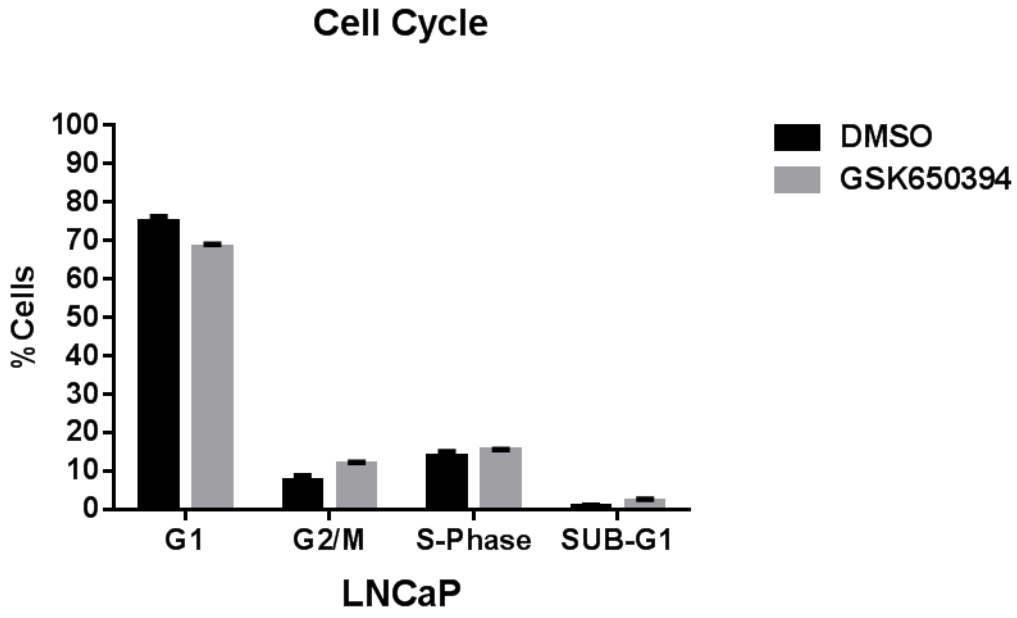

Figure 5-18 GSK650394 leads to increased arrest of LNCaP cells at G2/M

LNCaP cells were seeded out on 6-well plates. The cells were grown in full medium and the following day the cells were treated with 2.82μM GSK650394 for 72 hours, with DMSO used as a control. Error bars represent the mean ± SD for triplicate independent experiments.

5.2.16 GSK650394 arrests LNCaP-ENZ-R cells at G2/M and Sub-G1

A validation of the effect of the SGK1 inhibitor on the cell phenotype was extended to the LNCaP-ENZ-R cell line by using cell cycle analysis. LNCaP-ENZ-R cells were treated with SGK1 inhibitor for 3 days, then the cells were collected to investigate the cell cycle using Flow cytometry. The cells were collected and washed with PBS, then fixed with a citrate buffer and later the DNA was stained with propidium iodide (PI). RNase was added for 40 minutes to degrade RNA. PI binding to DNA was quantified using a BD FACsCalibur capturing 10,000 events per sample. Only single cells were gated, which represented subG1, G1, S and G2/M in a FL2-W vs FL2-A plot. The results demonstrate that SGK1 inhibition causes a significant increase in the number of cells demonstrating arrest at the G2 stage and sub-G1 stage (Figure 5-19).

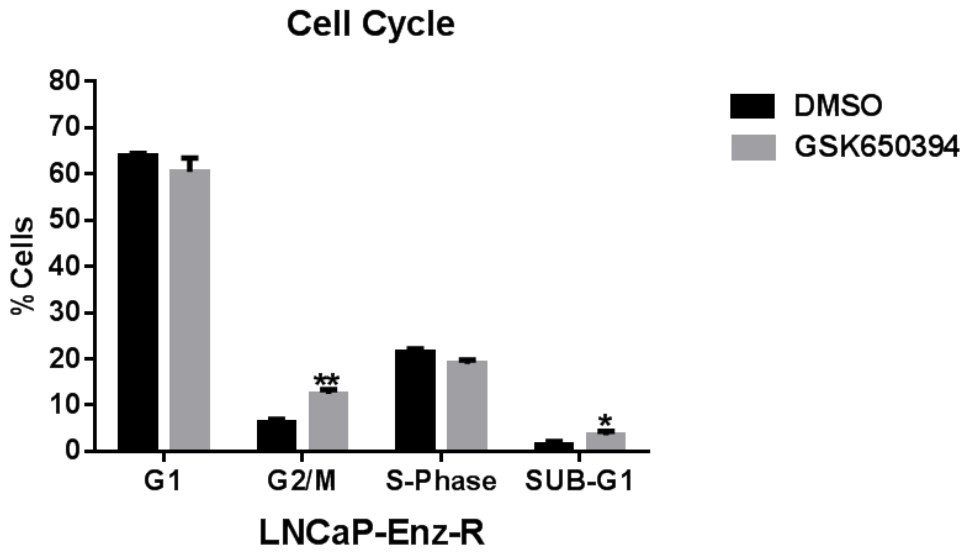

Figure 5-19 GSK650394 leads to increased arrest of LNCaP-ENZ-R cells at G2/M and Sub-G1

LNCaP-ENZ-R cells were seeded out on 6-well plates. The cells were grown in full media. The following day the cells were treated with 2.23µM GSK650394 for 72 hours. All data analysis was carried out using FlowJo_V10 software. Error bars represent the mean ± SD for triplicate independent experiments. p-values were determined by using student t-test (* p-value <0.05, ** p-value <0.01).

5.2.17 GSK650394 has no effect on the migration of LNCaP cells

To further validate the role of the SGK1 inhibitor in cell phenotype, LNCaP cells were treated with SGK1 inhibitor and a wound healing assay was used to quantify migration of the cells. The cells were left until near 100% confluency. After that a perpendicular scratch was performed using p20 filter tips. The media was replaced with fresh media with and without 2.82µM GSK650394. Images were taken of three separate fields for each well at 0h, 6h, 24h and 48h. The width of the "wound" was measured using ImageJ software. This was achieved by overlaying a 20 square grid over each image, taking an average and normalising to the 0 hour control. The results showed that SGK1 inhibition does not reduce parental LNCaP cells migration at 6 and 12 hours. However, a non-significant effect of SGK1 inhibitor was noticed after 24 hours (Figure 5-20).

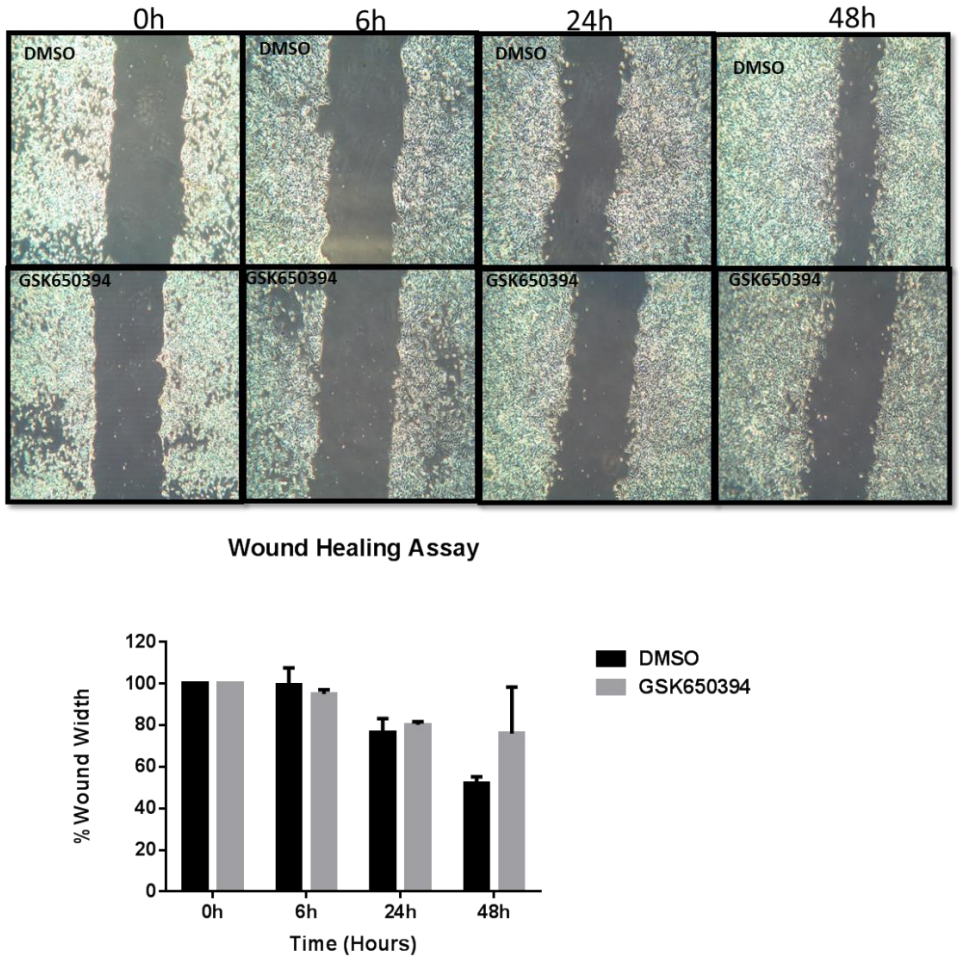

Figure 5-20 GSK650394 has no effect on the migration of LNCaP cells

LNCaP cells were seeded into 6-well plates in full media and the cells left to near 100% confluency. After that a perpendicular scratch was performed and the cells treated with 2.82µM GSK650394. The width of wound was measured by using ImageJ software. Error bars represent the mean ± SD for triplicate independent experiments.

5.2.18 GSK650394 significantly decreases migration of LNCaP-ENZ-R cells

To further validate the role of the SGK1 inhibitor in cell phenotype, LNCaP-ENZ-R cells were treated with the SGK1 inhibitor and a wound healing assay was used to quantify migration of the cells. The cells were left until near 100% confluency. After that a perpendicular scratch was performed using p20 filter tips. The media was replaced with fresh media with and without 2.23µM GSK650394. Images were taken of three separate fields for each well at 0h, 6h, 24h and 48h. The width of the "wound" was measured using ImageJ software. This was achieved by overlaying a 20 square grid over each image, taking an average and normalising to the 0 hour control. The results showed that SGK1 inhibitor significantly reduced migration of the cells at 24 and 48 hours ($p < 0.05$) (Figure 5-21).

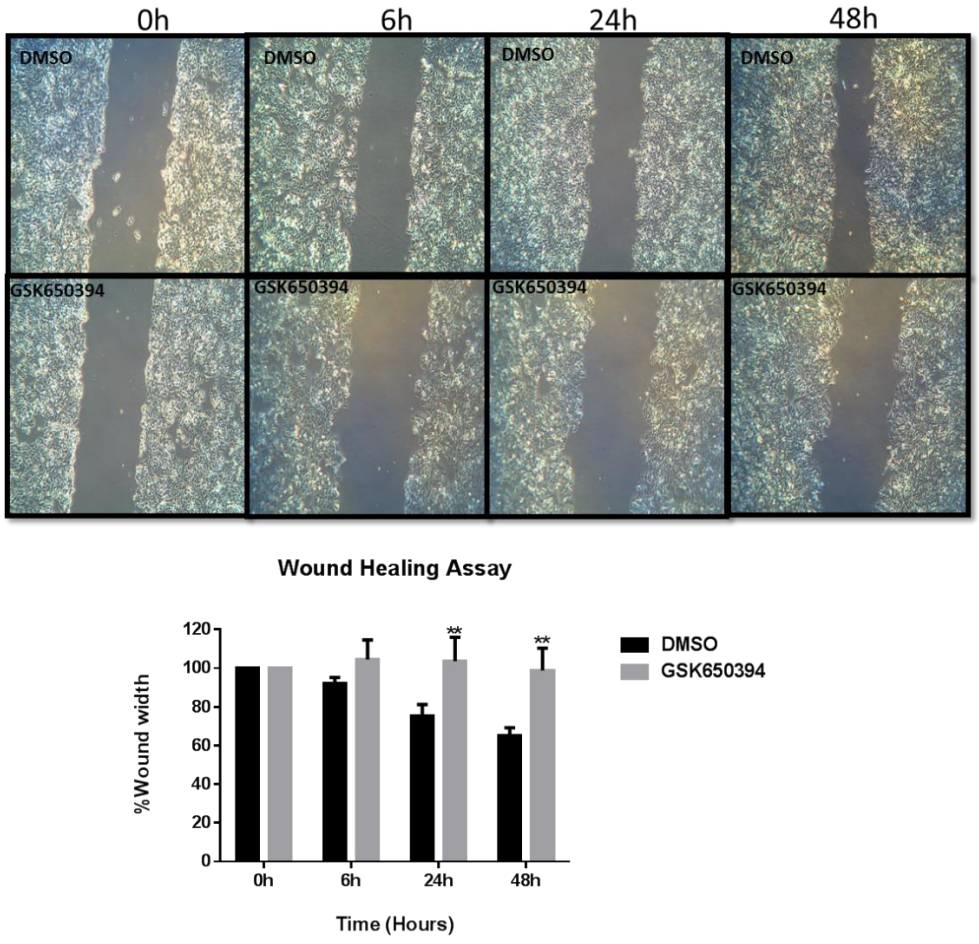

Figure 5-21 GSK650394 decreases migration of LNCaP-ENZ-R cells

LNCaP-ENZ-R cells were seeded into 6-well plates in full media and the cells left to near 100% confluency. After that, a perpendicular scratch was performed and the cells treated with 2.23µM GSK650394. The width of wound was measured by using ImageJ software. Error bars represent the mean ± SD for triplicate independent experiments. p-values were determined by using TWO-WAY ANOVA (* p-value <0.05, ** p-value <0.01).

5.2.19 Proliferation of parental LNCaP and LNCaP-ENZ-R cells is reduced in response to combined GR knockdown and SGK1 inhibition

From the data obtained in Figure 5-19, the cell cycle was significantly affected by GSK650394 in LNCaP-ENZ-R cells, with cell cycle arrest seen at G2/M. A significant increase in the percentage of the cells at the sub-G1 phase was also seen. This increase in cells in the sub-G1 phase was not seen in LNCaP cells in response to GSK650394. A significant reduction in AR target genes in response to GR knockdown using two selected oligos was demonstrated in (Figure 5-11). In an attempt to understand the possible effects of an SGK1 inhibitor with or without GR knockdown on the proliferation of LNCaP and LNCaP-ENZ-R cells. Both cell lines were reverse transfected with two oligos against GR for 72 hours, followed by treatment with GSK650394 for 16 hours. Then the plates were placed in the IncuCyte® ZOOM System enabling observation and quantification of cell phenotype over time by automatically gathering and analysing images every 2 hours for 7 days. The data was normalized to the zero hours for each condition. This was to avoid problems with seeding out. The data showed a non-significant decrease in proliferation of LNCaP cells in response to GSK650394 or GR knockdown, while a combination of GSK650394 plus GR knockdown led to a significant decrease in proliferation of the parental LNCaP cells (Figure 5-22 A). A similar trend was also obtained in LNCaP-ENZ-R cells in response to the same experimental condition, where a significant ($p< 0.05$) reduction in proliferation was also detected (Figure 5-22 B).

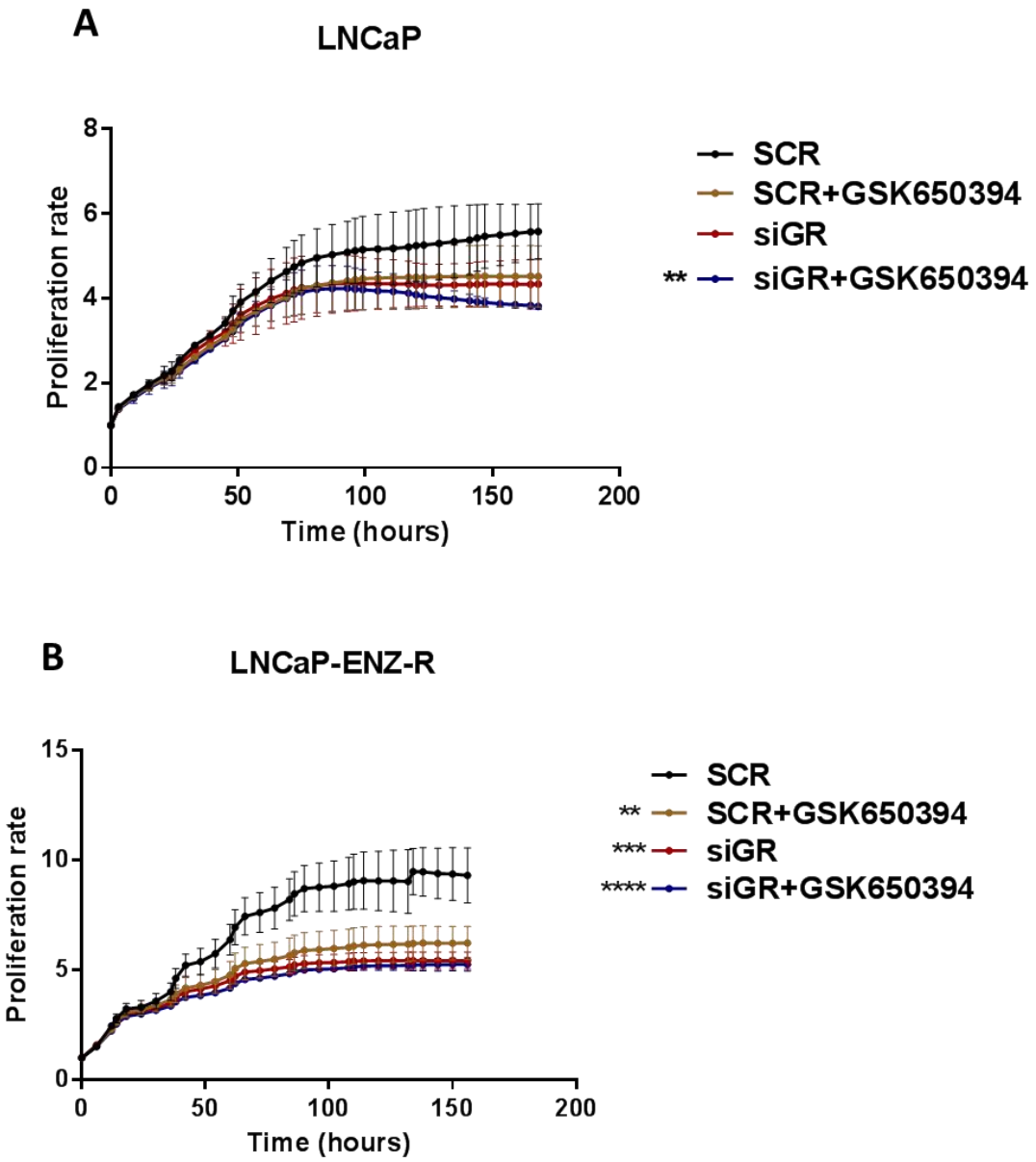

Figure 5-22 Parental LNCaP and LNCaP-ENZ-R cells proliferation is reduced in response to combined of GR knockdown and GSK650394 treatment

LNCaP and LNCaP-ENZ-R cells were reverse transfected with a selected oligo against GR on 6-well plates format. Non-silencing oligo was used as a control. The cells were transferred to 96-well plates, followed by GSK650394 treatment. Error bars represent the mean ± SD for triplicate independent experiments. p-values were determined by using student t-test (* p-value <0.05, ** p-value <0.01 and ** p-value <0.01, *** p-value <0.001 and **** p- value < 0.0001).

5.2.20 High expression of SGK1 in relapsed patients compared to naïve patients

Previously, the data generated from the microarray experiment showed a high expression of SGK1 in the enzalutamide-resistant cell line compared to the parental LNCaP cells. To compare this interesting laboratory finding in clinical samples from patients with known prostate cancer, our in-house generated TMA5 was selected to investigate the expression of SGK1. TMA5 is a very interesting cohort of patient samples, with samples taken from the same patients before and after hormone ablation treatment was received. The pairs were divided into three groups: firstly a hormone naïve group containing patients tissues which never received hormone treatment. Secondly hormone sensitive group containing patients tissues which had subsequently received ADT to good effect and continued to be sensitive to the treatment. Then the final castrate resistant group, which included patients who received hormone treatment, initially to good effect, but had relapsed and subsequently found to have castration resistant PC.

The results demonstrated that SGK1 expression is seen in the nuclear compartment of the cell and does not significantly change between matched patients who belonged to the continued treatment naïve group. These patients had not received any treatment. However, a suggestion of higher expression of SGK1 was seen in matched patients in the second, hormone sensitive treatment group, but this did not reach significance. Interestingly, there was a significant change in nuclear expression of SGK1 in matched samples taken from patients who were relapsed following treatment. The data also showed an increase in the expression of SGK1 in sensitive-to-treatment group compared to the naïve group, while a significant increase was noticed in the relapsed group compared to the naïve group (Figure 5-23 A, B, C, D).

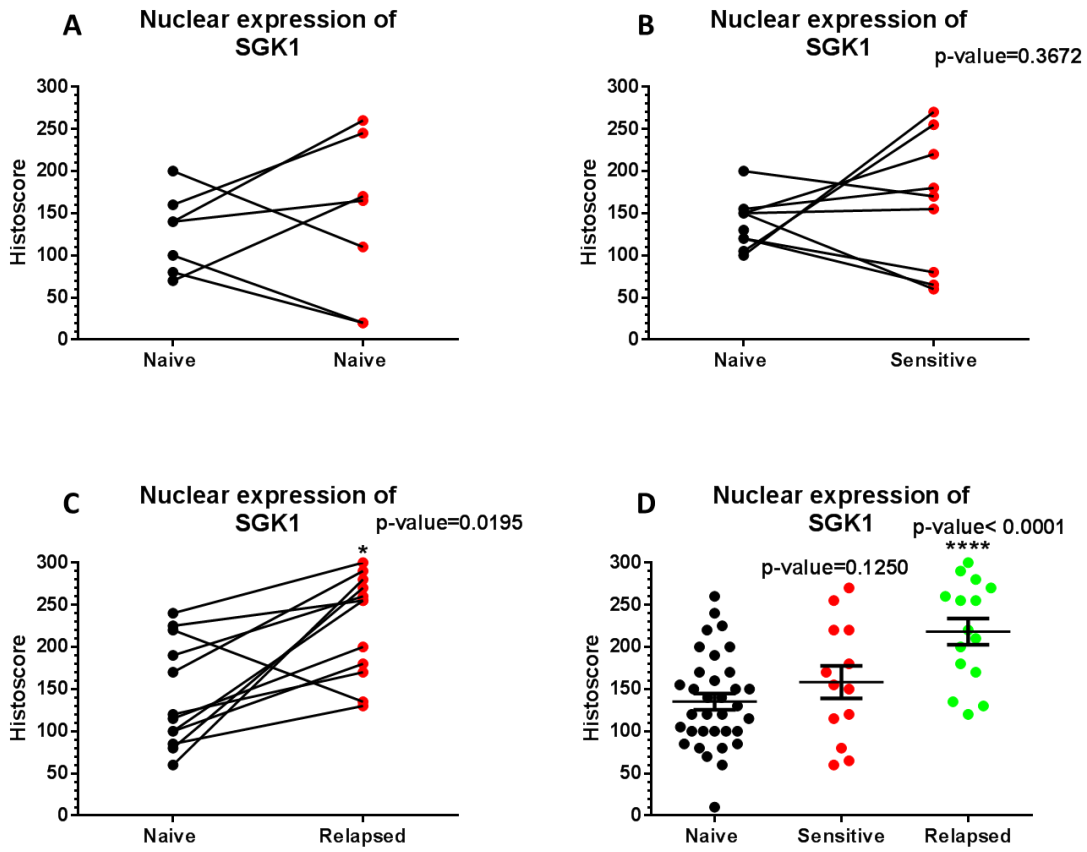

Figure 5-23 Nuclear expression of SGK1 in matched patients who were naïve, sensitive to the androgen withdrawal treatment and relapsed patients who were resistant to hormone treatment.

A. There was no significant change in SGK1 expression in matched samples from patients who had not received any treatment for their prostate cancer. **B.** An increase and decrease in SGK1 expression was observed in matched samples from patients who were sampled before treatment and again after they were established on hormone treatment and were still sensitive to the hormone treatment at the time of their second biopsy. **C.** There was a significant change in nuclear SGK1 expression in matched samples taken from patients who had a second sample taken after they had relapsed and were no longer sensitive to their hormone treatment. **D.** Higher expression of SGK1 in the sensitive to treatment group compared to naïve group, while a significant increase was noticed in relapsed group compared to the treatment naïve group.

5.3 Discussion:

Attempts to abrogate testicular androgen production are still a mainstay in the treatment of locally advanced and metastatic PC. However, eventually and inevitably this treatment fails when PC progresses despite apparent low levels of testosterone (Chen *et al.*, 2008). Although there may be low levels of circulating androgen in CRPC following chemical or surgical castration, AR signaling continues in CRPC (Scher *et al.*, 2012). Enzalutamide is used as a second line anti-androgen to block AR activity, resulting in a significant improvement of overall patient's survival with CPRC progression. Unfortunately median survival for patients with CRPC following treatment with enzalutamide remains less than a year, with an overall median survival of 4.8 months (Chen *et al.*, 2008; Scher *et al.*, 2012). The glucocorticoid receptor (GR), progesterone receptor (PR) and the androgen receptor (AR) bind with high affinity to DNA elements. Hormone response element (Epstein *et al.*) sites, which are located in the DNA are identical for GR, PR and AR. There are many genes that can be regulated by more than one steroid receptor, the relevance here being that like the AR, GR can induce PSA activity. Similarly, dexamethasone has previously been shown to stimulate PSA expression (Cleutjens *et al.*, 1997). Other studies have demonstrated that SGK1 is a downstream target of both AR and GR in CWR22R1 and LNCaPC4 (Isikbay *et al.*, 2014). However, the role of the GR and AR in the regulation of SGK1 in drug-resistant prostate cancer remains unclear. This chapter aimed to investigate the possible mechanism governing this relationship, or at least the generation of some data to begin to answer this query. Firstly, an investigation of SGK1 expression at the protein level was performed on LNCaP and LNCaP-ENZ-R cells in the presence and absence of enzalutamide for 48 hours. Similarly, the expression at the mRNA level showed an increase in the expression of the SGK1 in LNCaP-ENZ-R cells compared to the LNCaP control (Figure 5-2). These results might suggest that SGK1 plays a role in enzalutamide-resistance, which is consistent with a group working on breast cancer (Sommer *et al.*, 2013) who demonstrated that SGK1 is significantly elevated in breast cancer Akt inhibitor-resistant cell lines.

SGK1 antibody was validated by identify the band on the size 50 KD. also SGK1 antibody was validated by activated SGK1 with DHT and dexamethasone and the results showed increased SGK1 protein level in response for DHT and dexamethasone, which prove specify of this antibody.

To test the role of AR in the regulation of the SGK1 in both LNCaP and LNCaP-ENZ-R cell lines (cellular models of hormone-sensitive and hormone-resistant disease, respectively), they were stimulated with DHT for 24 and 48 hours. The results of this

study might indicated an increase in the expression of SGK1 at the mRNA and protein levels in response to the DHT stimulation in both cell lines. Interestingly, the data might suggest that AR regulates of SGK1 expression in LNCaP cells (Figure 5-3). This is in agreement with Sherk *et al.* (2008) who demonstrated that activation of AR leads to increased SGK1 expression in parental prostate cancer cell line. This study also showed that AR regulates SGK1 expression in LNCaP-ENZ-R cells (Figure 5-4).

To study the role of the GR in regulation of SGK1 in LNCaP and LNCaP-ENZ-R cells, both cell lines were activated with dexamethasone for 24 and 48 hours. The results showed an increase in the expression of SGK1 in response to dexamethasone stimulation in LNCaP cells, at the mRNA level. However, no effect was observed at the protein level (Figure 5-5), which perhaps suggests that activation by dexamethasone correlates with activation of SGK1 and requires a functional glucocorticoid receptor (Wang *et al.*, 2007). On the other hand, increases in mRNA and protein expression of SGK1 were observed in LNCaP-ENZ-R cells (Figure 5-6) in response to dexamethasone activation, which might suggest that LNCaP-ENZ-R cells contains a functional GR to activate SGK1.

Further investigation of the functionality of GR was then explored. Firstly, GR expression was detected at the protein level by Western blot analysis and the results showed an increase in the expression of GR in response to AR inhibition by enzalutamide in parental LNCaP cells. However, in LNCaP-ENZ-R cell line, the results showed an increase in the expression of GR in the presence and absence of enzalutamide for 48 hours compared to the parental LNCaP. At the mRNA level, the results indicated that blocking AR activity with enzalutamide for 48 hours increases the expression of GR in LNCaP and LNCaP-ENZ-R cells (Figure 5-7), which is in agreement with another group (Isikbay *et al.*, 2014), who described that GR expression increases in the androgen-sensitive LNCaP and VCaP cell lines, following AR inhibition by enzalutamide. One could perhaps therefore suggest that increased GR expression mediates PC resistance to enzalutamide.

A further investigation of GR in LNCaP-ENZ-R cells compared to the parental LNCaP cells was applied, by activating both cell lines with dexamethasone for 24 hours. This experiment showed that no significant changes of selected AR target genes were noticed in LNCaP cells (Figure 5-8). However, a significant increase of the AR target genes *KLK3*, *KLK2*, *FKPB5* and *TMPRSS2* was observed in response to dexamethasone stimulation in LNCaP-ENZ-R cells (Figure 5-9). To confirm the results from previous experiment (Figure 5-9), GR knockdown was achieved by using two selected siRNA oligos against GR in parental LNCaP cells and AR target genes were identified mRNA level. GR knockdown was validated by QRT-PCR only, the limitation of this experiment

is not confirming GR knockdown at the protein level, which might need to be consider in future.

The results from this study showed no significant change in the expression of the chosen AR target genes in response to GR knockdown in the parental LNCaP cells (Figure 5-10). However, a significant decrease in the expression of the AR target genes was noticed in response to GR knockdown in LNCaP-ENZ-R cells (Figure 5-11). It can thus be suggested that GR can bypass AR and regulate AR target genes known to be involved in the proliferation and growth of resistant cell line models.

From this data, this study suggests that SGK1 is predominantly regulated by AR in parental LNCaP cells, while both GR and AR are involved in the regulation of SGK1 in LNCaP-ENZ-R cells. To test this theory, both parental LNCaP and LNCaP-ENZ-R cells were grown in full medium and transfected with siRNA against GR for 72 hours. The cells were kept with or without enzalutamide. The data from this experiment demonstrated that blocking AR led to a decrease in the expression of *SGK1, KLK3* and *FKBP5* and no significant effects were noticed in the expression of *SGK1, KLK3* and *FKBP5* in response to GR knockdown in parental LNCaP cells. Enzalutamide was able to reduce the GR knockdown effects on the expression of *SGK1, KLK3* and *FKBP5* (Figure 5-12 A, B, C). To confirm the previous suggestion, parental LNCaP cells were transfected with siRNA against GR for 72 hours in SDM, then the cells were stimulated with DHT for 24 hours. This data showed that stimulation of AR with DHT led to an increase in the expression of *SGK1, KLK3* and *FKBP5*. However, no effect of GR knockdown was observed on the expression of *SGK1, KLK3* and *FKBP5*, adding weight to the results of the previous experiment. Also this study showed that knockdown of GR does not abrogate the AR stimulation effects on the expression *SGK1, KLK3* and *FKBP5* in LNCaP cells (Figure 5-12 D, E, F). This might suggest that AR regulates SGK1, while no significant effect of GR was noticed in the regulation of SGK1 and other AR target genes in parental LNCaP and GR knockdown had no effect on blocking or activation of AR effects on the expression of SGK1 and other AR target genes. Also this study noticed that KLK3 and FKBP5 reduced expression with GR knockdown, but in the presence of DHT compared to GR knockdown arm. This might suggest that DHT can activate GR-mediated gene expression. The limitation of this experiment is not confirming GR knockdown at the protein level, which might need to be consider in future.

Further experiments were applied to test this theory on LNCaP-ENZ-R cells. These cells were grown in full medium and transfected with siRNA against GR for 72 hours. The cells were kept with and or without enzalutamide. This study demonstrated that in the

present and absence of enzalutamide, there was no effect on SGK1 expression in LNCaP-ENZ-R cells and GR knockdown led to a decrease in the expression of SGK1 in the presence and the absence of enzalutamide. However, enzalutamide treatment led to an increase in the expression of *KLK3* and *FKBP5*, which supports the results obtained from Figure 5-7, that blocking AR increases the level of GR, which appears to be able to regulate AR target genes. A decrease in the expression of *KLK3* and *FKBP5* in response to GR knockdown, with or without enzalutamide, was noticed in this study (Figure 5-13 A, B, C). This perhaps suggests that SGK1 could be a biomarker for enzalutamide resistance, but more experiments are needed to confirm this finding. SGK1 is regulated by GR and enzalutamide does not abrogate GR activity in LNCaP-ENZ-R cells. However, blocking AR led to an increase in the expression of GR which then appears to regulate AR target genes. Again, enzalutamide does not abrogate the GR activity in regulation of AR target genes. In order to further investigate this theory, LNCaP-ENZ-R cells were transfected with siRNA against GR for 72 hours in SDM, then the cells were stimulated with DHT for 24 hours. This experiment indicated that stimulation of LNCaP-ENZ-R cells with DHT led to an increase in the expression of *SGK1, KLK3* and *FKBP5*, which adds weight to the results obtained from Figure 5-4 that AR may regulate SGK1 in LNCaP-ENZ-R cells. Also the results showed that GR knockdown led to a decrease in the expression of *SGK1, KLK3* and *FKBP5*, which confirm the results of the previous experiment. Interestingly, the data demonstrated that knockdown of GR does not abrogate the effects of DHT on the expression of SGK1. This confirms the results obtained from (Figure 5-4), (Figure 5-6) which indicated that AR and GR are both able to regulate SGK1. However, knockdown of GR abrogated AR stimulation effects on the expression of *KLK3* and *FKBP5* (Figure 5-13 D, E, F). Not confirming GR knockdown by western blot is one of the limitation of this experiment, which is need further investigation. Below a cartoon summarized the finding of this study (Figure 5-24).

To investigate the activity of SGK1 in the LNCaP and LNCaP-ENZ-R cell lines, pSGK1-Ser422 protein expression was measured in both cell lines, via western blot. The results from this experiment showed a gradual increase in the expression of pSGK1-Ser422 in LNCaP cells induced by increasing doses of dexamethasone, while consistent pSGK1-Ser422 expression was detected in LNCaP-ENZ-R cells, whether stimulated with dexamethasone or not. This potentially indicates that in LNCaP cells, stimulation is required to activate SGK1. However, in LNCaP-ENZ-R cells dexamethasone stimulation was not required, suggesting SGK1 may be constitutively active in these drug-resistant cells (Figure 5-14). The limitation of this experiment was total SGK1 not investigated.

However, the total SGK1 was investigated previously in this study but in different blot in response to dexamethasone (Figure 5-5, Figure 5-6).

Previously, the data showed that a high expression of pAkt was observed in LNCaP-ENZ-R cells, compared to parental LNCaP cells (Figure 3-4). An independent study demonstrated that Akt promotes activation of mTORC1 (Sommer *et al.*, 2013). Another study demonstrated that mTORC1 can mediate the activity of both pSGK1-Ser422 and pAkt-Ser473 (Hong *et al.*, 2008). Based on these studies and the previous data in this study, mTORC1 might be suggested to activate SGK1 through the activity of pAkt in the LNCaP-ENZ-R cells.

To further study the effect of SGK1 on the LNCaP and LNCaP-ENZ-R cells, an SGK1 inhibitor (GSK650394) was used. It has been shown GSK650394 inhibited the enzymatic activity of SGK1 and SGK2. In addition, GSK650394 is relatively selective for SGK1 over Akt, the most closely related AGC kinase. Also GSK650394 as a growth inhibitor might also be due to nonspecific inhibition of other kinases, particularly other members of the SGK protein family, SGK2 and SGK3 (Sherk *et al.*, 2008).

The GI50 doses (LNCaP 2.82µM, LNCaP-ENZ-R 2.23µM) were evaluated (Figure 5-17). The data from this study showed that GSK650394 arrests the cells at the G2/M and sub-G1 phases significantly ($p<0.05$) in LNCaP-ENZ-R cells (Figure 5-19). However, no significant changes were detected in parental LNCaP cells (Figure 5-18). The effect of GSK650394 on cell growth was previously suggested to be a non-specific inhibition of other kinases, particularly other members of the SGK protein family SGK2 and SGK3. A possible mechanism of how SGK1 may control the cell cycle in enzalutamide-resistant prostate cancer is through direct or indirect regulation of mTORC, which regulates cell cycle through cyclin D1 and D2 (Sherk *et al.*, 2008).

A further investigation of the effect of GSK650394 on LNCaP and LNCaP-ENZ-R cells was performed using a wound-healing assay to detect effects on cell migration. From the results, no significant effects of GSK650394 on cell migration was detected in parental LNCaP cells (Figure 5-20). However, a significant reduction of migration was observed in the LNCaP-ENZ-R cells starting from 6 hours of treatment (Figure 5-21). A previous study showed that SGK1 overexpression in colon cell lines enhances cell migration, also correlating with vinculin dephosphorylation (Schmidt *et al.*, 2012). Vinculin is an adhesion protein that participates in cell–cell adhesions and is known to regulate migration (Schmidt *et al.*, 2012). From the data above (Figure 5-11), it was observed that GR regulates the AR target genes responsible for proliferation. Moreover, the SGK1 inhibitor was able to arrest the cells in sub-G1. For that reason, both cell lines were treated

with GSK650394 in addition to GR knockdown to see if combination treatment may be advantageous (Figure 5-22). Interestingly, a stronger effect was noticed using a combination of GSK650394 with GR knockdown on the proliferation of LNCaP-ENZ-R cells, suggesting that inhibition of SGK1 activity combined with GR depletion may be a better approach to treat enzalutamide-resistant PC cases. However, further experiments are required to strengthen this hypothesis such as validate SGK1 and GR inhibition at the protein level by western blotting.

LNCaP-ENZ-R cells demonstrate upregulated GR signalling and as a consequence elevated SGK1 levels and is consistent with the clinical scenario in which patients resistant to the next-generation anti-androgen show a switch from androgen- to glucocorticoid-dependency.

High expression of SGK1 was noticed in enzalutamide-resistant cells compared to LNCaP parental cells. To investigate this result on patient tissue samples, TMA5 was selected as it contains three groups of matched pairs. The pairs were divided into three groups: a hormone naïve group containing patients tissues which never received hormone treatment; hormone sensitive groups containing patients tissues which had subsequently received ADT to good effect and continued to be sensitive to the treatment; and the final castrate resistant group. The data was consistent with SGK1 expression on the cellular level, as a significant increase was noticed in the relapsed group (representing castration resistant PC) as previously seen in the enzalutamide-resistant cells, suggesting that SGK1 could be a potential prognostic biomarker for enzalutamide-resistance in patients with prostate cancer (Figure 5-23). Again, further experiments are required to strengthen this hypothesis.

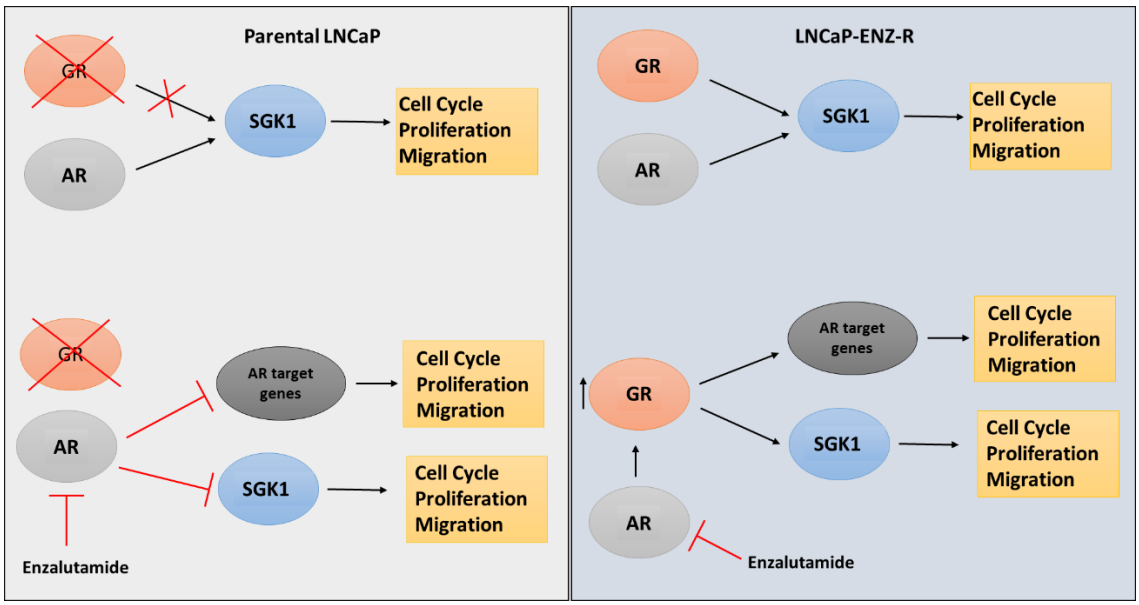

Figure 5-24 role of AR and GR in parental LNCaP compared to LNCaP-ENZ-R

Chapter 6. Identification of TROP-2 as a potential therapeutic target in castrate resistance prostate cancer

6.1 Introduction

Tumour-associated calcium signal transducer 2, also known as TROP-2, is a transmembrane glycoprotein encoded by the intronless *TACSTD2* gene located on chromosome 1p32. It is approximately 35 kDa in size. TROP-2 protein was originally detected in human trophoblasts and has been shown to be overexpressed in a variety of human carcinomas such as endometrial and cervical cancers, adenocarcinomas, squamous cell carcinomas and carcinosarcomas (McDougall *et al.*, 2011; Bignotti *et al.*, 2012).

TROP-2 consists of several domains that span the cell membrane and is composed of 323 amino acids (a.a.). It starts with a hydrophobic leader peptide (a.a.1-26), then an N-terminal domain extracellular domain (a.a. 27-274), which is the largest domain (also known as the ectodomain), next is the transmembrane domain (a.a. 275-297), anchored via a single transmembrane helix (TM) followed by a short intracellular cytoplasmic tail (a.a. 298-323) (Figure 6-1). TROP-2 is predicted to have N-linked glycosylation sites at residues 33, 120, 168 and 208. An extracellular EGF-like repeat domain is located between amino acid 1-274. A thyroglobulin type-1 domain is made up of the amino acids 70-145 within the extracellular domain (Cubas *et al.*, 2009). TROP-2 has been implicated in numerous signalling pathways that are crucial for survival, self-renewal, proliferation and invasion. TROP-2 transduces an intracellular calcium signal, which can occur without extracellular Ca^{2+}, suggesting a mobilization of Ca^{2+} from internal stores (Shvartsur and Bonavida, 2015).

TROP2 is a member of the GA733 family, which consists of GA733-1 (Trop2) and GA733-2 also known as EpCAM (epithelial cell adhesion molecule). EpCAM and TROP-2 have about 49% structural similarity and they are both transmembrane proteins with single transmembrane domains. Both proteins have an important role in cell to cell adhesion and cell signalling through c-MYC and cyclins that are crucial for migration, invasion, proliferation and differentiation. However, TROP-2 and EpCAM appear to have opposite biological effects. It has been reported using patient tissues samples from pulmonary adenocarcinoma that the expression of EpCAM was significantly related to a favourable outcome, while TROP-2 tended to be expressed in cases with an unfavourable outcome (Kobayashi *et al.*, 2010).

TROP-2 expression can lead to stimulation of the RAS/RAF/MEK signalling pathway and this pathway can be further activated by signals related to an increase of calcium. TROP-2 expression increases the levels of phosphorylated ERK1 and ERK2 and ERK signalling leads to induction of AP-1 transcription factor, which is involved in invasion and metastasis via MMPs (matrix metalloproteinases), proliferation via the cyclins and CDKs, apoptosis via pro-apoptotic Bcl-2 (B-cell lymphoma 2) and angiogenesis via VEGF (vascular endothelial growth factor). TROP-2 expression leads to a downregulation of p27 which is a cyclin-dependent kinase inhibitor 1B. Also, its expression increases levels of cyclin D1 and cyclin E, which helps mediate ERK1/2 cell cycle progression (Cubas *et al.*, 2010; Shvartsur and Bonavida, 2015).

According to DNA microarray and real-time PCR studies, TROP-2 mRNA is expressed in most cancers of epithelial origin such as breast, cervix, endometrium, oesophagus, fallopian tubes, kidney, pancreas, placenta, prostate, respiratory tract, salivary glands, seminal vesicles, stomach, tonsils, thymus and vagina (Trerotola *et al.*, 2013a). TROP-2 overexpression was detected in 83% of breast cancer cases compared to normal breast tissue according to a microarray analysis and tumour growth rates and progression were increased dramatically in the mice that were injected with TROP-2 overexpressing cells (Trerotola *et al.*, 2013a). A further study demonstrated that TROP-2 is up-regulated in locally advanced human PC (with extracapsular extension - stages pT3/pT4) as compared to organ-confined (stage pT2) PC (Trerotola *et al.*, 2015). TROP-2 has also been shown to be up-regulated in metastatic prostate tumours of transgenic adenocarcinoma of mouse prostate (TRAMP) mice (Trerotola *et al.*, 2015). Data from the same group has shown that β1- integrin-dependent cell adhesion to fibronectin is regulated by TROP-2 and it also promotes metastatic dissemination of prostate cancer cells *in vivo*. Also, TROP-2 promotes prostate cancer cell migration on fibronectinand its overexpression enhances directional cancer cell migration (Trerotola *et al.*, 2013b). However, the role of TROP-2 in enzalutamide-resistant prostate cancer is not clear. For that reason the aims of this chapter are:

1. Identify the expression of TROP-2 in parental LNCaP and LNCaP-ENZ-R cells
2. Study the effect of TROP-2 knockdown on the phenotype of parental LNCaP and LNCaP-ENZ-R cells
3. Investigate the pathways that might by affected by TROP-2 knockdown

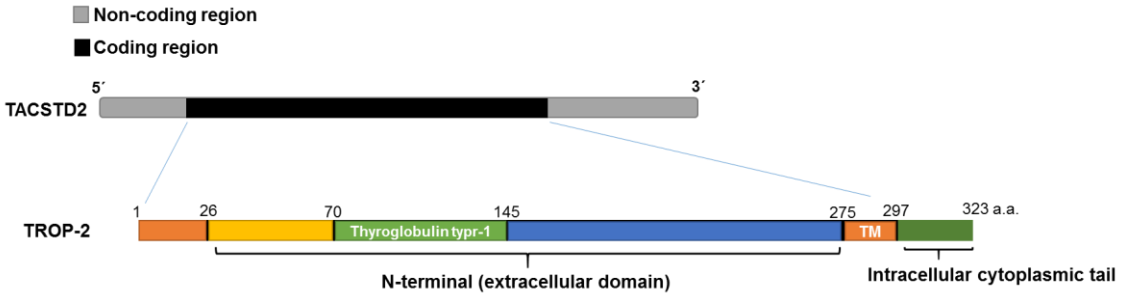

Figure 6-1 Schematic diagram of TACSTD2 gene and homologous domain representation of TROP-2 protein. Adapted from (Cubas *et al.*, 2009)

6.2 Results

6.2.1 High expression of TROP-2 protein in LNCaP-ENZ-R cells in the presence and absence of enzalutamide

An increase in the expression of *TACSTD2* in the LNCaP-ENZ-R cell line was detected in the presence of enzalutamide by microarray data (Figure 4-10 B). This was further validated at mRNA level using QRT-PCR (Figure 6-2 A). To validate the TROP-2 expression at the protein level, in the same experimental condition as in microarray study, an appropriate antibody was sourced and then validated to detect TROP-2. The data shows an increase in the expression of the TROP-2 in LNCaP-ENZ-R cell line at the protein level in the presence or absence of enzalutamide (Figure 6-2 B).

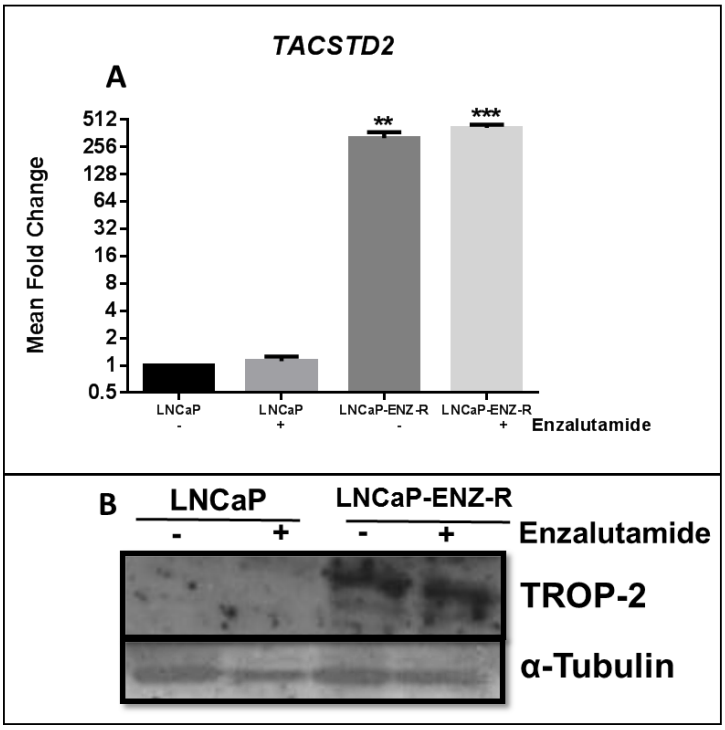

Figure 6-2 TROP-2 expression is increased in the LNCaP-ENZ-R cell line

LNCaP and LNCaP-ENZ-R cells were seeded out in 6-well plates. The cells were grown in full medium simultaneously with or without 10μM enzalutamide for 48 hours. DMSO was used as a control. **A.** TACSTD2 expression was determined by QRT-PCR using specific primers. The relative expression was measured by normalizing all samples to the parental LNCaP cells. **B.** TROP-2 protein expression in parental LNCaP and LNCaP-ENZ-R cells was determined by western blotting. Alpha-tubulin was used as a loading control. Error bars represent the mean ± SD for triplicate independent experiments. P-values were determined by using student t-test (* p-value <0.05, ** p-value <0.01, *** p-value <0.001 and **** p- value < 0.0001) (representative blot).

6.2.2 Confirmation of TROP-2 knockdown LNCaP-ENZ-R cells

To confirm that the protein band detected in the previous figure belongs to TROP-2 (Figure 6-2 B), three selected oligos against TROP-2 were used to achieve knockdown. A successful knockdown of TROP-2 was achieved in LNCaP-ENZ-R cell line at both the protein and mRNA level. However, TROP-2 showed no detectable expression in parental LNCaP which is in agreement with that previously described (Trerotola *et al.*, 2012) (Figure 6-3).

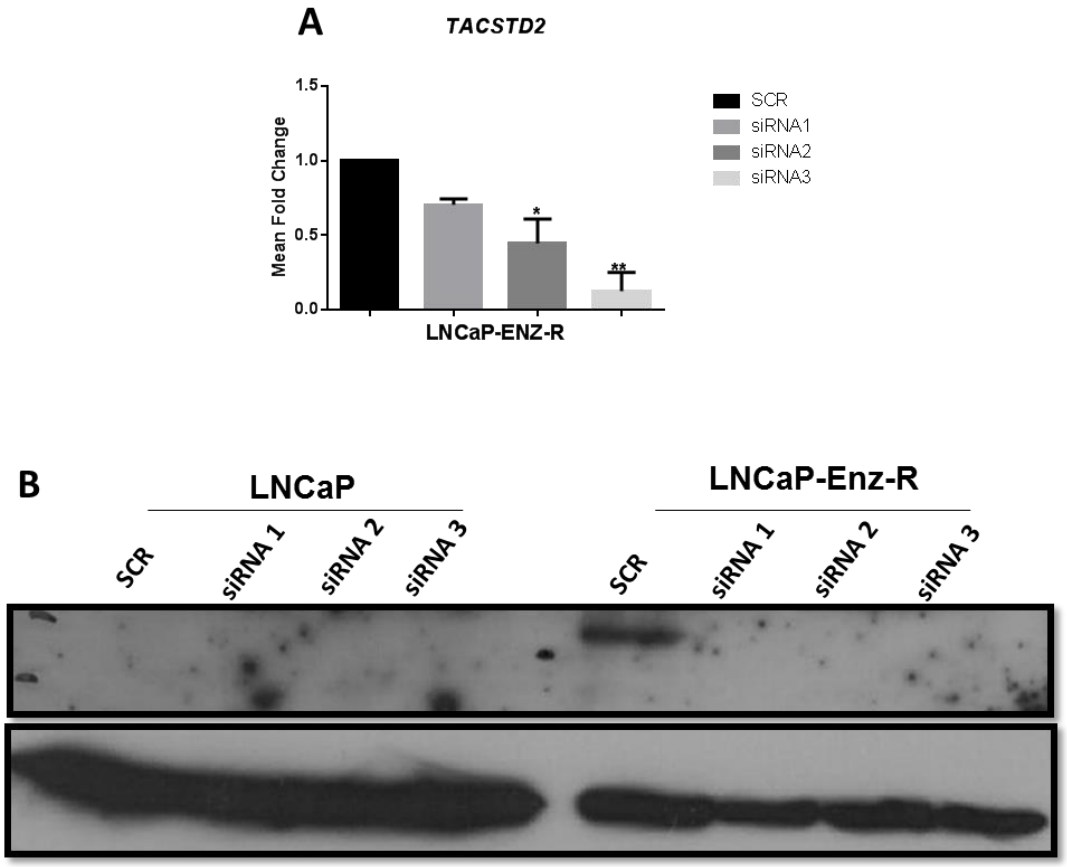

Figure 6-3 Confirmation of TROP-2 knockdown LNCaP-ENZ-R cells

LNCaP and LNCaP-ENZ-R cells were reverse transfected with three selected oligos, against TROP-2, for 72 hours. The cells were grown in full medium. Non-silencing oligo was used as a control. The cells were then lysed in RIPA buffer for protein samples and Trizol kits were used for RNA extraction. **A.** mRNA level of *TACSTD2*, the expression was determined by QRT-PCR and the relative expression was measured by normalization of all samples up to SCR. **B.** TROP-2 protein expression in parental LNCaP and LNCaP-ENZ-R cells. Alpha-tubulin was used as a loading control. Error bars represent the mean ± SD for triplicate independent experiments. p-values were determined by using student t-test (* p-value <0.05, ** p-value <0.01) (representative blot).

6.2.3 Knockdown of TROP-2 significantly decreases the proliferation of LNCaP-ENZ-R cells

To study the effect of TROP-2 on the proliferation of parental LNCaP and LNCaP-ENZ-R cells, TROP-2 knockdown was achieved by using three oligos against TROP-2 and the cells were counted by staining with Trypan blue. The results showed that knockdown of TROP-2 in LNCaP-ENZ-R cells significantly decreased proliferation. However, no significant effect on proliferation was detected in parental LNCaP cells (Figure 6-4).

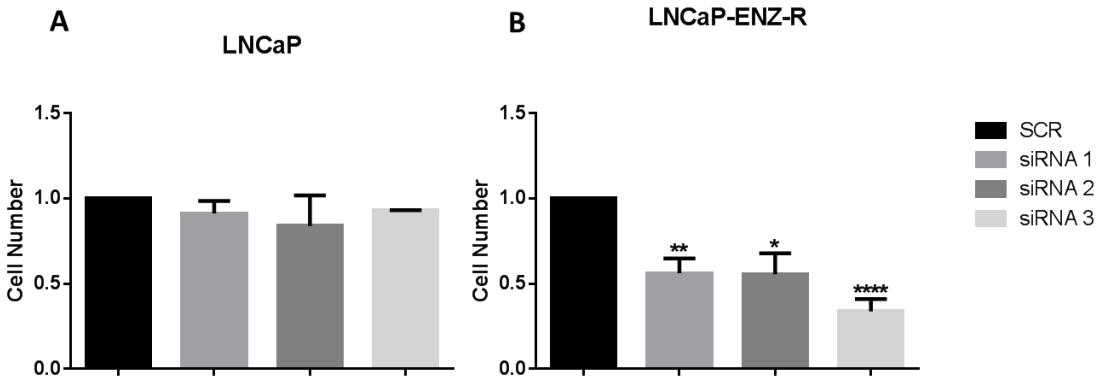

Figure 6-4 Cell counts of LNCaP and LNCaP-ENZ-R cells in response to TROP-2 knockdown

LNCaP and LNCaP-ENZ-R cells were reverse transfected with two selected oligos against TROP-2 for 72 hours. The cells were grown in full medium. **A**. Cell counts after LNCaP cells were transfected with three selected oligos against TROP-2 for 72 hours **B.** Cell counts after LNCaP-ENZ-R cells were transfected with three selected oligos against TROP-2, for 72 hours. Error bars represent the mean ± SD for triplicate independent experiments. p-values were determined by using student t-test (* p-value <0.05, ** p-value <0.01m, *** p-value <0.001 and **** p- value < 0.0001).

6.2.4 Knockdown of TROP-2 has no effect on the cell cycle in parental LNCaP cells

To observe the influence of TROP-2 on the cell cycle, two selected oligos against TROP-2 were used to achieve TROP-2 knockdown. The cells were collected and washed with PBS then fixed with a citrate buffer and subsequently the DNA was stained with propidium iodide (PI). RNase was added to degrade RNA for 40 minutes. PI binding to the DNA was quantified by a BD FACs Calibre capturing 10,000 events per sample. Only single cells were gated, which was represented sub-G1, G1, S and G2/M in a FL2-W vs FL2-A plot. The results show that knockdown of the TROP-2 had no detectable effect on the progress of the cell cycle in LNCaP cells (Figure 6-5).

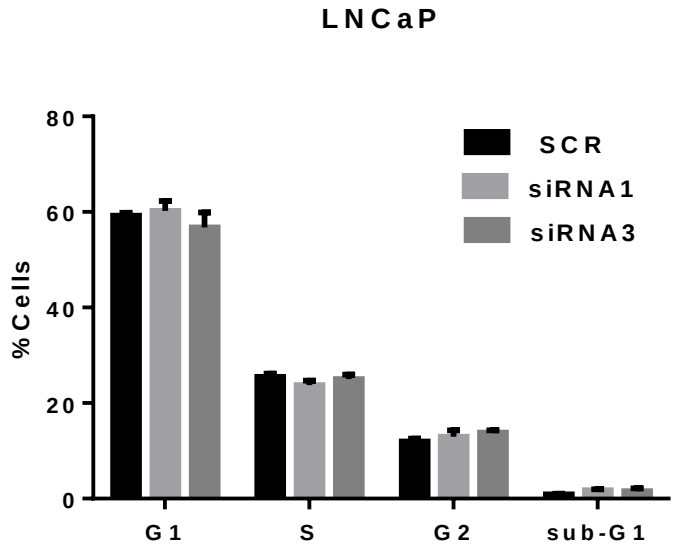

Figure 6-5 Knockdown of TROP-2 has no effect on cell cycle progression in parental LNCaP cells

LNCaP cells were reverse transfected with two selected oligos against TROP-2 for 72 hours. The cells were grown in full medium. A non-silencing oligo was used as a control. All data analysis was carried out using FlowJo_V10 software. Error bars represent the mean ± SD for triplicate independent experiments.

6.2.5 Knockdown of TROP-2 results in an increased accumulation of LNCaP-ENZ-R cells in sub-G1

An investigation of the effect of TROP-2 knockdown on the cell cycle was extended to the LNCaP-ENZ-R cell line. Two selected oligos against TROP-2 were used to achieve TROP-2 knockdown. The cells were collected and washed with PBS then fixed with a citrate buffer and the DNA was subsequently stained with propidium iodide (PI). RNase were added to degrade RNA for 40 minutes. PI binding to the DNA was quantified by a BD FACs Calibre capturing 10,000 events per sample. Only single cells were gated representing sub-G1, G1, S and G2/M in a FL2-W vs FL2-A plot. All data analysis was carried out using FlowJo_V10 software. The results showed that knockdown of the TROP-2 causes an accumulation of cells in the sub-G1 phase (Figure 6-6).

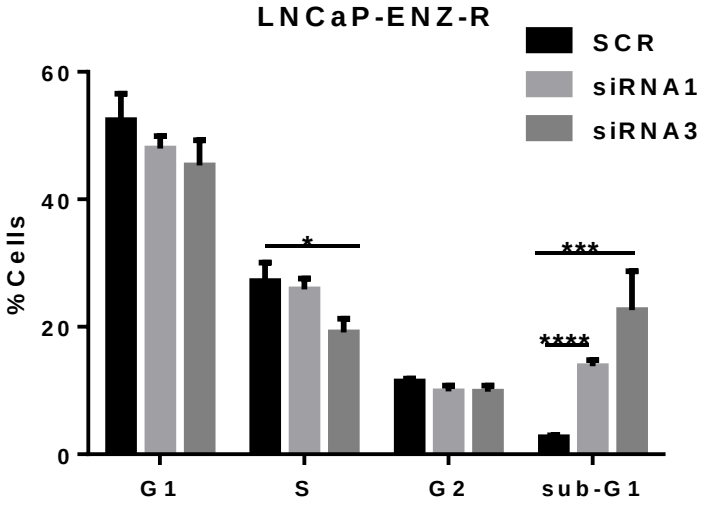

Figure 6-6 Knockdown of TROP-2 results in accumulation of LNCaP-ENZ-R cells in sub-G1

LNCaP-ENZ-R cells were reverse transfected with two selected oligos against TROP-2 for 72 hours. The cells were grown in full medium. A non-silencing oligo was used as a control. All data analysis was carried out using FlowJo_V10 software. Error bars represent the mean ± SD for triplicate independent experiments. p-values were determined by using student t-test (* p-value <0.05, ** p-value <0.01m, *** p-value <0.001 and **** p- value < 0.0001).

6.2.6 Knockdown of TROP-2 has no effect on migration of parental LNCaP cells

TROP-2 has previously been found to play an important role in cell adhesion by promoting prostate cancer cell detachment from the extra-cellular matrix (ECM), representing an aggressive phenotype of cancer, associated with a metastatic phenotype (Trerotola *et al.*, 2015). To investigate the effect of TROP-2 on the migration of parental LNCaP cells, TROP-2 knockdown was achieved by two oligos against TROP-2 and a wound healing assay used to investigate the migration of the cells. The cells were left until near 100% confluency. At this stage, a perpendicular scratch was performed using p20 filter tips. Images were taken of three separate fields for each well at 0h, 6h, 24h and 48h. The width of the "wound" was measured using ImageJ software. This was achieved by overlaying a 20 square grid over each image taking an average and normalising to the 0 hour control. The results showed that knockdown of TROP-2 in parental LNCaP cells had no effect on migration **(**Figure 6-7).

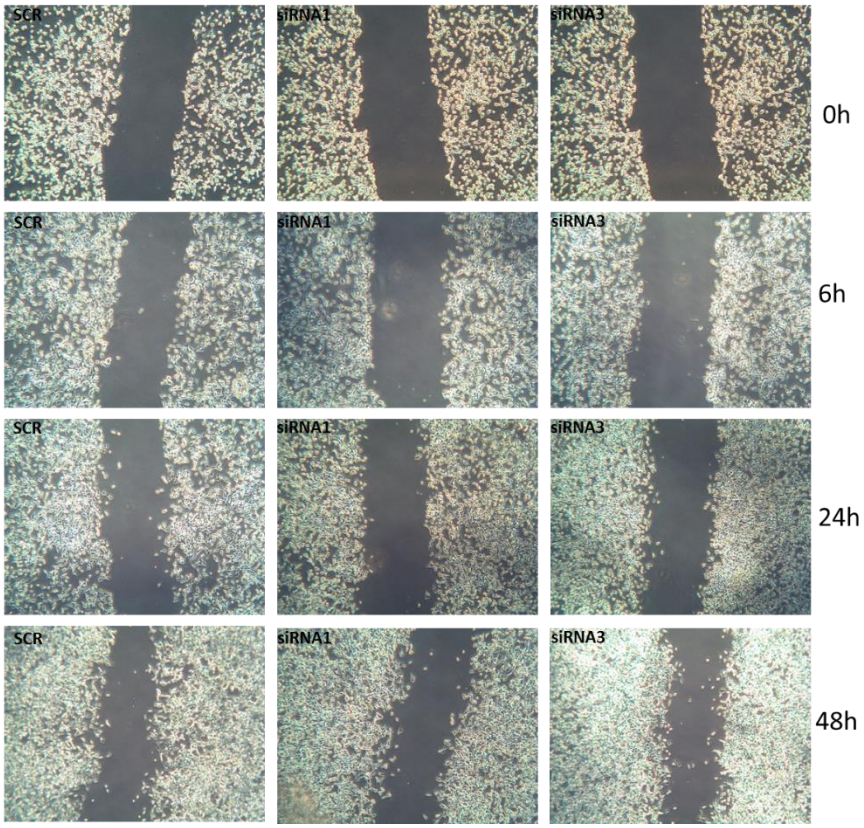

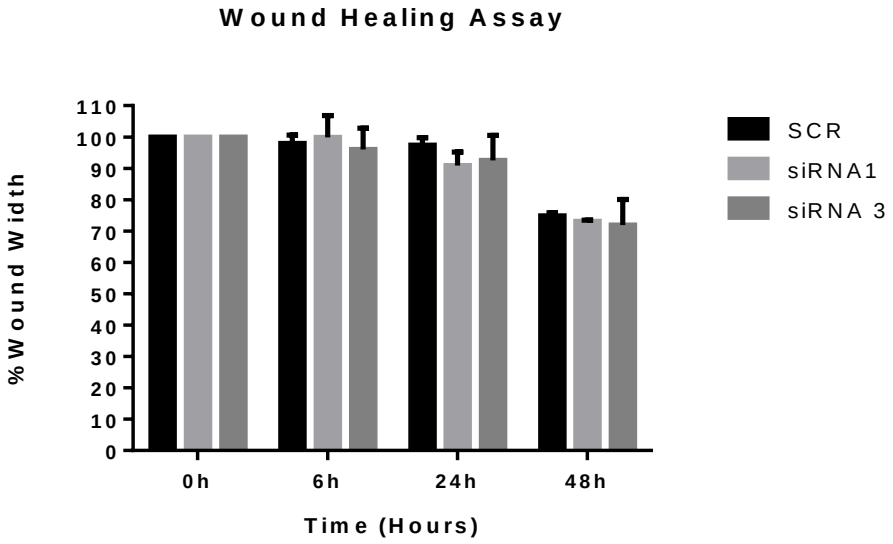

Figure 6-7 Knockdown of TROP-2 has no effect on migration of parental LNCaP cells

LNCaP cells were reverse transfected with two selected oligos against TROP-2 for 72 hours. Non-silencing oligo was used as a control. The cells were grown in full medium. Images were taken of three fields for each well at 0h, 6h, 24h and 48h. The width of wound was measured by using ImageJ software by overlaying a 20 square grid over each image, taking an average and normalising to the 0 hour control. Error bars represent the mean ± SD for triplicate independent experiments.

6.2.7 Knockdown of TROP-2 significantly decreases migration of LNCaP-ENZ-R cells

The same experimental conditions from the previous experiment (Figure 6-7) were applied to the LNCaP-ENZ-R cell line. The results showed that knockdown of TROP-2 decreases migration of the cells, with the effect being most pronounced with siRNA3 at 48 hours (Figure 6-8). Another effect detected during this experiment was increased cell death, which was observed down the microscope, further investigation is suggested for this finding.

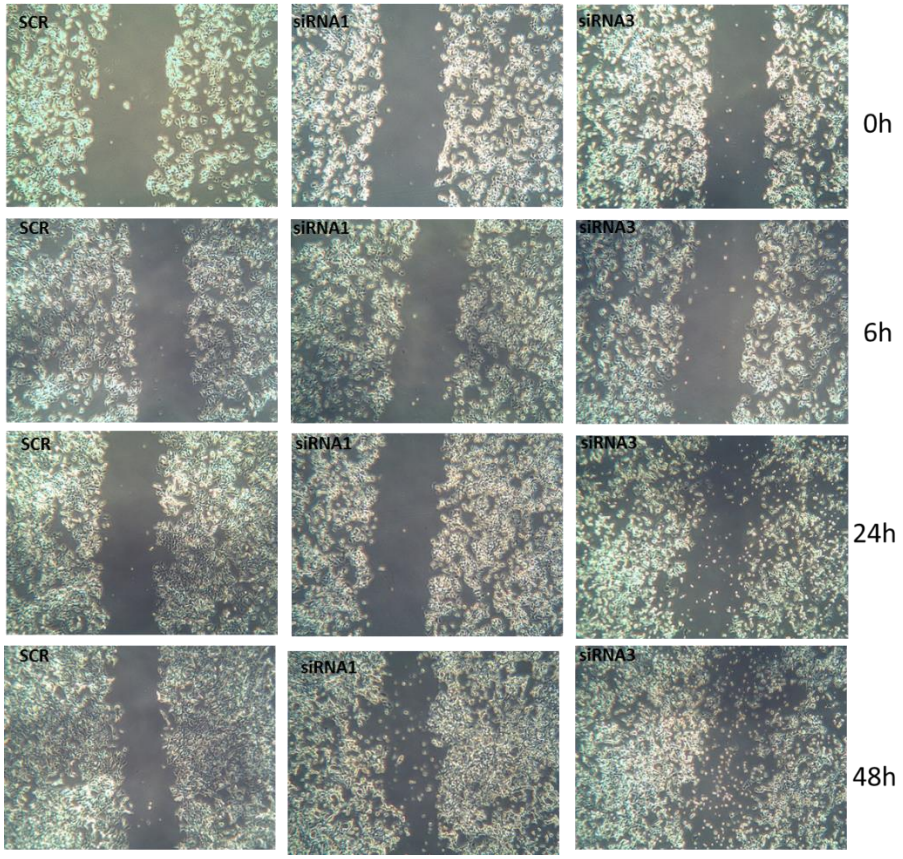

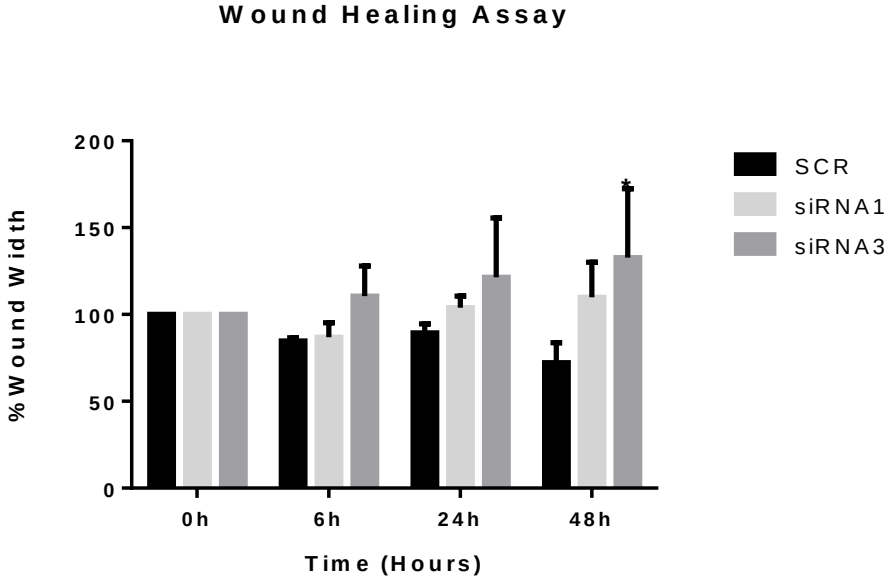

Figure 6-8 Knockdown of TROP-2 decreases migration of LNCaP-ENZ-R cells

LNCaP-ENZ-R cells were reverse transfected with two selected oligos against TROP-2, for 72 hours in full medium. A non-silencing oligo was used as a control. The cells were grown in full medium. Images were taken of three fields for each well at 0h, 6h, 24h and 48h. The width of wound was measured by using ImageJ software by overlaying a 20 square grid over each image, taking an average and normalising to the 0 hour control. Error bars represent the mean ± SD for triplicate independent experiments.

6.2.8 The effect of TROP-2 knockdown on the regulation of epithelial mesenchymal transition (EMT) in LNCaP-ENZ-R cells

To further investigate the effect of TROP-2 on migration, as observed in the previous experiment (Figure 6-8). Knockdown of TROP-2 was achieved and the expression of E-cadherin and Vimentin, which represents an epithelial and mesenchymal marker respectively, were detected by using QRT-PCR. The result shows that knockdown of TROP-2 with siRNA3 causes a significant increase in mRNA expression of E-cadherin, while significantly decreasing mRNA expression of Vimentin (Figure 6-9).

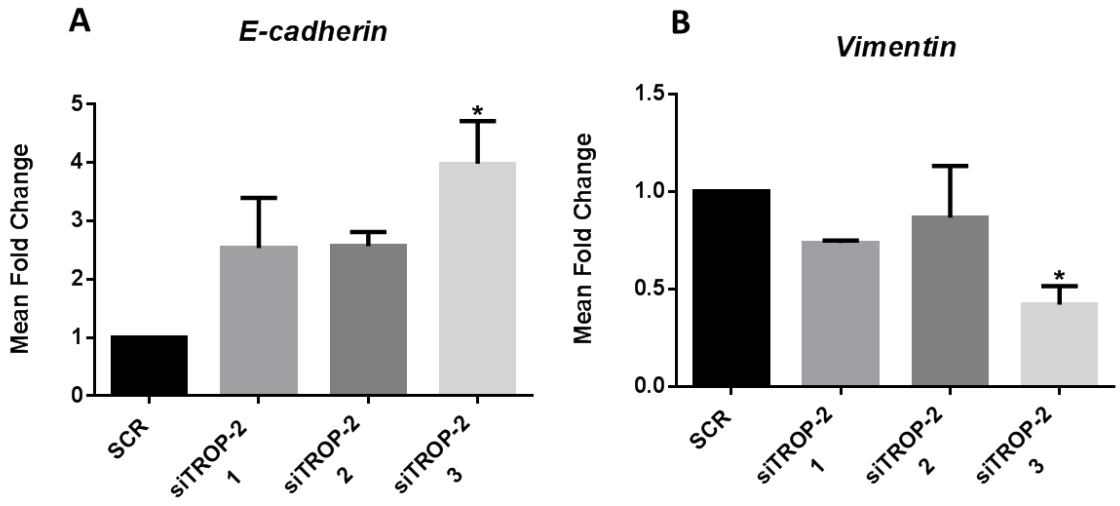

Figure 6-9 The effect of TROP-2 knockdown on epithelial mesenchymal transition (EMT) in LNCaP-ENZ-R cells

LNCaP-ENZ-R cells were reverse transfected with three selected oligos against TROP-2 for 72 hours. The cells were grown in full medium. A non-silencing oligo was used as a control. **A**. E-cadherin expression was determined by QRT-PCR using specific primers. The relative expression was measured by normalizing all samples up to the SCR control. **B**. Vimentin expression was determined by QRT-PCR using specific primers. The relative expression was measured by normalizing all samples to the SCR. Error bars represent the mean ± SD for triplicate independent experiments. p-values were determined by using student t-test (* p-value <0.05).

6.2.9 Expression of pAkt, pERK1/2, c-MYC and p27 in response to TROP-2 knockdown in LNCaP and LNCaP-ENZ-R cells

To further investigate the cell death that was observed during the cell cycle progression analysis of LNCaP-ENZ-R cells in response to TROP-2 knockdown (Figure 6-6), the protein expression of pAkt, pERK1/2, c-MYC and p27 were measured in response to TROP-2 knockdown utilizing western blotting. The results showed a decreased expression of pAkt, c-MYC and pERK1/2 and an increased expression of p27 in response to TROP-2 knockdown in LNCaP-ENZ-R cells (Figure 6-10 B). However, there was no obvious, similar effect of TROP-2 knockdown on pAkt, pERK1/2 and p27 noticed in LNCaP parental cells (Figure 6-10 A).

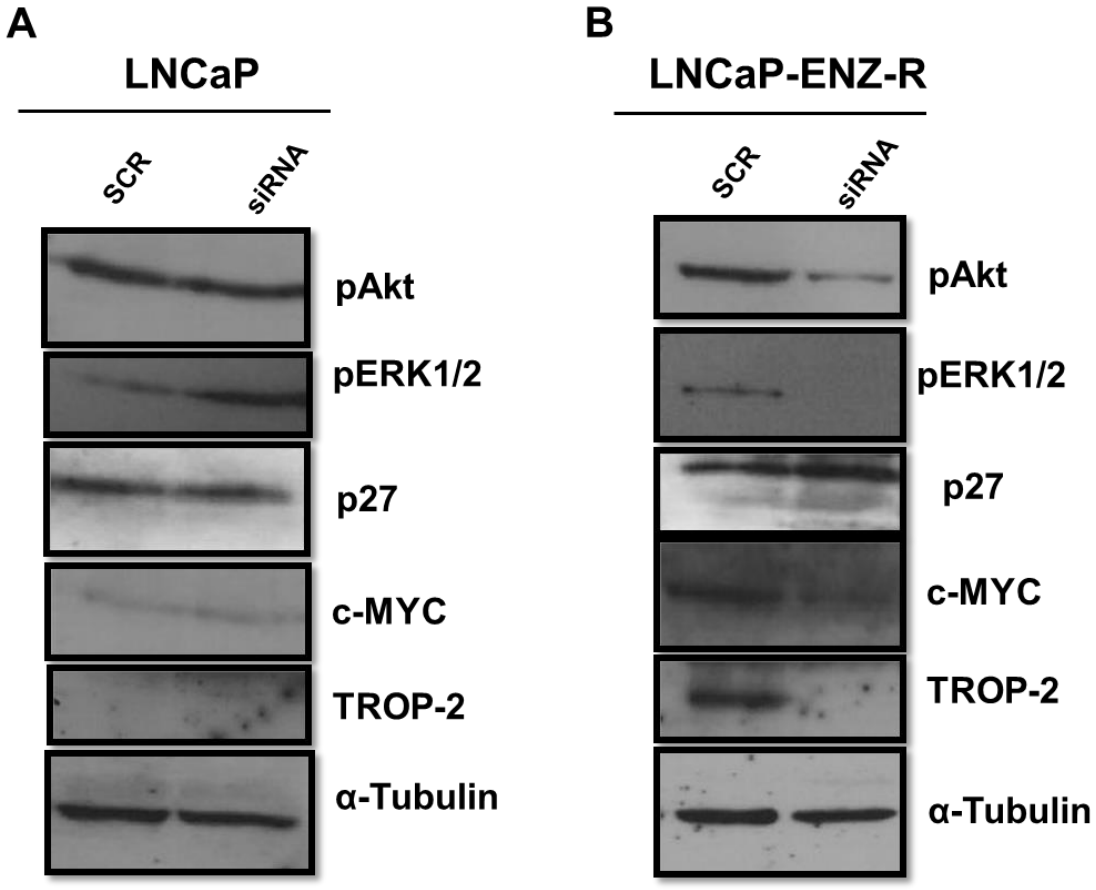

Figure 6-10 Expression of pAkt, pERK1/2, c-MYC and p27 in response to TROP-2 knockdown in LNCaP and LNCaP-ENZ-R cells

LNCaP and LNCaP-ENZ-R cells were reverse transfected with one selected oligo against TROP-2 for 72 hours. A non-silencing oligo was used as a control. The cells were grown in full medium. The cells were lysed using a RIPA buffer **A**. Protein expression of pAkt, pERK1/2, c-MYC, p27 and TROP-2 in LNCaP parental cells. **B**. Protein expression of pAkt, pERK1/2, p27 and TROP-2 in LNCaP-ENZ-R cells. Alpha-tubulin was used as a loading control (representative blot).

6.2.10 Higher expression of c-MYC in LNCaP-CDX-R, LNCaP-ENZ-R and LNCaP-ARN-R cells, compared to parental LNCaP cells

To further investigate the effect of TROP-2 on the transcription level of *c-MYC*. *c-MYC* expression at the mRNA level was measured in LNCaP-CDX-R, LNCaP-ENZ-R and LNCaP-ARN-R cells compared to parental LNCaP cells. The results showed a significantly higher expression of *c-MYC* in the LNCaP-CDX-R, LNCaP-ENZ-R and LNCaP-ARN-R cell lines compared to parental LNCaP cells ($p<0.05$) (Figure 6-11 A). TROP-2 knockdown was then achieved by using siRNA against TROP-2 in LNCaP-ENZ-R and LNCaP cells and *c-MYC* expression was detected by QRT-PCR. The data from this experiment showed that knockdown of TROP-2 led to a significant decrease ($p< 0.05$) of *c-MYC* expression in LNCaP-ENZ-R cells, while no significant change was noticed in LNCaP cells (Figure 6-11 B,C).

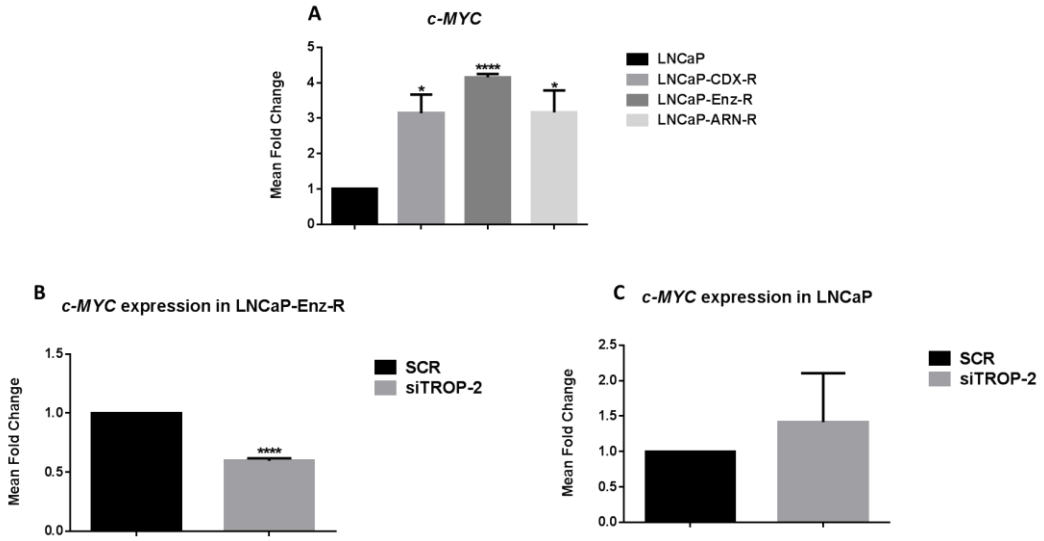

Figure 6-11 Higher expression of c-MYC in LNCaP-CDX-R, LNCaP-ENZ-R and LNCaP-ARN-R cells compared to parental LNCaP cells

Parental LNCaP and Casodex-, enzalutamide- and ARN509-resistant cell lines were seeded in 6-well plates in full medium for 24 hours. Trizol kits were used for RNA extraction. **A**. *c-MYC* expression was determined by quantitative PCR. **B**. LNCaP-ENZ-R cells were reverse transfected with one selected oligo against TROP-2 for 72 hours. A non-silencing oligo was used as a control. The *c-MYC* expression was determined by quantitative PCR using specific primers. **C**. LNCaP cells were reverse transfected with one selected oligo against TROP-2 for 72 hours. Non-silencing oligo was used as control. The *c-MYC* expression was determined by quantitative PCR using specific primers. p-values were determined by t-test (* p-value <0.05, ** p-value <0.01, *** p-value <0.001 and **** p- value < 0.0001).

6.2.11 Higher expression of TROP-2 in castrate-resistant patients, compared to hormone-naïve and hormone-sensitive patients

Previously, the data showed a higher expression of TROP-2 in resistant cell lines compared to the parental LNCaP cells. To seek validation of this data in patient samples, TMA5 was selected to investigate the expression of TROP-2. TMA5 was selected as the samples were taken from the same patients before and then some time after hormone therapy was initiated. The pairs were divided into three groups: firstly a hormone naïve group containing patient's tissues which never received hormone treatment. Secondly, hormone sensitive group containing patient's tissues which had subsequently received ADT to good effect and continued to be sensitive to the treatment. Then the final castrate resistant group, which included patients who received hormone treatment initially to good effect, but had relapsed and subsequently found to have castration resistant PC. The results showed that TROP-2 expression did not change between matched patients belonging to the continued treatment naïve group and the sensitive to treatment group. The results also demonstrated higher expression of TROP-2 in matched patients who relapsed after treatment. The data also showed a significant increase in the expression of TROP-2 in the relapsed group compared to the treatment naïve group (Figure 6-12).

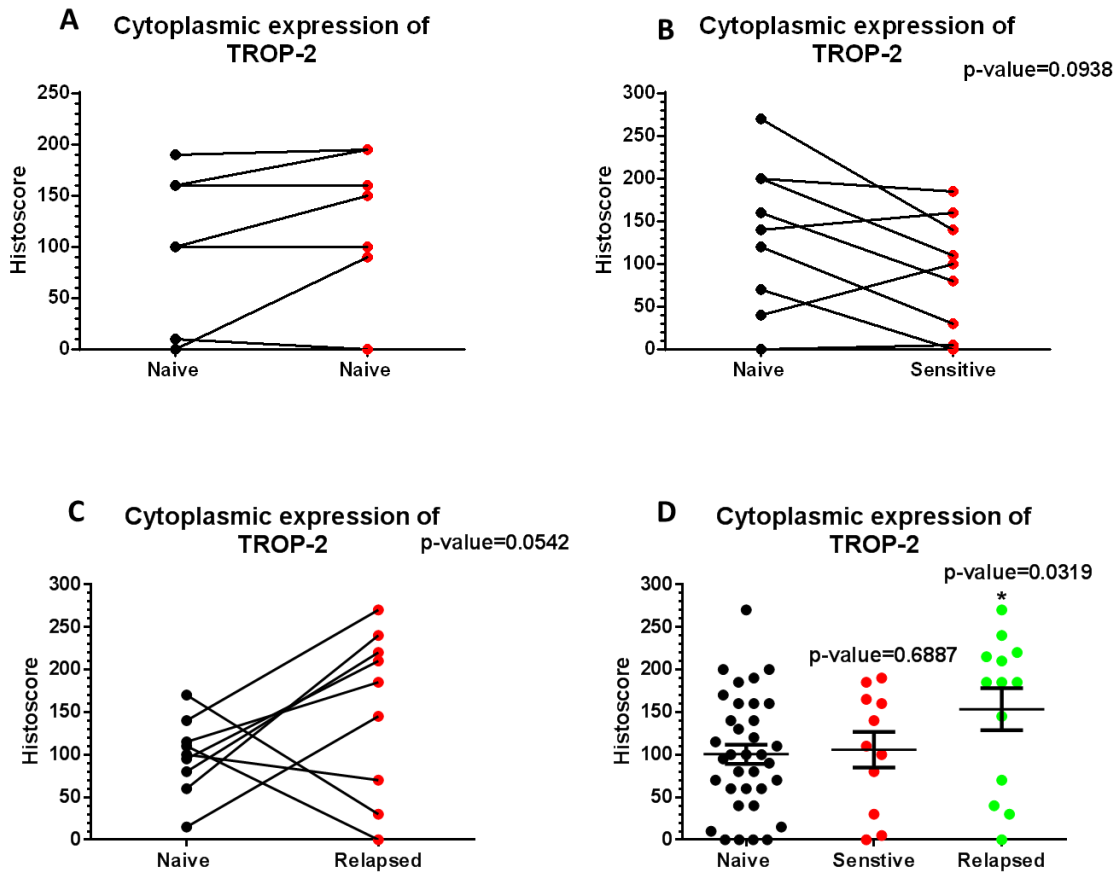

Figure 6-12 Cytoplasmic expression of TROP-2 in matched patients who were naïve, sensitive to the androgen withdrawal treatment and relapsed patients who were resistant to antiandrogens.

A. There was no significant change in TROP-2 expression in matched samples from patients with a diagnosis of prostate cancer who had not received any treatment. **B**. A non-significant decrease in TROP-2 expression was observed in matched samples from patients who were initially treatment naïve, received ADT(and were sensitive) and continued to be sensitive to this treatment when the second tissue sample was taken. **C**. There was a non-significant increase in cytoplasmic TROP-2 expression in matched samples taken from patients who were screened after they relapsed following treatment. **D.** A significant increase in TROP-2 expression was noticed in the relapsed patients compared to the treatment naïve group.

6.3 Discussion

*TACSTD*2 gene encodes a transmembrane Ca^{+} signal transducer 2 protein which is normally expressed in the trophoblast cells. It has been shown that TROP-2 is a biomarker associated with neoplastic and normal prostate stem cells (Trerotola *et al.*, 2010). Expression of TROP-2 is associated with poor outcome and aggressiveness of pancreatic, oral, colorectal, gastric and ovarian cancers, proposing that it has a role in cancer progression and it can be a target for anticancer immunotherapy (Trerotola *et al.*, 2013a). Anti-TROP-2 monoclonal antibodies have been reported to inhibit the proliferation of uterine serous papillar carcinoma cells and mediated cytotoxicity *in vitro*. However, TROP-2 was also detected in normal tissue making the use of inhibitors for TROP-2 challenging (Trerotola *et al.*, 2013a). A study has found that transfecting LNCaP cells with TROP-2 siRNA significantly reduces the percentage of viable cells 7 days after docetaxel withdrawal suggesting that the TROP-2 glycoprotein itself may play an active role in the recovery process, after chemotherapy and androgen ablation treatments. The same authors observed that high TROP-2 expression correlates with poor prognosis in cohorts of prostate cancer patients particularly in patients with low (Gleason 6) grade tumours (Xie *et al.*, 2016). Another study showed that TROP-2 was not expressed in androgen-sensitive LNCaP cells and forced overexpression of TROP-2 inhibits cell adhesion to fibronectin (Rothdiener *et al.*, 2010) suggesting the promotion of an aggressive phenotype of PC cells, since it is conceivable that more aggressive cells tend to be poorly adhesive and more motile than less aggressive cells. Another group suggested that TROP-2 expression is a requirement for cancer cells needing to detach from the extracellular matrix (ECM) (Trerotola *et al.*, 2012).

From the microarray data, high expression of *TACSTD*2 was detected in LNCaP-ENZ-R cells compared to parental LNCaP cells and QRT-PCR validation confirmed these results at the mRNA level (Figure 6-2 A). To confirm the results at the protein level, LNCaP cells and LNCaP-ENZ-R cells were grown in full medium and treated with or without enzalutamide for 48 hours. The results showed that TROP-2 is expressed in the LNCaP-ENZ-R cell line. However, no expression of TROP-2 was observed in parental LNCaP cells (Figure 6-2 B) which is consistent with Trerotola *et al.* (2012) results. They demonstrated that TROP-2 expression is found to be higher in aggressive DU145 and PC3 cells and undetectable in LNCaP cells. Thus, TROP-2 expression levels may reflect an aggressive phenotype of PC.

In the current study, an attempt was made to study the biological role of TROP-2 in enzalutamide-resistant cells and to investigate the effects of its expression on enzalutamide-resistant cell proliferation, cell cycle and migration compared to parental LNCaP cells. Three selected oligos against TROP-2 were used to achieve the knockdown. A successful knockdown of TROP-2 was achieved in LNCaP-ENZ-R cells at the protein and mRNA level. However, TROP-2 showed no detectable expression in parental LNCaP cells (Figure 6-3), in agreement with the previous experiment (Figure 6-2).

This study investigated the influence of TROP-2 on the proliferation of parental LNCaP and LNCaP-ENZ-R cells in response to loss of the TROP-2 transcriptome. TROP-2 knockdown was achieved by using three separate oligos and cells were counted to detect the proliferation. The results demonstrated that the knockdown of TROP-2 in LNCaP-ENZ-R cells significantly decreased proliferation. However, no effect on proliferation was detected in parental LNCaP cells. This suggests that TROP-2 may regulates the proliferation in the drug-resistant LNCaP-ENZ-R cells (Figure 6-4).

To further investigate the role of TROP-2 on proliferation, a cell cycle distribution analysis was applied to both cell lines after TROP-2 knockdown. As expected, the siRNAs against TROP-2 caused a significant accumulation of the LNCaP-ENZ-R cells at the sub-G1 phase. However, no effect of siRNAs against TROP-2 was noticed in the cell cycle progression of LNCaP parental cells (Figure 6-5, 6). This further suggests that the expression of TROP-2 is important for LNCaP-ENZ-R cell proliferation. This data are in agreement with Cubas *et al.* (2010) who reported that TROP-2 expression increased tumour growth in both subcutaneous and orthotopic pancreatic cancer murine models and also led to increased liver metastasis. Additionally, TROP-2 expression also increased the levels of phosphorylated ERK1/2 mediating cell cycle progression, by increasing the levels of cyclin D1 and cyclin E as well as downregulating p27.

Further investigation of the role of TROP-2 on the phenotype of LNCaP and LNCaP-ENZ-R cells was undertaken. A wound healing assay was used to investigate cell migration in response to TROP-2 knockdown. A long term wound healing assay more than 24 hours cannot distinguish cell proliferation from cell motility. In addition, some cells attached to the edge of the scratch after wounding. This study was tried to measure cell migration using the trans-well assay. The principle of this assay is based on two medium containing chambers separated by 8 µm porous membrane through which cells transmigrate. However, we faced a problem that LNCaP-ENZ-R cell lines was not able to pass through these pores as it was bigger size than parental LNCaP. This study

suggested that keep grown the LNCaP-ENZ-R in present of enzalutamide led to change in the morphology of these cells by became bigger in size and more irregular in shape and also slower in the growth than parental LNCaP.

For that reason this study select wound healing assay to measure the cell direction, and the results from this study showed that knockdown of TROP-2 in parental LNCaP cells had no effect on migration (Figure 6-7). However, knockdown of TROP-2 decreased migration of the LNCaP-ENZ-R cells at 6, 24 and 48 hours. Another effect visualised down the microscope was apparent increased cell death (Figure 6-8). The effect of TROP-2 on migration was described previously Cubas *et al.* (2010). Ectopically expressed TROP-2 in subcutaneous and orthotopic pancreatic cancer murine cells showed increase cell migration.

To further investigate the effect of TROP-2 on cell migration, epithelial mesenchymal transition (EMT) markers were examined in response to TROP-2 knockdown. EMT was identified as a biological process in which epithelial cells obtain a migratory and invasive mesenchymal phenotype. It is typically characterized by loss of epithelial markers such as E-cadherin and gain of mesenchymal biomarkers such as N-cadherin and vimentin. In particular, EMT has been reported to mediate cancer metastasis and confer resistance to therapeutic preclinical model systems of mammary, lung, pancreatic and bladder cancer. Moreover, EMT facilitates prostate cancer progression and metastasis (Sun *et al.*, 2012). The expression levels of both E-cadherin and Vimentin were determined in response to TROP-2 knockdown and the results showed an increased expression of E-cadherin, while a decrease in expression of Vimentin, in response to TROP-2 knockdown in LNCaP-ENZ-R cells was observed (Figure 6-9). This suggests that TROP-2 may perhaps also regulate EMT in this cell line. The data was consistent with Chen *et al.* (2014) who demonstrated that high TROP-2 expression was significantly associated with a loss of the epithelial marker E-Cadherin in gall bladder cancer patients tissue by using immunohistochemistry. This study noticed that siRNA3 provide a significant effect more than siRNA1 and siRNA2 on the expression of both N-cadherin and vimentin. This could be explained that siRNA3 led to a significant reduction in the expression of TROP-2 at mRNA more than siRNA1 and siRNA2 (Figure 6-3).

This study showed that loss of TROP-2 expression in the LNCaP-ENZ-R cell line led to a decreased number of viable cells. Similarly, cell cycle analysis showed an accumulation of the cells at the sub-G1 phase. Moreover, loss of TROP-2 transcriptome was able to reduce the LNCaP-ENZ-R cell line ability to migrate. This might be indicative that TROP-2 transduces a survival signal that has a crucial role in prostate cancer growth. To

validate such a theory, this study verified the role of TROP-2 in the regulation of PI3 Kinase (pAkt) and MAP Kinase (pERK1/2) pathway activity as this study had previously shown that both pathways are active in LNCaP-ENZ-R cells.

The data demonstrated that loss of TROP-2 expression led to a decrease in the protein expression of pAkt in LNCaP-ENZ-R cells (Figure 6-10). Previously, this study demonstrated a high expression of pAkt in LNCaP-ENZ-R cells (figure 3-6), compared to the parental LNCaP. This perhaps suggests that inhibition of TROP-2 leads to an increase in the sensitivity of LNCaP-ENZ-R cells to apoptosis by inhibition of the activity of Akt. This statement is based on the observation fact that activated Akt leads to the inhibition of apoptosis by inactivating several proapoptotic proteins, including BAD, BAX and caspase 9 and also by inducing the expression of anti-apoptotic proteins such as BCL2, BCLXL, FLIP, cIAP2, XIAP and survivins in myeloma cells (Mitsiades *et al.*, 2002).

A previous experiment demonstrated that TROP-2 might regulate Akt activity (Figure 6-10) due to cross-reaction between PI3K/Akt and MAP Kinase signalling pathways. This study hypothesised that TROP-2, as a transmembrane glycoprotein, might transduce apoptosis signalling through the MAP Kinase pathway. This might give an understanding of the increased apoptosis seen with TROP-2 knockdown in LNCaP-ENZ-R cells. The results from this study demonstrated that knockdown of TROP-2 protein leads to no detectable pERK1/2 (Figure 6-10), which may explain the increased apoptosis seen in the LNCaP-ENZ-R cell line. A previous study showed that Raf/MEK/ERK may promote cell cycle arrest in PC cells and this may be regulated by p53, as restoration of wild-type p53 results in enhanced sensitivity to chemotherapeutic drugs (McCubrey *et al.*, 2007). The same study indicated that both Raf/MEK/ERK and PI3K/PTEN/Akt pathways have anti-apoptotic and drug resistance effects on cells and also interact with the p53 pathway. The limitation of this experiment is not investigate total Akt and total ERK1/2, which might add a robust finding for this study.

The previous data suggests that TROP-2 regulates ERK1/2 activity (Figure 6-10) and a study has shown that ERKs can directly phosphorylate many transcription factors, including Ets-1, c-Jun and c-MYC (Zhao and Lee, 1999). This study examined the expression of c-MYC in LNCaP-CDX-R, LNCaP-ENZ-R and the LNCaP-ARN-R cell lines compared with parental LNCaP cells and c-MYC expression in response to TROP-2 knockdown. The data showed that a higher expression of c-MYC was detected in the drug-resistant LNCaP-CDX-R, LNCaP-ENZ-R and LNCaP-ARN-R cell lines compared

to parental LNCaP cells (Figure 6-11 A). The results from this study also demonstrated that loss of TROP-2 expression led to a decrease of c-MYC expression in LNCaP-ENZ-R cells, at the protein and mRNA level. As expected, no effect of TROP-2 knockdown on c-MYC expression in parental LNCaP was observed (Figure 6-11 B, C). This may be a further explanation for the reduction in proliferation seen in response to TROP-2 knockdown, as it has been shown that inhibition of c-Myc expression abrogates proliferation and blocks cell cycle progression of breast cancer cells (Butt *et al.*, 2005). This study suggests that TROP-2 regulates ERK1/2 signalling, which directly activates the transcription factor c-MYC, giving an explanation for the cell cycle arrest and proliferation inhibition seen in response to TROP-2 knockdown. Further investigation of the role of TROP-2 in the regulation of the cell cycle was examined in this study by investigating the expression of p27, a key regulator of cell cycle, in response to TROP-2 knockdown. The results showed that loss of TROP-2 protein led to a small increase in the expression of the p27 protein in LNCaP-ENZ-R cells, while no effect was noticed in LNCaP cells. However, no arrest of the LNCaP-ENZ-R cells in G1 or S-phase was seen in cell cycle analysis. It is known that p27 is a key regulator of G1 and S-phase (Porter *et al.*, 1997). This suggests that TROP-2 has less of an effect on the expression of p27. However, further experiments are certainly required to address this. Below is a cartoon summarized the finding of this chapter (Figure 6-13)

In the current study, a high expression of TROP-2 was noticed in enzalutamide-resistant cells, which are used as one tool to represent drug-resistant CRPC in the clinic, compared to LNCaP cells at the protein and mRNA levels. For that reason, it was hypothesised that TROP-2 may act as a prognostic biomarker in patients who relapsed after an initial good response to hormonal deprivation therapy. TMA5 was selected as it contains three groups of matched pairs; a naïve group, a drug sensitive group and a relapsed group. The data was consistent with TROP-2 expression on the cellular level, as a significant increase was noticed in the relapsed group (representing castrate resistant PC) to complement that seen in the enzalutamide-resistant cell line, suggesting that TROP-2 could be a potential prognostic biomarker for anti-androgen resistance patient (Figure 6-12). Again, further studies are required.

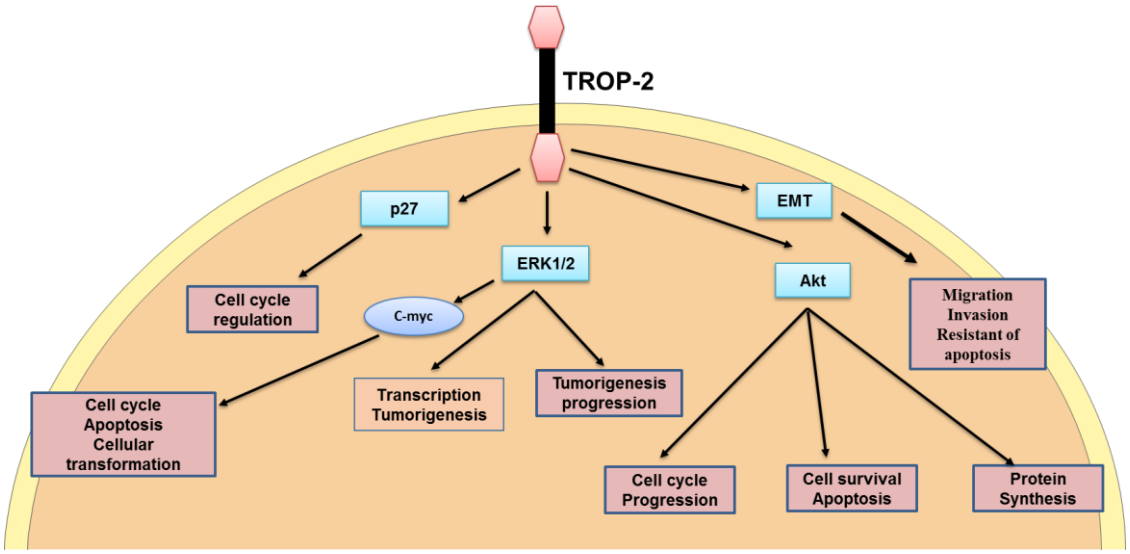

Figure 6-13 Functional role of TROP-2 in LNCaP-ENZ-R cell line

Chapter 7. General Discussion

7.1 General Discussion

The androgen receptor is a transcription factor that plays a crucial role in male sexual development and growth of the prostate gland. AR also plays an essential role in the development of human prostate cancer. In patients with clinically significant disease, not fit or not appropriate for curative treatments, ADT is largely used to inhibit tumour cell proliferation. However, tumour regrowth inevitably occurs following a period of treatment response. A hormone refractory or "castrate-resistant" stage of the disease is characterized by an increase in the expression of AR and AR target genes, such as PSA, suggesting that the AR pathway remains active in this advanced stage of the disease (Isaacs and Isaacs, 2004). As mentioned in the introductory chapter; HER2/HER3 signalling enhances AR stability and optimises binding of the AR to the promoter region of the AR target genes, suggesting that HER2/HER3 signalling is critical in hormone-refractory PC (Mellinghoff *et al.*, 2004). An initial objective of this project was to identify the role of HER2/HER3 in the available anti-androgen resistant models which have been generated in our laboratory, compared to the parental LNCaP cells. The results of this study indicated that the expression of HER2 and HER3 were significantly higher in all tested resistant cell lines (LNCaP-Casodex resistant, LNCaP-enzalutamide resistant and LNCaP-ARN509 resistant) than parental LNCaP cells, at the protein and at the mRNA levels, in cells grown in full media and basal media. Heregulin treatment leads to increased expression of HER2/HER3 at the mRNA level and this was more pronounced in the LNCaP-ENZ-R cell line.

Heregulin is known to activate HER2/HER3 through tyrosine residue phosphorylation (Gregory *et al.*, 2005). In this current study, the pathways that might be activated through stimulation of HER2/HER3 were investigated in the anti-androgen resistant models, compared to the parental cell line. The results of this study indicate that activation of HER2/HER3 in the LNCaP-ENZ-R cell line led to a stimulation of both PI3 Kinase (pAkt) and MAP Kinase (pERK1/2) signalling pathways in LNCaP-CDX-R, LNCaP-ENZ-R and LNCaP-ARN-R resistant cells, compared to parental LNCaP cells. The findings of the current study are consistent with Rao (2015) who discovered that HER2/3 have a prominent role in advanced prostate cancer. The same study showed that HER2/HER3 signalling: increases androgen receptor activity; increases downstream MAP Kinase and PI3 Kinase signalling activity; and increases cell proliferation, migration and invasion of PC cells. The results show that activating HER2/HER3 led to

a stimulation of both PI3 Kinase (pAkt) and MAP Kinase (pERK1/2) signalling pathways and this was seen to be more pronounced in LNCaP-ENZ-R cells. For that reason, the LNCaP-ENZ-R cell model was studied in more detail, always comparing to parental LNCaP cells in this study. First, the phenotypic differences between LNCaP-ENZ-R cells and parental LNCaP cells were investigated and the results of this study showed that LNCaP cellular proliferation was attenuated in SDM whereas heregulin increased the proliferation. However, proliferation of LNCaP-ENZ-R cells was not affected in steroid depleted media and enhanced with heregulin stimulation. Hence, it could conceivably be hypothesised that LNCaP-ENZ-R is an androgen independent cell line and that heregulin can enhance the proliferation of both cell lines.

The current study found that enzalutamide treatment led to a decrease in proliferation, cell cycle arrest and migration of parental LNCaP cells. However, no effect of enzalutamide on LNCaP-ENZ-R cells was noticed, which simply confirms the resistance of LNCaP-ENZ-R cells to enzalutamide drug. This result may be one reason to explain why blocking of the AR is usually very effective in the early stage of the disease and not as effective in the late stage of the disease.

This study also investigated the consequence of enzalutamide on LNCaP-ENZ-R cells, compared to parental LNCaP cells, at the genomic level. A microarray screen was applied to identify the genes which might regulate the LNCaP-ENZ-R phenotype and also to identify which proteins, coded by these genes, which are relevant in advanced, drug-resistant prostate cancer tissue and have the potential for identification by simple, inexpensive immunohistochemical techniques. The identification of such predictive biomarkers is of vital importance in drug-resistant disease.

In the current study, four conditions for the microarray screen were included: parental LNCaP, parental LNCaP with enzalutamide for 48 hours, LNCaP-ENZ-R without enzalutamide for 48 hours and LNCaP-ENZ-R with enzalutamide for 48 hours. Triplicates were generated for each sample and only samples that showed consistency and high integrity RNA were selected for the microarray screen. Relative expression of the LNCaP-ENZ-R cell line with enzalutamide condition was selected to compare with parental LNCaP cells, without enzalutamide. The microarray data analysis of LNCaP-ENZ-R cells with enzalutamide revealed that 280 genes were up-regulated significantly ($p<0.05$) and 501 genes were down-regulated significantly ($p<0.05$) compared with parental LNCaP.

From the microarray data, *SGK1, TACSTD2, RLN1, RLN2,* and *SYT4* genes were selected for further study as they were upregulated significantly ($p<0.05$) in LNCaP-ENZ-R cells compared to parental LNCaP and also are involved (directly or indirectly) in pathways that are crucial for cell proliferation, cell growth and cell signalling. Specific primers were used to validate these genes by QRT-PCR. The results were consistent with the microarray data, these genes were upregulated significantly ($p<0.05$) in LNCaP-ENZ-R cells compared to parental LNCaP cells. In addition, these genes were also upregulated at the mRNA levels in LNCaP-CDX-R and LNCaP-ARN-R cells, adding weight to the argument for the possible role of these genes in anti-androgen drug resistance.

A study in our research group found that SGK1 expression was highly expressed in the KUCaP xenograft model and a CRPC patient biopsy sample, both of which express the bicalutamide-activated receptor mutant (O'Neill *et al.*, 2015). In the same study, a SGK1 inhibitor was used on AR_{W741L} models and transcriptional and growth promoting activity was reduced, indicating opportunities for potential new and effective therapies for CRPC patients (O'Neill *et al.*, 2015). For that reason we selected SGK1 to investigate the effects of its increased expression in enzalutimde-resistant models on; proliferation, cell cycle, migration and a possible role of AR and GR in the regulation of SGK1. Similar to the mRNA level, there was higher SGK1 protein expression in LNCaP-ENZ-R cells compared to parental LNCaP cells, directing an investigation towards the consequences of increased SGK1 activity in LNCaP-ENZ-R cells (Figure 5-3). SGK1 is known as a downstream target of both AR and GR (Isikbay *et al.*, 2014). However, the role of the GR and AR in the regulation of SGK1 in advanced and enzalutimde-resistant prostate cancer remains unclear. In order to investigate the role of AR in regulation of SGK1, AR was first activated with DHT. The data from this study showed that the activation of AR led to an increase in the expression of SGK1 in both LNCaP-ENZ-R and parental LNCaP cells (Figure 5-3 and . It can therefore be assumed that the AR regulates SGK1 expression in androgen-dependent conditions and in enzalutamide-resistant conditions.

To test the alternative theory, that the GR regulates SGK1, both LNCaP-ENZ-R and parental LNCaP cells were activated with dexamethasone, which is known to activate GR. Although the activation of the GR led to an increase of SGK1 expression at the mRNA and protein level in LNCaP-ENZ-R cells (Figure 5-6), only the mRNA level of SGK1 was increased in response to dexamethasone stimulation (not at the protein level) in parental LNCaP cells (Figure 5-5). It is possible, therefore, that LNCaP-ENZ-R cells

contain a functional GR to activate SGK1, while no functional GR is able to activate SGK1 in parental LNCaP cells.

In order to test the functionality of GR in parental LNCaP and LNCaP-ENZ-R cells, in presence and absence of enzalutamide, both cell lines were kept with or without enzalutamide for 48 hours. The data showed that blocking AR with enzalutamide led to an increase in GR expression at the mRNA level in both cell lines. Similar to the mRNA level, an increase in the GR expression was noticed at the protein level in parental LNCaP cells. However, an increase in the GR was noticed in the presence and the absence of enzalutamide. This perhaps suggests LNCaP-ENZ-R cells contain a functional GR in the presence and the absence of anti-androgen blockade, therefore this might indicate that increased GR expression mediates PC resistance to enzalutamide. From the data above, the stimulation of GR led to increased SGK1 expression (Figure 5-6) and SGK1, downstream of AR (Figure 5-65). Further evidence for the role of GR in the regulation of other AR target genes was observed, such as upregulation of *KLK3*, *KLK2*, *FKPB5* and *TMPRSS2* genes in response to dexamethasone activation. We showed that no significant changes of these genes were observed in LNCaP cells (Figure 5-8). However, a significant increase of the AR target genes *KLK3*, *KLK2*, *FKPB5* and *TMPRSS2* were noticed in response to dexamethasone stimulation in LNCaP-ENZ-R cells (Figure 5-9). To confirm the previous finding, GR knockdown was achieved and AR target genes such as *KLK3*, *KLK2*, *FKPB5* and *TMPRSS2* were detected. GR knockdown led to a significant reduction in the expression of these genes in LNCaP-ENZ-R (Figure 5-11). However, no significant change in the expression of these genes was noticed in LNCaP.

From the data, this study suggests that SGK1 is regulated by AR alone in parental LNCaP cells, while both GR and AR are involved in the regulation of SGK1 in LNCaP-ENZ-R cells. This theory was tested by a demonstration that blockade of AR activity led to a decrease in the expression of SGK1 and AR target genes in parental LNCaP cells whereas no significant effects were noticed in the expression of SGK1, KLK3 and FKBP5 in response to GR knockdown in parental LNCaP cells (Figure 5-12 A, B, C). Also, stimulation of AR led to an increase in the expression of SGK1 and AR target genes in parental LNCaP cells. However, no effect of GR knockdown was observed on the expression of SGK1, KLK3 and FKBP5 which confirm the results of a previous experiment. Also, this study showed that knockdown of GR does not abrogate the AR stimulation effects on the expression of SGK1, KLK3 and FKBP5 (Figure 5-12 D, E, F). These findings suggest that AR regulates SGK1, while no significant effect of GR was

noticed in the regulation of SGK1 or other selected AR target genes in parental LNCaP cells.

The presence or absence of enzalutamide was demonstrated to have no differential effect on SGK1 expression in LNCaP-ENZ-R cells. Furthermore, GR knockdown led to a decrease in the expression of SGK1 in the presence or the absence of enzalutamide. However, enzalutamide treatment led to an increase in the expression of AR target genes, which support the results obtained from Figure 5-7 that blocking AR activity leads to an increase in the level of GR which appears to be able to regulate AR target genes. A decrease in the expression of AR target genes in response to GR knockdown with or without enzalutamide was seen in LNCaP-ENZ-R cells (Figure 5-13 A, B, C). This perhaps suggests that SGK1 could be a predictive biomarker for enzalutamide resistance, but more experiments are needed to confirm this finding. SGK1 is regulated by GR and enzalutamide does not abrogate the GR activity in LNCaP-ENZ-R cells. However, blocking AR led to an increase in the expression of GR, which then appears to regulate AR target genes and again enzalutamide does not abrogate the GR activity in the regulation of AR target genes (Figure 5-13 D, E, F).

Overall, these results indicate that GR levels remain unchanged, whether the cells are exposed to anti-androgens or not and that GR was able to regulate AR target genes such as SGK1. This might be an important factor for the proliferation of enzalutamide-resistant PC cells. So the next step undertaken was to decrease SGK1 and/or GR levels in enzalutamide-resistant cells by the use of a small molecule inhibitor and siRNA technology, respectively and investigate the phenotype of these cells, compared with parental LNCaP cells. Using the SGK1 inhibitor led to a significant decrease in the proliferation of LNCaP-ENZ-R and parental LNCaP cells. Also inhibition of SGK1 can cause a significant arrest of the cells at the G2/M and sub-G1 phases and in LNCaP-ENZ-R cells (Figure 5-19). However, no significant changes were detected in parental LNCaP cells (Figure 5-18). Also, inhibition of SGK1 activity led to a significant reduction in the migration of the LNCaP-ENZ-R cell line, starting from 24 hours of treatment (Figure 5-21). Again, no significant effects of GSK650394 on cell migration were detected in parental LNCaP cells (Figure 5-20). It can thus be suggested that SGK1 regulates proliferation and cell cycle progression of enzalutamide-resistant PC cells through the direct or indirect regulation of the activity of the mTOR protein. A previous study demonstrated that Akt promotes activation of mTOR (Sommer *et al.*, 2013).

Previously, the data from this study showed a high expression of pAkt, which was observed in LNCaP-ENZ-R cells (Figure 3-5). In addition, another study demonstrated that mTOR can mediate the activity of SGK1 (Hong *et al.*, 2008). This study gives another interesting suggestion: perhaps a high expression of pAkt promotes mTOR activation, which, in turn might regulate SGK1 activity in LNCaP-ENZ-R cells. Active mTOR contributes to an enhancement of the translation rates of various proteins involved in cell cycle progression, including cyclin D1 and D2 (Sherk *et al.*, 2008). This finding was supported by the next experiment, which demonstrated a consistently high expression of pSGK1-Ser422 in LNCaP-ENZ-R cells, with or without dexamethasone stimulation. Increasing doses of dexamethasone were able to induce incremental pSGK1-Ser422 activation in parental LNCaP cells. This suggests SGK1 may be constitutively active in the drug-resistant cells (Figure 5-14). We also showed that inhibition/knockdown of both GR and its downstream target SGK1 is a better approach to reduce the proliferation of the LNCaP-ENZ-R and the parental LNCaP cell lines (Figure 5-22).

Taken together, these results suggest that combination inhibition of SGK1 and GR is perhaps a better approach to treat patients who are resistant to enzalutamide, or as a method of delaying enzalutamide-resistance. However, further experiments will need to be undertaken in order to confirm this finding.

To test this finding in the tissue of patients with known prostate cancer, the matched pairs TMA5 was selected. The pairs were divided into three groups: a hormone naïve group containing patient's tissues which never received hormone treatment; hormone sensitive group containing patient's tissues which had subsequently received ADT to good effect and continued to be sensitive to the treatment; and the final castrate resistant group. The data obtained was consistent with SGK1 expression on the cellular level, as a significant increase in SGK1 expression was noticed in the relapsed group (representing castration resistant PC) agreeing with that seen in the enzalutamide-resistant cells, suggesting that SGK1 could be a potential predictive or prognostic biomarker for enzalutamide-resistance in patients with prostate cancer (Figure 5-23). Again, further experiments are required to strengthen this hypothesis.

From the microarray data, a significantly higher expression of the *TACSTD*2 gene was detected in LNCaP-ENZ-R cells, compared to parental LNCaP cells. *TACSTD*2 was selected to study in detail as it has previously been demonstrated that expression of TROP-2 is associated with poor outcome and aggressiveness of pancreatic, oral,

colorectal, gastric and ovarian cancers, proposing that it has a role in cancer progression (Trerotola *et al.*, 2013b). It was hypothesised that TROP-2 might have a role in the prostate cancer progression, aggressiveness and indeed enzalutamide-resistance. Firstly, the results were validated at mRNA and protein levels by using TROP-2 specific primers and a specific targeting antibody, respectively. mRNA levels agreed with the previous microarray data and Western blotting revealed that TROP-2 protein is expressed in the LNCaP-ENZ-R cell line, however, no protein expression of TROP-2 was observed in parental LNCaP cells (Figure 6-2 B), This finding is in agreement with Trerotola *et al.* (2012), who showed that TROP-2 expression is higher in aggressive DU145 and PC3 cells and undetectable in LNCaP cells. It can thus be suggested that TROP-2 expression levels may reflect an aggressive phenotype of PC.

In the current study, TROP-2 knockdown was applied to investigate the effects of its expression on enzalutamide-resistant cell proliferation, cell cycle distribution and migration. Loss of TROP-2 expression in the LNCaP-ENZ-R cells was shown to cause a significant decrease in cell number, compared to the non-silencing control. However, no effect on proliferation was detected in parental LNCaP cells. This suggests that TROP-2 may play an important role in regulation of the proliferation of LNCaP-ENZ-R cells (Figure 6-4).

Also, this study showed that loss of TROP-2 expression in the LNCaP-ENZ-R cells led to an increased number of cells entering sub-G1 phase. However, no effects of siRNA knockdown of TROP-2 were noticed on the cell cycle progression of parental LNCaP cells (Figure 6-5). This is further evidence that the expression of TROP-2 is important for LNCaP-ENZ-R cell proliferation. These data are in agreement with Cubas *et al.* (2010), who reported that TROP-2 expression increased tumour growth in both subcutaneous and orthotopic pancreatic cancer murine models.

A decrease in the ability of LNCaP-ENZ-R cells following TROP-2 knockdown to migrate was observed, even with the presence of serum in the media, at 6, 24 and 48 hours (Figure 6-8). Knockdown of TROP-2 in parental LNCaP cell had no effect on cell migration (Figure 6-7). These results are consistent with those of other studies where ectopically expressed TROP-2, in subcutaneous and orthotopic pancreatic cancer murine cells, showed increased cell migration (Cubas *et al.*, 2010).

Further investigation of the role of TROP-2 on cell migration included an analysis of EMT markers (E-cadherin and Vimentin), in response to TROP-2 knockdown. An increase in the mRNA expression of E-cadherin was observed, while a decrease in mRNA

expression of Vimentin was seen, in response to TROP-2 knockdown in LNCaP-ENZ-R cells (Figure 6-9). This suggests that TROP-2 may also regulate EMT in these cells. The findings of the current study are consistent with those of Chen *et al.* (2014), who demonstrated that high TROP-2 expression was significantly associated with a loss of the epithelial marker E-cadherin in gall bladder cancer patients tissue, by using immunohistochemical techniques.

This study indicated that TROP-2 knockdown in LNCaP-ENZ-R cells led to a decrease in their proliferation. Subsequently, cell cycle analysis showed an accumulation of the cells at the sub-G1 phase. Moreover, TROP-2 knockdown attenuated the ability of LNCaP-ENZ-R cell to migrate. This suggests that TROP-2 is a partner in a signalling cascade that may have a crucial role in the prostate cancer growth. To test this theory, this study verified the role of TROP-2 in the regulation of PI3 Kinase (pAkt) and MAP Kinase (pERK1/2) pathway activity, as this study showed that both pathways are active in the LNCaP-ENZ-R cell line (Figure 3-6).

The data from this study demonstrated that TROP-2 knockdown led to a decrease in pAkt in LNCaP-ENZ-R cells (Figure 6-10). Previously, we showed high expression of pAkt in LNCaP-ENZ-R cells, compared to the parental LNCaP (Figure 3-6). These findings further support the idea that loss of TROP-2 expression leads to an increase in the sensitivity of LNCaP-ENZ-R cells to cell death by inhibition of the Akt activity. This statement is based on the published finding that activated Akt leads to inhibition of apoptosis by inactivating several proapoptotic proteins, including BAD, BAX and caspase-9 and also by inducing the expression of anti-apoptotic proteins, such as BCL2, BCLXL, FLIP, cIAP2, XIAP and survivins, in myeloma cells (Mitsiades *et al.*, 2002).

The loss of TROP-2 expression was shown to lead a decrease in Akt activity. Based on the known cross-talk between the PI3K/Akt and MAP Kinase signalling pathways, it was hypothesised that TROP-2 might transmit an apoptosis signalling cascade, through the MAP Kinase pathway, which might give better understanding of the apoptosis phenotype related to TROP-2 knockdown in LNCaP-ENZ-R cell line. The most interesting finding was that knockdown of TROP-2 protein led to a complete loss of pERK1/2 (Figure 6-10), which may explain the increased apoptosis seen in the LNCaP-ENZ-R cells. These results match those observed in an earlier study demonstrating that Raf/MEK/ERK may promote cell cycle arrest in PC cells and that this activity may be regulated by p53, as a restoration of wild-type p53 resulted in enhanced sensitivity to chemotherapeutic drugs (McCubrey *et al.*, 2007). The same study indicated that both Raf/MEK/ERK and PI3K/PTEN/Akt

pathways have anti-apoptotic and drug-resistance effects on cells and also interact with the p53 pathway (McCubrey *et al.*, 2007).

In this study, higher expression of c-MYC was detected in LNCaP-CDX-R, LNCaP-ENZ-R and LNCaP-ARN-R cells, compared to parental LNCaP cells (Figure 6-11 A). The results from this study also demonstrated that loss of TROP-2 expression led to a decrease in c-MYC expression, at the protein and mRNA level, in LNCaP-ENZ-R cells. As expected, no effect of TROP-2 knockdown on c-MYC expression in parental LNCaP cells was observed (Figure 6-11 B, C). This may be a further explanation for the reduction in proliferation seen in response to TROP-2 knockdown, as it has been previously shown that inhibition of c-MYC expression abrogates proliferation and blocks cell cycle progression of breast cancer cells (Butt *et al.*, 2005). This study suggests that TROP-2 regulates ERK1/2 signalling, which directly activates the transcription factor c-MYC, giving an explanation for the cell cycle arrest and proliferation inhibition seen in response to TROP-2 knockdown.

Further investigation for the role of TROP-2 in the regulation of the cell cycle was examined in this study by investigating the expression of p27, a key regulator of cell cycle, in response to TROP-2 knockdown. The results showed that knockdown of TROP-2 led to a small increase in the expression of p27 protein in LNCaP-ENZ-R cells, while no effect was noticed in LNCaP cells. p27 is known as a key regulator of cell cycle progress (Porter *et al.*, 1997).

The current study found a high expression of TROP-2 in enzalutamide-resistant LNCaP cells, which are used as an in vitro model to represent anti-androgen-resistant CRPC in the clinic. For that reason, it was hypothesised that TROP-2 might act as a biomarker for patients who relapsed after an initial good response to hormonal deprivation therapy. A tissue microarray TMA5 was selected as this contains matched samples for individual patients. The paired samples were divided into three groups: a hormone naïve group containing patient tissues which never received hormone treatment; hormone sensitive group containing patient tissues which had subsequently received ADT to good effect and continued to be sensitive to the treatment; and the final castrate resistant group. The data was consistent with TROP-2 expression on the cellular level, as a significant increase was noticed in the relapsed group (representing castrate resistant PC) complementing that seen in the enzalutamide-resistant cell line. This suggests that TROP-2 could be a potential predictive biomarker for anti-androgen resistance in prostate cancer patients (Figure 6-12). Further work is required to confirm this suggestion.

Conclusion

The main goal of this study was to determine the genetic differences and the active pathways that are involved in the proliferation, cell cycle and migration of enzalutamide-resistant LNCaP cells, compared to parental LNCaP. This will give a better understanding regarding the mechanisms behind drug-resistance in prostate cancer patients and may also lead to the discovery of novel predictive and prognostic biomarkers.

This study has shown that there is a negative feedback effect of AR on HER3 expression. The investigation of this study has shown that the expression of HER2 and HER3 are significantly higher in all tested resistant cell lines (LNCaP-Casodex resistant, LNCaP-enzalutamide resistant and LNCaP-ARN509 resistant). Also, activating HER2/HER3 activates both PI3 Kinase (pAkt) and MAP Kinase (pERK1/2) signalling pathway in all tested resistant cell lines, though is more pronounced in LNCaP-ENZ-R cells. Additionally, this research has shown that LNCaP-ENZ-R is an androgen-independent cell line and that heregulin can enhance proliferation of both parental LNCaP and LNCaP-ENZ-R. One of the more significant findings to emerge from this study is that only AR regulates SGK1 expression in androgen-dependent cells, while both AR and GR are able to regulate SGK1 in enzalutamide-resistant cells. The second major finding was that on blocking AR activity, the GR level was found to be higher and that GR was able to regulate AR target genes such as SGK1. This might be a key factor responsible for the proliferation and continued growth of enzalutamide-resistant PCs. The evidence from this study suggests that inhibition of the GR and its downstream target SGK1 is a better approach to reducing the proliferation of the LNCaP-ENZ-R cells. This study suggests that SGK1 could be a potential prognostic or predictive biomarker for enzalutamide-resistance in patients with prostate cancer.

Despite its exploratory nature, this study also offers some insight into the role of TROP-2 in the regulation of proliferation, cell cycle and migration of enzalutamide-resistant LNCaP cells. The results of this investigation show that TROP-2 is expressed in LNCaP-ENZ-R cells, while no expression of TROP-2 was observed in parental LNCaP cells, at the protein level. The results of this study indicate that loss of TROP-2 expression in the LNCaP-ENZ-R cells led to decreased proliferation and an increased number of cells entering the sub-G1 phase. Multiple regression analysis revealed that a decrease in the ability of LNCaP-ENZ-R cells, with knockdown of TROP-2, to migrate, even with the

presence of serum in the media. However, knockdown of TROP-2 in parental LNCaP cells had no effect on the proliferation, cell cycle distribution and migration.

These findings enhance our understanding of the role of TROP-2 in the regulation of PI3 Kinase (pAkt) and MAP Kinase (pERK1/2) pathway activity in LNCaP-ENZ-R cells. The results of this research support the idea that TROP-2 regulates ERK1/2 signalling, which directly activates the transcription factor c-MYC, giving an explanation for the cell cycle arrest and proliferation inhibition seen in response to TROP-2 knockdown. Taken together, these results suggest that TROP-2 could be a potential predictive biomarker for anti-androgen resistance in prostate cancer patients.

Further research work

- It would be interesting to perform a second microarray experiment, this time including and assessing the effects of heregulin stimulation on the genetic expression profile in the LNCaP-enzalutamide resistant cell line. This would give a better understanding of the role of HER2 and HER3 in this model of anti-androgen-resistant disease. This would provide further evidence to justify a clinical trial of a pan-HER inhibitor, such as AZD8931, in carefully stratified patients, with advanced prostate cancer.

- This research has thrown up many questions in need of further investigation, such as the role of GR vs AR in the regulation of SGK1 in advanced prostate cancer. There is an opportunity to perform a research study on the validation of SGK1 as a therapeutic target in advanced and drug-resistant prostate cancer. This would involve: Further justification of SGK1 as a candidate therapeutic target in CRPC; an examination of the requirement for SGK1 in AR and GR signalling in CRPC *in-vitro*; and a validation of SGK1 as a therapeutic target in more translationally-relevant backgrounds, such as human PC biopsies, as either explants or organoids, from both hormone-naïve and enzalutamide-resistant patients.

- Future research should also assess the impact of TROP-2 knockdown or inhibition on the genetic expression profile of models of anti-androgen-resistance, such as LNCaP-enzalutamide-resistant cells, versus parental LNCaP cells. Potentially, TROP-2 could be an important predictive biomarker of enzalutamide-resistance, or a therapeutic target in its own right, to delay or combat enzalutamide-resistance.

Chapter 8. References

Abate-Shen, C. and Shen, M.M. (2000) 'Molecular genetics of prostate cancer', *Genes & development*, 14(19), pp. 2410-2434.
Abrahamsson, P.A. (1999) 'Neuroendocrine differentiation in prostatic carcinoma', *The Prostate*, 39(2), pp. 135-148.
Abreu-Martin, M.T., Chari, A., Palladino, A.A., Craft, N.A. and Sawyers, C.L. (1999) 'Mitogen-activated protein kinase kinase kinase 1 activates androgen receptor-dependent transcription and apoptosis in prostate cancer', *Molecular and cellular biology*, 19(7), pp. 5143-5154.
Agus, D.B., Akita, R.W., Fox, W.D., Lewis, G.D., Higgins, B., Pisacane, P.I., Lofgren, J.A., Tindell, C., Evans, D.P. and Maiese, K. (2002) 'Targeting ligand-activated ErbB2 signaling inhibits breast and prostate tumor growth', *Cancer cell*, 2(2), pp. 127-137.
Ahmad, I., Patel, R., Singh, L.B., Nixon, C., Seywright, M., Barnetson, R.J., Brunton, V.G., Muller, W.J., Edwards, J. and Sansom, O.J. (2011) 'HER2 overcomes PTEN (loss)-induced senescence to cause aggressive prostate cancer', *Proceedings of the National Academy of Sciences*, 108(39), pp. 16392-16397.
Ai, J., Wang, Y., Dar, J.A., Liu, J., Liu, L., Nelson, J.B. and Wang, Z. (2009) 'HDAC6 regulates androgen receptor hypersensitivity and nuclear localization via modulating Hsp90 acetylation in castration-resistant prostate cancer', *Molecular Endocrinology*, 23(12), pp. 1963-1972.
Albertelli, M.A., O'Mahony, O.A., Brogley, M., Tosoian, J., Steinkamp, M., Daignault, S., Wojno, K. and Robins, D.M. (2008) 'Glutamine tract length of human androgen receptors affects hormone-dependent and-independent prostate cancer in mice', *Human molecular genetics*, 17(1), pp. 98-110.
Amin, M., Khalid, A., Tazeen, N. and Yasoob, M. (2010) 'Zonal anatomy of prostate', *Annals of King Edward Medical University*, 16(3), p. 138.
Anantharaman, A. and Friedlander, T.W. (2016) *Urologic Oncology: Seminars and Original Investigations*. Elsevier. Available at: http://ac.els-cdn.com/S1078143915005554/1-s2.0-S1078143915005554-main.pdf?_tid=b56f4320-eec8-11e6-903d-00000aacb35e&acdnat=1486645828_7535a94e3a851a291bfc97ef384f56c9.
Arora, V.K., Schenkein, E., Murali, R., Subudhi, S.K., Wongvipat, J., Balbas, M.D., Shah, N., Cai, L., Efstathiou, E. and Logothetis, C. (2013) 'Glucocorticoid receptor confers resistance to antiandrogens by bypassing androgen receptor blockade', *Cell*, 155(6), pp. 1309-1322.
Baker, S.J. and Reddy, E.P. (2013) 'Understanding the temporal sequence of genetic events that lead to prostate cancer progression and metastasis', *Proceedings of the National Academy of Sciences*, 110(37), pp. 14819-14820.
Bakin, R.E., Gioeli, D., Sikes, R.A., Bissonette, E.A. and Weber, M.J. (2003) 'Constitutive activation of the Ras/mitogen-activated protein kinase signaling pathway promotes androgen hypersensitivity in LNCaP prostate cancer cells', *Cancer research*, 63(8), pp. 1981-1989.
Barber, L.E., Gerke, T.A., Markt, S.C., Parmigiani, G. and Mucci, L.A. (2016) 'A family affair: Prostate cancer risk and family history of breast or prostate cancer'. AACR, pp. 2543-2543.
Bassetto, M., Ferla, S., Giancotti, G., Pertusati, F., Westwell, A.D., Brancale, A. and McGuigan, C. (2017) 'Rational design and synthesis of novel phenylsulfonyl-benzamides as anti-prostate cancer agents', *MedChemComm*.
Beer, T.M., Armstrong, A.J., Rathkopf, D.E., Loriot, Y., Sternberg, C.N., Higano, C.S., Iversen, P., Bhattacharya, S., Carles, J. and Chowdhury, S. (2014) 'Enzalutamide in metastatic prostate cancer before chemotherapy', *New England Journal of Medicine*, 371(5), pp. 424-433.

Bianchini, D., Lorente, D., Rodriguez-Vida, A., Omlin, A., Pezaro, C., Ferraldeschi, R., Zivi, A., Attard, G., Chowdhury, S. and de Bono, J.S. (2014) 'Antitumour activity of enzalutamide (MDV3100) in patients with metastatic castration-resistant prostate cancer (CRPC) pre-treated with docetaxel and abiraterone', *European journal of cancer*, 50(1), pp. 78-84.
Bignotti, E., Zanotti, L., Calza, S., Falchetti, M., Lonardi, S., Ravaggi, A., Romani, C., Todeschini, P., Bandiera, E. and Tassi, R.A. (2012) 'Trop-2 protein overexpression is an independent marker for predicting disease recurrence in endometrioid endometrial carcinoma', *BMC clinical pathology*, 12(1), p. 22.
Bitting, R.L. and Armstrong, A.J. (2013) 'Targeting the PI3K/Akt/mTOR pathway in castration-resistant prostate cancer', *Endocrine-related cancer*, 20(3), pp. R83-R99.
Bogusz, A.M., Brickley, D.R., Pew, T. and Conzen, S.D. (2006) 'A novel N-terminal hydrophobic motif mediates constitutive degradation of serum-and glucocorticoid-induced kinase-1 by the ubiquitin–proteasome pathway', *FEBS Journal*, 273(13), pp. 2913-2928.
Bolla, M., Collette, L., Blank, L., Warde, P., Dubois, J.B., Mirimanoff, R.-O., Storme, G., Bernier, J., Kuten, A. and Sternberg, C. (2002) 'Long-term results with immediate androgen suppression and external irradiation in patients with locally advanced prostate cancer (an EORTC study): a phase III randomised trial', *The Lancet*, 360(9327), pp. 103-108.
Bostwick, D.G. (2000) 'Prostatic intraepithelial neoplasia', *Current urology reports*, 1(1), pp. 65-70.
Bostwick, D.G., Amin, M.B., Dundore, P., Marsh, W. and Schultz, D.S. (1993) 'Architectural patterns of high-grade prostatic intraepithelial neoplasia', *Human pathology*, 24(3), pp. 298-310.
Bostwick, D.G. and Brawer, M.K. (1987) 'Prostatic intra-epithelial neoplasia and early invasion in prostate cancer', *Cancer*, 59(4), pp. 788-794.
Bostwick, D.G. and Qian, J. (2004) 'High-grade prostatic intraepithelial neoplasia', *Modern pathology*, 17(3), pp. 360-379.
Brady, M.E., Ozanne, D.M., Gaughan, L., Waite, I., Cook, S., Neal, D.E. and Robson, C.N. (1999) 'Tip60 is a nuclear hormone receptor coactivator', *Journal of Biological Chemistry*, 274(25), pp. 17599-17604.
Brown, M. and Wittwer, C. (2000) 'Flow cytometry: principles and clinical applications in hematology', *Clinical chemistry*, 46(8), pp. 1221-1229.
Bubendorf, L., Kononen, J., Koivisto, P., Schraml, P., Moch, H., Gasser, T.C., Willi, N., Mihatsch, M.J., Sauter, G. and Kallioniemi, O.-P. (1999) 'Survey of gene amplifications during prostate cancer progression by high-throughput fluorescence in situ hybridization on tissue microarrays', *Cancer research*, 59(4), pp. 803-806.
Buchanan, G., Yang, M., Cheong, A., Harris, J.M., Irvine, R.A., Lambert, P.F., Moore, N.L., Raynor, M., Neufing, P.J. and Coetzee, G.A. (2004) 'Structural and functional consequences of glutamine tract variation in the androgen receptor', *Human molecular genetics*, 13(16), pp. 1677-1692.
Butt, A.J., McNeil, C.M., Musgrove, E.A. and Sutherland, R.L. (2005) 'Downstream targets of growth factor and oestrogen signalling and endocrine resistance: the potential roles of c-Myc, cyclin D1 and cyclin E', *Endocrine-related cancer*, 12(Supplement 1), pp. S47-S59.
Carrasco-García, E., Saceda, M., Grasso, S., Rocamora-Reverte, L., Conde, M., Gómez-Martínez, Á., García-Morales, P., Ferragut, J.A. and Martínez-Lacaci, I. (2011) 'Small tyrosine kinase inhibitors interrupt EGFR signaling by interacting with erbB3 and erbB4 in glioblastoma cell lines', *Experimental cell research*, 317(10), pp. 1476-1489.

Carter, H.B., Kettermann, A., Warlick, C., Metter, E.J., Landis, P., Walsh, P.C. and Epstein, J.I. (2007) 'Expectant management of prostate cancer with curative intent: an update of the Johns Hopkins experience', *The Journal of urology*, 178(6), pp. 2359-2365.
Carver, B.S., Chapinski, C., Wongvipat, J., Hieronymus, H., Chen, Y., Chandarlapaty, S., Arora, V.K., Le, C., Koutcher, J. and Scher, H. (2011) 'Reciprocal feedback regulation of PI3K and androgen receptor signaling in PTEN-deficient prostate cancer', *Cancer cell*, 19(5), pp. 575-586.
Chang, J.J., Shinohara, K., Bhargava, V. and C Jr, J. (1998) 'Prospective evaluation of lateral biopsies of the peripheral zone for prostate cancer detection', *The Journal of urology*, 160(6), pp. 2111-2114.
Chang, L., Graham, P.H., Ni, J., Hao, J., Bucci, J., Cozzi, P.J. and Li, Y. (2015) 'Targeting PI3K/Akt/mTOR signaling pathway in the treatment of prostate cancer radioresistance', *Critical reviews in oncology/hematology*, 96(3), pp. 507-517.
Chen, L., Siddiqui, S., Bose, S., Mooso, B., Asuncion, A., Bedolla, R.G., Vinall, R., Tepper, C.G., Gandour-Edwards, R. and Shi, X. (2010) 'Nrdp1-mediated regulation of ErbB3 expression by the androgen receptor in androgen-dependent but not castrate-resistant prostate cancer cells', *Cancer research*, 70(14), pp. 5994-6003.
Chen, M.-B., Wu, H.-F., Zhan, Y., Fu, X.-L., Wang, A.-K., Wang, L.-S. and Lei, H.-M. (2014) 'Prognostic value of TROP2 expression in patients with gallbladder cancer', *Tumor Biology*, 35(11), pp. 11565-11569.
Chen, Y.U., Sawyers, C.L. and Scher, H.I. (2008) 'Targeting the androgen receptor pathway in prostate cancer', *Current opinion in pharmacology*, 8(4), pp. 440-448.
Clegg, N.J., Wongvipat, J., Joseph, J.D., Tran, C., Ouk, S., Dilhas, A., Chen, Y., Grillot, K., Bischoff, E.D. and Cai, L. (2012) 'ARN-509: a novel antiandrogen for prostate cancer treatment', *Cancer research*, 72(6), pp. 1494-1503.
Cleutjens, C., Steketee, K., van Eekelen, C., Van der Korput, J., Brinkmann, A.O. and Trapman, J. (1997) 'Both Androgen Receptor and Glucocorticoid Receptor Are Able to Induce Prostate-Specific Antigen Expression, but Differ in Their Growth-Stimulating Properties of LNCaP Cells 1', *Endocrinology*, 138(12), pp. 5293-5300.
Cornford, P., Bellmunt, J., Bolla, M., Briers, E., De Santis, M., Gross, T., Henry, A.M., Joniau, S., Lam, T.B. and Mason, M.D. (2016) 'EAU-ESTRO-SIOG Guidelines on Prostate Cancer. Part II: treatment of relapsing, metastatic, and castration-resistant prostate cancer', *European Urology*.
Coyne, K.S., Sexton, C.C., Thompson, C.L., Milsom, I., Irwin, D., Kopp, Z.S., Chapple, C.R., Kaplan, S., Tubaro, A. and Aiyer, L.P. (2009) 'The prevalence of lower urinary tract symptoms (LUTS) in the USA, the UK and Sweden: results from the Epidemiology of LUTS (EpiLUTS) study', *BJU international*, 104(3), pp. 352-360.
Craft, N., Shostak, Y., Carey, M. and Sawyers, C.L. (1999) 'A mechanism for hormone-independent prostate cancer through modulation of androgen receptor signaling by the HER-2/neu tyrosine kinase', *Nature medicine*, 5(3), pp. 280-285.
Crawford, E.D., Shore, N.D., Moul, J.W., Tombal, B., Schröder, F.H., Miller, K., Boccon-Gibod, L., Malmberg, A., Olesen, T.K. and Persson, B.-E. (2014) 'Long-term tolerability and efficacy of degarelix: 5-year results from a phase III extension trial with a 1-arm crossover from leuprolide to degarelix', *Urology*, 83(5), pp. 1122-1128.
Cubas, R., Li, M., Chen, C. and Yao, Q. (2009) 'Trop2: a possible therapeutic target for late stage epithelial carcinomas', *Biochimica et Biophysica Acta (BBA)-Reviews on Cancer*, 1796(2), pp. 309-314.
Cubas, R., Zhang, S., Li, M., Chen, C. and Yao, Q. (2010) 'Trop2 expression contributes to tumor pathogenesis by activating the ERK MAPK pathway', *Molecular cancer*, 9(1), p. 253.

Cucchiara, V., Yang, J.C., Mirone, V., Gao, A.C., Rosenfeld, M.G. and Evans, C.P. (2017) 'Epigenomic Regulation of Androgen Receptor Signaling: Potential Role in Prostate Cancer Therapy', *Cancers*, 9(1), p. 9.
Culig, Z. (2016) 'Androgen receptor coactivators in regulation of growth and differentiation in prostate cancer', *Journal of cellular physiology*, 231(2), pp. 270-274.
D'amico, A.V., Whittington, R., Malkowicz, B., Schnall, M., Schultz, D., Cote, K., Tomaszewski, J.E. and Wein, A. (2000) 'Endorectal magnetic resonance imaging as a predictor of biochemical outcome after radical prostatectomy in men with clinically localized prostate cancer', *The Journal of urology*, 164(3), pp. 759-763.
Day, K.C., Hiles, G.L., Kozminsky, M., Dawsey, S.J., Paul, A., Broses, L.J., Shah, R., Kunja, L.P., Hall, C. and Palanisamy, N. (2017) 'HER2 and EGFR overexpression support metastatic progression of prostate cancer to bone', *Cancer Research*, 77(1), pp. 74-85.
De Bono, J.S., Logothetis, C.J., Molina, A., Fizazi, K., North, S., Chu, L., Chi, K.N., Jones, R.J., Goodman Jr, O.B. and Saad, F. (2011) 'Abiraterone and increased survival in metastatic prostate cancer', *New England Journal of Medicine*, 364(21), pp. 1995-2005.
DeSantis, C.E., Lin, C.C., Mariotto, A.B., Siegel, R.L., Stein, K.D., Kramer, J.L., Alteri, R., Robbins, A.S. and Jemal, A. (2014) 'Cancer treatment and survivorship statistics, 2014', *CA: a cancer journal for clinicians*, 64(4), pp. 252-271.
Dhupkar, P., Dowling, M., Cengel, K. and Chen, B. (2010) 'Effects of anti-EGFR antibody cetuximab on androgen-independent prostate cancer cells', *Anticancer research*, 30(6), pp. 1905-1910.
Di Lorenzo, G., Tortora, G., D'Armiento, F.P., De Rosa, G., Staibano, S., Autorino, R., D'Armiento, M., De Laurentiis, M., De Placido, S. and Catalano, G. (2002) 'Expression of epidermal growth factor receptor correlates with disease relapse and progression to androgen-independence in human prostate cancer', *Clinical Cancer Research*, 8(11), pp. 3438-3444.
Edlind, M.P. and Hsieh, A.C. (2014) 'PI3K-AKT-mTOR signaling in prostate cancer progression and androgen deprivation therapy resistance', *Asian journal of andrology*, 16(3), p. 378.
Edwards, J., Traynor, P., Munro, A.F., Pirret, C.F., Dunne, B. and Bartlett, J.M.S. (2006) 'The role of HER1-HER4 and EGFRvIII in hormone-refractory prostate cancer', *Clinical cancer research*, 12(1), pp. 123-130.
Epstein, J.I. (2010) 'An update of the Gleason grading system', *The Journal of urology*, 183(2), pp. 433-440.
Epstein, J.I., Allsbrook Jr, W.C., Amin, M.B., Egevad, L.L. and Committee, I.G. (2005) 'The 2005 International Society of Urological Pathology (ISUP) consensus conference on Gleason grading of prostatic carcinoma', *The American journal of surgical pathology*, 29(9), pp. 1228-1242.
Epstein, J.I., Egevad, L., Amin, M.B., Delahunt, B., Srigley, J.R., Humphrey, P.A. and Grading, C. (2016) 'The 2014 International Society of Urological Pathology (ISUP) consensus conference on Gleason grading of prostatic carcinoma: definition of grading patterns and proposal for a new grading system', *The American journal of surgical pathology*, 40(2), pp. 244-252.
Feldman, B.J. and Feldman, D. (2001a) 'The development of androgen-independent prostate cancer', *Nature Reviews Cancer*, 1(1), pp. 34-45.
Feldman, B.J. and Feldman, D. (2001b) 'The development of androgen-independent prostate cancer', *Nature reviews. Cancer*, 1(1), p. 34.
Feng, S., Agoulnik, I.U., Bogatcheva, N.V., Kamat, A.A., Kwabi-Addo, B., Li, R., Ayala, G., Ittmann, M.M. and Agoulnik, A.I. (2007) 'Relaxin promotes prostate cancer progression', *Clinical Cancer Research*, 13(6), pp. 1695-1702.

Ferrell, J.E. (1996) 'Tripping the switch fantastic: how a protein kinase cascade can convert graded inputs into switch-like outputs', *Trends in biochemical sciences*, 21(12), pp. 460-466.
García-Martínez, J.M. and Alessi, D.R. (2008) 'mTOR complex 2 (mTORC2) controls hydrophobic motif phosphorylation and activation of serum-and glucocorticoid-induced protein kinase 1 (SGK1)', *Biochemical Journal*, 416(3), pp. 375-385.
Gaughan, L., Logan, I.R., Neal, D.E. and Robson, C.N. (2005) 'Regulation of androgen receptor and histone deacetylase 1 by Mdm2-mediated ubiquitylation', *Nucleic acids research*, 33(1), pp. 13-26.
Gaughan, L., Stockley, J., Wang, N., McCracken, S.R.C., Treumann, A., Armstrong, K., Shaheen, F., Watt, K., McEwan, I.J. and Wang, C. (2011) 'Regulation of the androgen receptor by SET9-mediated methylation', *Nucleic acids research*, 39(4), pp. 1266-1279.
Gibbons, J.A., Ouatas, T., Krauwinkel, W., Ohtsu, Y., van der Walt, J.-S., Beddo, V., de Vries, M. and Mordenti, J. (2015) 'Clinical pharmacokinetic studies of enzalutamide', *Clinical pharmacokinetics*, 54(10), pp. 1043-1055.
Gioeli, D., Wunderlich, W., Sebolt-Leopold, J., Bekiranov, S., Wulfkuhle, J.D., Petricoin, E.F., Conaway, M. and Weber, M.J. (2011) 'Compensatory pathways induced by MEK inhibition are effective drug targets for combination therapy against castration-resistant prostate cancer', *Molecular cancer therapeutics*, 10(9), pp. 1581-1590.
Gleason, D.F. and Mellinger, G.T. (1974) 'Prediction of prognosis for prostatic adenocarcinoma by combined histological grading and clinical staging', *The Journal of urology*, 111(1), pp. 58-64.
Gnanapragasam, V.J., Kumar, V., Langton, D., Pickard, R.S. and Leung, H.Y. (2006) 'Outcome of transurethral prostatectomy for the palliative management of lower urinary tract symptoms in men with prostate cancer', *International journal of urology*, 13(6), pp. 711-715.
Goldenberg, M.M. (1999) 'Trastuzumab, a recombinant DNA-derived humanized monoclonal antibody, a novel agent for the treatment of metastatic breast cancer', *Clinical therapeutics*, 21(2), pp. 309-318.
Gosselaar, C., Roobol, M.J., Roemeling, S., de Vries, S.H., Cruijsen-Koeter, I.v.d., van der Kwast, T.H. and Schröder, F.H. (2006) 'Screening for prostate cancer without digital rectal examination and transrectal ultrasound: results after four years in the European Randomized Study of Screening for Prostate Cancer (ERSPC), Rotterdam', *The Prostate*, 66(6), pp. 625-631.
Greene, K.L., Albertsen, P.C., Babaian, R.J., Carter, H.B., Gann, P.H., Han, M., Kuban, D.A., Sartor, A.O., Stanford, J.L. and Zietman, A. (2009) 'Prostate specific antigen best practice statement: 2009 update', *The Journal of urology*, 182(5), pp. 2232-2241.
Gregory, C.W., Whang, Y.E., McCall, W., Fei, X., Liu, Y., Ponguta, L.A., French, F.S., Wilson, E.M. and Earp, H.S. (2005) 'Heregulin-induced activation of HER2 and HER3 increases androgen receptor transactivation and CWR-R1 human recurrent prostate cancer cell growth', *Clinical Cancer Research*, 11(5), pp. 1704-1712.
Hanahan, D. and Weinberg, R.A. (2000) 'The hallmarks of cancer', *cell*, 100(1), pp. 57-70.
Hanahan, D. and Weinberg, R.A. (2011) 'Hallmarks of cancer: the next generation', *cell*, 144(5), pp. 646-674.
He, B., Lanz, R.B., Fiskus, W., Geng, C., Yi, P., Hartig, S.M., Rajapakshe, K., Shou, J., Wei, L. and Shah, S.S. (2014) 'GATA2 facilitates steroid receptor coactivator recruitment to the androgen receptor complex', *Proceedings of the National Academy of Sciences*, 111(51), pp. 18261-18266.
Heidenreich, A., Bastian, P.J., Bellmunt, J., Bolla, M., Joniau, S., van der Kwast, T., Mason, M., Matveev, V., Wiegel, T. and Zattoni, F. (2014) 'EAU guidelines on prostate

cancer. Part II: treatment of advanced, relapsing, and castration-resistant prostate cancer', *European urology*, 65(2), pp. 467-479.
Hong, F., Larrea, M.D., Doughty, C., Kwiatkowski, D.J., Squillace, R. and Slingerland, J.M. (2008) 'mTOR-raptor binds and activates SGK1 to regulate p27 phosphorylation', *Molecular cell*, 30(6), pp. 701-711.
Horoszewicz, J.S., Leong, S.S., Chu, T.M., Wajsman, Z.L., Friedman, M., Papsidero, L., Kim, U., Chai, L.S., Kakati, S. and Arya, S.K. (1980) 'The LNCaP cell line--a new model for studies on human prostatic carcinoma', *Progress in clinical and biological research*, 37, p. 115.
Hsieh, A.C.a. and Moasser, M.M. (2007) 'Targeting HER proteins in cancer therapy and the role of the non-target HER3', *British journal of cancer*, 97(4), pp. 453-457.
Hsu, F.-N., Yang, M.-S., Lin, E., Tseng, C.-F. and Lin, H. (2011) 'The significance of Her2 on androgen receptor protein stability in the transition of androgen requirement in prostate cancer cells', *American Journal of Physiology-Endocrinology And Metabolism*, 300(5), pp. E902-E908.
Huffman, J.L., Sundheim, O. and Tainer, J.A. (2005) 'DNA base damage recognition and removal: new twists and grooves', *Mutation Research/Fundamental and Molecular Mechanisms of Mutagenesis*, 577(1), pp. 55-76.
Ihle, N.T., Lemos, R., Wipf, P., Yacoub, A., Mitchell, C., Siwak, D., Mills, G.B., Dent, P., Kirkpatrick, D.L. and Powis, G. (2009) 'Mutations in the phosphatidylinositol-3-kinase pathway predict for antitumor activity of the inhibitor PX-866 whereas oncogenic Ras is a dominant predictor for resistance', *Cancer research*, 69(1), pp. 143-150.
Imada, K., Shiota, M., Kohashi, K., Kuroiwa, K., Song, Y., Sugimoto, M., Naito, S. and Oda, Y. (2013) 'Mutual regulation between Raf/MEK/ERK signaling and Y-box–binding protein-1 promotes prostate cancer progression', *Clinical Cancer Research*, 19(17), pp. 4638-4650.
Isaacs, J.T. and Isaacs, W.B. (2004) 'Androgen receptor outwits prostate cancer drugs', *Nature medicine*, 10(1), pp. 26-27.
Isikbay, M., Otto, K., Kregel, S., Kach, J., Cai, Y., Vander Griend, D.J., Conzen, S.D. and Szmulewitz, R.Z. (2014) 'Glucocorticoid receptor activity contributes to resistance to androgen-targeted therapy in prostate cancer', *Hormones and Cancer*, 5(2), pp. 72-89.
Iwakura, Y. and Nawa, H. (2013) 'ErbB1-4-dependent EGF/neuregulin signals and their cross talk in the central nervous system: pathological implications in schizophrenia and Parkinson's disease', *Frontiers in cellular neuroscience*, 7, p. 4.
Jakób, M., Kołodziejczyk, R., Orłowski, M., Krzywda, S., Kowalska, A., Dutko-Gwóźdź, J., Gwóźdź, T., Kochman, M., Jaskólski, M. and Ożyhar, A. (2007) 'Novel DNA-binding element within the C-terminal extension of the nuclear receptor DNA-binding domain', *Nucleic acids research*, 35(8), pp. 2705-2718.
Jendrossek, V., Henkel, M., Hennenlotter, J., Vogel, U., Ganswindt, U., Müller, I., Handrick, R., Anastasiadis, A.G., Kuczyk, M. and Stenzl, A. (2008) 'Analysis of complex protein kinase B signalling pathways in human prostate cancer samples', *BJU international*, 102(3), pp. 371-382.
Joseph, J.D., Lu, N., Qian, J., Sensintaffar, J., Shao, G., Brigham, D., Moon, M., Maneval, E.C., Chen, I. and Darimont, B. (2013) 'A clinically relevant androgen receptor mutation confers resistance to second-generation antiandrogens enzalutamide and ARN-509', *Cancer discovery*, 3(9), pp. 1020-1029.
Josson, S., Matsuoka, Y., Chung, L.W.K., Zhau, H.E. and Wang, R. (2010) *Seminars in cell & developmental biology*. Elsevier.
K Jathal, M., Chen, L., Mudryj, M. and M Ghosh, P. (2011) 'Targeting ErbB3: the new RTK (id) on the prostate cancer block', *Immunology, Endocrine & Metabolic Agents in Medicinal Chemistry (Formerly Current Medicinal Chemistry-Immunology, Endocrine and Metabolic Agents)*, 11(2), pp. 131-149.

Keller, E.T., Fu, Z., Yeung, K. and Brennan, M. (2004) 'Raf kinase inhibitor protein: a prostate cancer metastasis suppressor gene', *Cancer letters*, 207(2), pp. 131-137.
Kirby, R.S. and Gilling, P.J. (2011) *Fast facts: benign prostatic hyperplasia*. Health Press Abingdon, Oxfordshire.
Kirkegaard, T., Edwards, J., Tovey, S., McGlynn, L.M., Krishna, S.N., Mukherjee, R., Tam, L., Munro, A.F., Dunne, B. and Bartlett, J.M.S. (2006) 'Observer variation in immunohistochemical analysis of protein expression, time for a change?', *Histopathology*, 48(7), pp. 787-794.
Kobayashi, H., Minami, Y., Anami, Y., Kondou, Y., Iijima, T., Kano, J., Morishita, Y., Tsuta, K., Hayashi, S. and Noguchi, M. (2010) 'Expression of the GA733 gene family and its relationship to prognosis in pulmonary adenocarcinoma', *Virchows Archiv*, 457(1), pp. 69-76.
Koivisto, P., Visakorpi, T. and Kallioniemi, O.-P. (1996) 'Androgen receptor gene amplification: a novel molecular mechanism for endocrine therapy resistance in human prostate cancer', *Scandinavian Journal of Clinical and Laboratory Investigation*, 56(sup226), pp. 57-63.
Korpal, M., Korn, J.M., Gao, X., Rakiec, D.P., Ruddy, D.A., Doshi, S., Yuan, J., Kovats, S.G., Kim, S. and Cooke, V.G. (2013) 'An F876L mutation in androgen receptor confers genetic and phenotypic resistance to MDV3100 (enzalutamide)', *Cancer discovery*, 3(9), pp. 1030-1043.
Koryakina, Y., Ta, H.Q. and Gioeli, D. (2014) 'Androgen receptor phosphorylation: biological context and functional consequences', *Endocrine-related cancer*, 21(4), pp. T131-T145.
Kuban, D.A., Tucker, S.L., Dong, L., Starkschall, G., Huang, E.H., Cheung, M.R., Lee, A.K. and Pollack, A. (2008) 'Long-term results of the MD Anderson randomized dose-escalation trial for prostate cancer', *International Journal of Radiation Oncology* Biology* Physics*, 70(1), pp. 67-74.
Ladomery, M. (2013) 'Aberrant alternative splicing is another hallmark of cancer', *International journal of cell biology*, 2013, pp. 2-6.
Lallous, N., Dalal, K., Cherkasov, A. and Rennie, P.S. (2013) 'Targeting alternative sites on the androgen receptor to treat castration-resistant prostate cancer', *International journal of molecular sciences*, 14(6), pp. 12496-12519.
Lee, J.T., Steelman, L.S. and McCubrey, J.A. (2004) 'Phosphatidylinositol 3′-kinase activation leads to multidrug resistance protein-1 expression and subsequent chemoresistance in advanced prostate cancer cells', *Cancer Research*, 64(22), pp. 8397-8404.
Lee, J.T., Steelman, L.S. and McCubrey, J.A. (2005) 'Modulation of Raf/MEK/ERK kinase activity does not affect the chemoresistance profile of advanced prostate cancer cells', *International journal of oncology*, 26(6), pp. 1637-1644.
Leevers, S.J., Vanhaesebroeck, B. and Waterfield, M.D. (1999) 'Signalling through phosphoinositide 3-kinases: the lipids take centre stage', *Current opinion in cell biology*, 11(2), pp. 219-225.
Leung, H.Y., Weston, J., Gullick, W.J. and Williams, G. (1997) 'A potential autocrine loop between heregulin-alpha and erbB-3 receptor in human prostatic adenocarcinoma', *British journal of urology*, 79(2), pp. 212-216.
Li, J. and Al-Azzawi, F. (2009) 'Mechanism of androgen receptor action', *Maturitas*, 63(2), pp. 142-148.
Li, Q., Yuan, Z. and Cao, B. (2013a) 'The function of human epidermal growth factor receptor-3 and its role in tumors (Review)', *Oncology reports*, 30(6), pp. 2563-2570.
Li, Y., Chan, S.C., Brand, L.J., Hwang, T.H., Silverstein, K.A.T. and Dehm, S.M. (2013b) 'Androgen receptor splice variants mediate enzalutamide resistance in castration-resistant prostate cancer cell lines', *Cancer research*, 73(2), pp. 483-489.

Liao, R.S., Ma, S., Miao, L., Li, R., Yin, Y. and Raj, G.V. (2013) 'Androgen receptor-mediated non-genomic regulation of prostate cancer cell proliferation', *Translational andrology and urology*, 2(3), p. 187.
Lilja, H., Oldbring, J., Rannevik, G. and Laurell, C.B. (1987) 'Seminal vesicle-secreted proteins and their reactions during gelation and liquefaction of human semen', *Journal of Clinical Investigation*, 80(2), p. 281.
Liu, A.Y., True, L.D., LaTray, L., Nelson, P.S., Ellis, W.J., Vessella, R.L., Lange, P.H., Hood, L. and Van Den Engh, G. (1997) 'Cell–cell interaction in prostate gene regulation and cytodifferentiation', *Proceedings of the National Academy of Sciences*, 94(20), pp. 10705-10710.
Liu, C., Lou, W., Zhu, Y., Yang, J.C., Nadiminty, N., Gaikwad, N.W., Evans, C.P. and Gao, A.C. (2015) 'Intracrine androgens and AKR1C3 activation confer resistance to enzalutamide in prostate cancer', *Cancer research*, 75(7), pp. 1413-1422.
Lonergan, P.E. and Tindall, D.J. (2011) 'Androgen receptor signaling in prostate cancer development and progression', *Journal of carcinogenesis*, 10(1), p. 20.
Ma, J., Lyu, H., Huang, J. and Liu, B. (2014) 'Targeting of erbB3 receptor to overcome resistance in cancer treatment', *Molecular cancer*, 13(1), p. 105.
Maiyar, A.C., Phu, P.T., Huang, A.J. and Firestone, G.L. (1997) 'Repression of glucocorticoid receptor transactivation and DNA binding of a glucocorticoid response element within the serum/glucocorticoid-inducible protein kinase (sgk) gene promoter by the p53 tumor suppressor protein', *Molecular Endocrinology*, 11(3), pp. 312-329.
Manning, B.D. and Cantley, L.C. (2007) 'AKT/PKB signaling: navigating downstream', *Cell*, 129(7), pp. 1261-1274.
Mark, H.F.L., Feldman, D., Das, S., Kye, H., Mark, S., Sun, C.-L. and Samy, M. (1999) 'Fluorescence in situ hybridization study of HER-2/neu oncogene amplification in prostate cancer', *Experimental and molecular pathology*, 66(2), pp. 170-178.
Matsumoto, T., Sakari, M., Okada, M., Yokoyama, A., Takahashi, S., Kouzmenko, A. and Kato, S. (2013) 'The androgen receptor in health and disease', *Annual review of physiology*, 75, pp. 201-224.
McCall, P., Gemmell, L.K., Mukherjee, R., Bartlett, J.M.S. and Edwards, J. (2008) 'Phosphorylation of the androgen receptor is associated with reduced survival in hormone-refractory prostate cancer patients', *British journal of cancer*, 98(6), pp. 1094-1101.
McCubrey, J.A., Steelman, L.S., Chappell, W.H., Abrams, S.L., Wong, E.W.T., Chang, F., Lehmann, B., Terrian, D.M., Milella, M. and Tafuri, A. (2007) 'Roles of the Raf/MEK/ERK pathway in cell growth, malignant transformation and drug resistance', *Biochimica et Biophysica Acta (BBA)-Molecular Cell Research*, 1773(8), pp. 1263-1284.
McDougall, A.R.A., Hooper, S.B., Zahra, V.A., Sozo, F., Lo, C.Y., Cole, T.J., Doran, T. and Wallace, M.J. (2011) 'The oncogene Trop2 regulates fetal lung cell proliferation', *American Journal of Physiology-Lung Cellular and Molecular Physiology*, 301(4), pp. L478-L489.
McLaughlin, P.W., Troyer, S., Berri, S., Narayana, V., Meirowitz, A., Roberson, P.L. and Montie, J. (2005) 'Functional anatomy of the prostate: implications for treatment planning', *International Journal of Radiation Oncology* Biology* Physics*, 63(2), pp. 479-491.
McNeal, J.E. (1988) 'Normal histology of the prostate', *The American journal of surgical pathology*, 12(8), pp. 619-633.
Medina, P.J. and Goodin, S. (2008) 'Lapatinib: a dual inhibitor of human epidermal growth factor receptor tyrosine kinases', *Clinical therapeutics*, 30(8), pp. 1426-1447.
Mellinghoff, I.K., Vivanco, I., Kwon, A., Tran, C., Wongvipat, J. and Sawyers, C.L. (2004) 'HER2/neu kinase-dependent modulation of androgen receptor function through effects on DNA binding and stability', *Cancer cell*, 6(5), pp. 517-527.

Merrick, G.S., Butler, W.M., Wallner, K.E., Galbreath, R.W. and Adamovich, E. (2004) 'Permanent interstitial brachytherapy in younger patients with clinically organ-confined prostate cancer', *Urology*, 64(4), pp. 754-759.
Mitsiades, C.S., Mitsiades, N., Poulaki, V., Schlossman, R., Akiyama, M., Chauhan, D., Hideshima, T., Treon, S.P., Munshi, N.C. and Richardson, P.G. (2002) 'Activation of NF-[kappa] B and upregulation of intracellular anti-apoptotic proteins via the IGF-1/Akt signaling in human multiple myeloma cells: therapeutic implications', *Oncogene*, 21(37), pp. 5673-5683.
Moasser, M.M. (2007) 'The oncogene HER2: its signaling and transforming functions and its role in human cancer pathogenesis', *Oncogene*, 26(45), pp. 6469-6487.
Montano, X. and Djamgoz, M. (2004) 'Epidermal growth factor, neurotrophins and the metastatic cascade in prostate cancer', *FEBS letters*, 571(1-3), pp. 1-8.
Montgomery, R.B., Mostaghel, E.A., Vessella, R., Hess, D.L., Kalhorn, T.F., Higano, C.S., True, L.D. and Nelson, P.S. (2008) 'Maintenance of intratumoral androgens in metastatic prostate cancer: a mechanism for castration-resistant tumor growth', *Cancer research*, 68(11), pp. 4447-4454.
Morgan, T.M., Koreckij, T.D. and Corey, E. (2009) 'Targeted therapy for advanced prostate cancer: inhibition of the PI3K/Akt/mTOR pathway', *Current cancer drug targets*, 9(2), pp. 237-249.
Mu, Z., Klinowska, T., Dong, X., Foster, E., Womack, C., Fernandez, S.V. and Cristofanilli, M. (2014) 'AZD8931, an equipotent, reversible inhibitor of signaling by epidermal growth factor receptor (EGFR), HER2, and HER3: preclinical activity in HER2 non-amplified inflammatory breast cancer models', *Journal of Experimental & Clinical Cancer Research*, 33(1), p. 47.
Mujoo, K., Choi, B.-K., Huang, Z., Zhang, N. and An, Z. (2014) 'Regulation of ERBB3/HER3 signaling in cancer', *Oncotarget*, 5(21), pp. 10222-36.
Mukherjee, R., McGuinness, D.H., McCall, P., Underwood, M.A., Seywright, M., Orange, C. and Edwards, J. (2011) 'Upregulation of MAPK pathway is associated with survival in castrate-resistant prostate cancer', *British journal of cancer*, 104(12), pp. 1920-1928.
Mulholland, D.J., Kobayashi, N., Ruscetti, M., Zhi, A., Tran, L.M., Huang, J., Gleave, M. and Wu, H. (2012) 'Pten loss and RAS/MAPK activation cooperate to promote EMT and metastasis initiated from prostate cancer stem/progenitor cells', *Cancer research*, 72(7), pp. 1878-1889.
Mulholland, D.J., Tran, L.M., Li, Y., Cai, H., Morim, A., Wang, S., Plaisier, S., Garraway, I.P., Huang, J. and Graeber, T.G. (2011) 'Cell autonomous role of PTEN in regulating castration-resistant prostate cancer growth', *Cancer cell*, 19(6), pp. 792-804.
Muniyan, S., Chen, S.-J., Lin, F.-F., Wang, Z., Mehta, P.P., Batra, S.K. and Lin, M.-F. (2015) 'ErbB-2 signaling plays a critical role in regulating androgen-sensitive and castration-resistant androgen receptor-positive prostate cancer cells', *Cellular signalling*, 27(11), pp. 2261-2271.
Munkley, J., Livermore, K., Rajan, P. and Elliott, D.J. (2017) 'RNA splicing and splicing regulator changes in prostate cancer pathology', *Human Genetics*, pp. 1-12.
O'Neill, D., Jones, D., Wade, M., Grey, J., Nakjang, S., Guo, W., Cork, D., Davies, B.R., Wedge, S.R. and Robson, C.N. Gaughan, L. (2015) 'Development and exploitation of a novel mutant androgen receptor modelling strategy to identify new targets for advanced prostate cancer therapy', *Oncotarget*, 6(28), p. 26029.
O'Neill, D.J. (2014) *Determining the efficacy of novel anti-androgens in models of castrate resistant prostate cancer*. PhD thesis. University of Newcastle upon Tyne.
Park, H., Kim, Y., Sul, J.W., Jeong, I.G., Yi, H.J., Ahn, J.B., Kang, J.S., Yun, J., Hwang, J.J. and Kim, C.S. (2015) 'Synergistic anticancer efficacy of MEK inhibition and dual

PI3K/mTOR inhibition in castration-resistant prostate cancer', *The Prostate*, 75(15), pp. 1747-1759.
Park, J.-I. (2014) 'Growth arrest signaling of the Raf/MEK/ERK pathway in cancer', *Frontiers in biology*, 9(2), pp. 95-103.
Peisch, S.F., Van Blarigan, E.L., Chan, J.M., Stampfer, M.J. and Kenfield, S.A. (2016) 'Prostate cancer progression and mortality: a review of diet and lifestyle factors', *World Journal of Urology*, pp. 1-8.
Penson, D.F., Armstrong, A.J., Concepcion, R., Agarwal, N., Olsson, C., Karsh, L., Dunshee, C., Wang, F., Wu, K. and Krivoshik, A. (2016) 'Enzalutamide versus bicalutamide in castration-resistant prostate cancer: the STRIVE trial', *Journal of Clinical Oncology*, 34(18), pp. 2098-2106.
Perner, S., Cronauer, M.V., Schrader, A.J., Klocker, H., Culig, Z. and Baniahmad, A. (2015) 'Adaptive responses of androgen receptor signaling in castration-resistant prostate cancer', *Oncotarget*, 6(34), pp. 35542-35555.
Peterson, C.L. and Laniel, M.-A. (2004) 'Histones and histone modifications', *Current Biology*, 14(14), pp. R546-R551.
Phin, S., Moore, M. and Cotter, P.D. (2013) 'Genomic rearrangements of PTEN in prostate cancer', *Frontiers in oncology*, 3, p. 240.
Poovassery, J.S., Kang, J.C., Kim, D., Ober, R.J. and Ward, E.S. (2015) 'Antibody targeting of HER2/HER3 signaling overcomes heregulin-induced resistance to PI3K inhibition in prostate cancer', *International journal of cancer*, 137(2), pp. 267-277.
Porta, C., Paglino, C. and Mosca, A. (2014) 'Targeting PI3K/Akt/mTOR signaling in cancer', *Targeting PI3K/mTOR signaling in cancer*, p. 47.
Porter, P.L., Malone, K.E., Heagerty, P.J., Alexander, G.M., Gatti, L.A., Firpo, E.J., Daling, J.R. and Roberts, J.M. (1997) 'Expression of cell-cycle regulators p27Kip1 and cyclin E, alone and in combination, correlate with survival in young breast cancer patients', *Nature medicine*, 3(2), pp. 222-225.
Poyet, P. and Labrie, F. (1985) 'Comparison of the antiandrogenic/androgenic activities of flutamide, cyproterone acetate and megestrol acetate', *Molecular and cellular endocrinology*, 42(3), pp. 283-288.
Qian, J., Jenkins, R.B. and Bostwick, D.G. (1999) 'Genetic and chromosomal alterations in prostatic intraepithelial neoplasia and carcinoma detected by fluorescence in situ hybridization', *European urology*, 35(5-6), pp. 479-483.
Qin, J., Lee, H.-J., Wu, S.-P., Lin, S.-C., Lanz, R.B., Creighton, C.J., DeMayo, F.J., Tsai, S.Y. and Tsai, M.-J. (2014) 'Androgen deprivation–induced NCoA2 promotes metastatic and castration-resistant prostate cancer', *The Journal of clinical investigation*, 124(11), pp. 5013-5026.
Qiu, X.-B. and Goldberg, A.L. (2002) 'Nrdp1/FLRF is a ubiquitin ligase promoting ubiquitination and degradation of the epidermal growth factor receptor family member, ErbB3', *Proceedings of the National Academy of Sciences*, 99(23), pp. 14843-14848.
Rao, K. (2015) *The Role of the Epidermal Growth Factor Receptor Family in Prostate Cancer and their Potential as Therapeutic Targets*. PhD thesis. Newcastle University.
Rebbeck, T.R. (2017) *Seminars in Radiation Oncology*. Elsevier.
Robinson, D., He, F., Pretlow, T. and Kung, H.-J. (1996) 'A tyrosine kinase profile of prostate carcinoma', *Proceedings of the National Academy of Sciences*, 93(12), pp. 5958-5962.
Robinson, S., Laniado, M. and Montgomery, B. (2017) 'Prostate specific antigen and acinar density: a new dimension, the "Prostatocrit"', *International braz j urol*, 43(2), pp. 230-238.
Rosenberg, S.A. (1989) *Cancer: Principles & Practice of Oncology*. Lippincott.
Rothdiener, M., Müller, D., Castro, P.G., Scholz, A., Schwemmlein, M., Fey, G., Heidenreich, O. and Kontermann, R.E. (2010) 'Targeted delivery of SiRNA to CD33-

positive tumor cells with liposomal carrier systems', *Journal of controlled release*, 144(2), pp. 251-258.
Ryan, C.J., Smith, M.R., De Bono, J.S., Molina, A., Logothetis, C.J., De Souza, P., Fizazi, K., Mainwaring, P., Piulats, J.M. and Ng, S. (2013) 'Abiraterone in metastatic prostate cancer without previous chemotherapy', *New England Journal of Medicine*, 368(2), pp. 138-148.
Sakkiah, S., Ng, H.W., Tong, W. and Hong, H. (2016) 'Structures of androgen receptor bound with ligands: advancing understanding of biological functions and drug discovery', *Expert opinion on therapeutic targets*, 20(10), pp. 1267-1282.
Scher, H.I., Fizazi, K., Saad, F., Taplin, M.-E., Sternberg, C.N., Miller, K., de Wit, R., Mulders, P., Chi, K.N. and Shore, N.D. (2012) 'Increased survival with enzalutamide in prostate cancer after chemotherapy', *New England Journal of Medicine*, 367(13), pp. 1187-1197.
Schmidt, E.M., Gu, S., Anagnostopoulou, V., Alevizopoulos, K., Föller, M., Lang, F. and Stournaras, C. (2012) 'Serum-and glucocorticoid-dependent kinase-1-induced cell migration is dependent on vinculin and regulated by the membrane androgen receptor', *Febs Journal*, 279(7), pp. 1231-1242.
Schoeberl, B., Faber, A.C., Li, D., Liang, M.-C., Crosby, K., Onsum, M., Burenkova, O., Pace, E., Walton, Z. and Nie, L. (2010) 'An ErbB3 antibody, MM-121, is active in cancers with ligand-dependent activation', *Cancer research*, 70(6), pp. 2485-2494.
Schulz, W.A., Burchardt, M. and Cronauer, M.V. (2003) 'Molecular biology of prostate cancer', *Molecular human reproduction*, 9(8), pp. 437-448.
Sciarra, A., Panebianco, V., Cattarino, S., Busetto, G.M., De Berardinis, E., Ciccariello, M., Gentile, V. and Salciccia, S. (2012) 'Multiparametric magnetic resonance imaging of the prostate can improve the predictive value of the urinary prostate cancer antigen 3 test in patients with elevated prostate-specific antigen levels and a previous negative biopsy', *BJU international*, 110(11), pp. 1661-1665.
Shah, N., Wang, P., Wongvipat, J., Karthaus, W.R., Abida, W., Armenia, J., Rockowitz, S., Drier, Y., Bernstein, B.E. and Long, H.W. (2017) 'Regulation of the glucocorticoid receptor via a BET-dependent enhancer drives antiandrogen resistance in prostate cancer', *eLife*, 6.
Shah, R.B., Ghosh, D. and Elder, J.T. (2006) 'Epidermal growth factor receptor (ErbB1) expression in prostate cancer progression: correlation with androgen independence', *The Prostate*, 66(13), pp. 1437-1444.
Sharifi, N., Li, J., Alyamani, M., Zhang, A., Chang, K.-H., Berk, M., Li, Z., Zhu, Z., Petro, M. and Taplin, M.-E. (2017) 'Aberrant tumor metabolism to enable glucocorticoid receptor takeover in enzalutamide-resistant prostate cancer'. American Society of Clinical Oncology.
Shatnawi, A., Norris, J.D., Chaveroux, C., Jasper, J.S., Sherk, A.B., McDonnell, D.P. and Giguere, V. (2014) 'ELF3 is a repressor of androgen receptor action in prostate cancer cells', *Oncogene*, 33(7), pp. 862-871.
Sherk, A.B., Frigo, D.E., Schnackenberg, C.G., Bray, J.D., Laping, N.J., Trizna, W., Hammond, M., Patterson, J.R., Thompson, S.K. and Kazmin, D. (2008) 'Development of a small-molecule serum-and glucocorticoid-regulated kinase-1 antagonist and its evaluation as a prostate cancer therapeutic', *Cancer research*, 68(18), pp. 7475-7483.
Shiota, M., Bishop, J.L., Takeuchi, A., Nip, K.M., Cordonnier, T., Beraldi, E., Kuruma, H., Gleave, M.E. and Zoubeidi, A. (2015) 'Inhibition of the HER2-YB1-AR axis with Lapatinib synergistically enhances Enzalutamide anti-tumor efficacy in castration resistant prostate cancer', *Oncotarget*, 6(11), p. 9086.
Shiota, M., Yokomizo, A., Masubuchi, D., Tada, Y., Inokuchi, J., Eto, M., Uchiumi, T., Fujimoto, N. and Naito, S. (2010) 'Tip60 promotes prostate cancer cell proliferation by translocation of androgen receptor into the nucleus', *The Prostate*, 70(5), pp. 540-554.

Shvartsur, A. and Bonavida, B. (2015) 'Trop2 and its overexpression in cancers: regulation and clinical/therapeutic implications', *Genes & cancer*, 6(3-4), p. 84.
Sithanandam, G. and Anderson, L.M. (2008) 'The ERBB3 receptor in cancer and cancer gene therapy', *Cancer gene therapy*, 15(7), pp. 413-448.
Small, E.J., Halabi, S., Dawson, N.A., Stadler, W.M., Rini, B.I., Picus, J., Gable, P., Torti, F.M., Kaplan, E. and Vogelzang, N.J. (2004) 'Antiandrogen withdrawal alone or in combination with ketoconazole in androgen-independent prostate cancer patients: a phase III trial (CALGB 9583)', *Journal of clinical oncology*, 22(6), pp. 1025-1033.
Snoek, R., Cheng, H., Margiotti, K., Wafa, L.A., Wong, C.A., Wong, E.C., Fazli, L., Nelson, C.C., Gleave, M.E. and Rennie, P.S. (2009) 'In vivo knockdown of the androgen receptor results in growth inhibition and regression of well-established, castration-resistant prostate tumors', *Clinical Cancer Research*, 15(1), pp. 39-47.
Sobin, L.H. and Fleming, I.D. (1997) 'TNM classification of malignant tumors, (1997)', *Cancer*, 80(9), pp. 1803-1804.
Sommer, E.M., Dry, H., Cross, D., Guichard, S., Davies, B.R. and Alessi, D.R. (2013) 'Elevated SGK1 predicts resistance of breast cancer cells to Akt inhibitors', *Biochemical Journal*, 452(3), pp. 499-508.
Sridhar, S.S., Freedland, S.J., Gleave, M.E., Higano, C., Mulders, P., Parker, C., Sartor, O. and Saad, F. (2014) 'Castration-resistant prostate cancer: from new pathophysiology to new treatment', *European urology*, 65(2), pp. 289-299.
Sun, Y., Wang, B.-E., Leong, K.G., Yue, P., Li, L., Jhunjhunwala, S., Chen, D., Seo, K., Modrusan, Z. and Gao, W.-Q. (2012) 'Androgen deprivation causes epithelial–mesenchymal transition in the prostate: implications for androgen-deprivation therapy', *Cancer research*, 72(2), pp. 527-536.
Tammela, T. (2004) 'Endocrine treatment of prostate cancer', *The Journal of steroid biochemistry and molecular biology*, 92(4), pp. 287-295.
Tannock, I., Gospodarowicz, M., Meakin, W., Panzarella, T., Stewart, L. and Rider, W. (1989) 'Treatment of metastatic prostatic cancer with low-dose prednisone: evaluation of pain and quality of life as pragmatic indices of response', *Journal of Clinical Oncology*, 7(5), pp. 590-597.
Taplin, M.-E., Bubley, G.J., Ko, Y.-J., Small, E.J., Upton, M., Rajeshkumar, B. and Balk, S.P. (1999) 'Selection for androgen receptor mutations in prostate cancers treated with androgen antagonist', *Cancer research*, 59(11), pp. 2511-2515.
Taplin, M.-E., Regan, M.M., Ko, Y.-J., Bubley, G.J., Duggan, S.E., Werner, L., Beer, T.M., Ryan, C.W., Mathew, P. and Tu, S.-M. (2009) 'Phase II study of androgen synthesis inhibition with ketoconazole, hydrocortisone, and dutasteride in asymptomatic castration-resistant prostate cancer', *Clinical Cancer Research*, 15(22), pp. 7099-7105.
Taylor, B.S., Schultz, N., Hieronymus, H., Gopalan, A., Xiao, Y., Carver, B.S., Arora, V.K., Kaushik, P., Cerami, E. and Reva, B. (2010) 'Integrative genomic profiling of human prostate cancer', *Cancer cell*, 18(1), pp. 11-22.
Teng, D.H.F., Hu, R., Lin, H., Davis, T., Iliev, D., Frye, C., Swedlund, B., Hansen, K.L., Vinson, V.L. and Gumpper, K.L. (1997) 'MMAC1/PTEN mutations in primary tumor specimens and tumor cell lines', *Cancer research*, 57(23), pp. 5221-5225.
Thiruchelvam, N. (2014) 'Benign prostatic hyperplasia', *Surgery (Oxford)*, 32(6), pp. 314-322.
Tomas, A., Futter, C.E. and Eden, E.R. (2014) 'EGF receptor trafficking: consequences for signaling and cancer', *Trends in cell biology*, 24(1), pp. 26-34.
Torre, L.A., Siegel, R.L., Ward, E.M. and Jemal, A. (2016) 'Global cancer incidence and mortality rates and trends—an update', *Cancer Epidemiology and Prevention Biomarkers*, 25(1), pp. 16-27.
Tran, C., Ouk, S., Clegg, N.J., Chen, Y., Watson, P.A., Arora, V., Wongvipat, J., Smith-Jones, P.M., Yoo, D. and Kwon, A. (2009) 'Development of a second-generation

antiandrogen for treatment of advanced prostate cancer', *Science*, 324(5928), pp. 787-790.
Trerotola, M., Cantanelli, P., Guerra, E., Tripaldi, R., Aloisi, A.L., Bonasera, V., Lattanzio, R., De Lange, R., Weidle, U.H. and Piantelli, M. (2013a) 'Upregulation of Trop-2 quantitatively stimulates human cancer growth', *Oncogene*, 32(2), pp. 222-233.
Trerotola, M., Ganguly, K.K., Fazli, L., Fedele, C., Lu, H., Dutta, A., Liu, Q., De Angelis, T., Riddell, L.W. and Riobo, N.A. (2015) 'Trop-2 is up-regulated in invasive prostate cancer and displaces FAK from focal contacts', *Oncotarget*, 6(16), p. 14318.
Trerotola, M., Jernigan, D.L., Liu, Q., Siddiqui, J., Fatatis, A. and Languino, L.R. (2013b) 'Trop-2 promotes prostate cancer metastasis by modulating β1 integrin functions', *Cancer research*, 73(10), pp. 3155-3167.
Trerotola, M., Li, J., Alberti, S. and Languino, L.R. (2012) 'Trop-2 inhibits prostate cancer cell adhesion to fibronectin through the β1 integrin-RACK1 axis', *Journal of cellular physiology*, 227(11), pp. 3670-3677.
Trerotola, M., Rathore, S., Goel, H.L., Li, J., Alberti, S., Piantelli, M., Adams, D., Jiang, Z. and Languino, L.R. (2010) 'CD133, Trop-2 and α2β1 integrin surface receptors as markers of putative human prostate cancer stem cells', *American journal of translational research*, 2(2), p. 135.
van den Bergh, R.C.N., van Casteren, N.J., Van den Broeck, T., Fordyce, E.R., Gietzmann, W.K.M., Stewart, F., MacLennan, S., Dabestani, S., Bellmunt, J. and Bolla, M. (2016) 'Role of hormonal treatment in prostate cancer patients with nonmetastatic disease recurrence after local curative treatment: a systematic review', *European urology*, 69(5), pp. 802-820.
Van der Roest, R.C.V., van Houdt, P.J., Heijmink, S.W., de Jong, J., Bergman, A.M., Zwart, W., van der Heide, U.A. and van der Poel, H.G. (2016) 'The Effects of Enzalutamide Monotherapy on Multiparametric 3T MR Imaging in Prostate Cancer', *Urology Case Reports*, 7, pp. 67-69.
Vias, M., Burtt, G., Culig, Z., Veerakumarasivam, A., Neal, D.E. and Mills, I.G. (2007) 'A role for neurotensin in bicalutamide resistant prostate cancer cells', *The Prostate*, 67(2), pp. 190-202.
Villers, A.A., McNeal, J.E., Freiha, F.S. and Stamey, T.A. (1991) 'Development of prostatic carcinoma: morphometric and pathologic features of early stages', *Acta Oncologica*, 30(2), pp. 145-151.
Visakorpi, T., Hyytinen, E., Koivisto, P., Tanner, M., Keinänen, R., Palmberg, C., Palotie, A., Tammela, T., Isola, J. and Kallioniemi, O.-P. (1995) 'In vivo amplification of the androgen receptor gene and progression of human prostate cancer', *Nature genetics*, 9(4), pp. 401-406.
Vivanco, I. and Sawyers, C.L. (2002) 'The phosphatidylinositol 3-kinase–AKT pathway in human cancer', *Nature Reviews Cancer*, 2(7), pp. 489-501.
Wadosky, K.M. and Koochekpour, S. (2017) 'Androgen receptor splice variants and prostate cancer: From bench to bedside', *Oncotarget*, 8, pp. 18550-18576.
Waltering, K.K., Urbanucci, A. and Visakorpi, T. (2012) 'Androgen receptor (AR) aberrations in castration-resistant prostate cancer', *Molecular and cellular endocrinology*, 360(1), pp. 38-43.
Wang, D., Zhang, H., Lang, F. and Yun, C.C. (2007) 'Acute activation of NHE3 by dexamethasone correlates with activation of SGK1 and requires a functional glucocorticoid receptor', *American Journal of Physiology-Cell Physiology*, 292(1), pp. C396-C404.
Watson, P.A., Arora, V.K. and Sawyers, C.L. (2015) 'Emerging mechanisms of resistance to androgen receptor inhibitors in prostate cancer', *Nature Reviews Cancer*, 13, pp. 701–711.

Watson, P.A., Chen, Y.F., Balbas, M.D., Wongvipat, J., Socci, N.D., Viale, A., Kim, K. and Sawyers, C.L. (2010) 'Constitutively active androgen receptor splice variants expressed in castration-resistant prostate cancer require full-length androgen receptor', *Proceedings of the national academy of sciences*, 107(39), pp. 16759-16765.
Weinstein-Oppenheimer, C.R., Blalock, W.L., Steelman, L.S., Chang, F. and McCubrey, J.A. (2000) 'The Raf signal transduction cascade as a target for chemotherapeutic intervention in growth factor-responsive tumors', *Pharmacology & therapeutics*, 88(3), pp. 229-279.
Whalen, R.E. and Edwards, D.A. (1969) 'Effects of the anti-androgen cyproterone acetate on mating behavior and seminal vesicle tissue in male rats', *Endocrinology*, 84(1), pp. 155-156.
Wise, D., Louw, J., Krupa, R., Schreiber, N.A., Sawyers, C.L., Dittamore, R.V. and Scher, H.I. (2016) 'Detection of glucocorticoid receptor (GR) expression in circulating tumor cells (CTCs) from patients (pts) with metastatic castration-resistant prostate cancer (mCRPC)'. American Society of Clinical Oncology.
Woods, D., Parry, D., Cherwinski, H., Bosch, E., Lees, E. and McMahon, M. (1997) 'Raf-induced proliferation or cell cycle arrest is determined by the level of Raf activity with arrest mediated by p21Cip1', *Molecular and cellular biology*, 17(9), pp. 5598-5611.
Xie, J., Mølck, C., Paquet-Fifield, S., Butler, L., Sloan, E., Ventura, S., Hollande, F. and Australian Prostate Cancer, B. (2016) 'High expression of TROP2 characterizes different cell subpopulations in androgen-sensitive and androgen-independent prostate cancer cells', *Oncotarget*, 7(28), p. 44492.
Yan, M., Schwaederle, M., Arguello, D., Millis, S.Z., Gatalica, Z. and Kurzrock, R. (2015) 'HER2 expression status in diverse cancers: review of results from 37,992 patients', *Cancer and Metastasis Reviews*, 34(1), pp. 157-164.
Yarden, Y. and Pines, G. (2012) 'The ERBB network: at last, cancer therapy meets systems biology', *Nature reviews Cancer*, 12(8), pp. 553-563.
Yeh, S., Lin, H.-K., Kang, H.-Y., Thin, T.H., Lin, M.-F. and Chang, C. (1999) 'From HER2/Neu signal cascade to androgen receptor and its coactivators: a novel pathway by induction of androgen target genes through MAP kinase in prostate cancer cells', *Proceedings of the National Academy of Sciences*, 96(10), pp. 5458-5463.
Yemelyanov, A., Bhalla, P., Yang, X., Ugolkov, A., Iwadate, K., Karseladze, A. and Budunova, I. (2012) 'Differential targeting of androgen and glucocorticoid receptors induces ER stress and apoptosis in prostate cancer cells: a novel therapeutic modality', *Cell cycle*, 11(2), pp. 395-406.
Yemelyanov, A., Czwornog, J., Gera, L., Joshi, S., Chatterton, R.T. and Budunova, I. (2008) 'Novel steroid receptor phyto-modulator compound a inhibits growth and survival of prostate cancer cells', *Cancer research*, 68(12), pp. 4763-4773.
Yuan, X., Cai, C., Chen, S., Yu, Z. and Balk, S.P. (2014) 'Androgen receptor functions in castration-resistant prostate cancer and mechanisms of resistance to new agents targeting the androgen axis', *Oncogene*, 33(22), pp. 2815-2825.
Zhang, N., Chang, Y., Rios, A. and An, Z. (2016) 'HER3/ErbB3, an emerging cancer therapeutic target', *Acta Biochim Biophys Sin (Shanghai)*, 48(1), pp. 39-48.
Zhao, Q. and Lee, F.S. (1999) 'Mitogen-activated protein kinase/ERK kinase kinases 2 and 3 activate nuclear factor-κB through IκB kinase-α and IκB kinase-β', *Journal of Biological Chemistry*, 274(13), pp. 8355-8358.
Zhou, C.K., Check, D.P., Lortet-Tieulent, J., Laversanne, M., Jemal, A., Ferlay, J., Bray, F., Cook, M.B. and Devesa, S.S. (2016) 'Prostate cancer incidence in 43 populations worldwide: an analysis of time trends overall and by age group', *International Journal of Cancer*, 138(6), pp. 1388-1400.

9.1 Microarray screen

Appendix 9-1 microarray samples

Sample ID	Description	Enzalutamide
1, 5, 9	Parental LNCaP	-
4, 10, 12	Parental LNCaP	+
2, 7, 11	LNCaP-ENZ-R	-
3, 6, 8	LNCaP-ENZ-R	+

9.1.1 Technical and Sample QC Metrics

Quality Control is a fundamental aspect of successful microarray data analysis. QC metrics is used for assessing the quality of RNA samples and of the intermediate stages of sample preparation and hybridization.

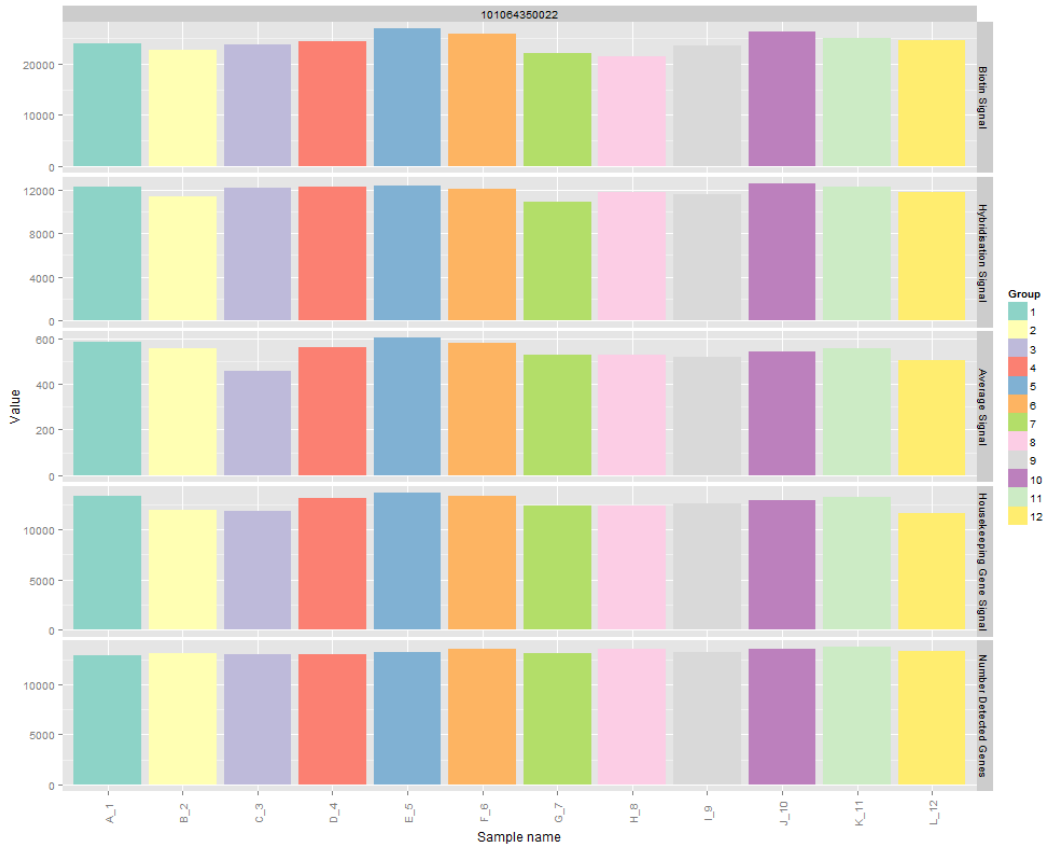

Appendix 9-2 The QC metrics.

This figure shows the samples ordered by chip and position (A-L) and coloured by the groups listed in the sample sheet. The control probes for biotin and hybridization (rows 1&2) are sample-independent and give consistently high signal, indicating that the experimental steps were successful. The sample-dependent plots of average signal intensity and signal from housekeeping genes are shown in rows 3&4. Any variability here can be attributed to several different factors (sample quality, labelling efficiency, amount of material loaded etc) and should largely be corrected by normalization. All the samples give good overall signal, and housekeeping gene signal is very high as expected. The number of detected genes (row 5) is also consistently high. No individual sample gives any cause for concern based on these metrics.

9.1.2 Data Preprocessing

The VSN (variance-stabilisation and normalisation) algorithm were used to process raw data from Illumina gene expression arrays and this works very well in the vast majority of cases. This pre-processing performs two main steps to make the data suitable for further analysis: (i) stabilises the variance to better meet the assumptions of the statistical test for differential expression and (ii) normalises signal intensities from different samples so that they are comparable.

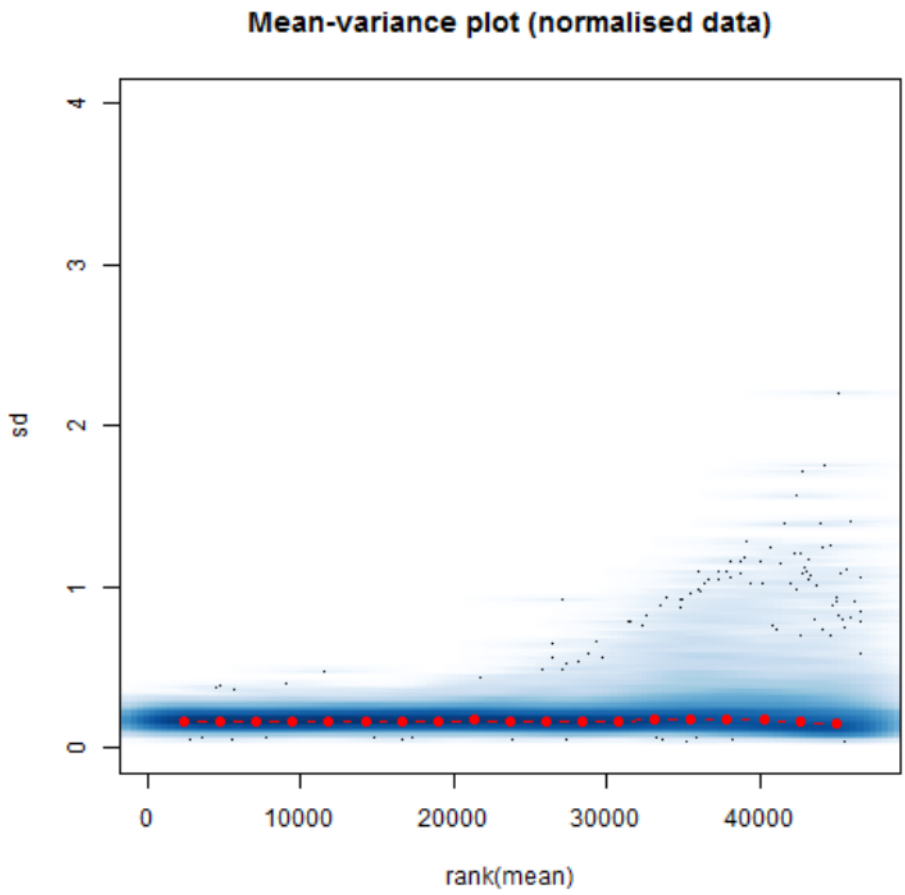

Appendix 9-3 Mean-variance plot after VSN processing.

A mean-variance plot should show approximately constant variance across the entire intensity range (the red dots should be roughly in a straight line).

9.1.3 Exploratory QC plots

We next generate further QC plots to explore various features of the data, looking at overall data quality, potential outlier samples and the main sources of variation. Firstly, the distribution of probe intensities (VSN normalized data) can be visualized for each sample as density plots (Appendix 9-4: left shows data for all 47,231 probes; right shows data for 23,463 probes after filtering to remove probes not detected in any of the samples). The filtered data is also shown as boxplots in Appendix 9-5. The profile for the probe intensity distribution is characteristic of high quality data and the samples are highly consistent with each other.

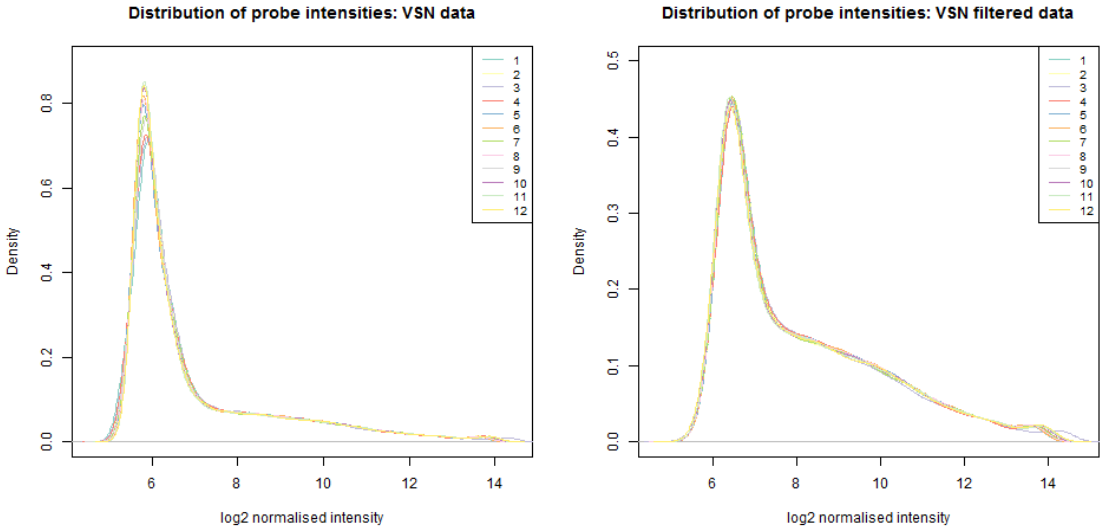

Appendix 9-4 Density distributions for the full dataset (left) and after filtering to remove probes not detected above background levels (right)

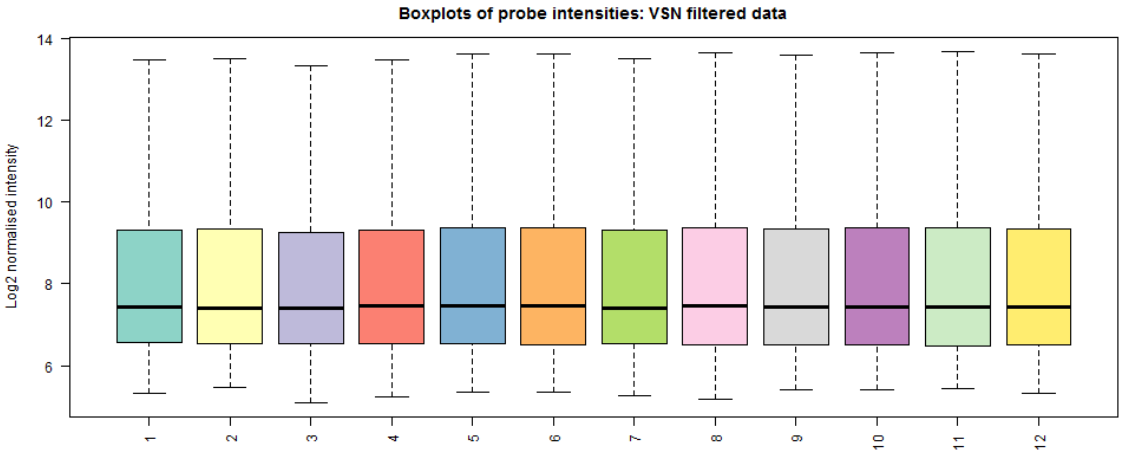

Appendix 9-5 Boxplots of filtered data for each sample

9.1.4 Hierarchical clustering analysis

Hierarchical clustering and principal components analysis (PCA) can be used to identify outlier samples and assess the main factors influencing the expression profile (e.g. experimental condition or technical factors such as batch or chip). Clustering of the filtered data suggests that samples 4 and 12 have the most distinct expression profiles, while 3 and 7 also form a separate branch (Appendix 9-6). Additional experimental information is required to comment further on the clustering pattern observed.

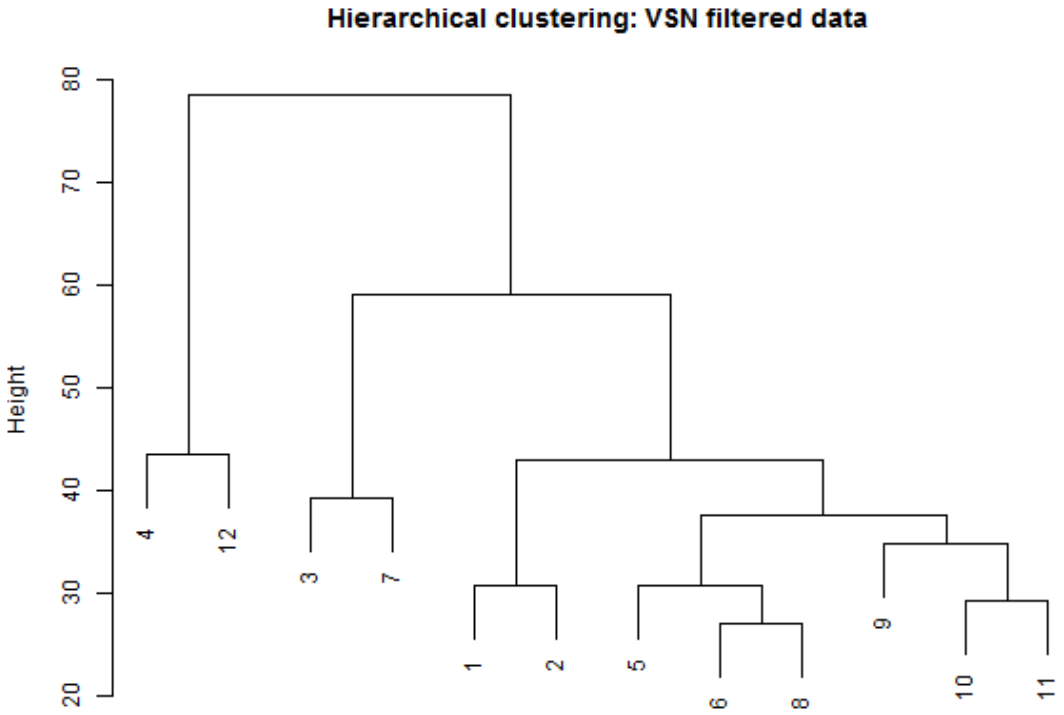

Appendix 9-6 Hierarchical clustering of the VSN-processed and filtered data

In the PCA plots below (Appendix 9-7), samples close together have similar overall expression profiles and the primary source of variation will separate samples on the x-axis (PC1) and secondary source on the y-axis (PC2). The pattern here is mostly consistent with the hierarchical clustering, with 4 and 12 found to the right of the plot, and 3 and 7 to the left. Note that sample 11 appears more similar to 6 and 8 than in Figure 5, and the PCA probably gives a better assessment of the relationship between samples. PC1 accounts for approximately 40% of the total variance, suggesting fairly large differences between the samples. However, the biological meaning of this is unclear in the absence of experimental details.

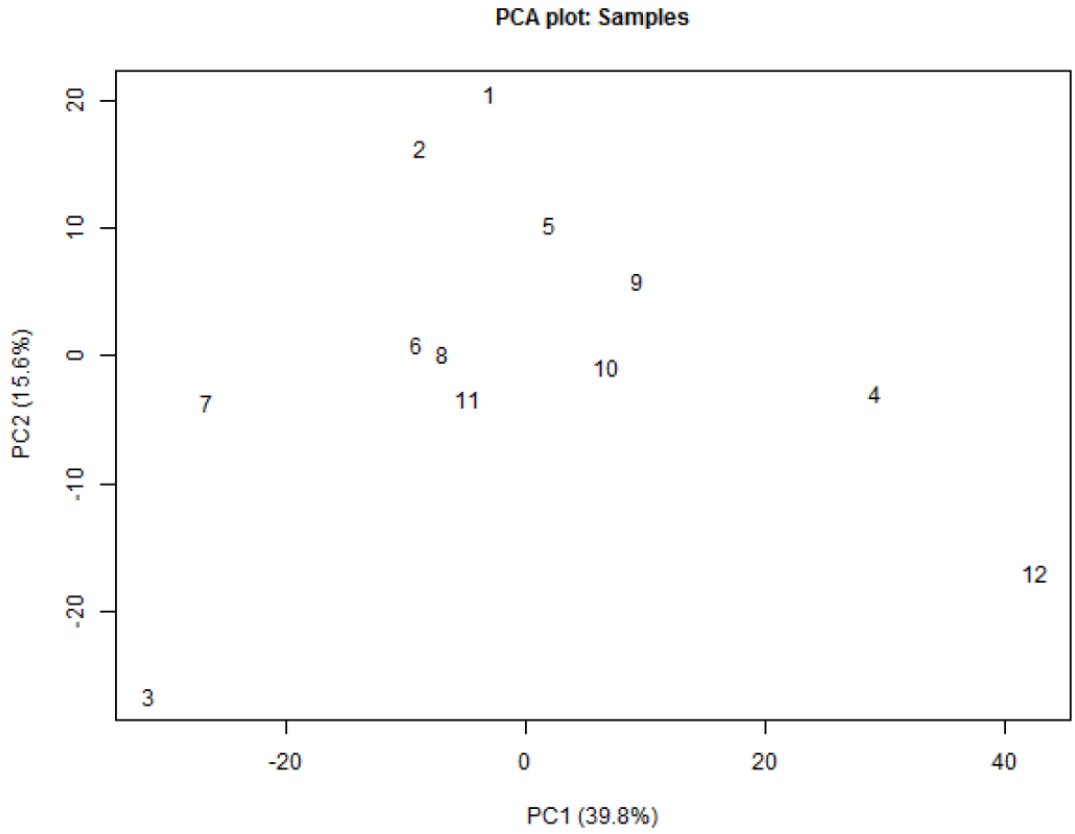

Appendix 9-7 PCA of the VSN-processed and filtered dataset, labelled by sample

Table 9-1 microarray data analysis: The up-regulated genes and down-regulated genes in LNCaP-ENZ-R in present of enzalutamide

ID	symbol	Fold Change	P.Value
ILMN_1796490	GRINA	2.010617	0.029181
ILMN_2396956	AKAP13	1.890986	0.006564
ILMN_1766309	ANKRD54	1.666811	0.00894
ILMN_1714710	CCDC120	1.653325	0.002108
NM_006911.2	RLN1	1.652356	0.000879
ILMN_1801403	DCUN1D4	1.623944	0.044987
ILMN_3238633	SDHAF2	1.616603	0.00418
NM_020783.2	SYT4	1.614506	0.000364
ILMN_3240838	SLC25A6	1.60671	0.003564
ILMN_1675632	LINC01549	1.600436	0.024655
NM_002353.1	TACSTD2	1.572794	0.000121
ILMN_1656718	DEF8	1.564621	8.33E-05
ILMN_1671005	IRF2BP2	1.560454	0.002496
ILMN_2389429	DCUN1D4	1.556708	0.03429
ILMN_2216157	GNA12	1.556087	1.76E-05
ILMN_1693490	SEC11A	1.54727	0.000581
ILMN_1769517	PRKDC	1.545612	0.002198
ILMN_1808487	PLA2G12B	1.531139	0.037923
ILMN_1779558	GAS6	1.512373	0.012286
ILMN_1659744	PRMT1	1.48603	0.0202
ILMN_1656185	DEF8	1.478261	0.000252
ILMN_1653115	ECH1	1.468967	2.8E-05
ILMN_1693220	AKAP11	1.465837	0.012869
ILMN_3308505	MIR129-2	1.44548	7.61E-05
ILMN_1779147	ENC1	1.441394	0.016655
ILMN_2393296	GK	1.427782	0.002277
ILMN_1783120	SLMAP	1.424937	0.0077
ILMN_3270972	ASAP2	1.413429	0.000204
ILMN_1657148	CIRBP-AS1	1.4096	0.00089
ILMN_1767509	DEF8	1.399229	0.001817
ILMN_1815745	SOX4	1.398091	0.003292
ILMN_2142695	RNF4	1.39446	0.018001
ILMN_2205050	PRKX	1.391202	0.019139
ILMN_2089167	RHOD	1.376596	0.000266
ILMN_1721833	IER5	1.375614	0.007263
ILMN_1771966	BCCIP	1.373546	0.000358
ILMN_1665455	DCUN1D3	1.372785	0.028524
ILMN_1795286	C6orf47	1.369793	0.000497
ILMN_1768282	SNX21	1.368862	0.001555
ILMN_1664630	CHEK1	1.366026	0.004413
ILMN_2166831	RPS4X	1.358629	0.000753

ILMN_1666179	HIST2H3C	1.354063	0.000658
ILMN_2371397	SLC25A45	1.34968	0.006656
ILMN_1674376	ANGPTL4	1.345407	0.006269
ILMN_1688938	KCNRG	1.34494	0.010478
ILMN_1741005	TRMT10A	1.340242	0.04308
ILMN_2408877	KMT2C	1.339958	0.000588
ILMN_1776088	NAT9	1.339746	0.007114
ILMN_1757697	NEIL3	1.338122	0.000946
ILMN_2412549	GAR1	1.336848	0.002225
ILMN_1795218	DHX30	1.328926	0.001205
ILMN_1772131	IL1R2	1.328752	0.0396
ILMN_1738783	GDF9	1.326873	0.013238
ILMN_1797499	PRKDC	1.326116	0.001977
ILMN_2221673	ASNSD1	1.325991	0.001236
ILMN_2270443	LIMK2	1.325988	0.0048
ILMN_1698404	ERN1	1.325085	0.000848
ILMN_2360705	ACSL3	1.323809	0.015924
ILMN_2315289	PEX10	1.319608	0.010351
ILMN_1729599	GDPD1	1.318378	0.017299
ILMN_1706246	CCT5	1.31282	0.001148
ILMN_1669584	ILF3	1.31195	0.005017
ILMN_2384536	ECI2	1.31189	0.029444
ILMN_1748916	TIMM21	1.311621	0.017652
ILMN_1803036	TARBP1	1.309058	0.00234
ILMN_1672565	TRMT10C	1.308217	0.009275
ILMN_2352326	COASY	1.308175	0.000931
ILMN_1665982	AKTIP	1.307848	0.009086
ILMN_1696046	SIVA1	1.307559	0.015595
ILMN_1682763	ALB	1.305131	0.002149
ILMN_1720124	RCC2	1.301621	0.001842
ILMN_2262462	CACTIN	1.301556	0.021969
ILMN_1702487	SGK1	1.301466	0.000216
ILMN_1677200	CYFIP2	1.300217	0.025698
ILMN_1732688	DUT	1.295431	0.008352
ILMN_1652412	PHKB	1.294255	0.001755
ILMN_1712067	DRC7	1.293823	0.011716
ILMN_1771599	PLOD2	1.293758	0.002256
ILMN_1759350	MED27	1.292923	0.058793
ILMN_1745172	ILF2	1.291021	0.000392
ILMN_1685641	BCHE	1.288714	0.003921
ILMN_3244592	SNORA68	1.288416	0.005572
ILMN_2395913	ARHGAP11A	1.288058	0.008052
ILMN_1772132	ATP5B	1.287876	0.002027
ILMN_1666599	SNORD30	1.287589	0.011499
ILMN_1758474	PRKRA	1.287233	0.020135
ILMN_2372698	RGN	1.286383	0.002845

ILMN_2161286	STRIP2	1.285769	0.000485
ILMN_2143250	FAR1	1.285158	0.007641
ILMN_1730363	STAU1	1.284815	0.000183
ILMN_1679428	CHIC2	1.284763	0.003788
ILMN_3237665	COX7A2L	1.284186	0.000196
ILMN_1746696	PDS5B	1.284024	0.008806
ILMN_1741957	RABEPK	1.283601	0.000252
ILMN_1659544	STX3	1.283543	0.036087
ILMN_2076658	MRPL1	1.283074	0.001345
ILMN_1776121	KIAA1211L	1.282864	0.01613
ILMN_1706426	DSTN	1.281214	0.006745
ILMN_1707336	ARPC4	1.2809	0.010378
ILMN_1684054	ASAH1	1.280437	0.016323
ILMN_1687495	SLC37A1	1.280405	0.000303
ILMN_1728517	FNTB	1.278742	0.001098
ILMN_2109994	RAB4B	1.27762	0.000892
ILMN_2355738	INCENP	1.276341	0.002957
ILMN_1756360	RPL35A	1.275338	0.008799
ILMN_2354478	CYFIP2	1.27525	0.02711
ILMN_1805024	ERBB2IP	1.275055	0.003316
ILMN_1756910	PLA2G15	1.274976	0.015732
ILMN_1792748	CPS1	1.274276	0.001021
ILMN_2357062	IL1RAP	1.273973	0.022879
ILMN_1721008	DUT	1.272114	0.002737
ILMN_1755758	RIF1	1.271775	0.00554
ILMN_1810085	ABCF3	1.270755	0.016288
ILMN_1788489	HIST1H3F	1.270069	0.009743
ILMN_3262348	IP6K2	1.26964	0.03409
ILMN_2123730	TBC1D22B	1.269571	0.002354
ILMN_1765649	IRF3	1.269491	0.008086
ILMN_1719158	CTBP1	1.26791	0.00073
ILMN_1770936	COQ5	1.267592	0.000922
ILMN_1681670	SLC25A4	1.267448	0.009039
ILMN_1725471	GK	1.266746	0.017999
ILMN_2222991	ETF1	1.265447	0.000404
ILMN_1751636	ANKS3	1.265403	0.022063
ILMN_1759048	SDHAP1	1.264963	0.009091
ILMN_1685952	ACSM3	1.26452	0.052348
ILMN_1796341	GLT8D1	1.262995	0.006095
ILMN_1691393	DNPEP	1.26277	0.005535
ILMN_1654468	ACRV1	1.26059	0.02006
ILMN_1684042	BET1	1.260242	0.016273
ILMN_1753353	SLBP	1.260026	0.004499
ILMN_1666546	DUSP14	1.259212	0.02157
ILMN_1701293	COX7A2	1.257948	0.001675
ILMN_1720422	G3BP2	1.25556	0.025067

ILMN_1729691	SLC16A6	1.25513	0.035571
ILMN_1760303	PIK3R1	1.255126	0.000982
ILMN_1724490	PSPC1	1.252759	0.018556
ILMN_1752046	SH2B3	1.251564	0.020742
ILMN_1811877	ANTXR1	1.251347	0.00048
ILMN_2103024	RBP5	1.250988	0.01487
ILMN_1817048	NA	1.250958	0.01383
ILMN_1659524	NDUFAF4	1.250661	0.04493
ILMN_2071937	ATP6V0E1	1.250381	0.004627
ILMN_1690066	TIGD2	1.250302	0.012865
ILMN_1757631	DBNDD1	1.249598	0.016479
ILMN_1734472	PEBP4	1.248045	0.046586
ILMN_2234343	ACP6	1.247937	0.019029
ILMN_1725680	LRRC1	1.247546	0.015213
ILMN_1736974	SOX12	1.246386	0.036007
ILMN_1814650	TRAPPC4	1.245596	0.000531
ILMN_3305949	NA	1.245481	0.003557
ILMN_1793859	ALDH2	1.245071	0.000977
ILMN_1892599	NA	1.244517	0.025931
ILMN_1807737	AKAP17A	1.243828	0.004122
ILMN_1720266	ZGRF1	1.242187	0.001884
ILMN_1777660	RNF144A	1.242053	0.00612
ILMN_1696591	RB1	1.241965	0.006107
ILMN_1666652	BRCA1	1.241701	0.02484
ILMN_1873620	TSPAN14	1.241056	0.007906
ILMN_3238001	NA	1.240797	0.042563
ILMN_1712027	RSBN1L	1.240638	0.015606
ILMN_1730848	KRT18	1.240061	0.017887
ILMN_2138765	PLIN2	1.239942	0.01169
ILMN_1708891	SCFD2	1.23989	0.006933
ILMN_2317463	INTS1	1.238729	0.01029
ILMN_2129877	PARP11	1.238243	0.008558
ILMN_2232084	ABCA11P	1.237664	0.010497
ILMN_1853738	SYCE2	1.237074	0.003996
ILMN_1800786	NA	1.236051	0.002968
ILMN_3237419	NA	1.235436	0.018881
ILMN_1746465	FJX1	1.234991	0.000718
ILMN_1779423	MRPS14	1.23484	0.009018
ILMN_1740231	ELMO1	1.234703	0.008988
ILMN_2363065	RTN3	1.234472	0.005854
ILMN_2281069	GPATCH4	1.234394	0.00648
ILMN_1793915	MXI1	1.233547	0.005792
ILMN_1767324	EIF4EBP1	1.233174	0.004206
ILMN_1810577	RPS4X	1.232911	0.00689
ILMN_1774589	IQCC	1.232664	0.00558
ILMN_1780141	SARAF	1.232273	0.008395

ILMN_2394193	VCPKMT	1.231153	0.001949
ILMN_3194508	ASAP2	1.230465	0.004073
ILMN_1678075	NA	1.229651	0.002166
ILMN_1730630	CXorf56	1.229293	0.002103
ILMN_1713935	C3orf33	1.229154	0.002238
ILMN_3236358	NOP14	1.229076	0.0091
ILMN_1674024	NA	1.228286	0.001863
ILMN_1713322	CCZ1B	1.227416	0.004194
ILMN_3243744	EAPP	1.227046	0.003343
ILMN_1737541	HGD	1.226925	0.020971
ILMN_1780699	THAP11	1.22689	0.006958
ILMN_1740395	RAVER1	1.226768	0.002398
ILMN_1789244	SOX8	1.226549	0.02675
ILMN_1651767	MKL1	1.226481	0.005865
ILMN_1751028	SERPINH1	1.226334	0.000563
ILMN_1669102	ATP5G2	1.226254	0.005769
ILMN_1669851	STAG3L4	1.226153	0.018509
ILMN_1753370	ABTB2	1.225226	0.002265
ILMN_3235632	ANXA2P2	1.224915	0.01063
ILMN_1765547	IRF2	1.224782	0.007353
ILMN_1821517	NA	1.22463	0.05008
ILMN_1851906	NA	1.224477	0.002941
ILMN_3310151	MIR1909	1.22442	0.00353
ILMN_1810116	INPP5B	1.224395	0.008213
ILMN_2117716	AKAP17A	1.224283	0.022596
ILMN_2090123	DHX29	1.223701	0.010663
ILMN_2224907	SMIM14	1.22347	0.004449
ILMN_2364088	GEMIN8	1.223337	0.001993
ILMN_1794711	NA	1.221163	0.035966
ILMN_1812688	SLC35F6	1.220472	0.039283
ILMN_2355559	PSAP	1.220068	0.002112
ILMN_2056032	CD99	1.219876	0.007171
ILMN_1794074	MXI1	1.218981	0.003669
ILMN_1721713	EXOSC9	1.218715	0.006514
ILMN_2395236	CHEK2	1.217774	0.01379
ILMN_1799628	NA	1.216309	0.014434
ILMN_1716524	RAB7A	1.216227	0.038482
ILMN_1659782	STK19	1.216186	0.007195
ILMN_2152711	ACVR2A	1.216026	0.012033
ILMN_1691428	NA	1.215172	0.043349
ILMN_2285568	NAAA	1.215084	0.012333
ILMN_3247653	LRFN1	1.214948	0.05191
ILMN_1693394	BCKDK	1.214047	0.001766
ILMN_1701854	GNG5	1.214002	0.001585
ILMN_1759987	HS6ST1	1.212923	0.031729
ILMN_1772957	FOXRED2	1.212795	0.002696

ILMN_1717674	PEPD	1.212743	0.004965
ILMN_3238797	FAM72A	1.212555	0.008584
ILMN_2197846	HADHB	1.211599	0.007435
ILMN_1769027	CDC42SE1	1.210803	0.013873
ILMN_2385647	ALAS1	1.210724	0.006646
ILMN_1815023	PIM1	1.210466	0.019329
ILMN_1769299	MTMR11	1.210353	0.00422
ILMN_1710216	AVEN	1.209396	0.010398
ILMN_1673682	GATAD2A	1.209388	0.019236
ILMN_2369286	NME7	1.209207	0.017948
ILMN_1737685	CRLS1	1.208279	0.009521
ILMN_1744914	FUCA2	1.207593	0.004555
ILMN_1671603	MED30	1.207233	0.01559
ILMN_1674411	CKAP2	1.20586	0.003177
ILMN_1805968	TCAF1	1.205629	0.035054
ILMN_2196588	C18orf32	1.203844	0.00325
ILMN_1804834	OARD1	1.203783	0.032222
ILMN_3309829	MIR373	1.203232	0.002739
ILMN_1808602	LINC01547	1.202984	0.053696
ILMN_3251388	TMEM183A	1.202716	0.011018
ILMN_2333829	NXF2	1.202447	0.003569
ILMN_1752270	SLC25A40	1.202105	0.005562
ILMN_1773200	CCP110	1.201295	0.003011
ILMN_1743194	EEA1	1.201203	0.038626
ILMN_1705064	NDEL1	1.200128	0.006722
ILMN_1704472	EID2	0.914898	0.058282
ILMN_1744963	ERO1A	0.914534	0.057771
ILMN_1673844	NA	0.913109	0.05197
ILMN_1663631	BANP	0.912925	0.051344
ILMN_3282436	NA	0.910992	0.050511
ILMN_3243274	LINC00200	0.91037	0.054374
ILMN_1746917	NA	0.910116	0.047759
ILMN_3239959	TEN1	0.90936	0.052622
ILMN_1656042	KIAA0319L	0.908854	0.050003
ILMN_1762281	DCTN3	0.908252	0.056336
ILMN_1694223	DGCR8	0.908064	0.043679
ILMN_2143685	CLDN7	0.908013	0.054085
ILMN_1728199	POLE	0.907958	0.053826
ILMN_3229570	NA	0.907817	0.055562
ILMN_1795826	ATP6V0D1	0.906847	0.055259
ILMN_3201975	NA	0.906593	0.04423
ILMN_1776582	PDK3	0.905898	0.052029
ILMN_1777526	MED20	0.905025	0.056268
ILMN_2141452	RPL18A	0.904489	0.057522
ILMN_3302701	NA	0.904437	0.038889
ILMN_1718898	HOXC9	0.904405	0.052725

ILMN_1651259	NA	0.90421	0.052881
ILMN_3298824	NA	0.904115	0.039955
ILMN_1758164	STC1	0.904076	0.049281
ILMN_3306730	RBM47	0.903046	0.045258
ILMN_1695475	SEMA3C	0.902972	0.042471
ILMN_1713496	ST3GAL5	0.90272	0.05315
ILMN_1759252	ADD1	0.90271	0.037855
ILMN_1753063	KIF15	0.902611	0.036171
ILMN_1725485	RGS17	0.902592	0.038872
ILMN_3240247	NOP10	0.902471	0.052858
ILMN_1758673	SLC44A1	0.902413	0.048888
ILMN_2169025	JOSD2	0.900981	0.045363
ILMN_1721876	TIMP2	0.900879	0.052516
ILMN_3246242	NA	0.900687	0.04103
ILMN_1790100	DDIAS	0.900596	0.050914
ILMN_1684258	NA	0.900299	0.043208
ILMN_1808391	DUSP4	0.900192	0.034728
ILMN_1782621	RPS12	0.899938	0.037907
ILMN_1764423	NA	0.899911	0.052283
ILMN_1681754	GGH	0.89988	0.047909
ILMN_1756308	NAE1	0.899814	0.047536
ILMN_1913021	NA	0.899581	0.052
ILMN_1761072	NA	0.899166	0.044465
ILMN_1786759	TMEM258	0.898628	0.048785
ILMN_1812473	MLLT3	0.898387	0.058626
ILMN_1678754	PFDN2	0.898338	0.038057
ILMN_1808202	R3HDM4	0.898337	0.049465
ILMN_2041648	TMPRSS7	0.898328	0.044813
ILMN_1716728	SAYSD1	0.8982	0.022471
ILMN_2075927	STK40	0.898155	0.055425
ILMN_2052598	ARMC10	0.897304	0.04252
ILMN_1674768	NA	0.897245	0.037813
ILMN_1879480	CCNG2	0.897004	0.035515
ILMN_2233099	SSRP1	0.896875	0.049009
ILMN_1721167	MYT1	0.896867	0.054639
ILMN_1785290	DOK6	0.896617	0.040911
ILMN_1815107	MATR3	0.896587	0.027159
ILMN_1780842	RANBP6	0.896551	0.056038
ILMN_1752798	NA	0.896532	0.054277
ILMN_2159859	LYSMD4	0.896255	0.022218
ILMN_3195203	OGFOD3	0.896077	0.037897
ILMN_2278265	PAOX	0.895901	0.037636
ILMN_2112460	MAD2L1	0.895675	0.032257
ILMN_3256801	ATP1A1-AS1	0.895637	0.035736
ILMN_2187718	COX17	0.895345	0.048737
ILMN_1687867	NA	0.895242	0.052015

ILMN_1771126	RORC	0.89505	0.03067
ILMN_3304519	NA	0.894677	0.05496
ILMN_3218820	NA	0.894629	0.033934
ILMN_1697959	SLC35B4	0.894346	0.037373
ILMN_1704238	DTD2	0.89405	0.030501
ILMN_2367172	AMACR	0.893588	0.044167
ILMN_1673788	CDV3	0.89342	0.025818
ILMN_1762021	TRIM48	0.893322	0.04717
ILMN_1745900	NA	0.893199	0.046827
ILMN_2400644	SRGAP3	0.893166	0.041095
ILMN_1728984	PA2G4	0.89316	0.059891
ILMN_2108735	EEF1A2	0.892994	0.021188
ILMN_1713086	RPL27A	0.892975	0.053377
ILMN_1815308	SDC1	0.892856	0.053691
ILMN_3243700	RPS8	0.892665	0.043981
ILMN_1684402	STXBP5	0.892591	0.048818
ILMN_1748616	GTF2F1	0.892141	0.044009
ILMN_1767747	HDAC2	0.892136	0.027134
ILMN_1660585	C15orf40	0.891995	0.051446
ILMN_3304012	NA	0.891655	0.050049
ILMN_1798270	SMCO4	0.891554	0.03977
ILMN_1810228	TTF2	0.891374	0.020346
ILMN_1823013	NA	0.891205	0.037673
ILMN_1663640	MAOA	0.89103	0.050187
ILMN_1762327	DHRS12	0.890814	0.02107
ILMN_1699887	ST14	0.890802	0.05152
ILMN_1758613	RAPGEFL1	0.890788	0.047135
ILMN_1807304	MBNL1	0.890559	0.032041
ILMN_2386008	MPZL1	0.890403	0.0202
ILMN_1691418	CDRT4	0.890194	0.051839
ILMN_3234513	NA	0.889998	0.026887
ILMN_1663447	HNRNPA1	0.889935	0.04769
ILMN_1662427	PTP4A3	0.889482	0.053654
ILMN_1805131	OXLD1	0.889325	0.024037
ILMN_1683054	NA	0.889252	0.037234
ILMN_1793201	HAGHL	0.88912	0.052796
ILMN_1842797	NA	0.889074	0.041808
ILMN_1704529	PPIA	0.889027	0.04507
ILMN_1689869	NA	0.889013	0.031015
ILMN_3244192	NA	0.888857	0.055758
ILMN_1812570	SHC1	0.888854	0.047084
ILMN_1765159	ELMOD2	0.888817	0.033096
ILMN_1784256	HDGFRP3	0.88871	0.046966
ILMN_3280735	NA	0.888639	0.047031
ILMN_1749838	MZF1	0.888637	0.056058
ILMN_2387784	DEAF1	0.888404	0.054635

ILMN_1688127	NA	0.888378	0.043786
ILMN_1729980	RNF216	0.888236	0.031493
ILMN_1732343	SIK3	0.887792	0.034508
ILMN_1691291	PIGS	0.887611	0.051577
ILMN_1799168	NA	0.887466	0.030041
ILMN_3240354	CYCSP52	0.887457	0.052372
ILMN_1743755	NA	0.887421	0.047138
ILMN_2310968	RUFY1	0.887114	0.035342
ILMN_2354649	SRSF10	0.887113	0.03876
ILMN_1788356	AKIP1	0.887039	0.024135
ILMN_2412384	CCNE2	0.886952	0.033186
ILMN_3258046	NA	0.886905	0.026184
ILMN_2356654	LGALS8	0.886758	0.042339
ILMN_1654398	RGL1	0.886749	0.035353
ILMN_2044027	NCOR1P1	0.886683	0.050667
ILMN_1740523	KTN1	0.886571	0.02727
ILMN_1815345	EIF3J	0.886557	0.040782
ILMN_1687821	C16orf45	0.886374	0.054735
ILMN_1656886	LIN37	0.886133	0.046686
ILMN_1739001	TACSTD2	0.885533	0.042489
ILMN_3187852	KANSL3	0.885513	0.049171
ILMN_1797950	EXTL2	0.885483	0.018949
ILMN_1808568	PYCR2	0.885436	0.018068
ILMN_1797005	PGLS	0.885435	0.02727
ILMN_1810875	SYNGR1	0.88536	0.022721
ILMN_2276933	GDAP1	0.88512	0.03249
ILMN_2151817	PFN1	0.884892	0.036845
ILMN_1676625	SS18L1	0.884808	0.030185
ILMN_1774312	MRPL57	0.884374	0.036792
ILMN_1696394	IL6R	0.884334	0.02503
ILMN_2404795	SULT1A1	0.88397	0.050179
ILMN_1706386	SLC39A4	0.883552	0.012848
ILMN_1768197	PTBP3	0.882962	0.023259
ILMN_1719149	NA	0.882329	0.036733
ILMN_1786606	NA	0.882262	0.058948
ILMN_1896892	NA	0.882254	0.024925
ILMN_1679185	LEF1	0.88219	0.04814
ILMN_2401978	STAT3	0.882178	0.030606
ILMN_1726647	NA	0.881905	0.019918
ILMN_1666553	SLC25A19	0.881868	0.02299
ILMN_1667016	FAF1	0.881819	0.027567
ILMN_1805766	POU6F1	0.881813	0.037609
ILMN_1659688	LGALS3BP	0.881707	0.045112
ILMN_1658830	WBP1L	0.881574	0.053488
ILMN_2321634	RAD17	0.881549	0.038201
ILMN_1748661	AKT1	0.880926	0.020581

ILMN_1681695	DNASE1L1	0.880803	0.045839
ILMN_1779182	TMEM98	0.880708	0.041026
ILMN_1687440	HIPK2	0.880579	0.045223
ILMN_1680091	POP7	0.880456	0.053946
ILMN_1753980	NA	0.880445	0.014512
ILMN_1839750	NA	0.880077	0.033446
ILMN_2145050	POM121	0.880036	0.031203
ILMN_1730575	GCLC	0.879995	0.018656
ILMN_1670540	SMAD1	0.879939	0.023909
ILMN_3236825	RAPGEF5	0.879878	0.022989
ILMN_2072091	HNRNPUL2	0.879549	0.033952
ILMN_1801130	STOML1	0.879287	0.019843
ILMN_3297510	NA	0.878908	0.015077
ILMN_1829845	NA	0.878765	0.057412
ILMN_3238782	NA	0.878722	0.047084
ILMN_2053829	CBLN3	0.878639	0.020486
ILMN_3279414	NA	0.87831	0.05453
ILMN_2041327	MRPL37	0.877825	0.03252
ILMN_1680193	PAXIP1	0.877748	0.043428
ILMN_1849941	NA	0.877523	0.01843
ILMN_1746720	TTC39C	0.877392	0.043763
ILMN_1813671	SLC25A1	0.877373	0.048472
ILMN_1737849	NA	0.876997	0.018899
ILMN_1735979	BCKDHA	0.876894	0.024374
ILMN_2266309	CEPT1	0.876618	0.026567
ILMN_2151818	PSMA6	0.87661	0.044704
ILMN_1801710	APBB1IP	0.876531	0.033713
ILMN_3202883	NA	0.876413	0.046262
ILMN_1762678	NMT1	0.876366	0.013666
ILMN_1760563	PRRC2A	0.876137	0.021704
ILMN_3247390	NA	0.876129	0.018419
ILMN_2192281	CARD8	0.876091	0.038487
ILMN_1682658	EPM2AIP1	0.875765	0.059436
ILMN_1837935	TNPO1	0.875708	0.038459
ILMN_2328433	NOP2	0.875611	0.038545
ILMN_1750549	PI4K2A	0.875472	0.050944
ILMN_1682428	HENMT1	0.875326	0.045273
ILMN_2365484	SNX1	0.87499	0.024856
ILMN_1795922	ZNF830	0.874618	0.046052
ILMN_3284036	NA	0.874368	0.033658
ILMN_1737517	RPL29	0.874243	0.025342
ILMN_1821397	NA	0.874057	0.029573
ILMN_1808218	NA	0.874043	0.018742
ILMN_1761131	ECI2	0.874013	0.017817
ILMN_1671703	ACTA2	0.873964	0.018045
ILMN_1659058	PPP1R10	0.873924	0.01902

ILMN_1788416	ABHD17C	0.873883	0.040198
ILMN_1738962	SYCN	0.873738	0.046007
ILMN_1765043	RPL38	0.873577	0.017006
ILMN_1805228	LRG1	0.873568	0.010044
ILMN_1699820	TNPO1	0.873243	0.029831
ILMN_1704760	BZW1	0.873234	0.010516
ILMN_2366587	SPDYA	0.8732	0.022402
ILMN_1704045	DEAF1	0.872879	0.017794
ILMN_1800795	NA	0.872588	0.049335
ILMN_1810560	NUPR1	0.872334	0.023255
ILMN_1706687	KLHL5	0.872072	0.020218
ILMN_1678730	NOMO1	0.872044	0.055814
ILMN_1655517	NA	0.871712	0.019061
ILMN_1678934	POLR1E	0.871353	0.033014
ILMN_1783707	SPECC1	0.87132	0.021702
ILMN_1753279	HNRNPA0	0.870706	0.042508
ILMN_1674758	NA	0.870081	0.033075
ILMN_1797082	SNX13	0.870029	0.029833
ILMN_1661424	THAP6	0.869917	0.017978
ILMN_1663605	RNF123	0.869875	0.014633
ILMN_2153485	NMNAT3	0.869854	0.012718
ILMN_1756402	TMEM177	0.869494	0.021279
ILMN_3236259	NA	0.869391	0.037137
ILMN_1683328	IP6K2	0.869377	0.021415
ILMN_1795639	MGMT	0.869203	0.023086
ILMN_1705114	NUMB	0.869176	0.028364
ILMN_1772455	HDAC3	0.869112	0.01234
ILMN_1687291	CDNF	0.869067	0.025857
ILMN_3306977	IMPDH1	0.8687	0.020795
ILMN_1896406	ZXDA	0.868587	0.027761
ILMN_2375418	DPH2	0.86857	0.057437
ILMN_1675387	LIMS1	0.868543	0.03885
ILMN_3245738	NA	0.868139	0.041891
ILMN_3242120	RAP1BL	0.868038	0.03908
ILMN_1671045	NA	0.867945	0.013019
ILMN_1723871	OTUB1	0.867944	0.038561
ILMN_1784328	SNORD25	0.867738	0.056998
ILMN_1677868	ADRA2B	0.867723	0.050324
ILMN_1804642	SMUG1	0.867173	0.045117
ILMN_1671158	MRPL13	0.867097	0.015247
ILMN_1784299	C19orf43	0.866949	0.027586
ILMN_1838372	NA	0.866826	0.043601
ILMN_1657810	PPM1M	0.866658	0.007758
ILMN_1708660	RWDD4	0.866622	0.015533
ILMN_2362681	CES2	0.866598	0.038438
ILMN_1738691	POU4F1	0.866484	0.012251

ILMN_1811729	CBLC	0.86643	0.023728
ILMN_2361163	SSBP3	0.86641	0.0167
ILMN_1689378	NOCT	0.866354	0.014268
ILMN_2047112	DPCD	0.866307	0.01605
ILMN_2247594	RPLP1	0.866256	0.014004
ILMN_3308743	MIR125B2	0.866238	0.038928
ILMN_1798690	ADAMTSL3	0.866063	0.040581
ILMN_2123665	SBF2	0.865596	0.050232
ILMN_2322986	MINA	0.865379	0.043137
ILMN_1737298	MAT2A	0.865376	0.024607
ILMN_1725946	IRF6	0.865289	0.029264
ILMN_1789106	IPP	0.865235	0.005978
ILMN_3211079	NA	0.865025	0.054596
ILMN_1798181	IRF7	0.864489	0.037876
ILMN_1755589	DIP2B	0.86418	0.029748
ILMN_1751753	IDH2	0.863873	0.03216
ILMN_2328986	SREBF1	0.863693	0.006386
ILMN_1708369	EPS15L1	0.863591	0.04989
ILMN_1677542	TRIM14	0.863458	0.045323
ILMN_1724897	C14orf93	0.863398	0.052023
ILMN_1731178	ARHGAP28	0.863303	0.032873
ILMN_1724825	PCBP2	0.862691	0.037808
ILMN_1784206	NA	0.862503	0.027627
ILMN_1751264	CCDC126	0.86245	0.019068
ILMN_1759250	TAP2	0.862359	0.035989
ILMN_1792076	TRERF1	0.862188	0.039916
ILMN_3243233	KATNBL1P6	0.861941	0.05726
ILMN_1701413	PIGQ	0.861478	0.004507
ILMN_1741780	DUSP28	0.860232	0.01532
ILMN_1750256	ALS2	0.859995	0.050252
ILMN_1679217	FAM110B	0.859972	0.042974
ILMN_3238570	EIF3CL	0.859667	0.029926
ILMN_3185709	IP6K2	0.859218	0.052796
ILMN_1758173	TMEM99	0.858975	0.051158
ILMN_3250585	NA	0.858565	0.050124
ILMN_1663033	TMEM129	0.858358	0.018189
ILMN_2387505	AP1B1	0.85834	0.049903
ILMN_2356838	CEPT1	0.85781	0.045765
ILMN_1709227	CCDC84	0.857733	0.05493
ILMN_1665066	NOA1	0.857529	0.058539
ILMN_1737380	BCAP29	0.857508	0.055796
ILMN_2375003	MAP4K4	0.857099	0.023207
ILMN_3220792	NA	0.857072	0.012393
ILMN_2341793	CCT7	0.856946	0.013907
ILMN_1682339	C19orf57	0.856891	0.016088
ILMN_1809483	HSD17B14	0.856886	0.044123

ILMN_2252701	SLC6A9	0.856767	0.016942
ILMN_1726025	ASXL1	0.85658	0.018572
ILMN_1720857	GUSBP2	0.856564	0.050821
ILMN_1667417	RAB23	0.856335	0.015943
ILMN_1720578	PRAF2	0.856246	0.042596
ILMN_1706326	MRPL33	0.856228	0.012899
ILMN_1750722	RPS7	0.856204	0.014392
ILMN_1730998	TSPAN6	0.855505	0.042912
ILMN_1831404	NA	0.85549	0.019633
ILMN_1739573	TNRC6A	0.855415	0.012802
ILMN_1748770	CKAP5	0.855168	0.015463
ILMN_2086077	JUNB	0.855053	0.0097
ILMN_1827736	PDK3	0.854883	0.041015
ILMN_1803318	PPFIA2	0.854609	0.01031
ILMN_1773567	LAMA5	0.854073	0.044508
ILMN_3244640	SNORD96A	0.854	0.023195
ILMN_1858001	NA	0.853818	0.003846
ILMN_1805448	EPB41L2	0.853564	0.014755
ILMN_1700728	KRTCAP3	0.853339	0.0119
ILMN_1697614	SNU13	0.852982	0.031804
ILMN_1792837	CIAO1	0.852545	0.047205
ILMN_2358626	ADK	0.852165	0.010291
ILMN_1884886	NA	0.852049	0.011742
ILMN_3289346	NA	0.851533	0.05234
ILMN_3242357	LOC100132418	0.85125	0.021742
ILMN_1804476	GMPPA	0.851228	0.013275
ILMN_1842448	NA	0.851114	0.014951
ILMN_1718766	MT1F	0.850891	0.033193
ILMN_1748476	NOP58	0.850766	0.004924
ILMN_2290808	RPL21	0.850719	0.018166
ILMN_1808163	C11orf24	0.85064	0.009811
ILMN_3304175	NA	0.850381	0.047231
ILMN_1672024	ISCA1P1	0.850139	0.031476
ILMN_1751452	NDFIP1	0.849785	0.013139
ILMN_2060145	GRHL2	0.849689	0.035189
ILMN_1666852	TRIM62	0.848942	0.002049
ILMN_2407389	GPNMB	0.848759	0.009962
ILMN_1693323	SMIM8	0.848375	0.010182
ILMN_2169856	C12orf43	0.848148	0.026351
ILMN_2325112	CDPF1	0.848073	0.009405
ILMN_1888264	NA	0.847997	0.027459
ILMN_2168952	DENR	0.847767	0.023168
ILMN_1762787	RNF26	0.847573	0.032398
ILMN_1702759	TMX4	0.846911	0.031546
ILMN_2318811	RANBP3	0.846793	0.05737
ILMN_1796069	CBLN2	0.846391	0.017179

ILMN_1709814	NMRAL1	0.846316	0.011531
ILMN_1745256	CXXC5	0.845511	0.007958
ILMN_2347424	MBOAT2	0.845489	0.020465
ILMN_3308490	MIR564	0.845027	0.043066
ILMN_1754068	NA	0.844933	0.034042
ILMN_2364828	OGT	0.844609	0.044648
ILMN_1731224	PARP9	0.84405	0.05857
ILMN_2049642	RPA1	0.843488	0.013349
ILMN_1784272	CD1E	0.84325	0.048926
ILMN_2180624	TMCO6	0.843244	0.042404
ILMN_1691949	NA	0.843156	0.004643
ILMN_1745533	FAM117A	0.842559	0.04803
ILMN_3241756	FAM136BP	0.841385	0.008469
ILMN_2082244	FOXK1	0.841208	0.006725
ILMN_3187328	IP6K1	0.841129	0.027995
ILMN_3297898	NA	0.841062	0.039231
ILMN_2126957	NOMO1	0.841056	0.012667
ILMN_1674072	RBAK	0.840407	0.011538
ILMN_1789839	GTF3C1	0.839995	0.011136
ILMN_3302484	NA	0.839856	0.033918
ILMN_1651652	RTN3	0.838359	0.017053
ILMN_1751886	REC8	0.837758	0.005973
ILMN_2369924	NDUFB6	0.837561	0.037343
ILMN_2374770	TAX1BP1	0.837516	0.027338
ILMN_1789001	SLC35B2	0.8371	0.010273
ILMN_1660323	NA	0.837032	0.013613
ILMN_1841620	NA	0.836853	0.008576
ILMN_1712505	KDELC1	0.836757	0.018607
ILMN_1689749	NA	0.836755	0.015925
ILMN_1687140	STARD7	0.836036	0.015652
ILMN_1682368	LRWD1	0.835802	0.02831
ILMN_3182422	NA	0.835324	0.031224
ILMN_1882000	TXLNG	0.83525	0.053003
ILMN_1684439	MLF1	0.83521	0.030948
ILMN_1657495	MLEC	0.835113	0.036012
ILMN_2372639	TRAPPC5	0.83507	0.035354
ILMN_1671933	CLCC1	0.835016	0.026175
ILMN_1751266	NA	0.834697	0.030572
ILMN_1754970	NA	0.833254	0.009513
ILMN_2273447	NPRL3	0.833055	0.005626
ILMN_1744048	NA	0.833032	0.046532
ILMN_1703886	SLC16A2	0.832769	0.001338
ILMN_3290199	NA	0.832714	0.003119
ILMN_1857861	NA	0.832327	0.001704
ILMN_1702211	TGIF1	0.832307	0.024106
ILMN_3209193	NA	0.8323	0.005584

ILMN_1841002	NA	0.831549	0.008805
ILMN_1659122	KLF10	0.828148	0.016553
ILMN_1766269	HM13	0.827554	0.018637
ILMN_1728331	ACPT	0.827375	0.047479
ILMN_1693830	LACTB	0.82713	0.049452
ILMN_1652306	MEGF10	0.826929	0.017558
ILMN_3246832	NA	0.826691	0.027192
ILMN_2083946	TGFA	0.826668	0.007304
ILMN_1814074	PHKA2	0.826578	0.004032
ILMN_1786920	KDM5A	0.826474	0.004932
ILMN_1738529	BCS1L	0.82559	0.040485
ILMN_3239946	FAM86HP	0.824206	0.049623
ILMN_1718712	FAM217B	0.824199	0.044694
ILMN_3241607	NA	0.824135	0.005552
ILMN_1722900	EIF4A1	0.823689	0.026601
ILMN_1707240	PTBP2	0.823389	0.005445
ILMN_2324561	SLC7A6	0.823244	0.009051
ILMN_1690036	NA	0.823157	0.011121
ILMN_2182531	TIMM21	0.82306	0.007382
ILMN_2319994	RPL3	0.822962	0.007072
ILMN_2167617	NACA	0.822895	0.020493
ILMN_1689446	EIF3G	0.822132	0.007355
ILMN_1754988	N6AMT1	0.821221	0.00672
ILMN_3234124	OGFOD3	0.821039	0.02155
ILMN_1686043	ZC2HC1C	0.820692	0.023772
ILMN_1772261	GLG1	0.82046	0.008326
ILMN_1828438	NA	0.820315	0.040264
ILMN_1741224	GPR137C	0.820081	0.003097
ILMN_1683859	SLC7A1	0.820074	0.009572
ILMN_1773066	CDKN2AIP	0.817977	0.023262
ILMN_1708047	NA	0.817873	0.001589
ILMN_1781942	HMMR	0.817591	0.005191
ILMN_3307901	GAN	0.817257	0.012584
ILMN_1753745	HDDC2	0.81674	0.016603
ILMN_2323633	TPD52L2	0.816715	0.02133
ILMN_1771746	C6orf165	0.81527	0.028306
ILMN_1731644	SETDB2	0.81442	0.008616
ILMN_1712352	DOCK3	0.814343	0.008034
ILMN_1656378	NMT2	0.814336	0.013004
ILMN_1719649	TMEM63A	0.814258	0.010684
ILMN_1775058	CSNK1A1	0.813275	0.023973
ILMN_2319996	RPL3	0.813191	0.012246
ILMN_1761969	DERL2	0.813059	0.014867
ILMN_2410864	RAB28	0.812978	0.002228
ILMN_1731922	NA	0.812175	0.023578
ILMN_1881909	SNAR-A1	0.811886	0.002212

ILMN_1668027	NA	0.811752	0.001939
ILMN_1680867	NA	0.811523	0.001298
ILMN_3237324	MMS19	0.810754	0.004016
ILMN_1719392	FH	0.810566	0.005553
ILMN_1696654	IFIT5	0.809986	0.041042
ILMN_3308663	MIR1228	0.809191	0.000961
ILMN_3239284	B9D1	0.807655	0.01377
ILMN_1738736	SNX4	0.806837	0.021512
ILMN_2107004	GPR1	0.806526	0.015353
ILMN_1690965	DHX9	0.806038	0.002444
ILMN_2247664	SON	0.804023	0.008247
ILMN_1654773	CASK	0.803767	0.013505
ILMN_2276290	RALGPS2	0.803648	0.019395
ILMN_1795719	RPA1	0.803087	0.051111
ILMN_1821483	NA	0.802798	0.005746
ILMN_1798311	MBTPS2	0.800976	0.005472
ILMN_1789567	MAGED2	0.800701	0.001913
ILMN_1811363	NOVA1	0.800107	0.001353
ILMN_1794740	CD151	0.799805	0.000654
ILMN_1774528	GPRC5C	0.799306	0.010729
ILMN_1774028	MTFR1	0.799192	0.030466
ILMN_1758827	RTN4IP1	0.79881	0.015196
ILMN_1802380	RERE	0.798117	0.002097
ILMN_1718207	SETDB1	0.796592	0.004736
ILMN_2377496	ERCC1	0.796581	0.008502
ILMN_1665909	LASP1	0.794413	0.058998
ILMN_1707631	MED10	0.793853	0.005153
ILMN_1731498	GPR156	0.792855	0.005505
ILMN_1687036	MRPL47	0.791167	0.029046
ILMN_1725992	RAPGEF6	0.790022	0.001986
ILMN_1800308	GTF2H4	0.789576	0.014807
ILMN_2350114	TRIM13	0.788289	0.027932
ILMN_2393573	RASSF1	0.78756	0.001297
ILMN_1740772	APBB3	0.786663	0.011611
ILMN_1679071	MTX3	0.78615	0.023633
ILMN_2095133	SPTAN1	0.785969	0.014966
ILMN_1785330	SH3BP4	0.783012	0.005051
ILMN_1787415	SNX16	0.781027	0.025303
ILMN_2100000	DHX36	0.780477	0.000274
ILMN_1697549	BAGE4	0.780374	0.001147
ILMN_3239426	GPN3	0.779776	0.03357
ILMN_1771689	EXD2	0.779452	0.037182
ILMN_1747556	CDK9	0.779346	0.001281
ILMN_2403730	ATP6V1H	0.779151	0.002809
ILMN_2205245	GPN2	0.777978	0.020883
ILMN_1739428	IFIT2	0.77479	0.035681

ILMN_2354855	OTUB1	0.773328	0.000902
ILMN_1700044	SAP130	0.770567	0.044316
ILMN_1737163	SH3BGRL3	0.763238	0.002803
ILMN_1797793	BLVRB	0.760857	0.00219
ILMN_2192683	DHX37	0.758502	0.012786
ILMN_2352097	ADGRG1	0.753062	0.000115
ILMN_2181968	CBL	0.750826	0.0033
ILMN_1714167	CYB5A	0.750047	0.003238
ILMN_1793241	SRD5A1	0.74936	0.000235
ILMN_1777113	NEURL2	0.740627	0.05192
ILMN_2352090	GPRC5C	0.740182	0.015712
ILMN_2218935	GPR37	0.739463	0.000702
ILMN_1804938	TPRA1	0.737698	0.031144
ILMN_1720267	TARSL2	0.7374	0.000232
ILMN_2375002	MAP4K4	0.736038	0.002013
ILMN_1739497	GTF2H5	0.733133	0.032535
ILMN_2121816	GPR137B	0.732951	0.000119
ILMN_1738976	OR2A20P	0.730877	0.006324
ILMN_1793118	TAX1BP1	0.725763	0.000169
ILMN_1687023	GJC1	0.725578	0.007458
ILMN_1753913	WLS	0.724483	0.000394
ILMN_1654703	GPR157	0.72385	0.000752
ILMN_2384122	ADGRG1	0.721709	0.020936
ILMN_1707326	TASP1	0.71138	0.003487
ILMN_1755664	RPS26	0.708509	0.014651
ILMN_1772719	GPN1	0.707997	0.000235
ILMN_2270015	AADAT	0.707018	0.000429
ILMN_1726306	HMBS	0.70559	0.000154
ILMN_2330371	TATDN3	0.685725	0.006771
ILMN_1657746	BPHL	0.684207	0.019896
ILMN_1744316	TATDN3	0.683759	3.33E-05
ILMN_1671260	WLS	0.682365	0.003087
ILMN_1660549	WLS	0.680088	0.008032
ILMN_2390853	CTSH	0.679611	4.54E-05
ILMN_2399769	WLS	0.677365	0.001139
ILMN_3250850	RFESD	0.674182	0.003152
ILMN_1692539	SH3BP1	0.672936	4.53E-05
ILMN_2209027	RPS26	0.672186	0.009045
ILMN_1802414	CA13	0.667112	0.004219
ILMN_1804332	GPR137	0.66509	1.82E-05
ILMN_2179397	TATDN1	0.659317	0.005511
ILMN_1759030	MAP4K5	0.655264	0.000255
ILMN_2283325	WLS	0.648223	0.000793
ILMN_1906397	LINC01311	0.638228	0.002672
ILMN_2207533	RPS17	0.634552	3.07E-05
ILMN_1809959	AADAT	0.63332	0.006285

ILMN_1762764	SH3BGRL2	0.632543	5.71E-05
ILMN_1757317	LARS	0.630439	0.000581
ILMN_1652631	GLIPR2	0.620768	0.000865
ILMN_2239754	IFIT3	0.618062	0.001876
ILMN_1666019	ADNP	0.613996	0.00017
ILMN_1737312	SLC25A17	0.595498	0.020668

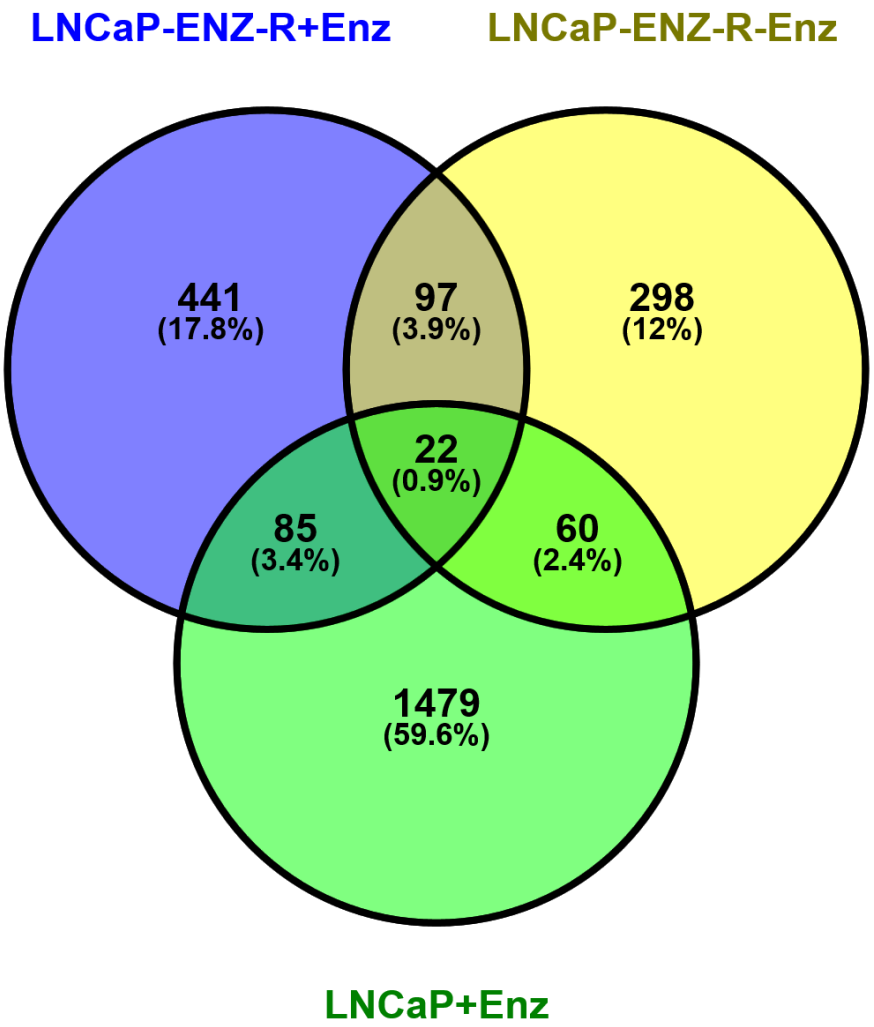

Appendix 9-8 Venn's diagram. This figure shows the list of genes for each condition of microarray and also the common genes between conditions. This adapted from Oliveros, J.C. (2007-2015) Venny. An interactive tool for comparing lists with Venn's diagrams. tp://bioinfogp.cnb.csic.es/tools/venny/index.html

Table 9-2 Common genes of microarray condition

97 common genes in LNCaP-ENZ-R+Enz and LNCaP-ENZ-R-Enz	22 common genes in LNCaP-ENZ-+Enz And LNCaP-ENZ-R-Enz And LNCaP+Enz	85 common genes in LNCaP-ENZ-R+Enz and LNCaP+Enz	60 common gens in LNCaP-ENZ-R-Enz and LNCaP+Enz
GNA12, GPR137,	ECH1, TACSTD2	CTSH, TARSL2	AKAP7, RECQL4
RLN1, DEF8	SYT4, SGK1	MAP4K5, WLS	AGAP3, PAXBP1
ADGRG1. COX7A2L	PIK3R1, CPS1	ANTXR1, LARS	CS, CTSL, LRBA
ASAP2, RABEPK	NA, GK, CKAP2	COASY, ALDH2	MTOR, STRA13
TACSTD2,	SLC25A40, SDHAP1	RASSF1, GAR1	SCPEP1, GART
BCCIP, TRAPPC4	PLIN2, GAS6, LRRC1	RAB28, RAVER1	PI4KAP1, PPIC
KMT2C, FJX1	RAB23, IL6R,	FOXRED2, INCENP	PRDX2, SLC35A2
ERN1, MIR1228	MAD2L1, POLR1E	CYB5A, SLC25A6	AMD1, OCRL
ASNSD1, BCKDK	MLEC, LGALS8	NXF2, BCHE	NOL12, SMPDL3A
PRKDC, GEMIN8	PAXIP1, MYT1	MMS19, EIF4EBP1	CCDC15, SKP2
ATP5B, CCDC120		SLBP, SH3BP4	NDUFB4, CYTH3
PSAP, PLOD2		HMMR, IQCC	MAGEA6, NIPAL3
ABTB2, TARBP1		HADHB, ERCC1	FOLH1, PIGP
IRF2BP2, SOX4		SETDB2, NOP14	SPAG9, C9orf152
MXI1, CHIC2		SLC7A1, PPFIA2	EIF4A3, NDUFAF5
MED10, MBTPS2		PEX10, GPRC5C	HIST1H4E, PIK3R2
			NAP1L4, SNX3
			DNAJC12, CSE1L
			AFMID, CTSC
			GTF3C2, LAMP2
			EME1, GRN
			ITGB5, PYROXD2
			RPS29, F2RL1
			EXOC4, MR1

SGK1, NPRL3		SNORD30, CHEK2	PSMG4, KLK15
MKL1, GPATCH4		EPB41L2, RTN4IP1	CENPN, GLRX2
AKAP13, NDEL1		MED30, ACSL3	RFC1, BIRC5
THAP11, CD99		RNF4, EXTL2	CCDC34, FKBP5
SLMAP, PPM1M		MBOAT2, IMPDH1	BEND3, MOB1A
INPP5B, FAM136BP		HGD, SPECC1	PPFIBP1
ANKRD54, SLC25A4		SLC25A19, MGMT	
AKTIP, CDPF1		PTBP3, G3BP2	
CRLS1, JUNB		CYFIP2, TNPO1	
ARPC4, ABCA11P		ISCA1P1, TMX4	
ANXA2P2, DRC7		CCNE2, GRHL2	
KRTCAP3, ACVR2A		RGL1, TRAPPC5	
NAAA, GAN		SLC16A6, IFIT2	
NOMO1, NMNAT3		KIF15, ADD1	
AKAP11, NOCT		PFDN2, SMCO4	
DERL2, SPTAN1		SRGAP3, MIR564	
SIVA1, RSBN1L		HSD17B14, PSMA6	
DBNDD1, ACTA2		HENMT1, TRIM48	
ASXL1, PRKX		NAE1, GGH	
PRMT1, AKT1		KANSL3, MAOA	
SH2B3, OGFOD3		NCOR1P1, GUSBP2	
SYNGR1, AKIP1		DDIAS, ACSM3	
BCKDHA, BRCA1		TIMP2, HOXC9	
C12orf43, PGLS		TXLNG, POLE	

ZXDA, STAT3 OARD1. ELMOD2 ATP1A1-AS1. CES2 SRSF10, RAP1BL PRAF2. OGT PPIA, HNRNPA1 KIAA0319L, STY4 ST14, C16orf45 SNORD25		BCAP29, DPH2 ERO1A, MED27 PA2G4	

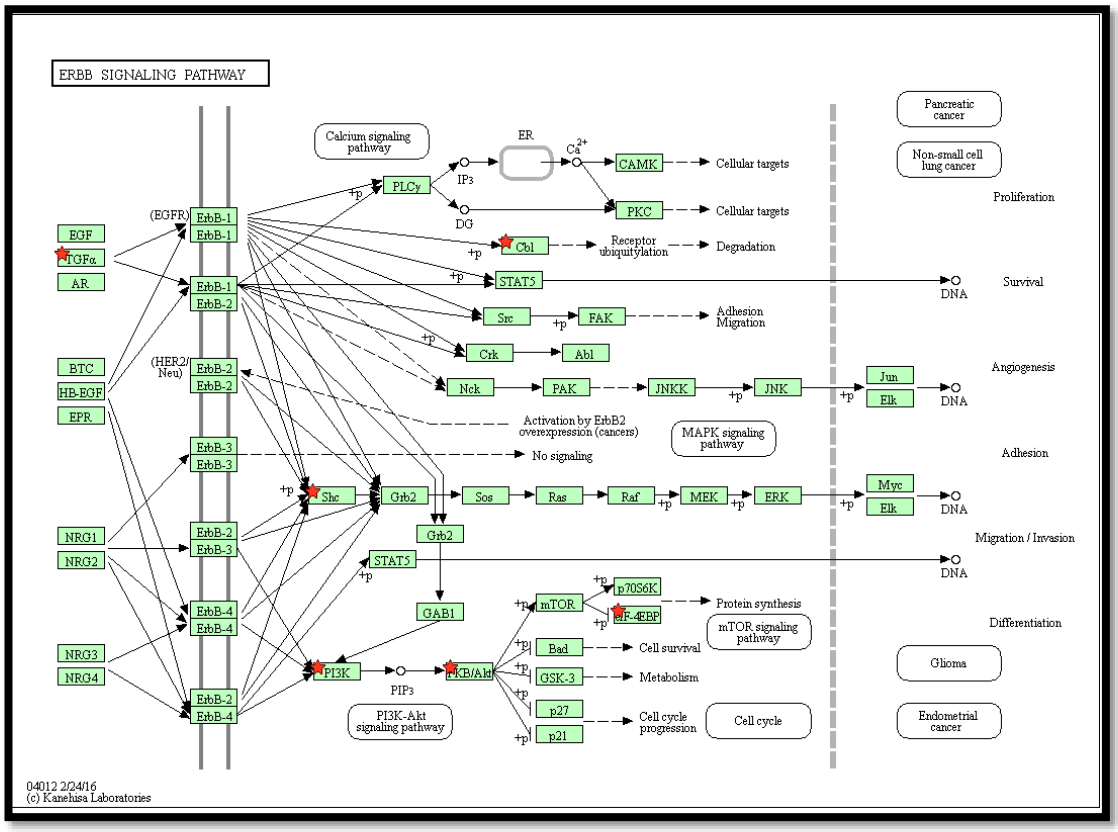

Appendix 9-9 ERBB signalling pathway. Genes included in the microarray data labelled by stars. Database for Annotation, Visualisation and Integrated Discovery (DAVID), v6.7 was used to analyse large gene lists and perform comprehensive clustering to outline genes with a similar function or biological theme. KEGG pathway analysis on steroid biosynthesis was included in the DAVID output.

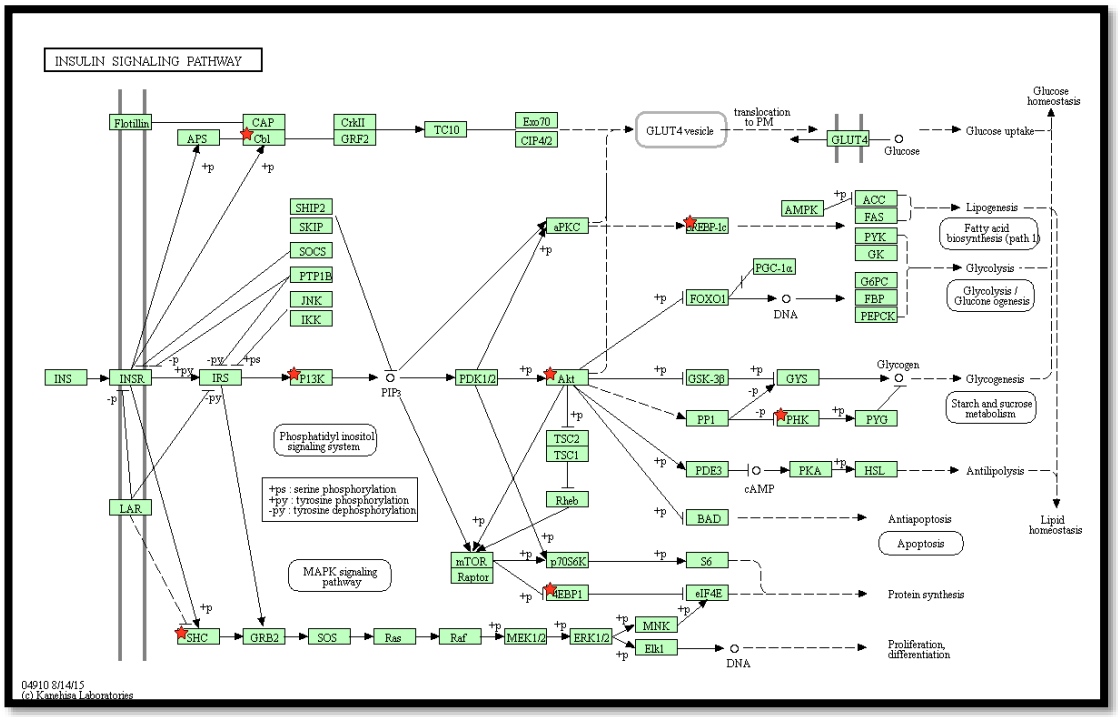

Appendix 9-10 Insulin signalling pathway. Genes included in the microarray data labelled by stars. Database for Annotation, Visualisation and Integrated Discovery (DAVID), v6.7 was used to analyse large gene lists and perform comprehensive clustering to outline genes with a similar function or biological theme. KEGG pathway analysis on steroid biosynthesis was included in the DAVID output.

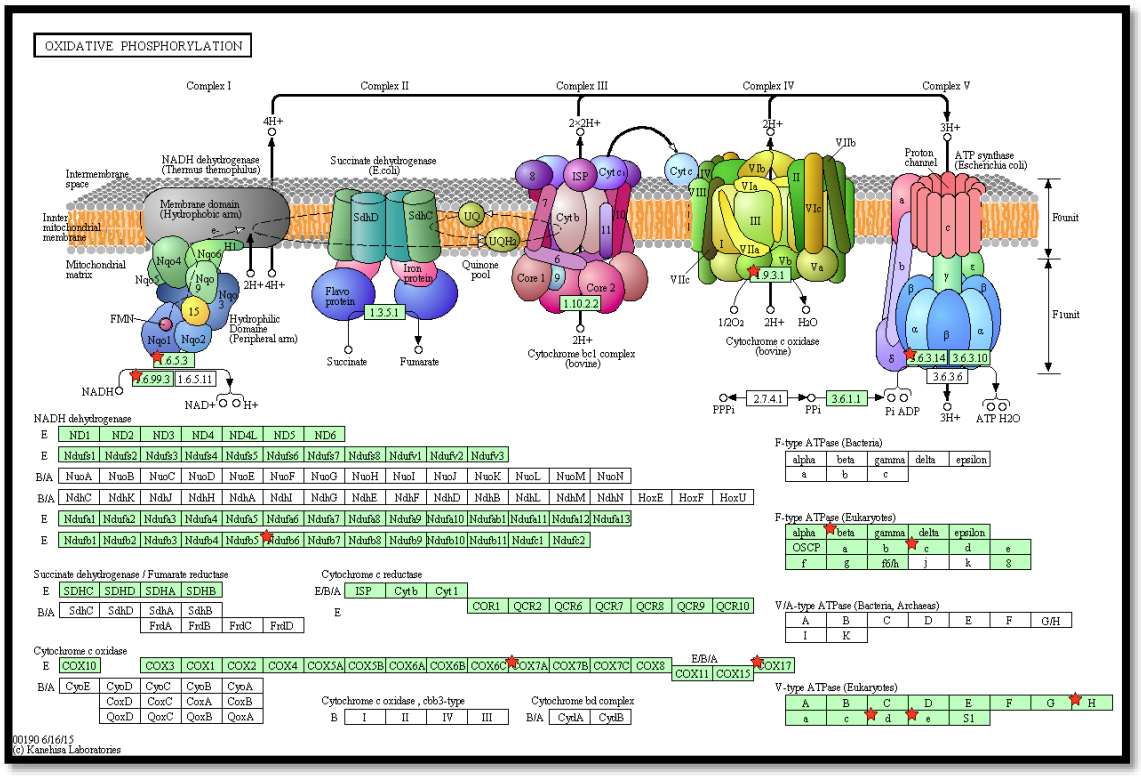

Appendix 9-11 Oxidative phosphorylation. Genes included in the microarray data labelled by stars. Database for Annotation, Visualisation and Integrated Discovery (DAVID), v6.7 was used to analyse large gene lists and perform comprehensive clustering to outline genes with a similar function or biological theme. KEGG pathway analysis on steroid biosynthesis was included in the DAVID output.

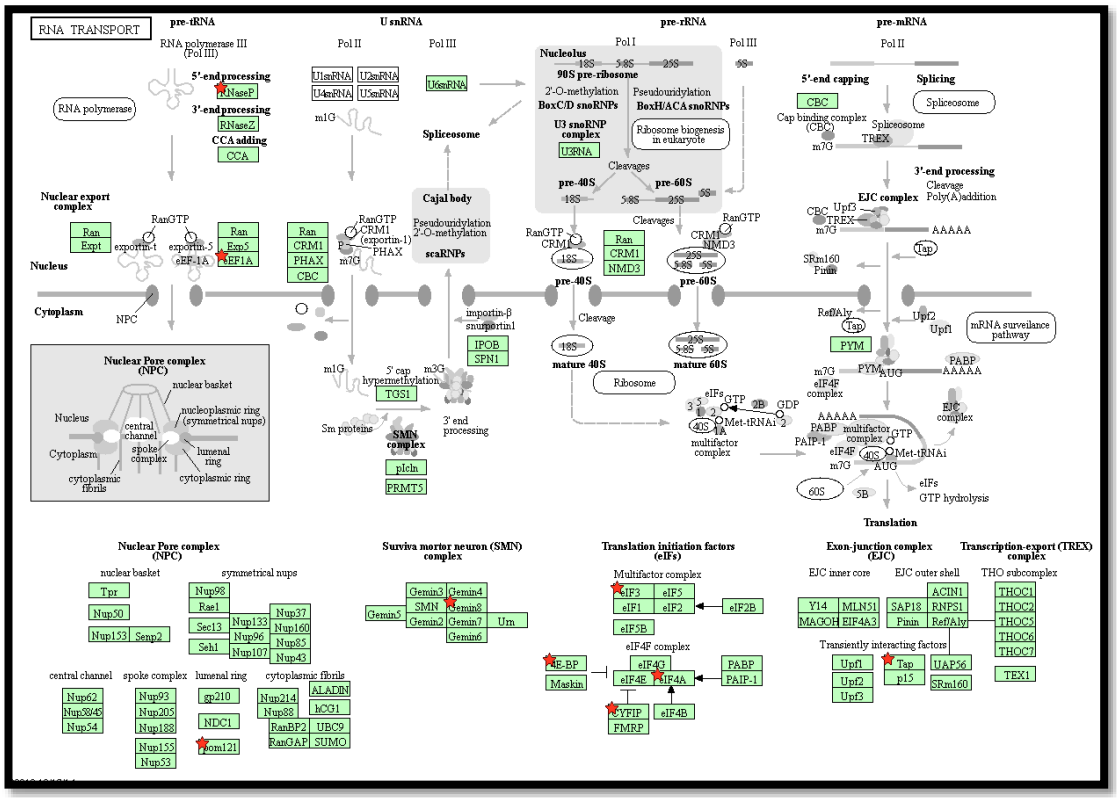

Appendix 9-12 RNA transport pathway. Genes included in the microarray data labelled by stars. Database for Annotation, Visualisation and Integrated Discovery (DAVID), v6.7 was used to analyse large gene lists and perform comprehensive clustering to outline genes with a similar function or biological theme. KEGG pathway analysis on steroid biosynthesis was included in the DAVID output.

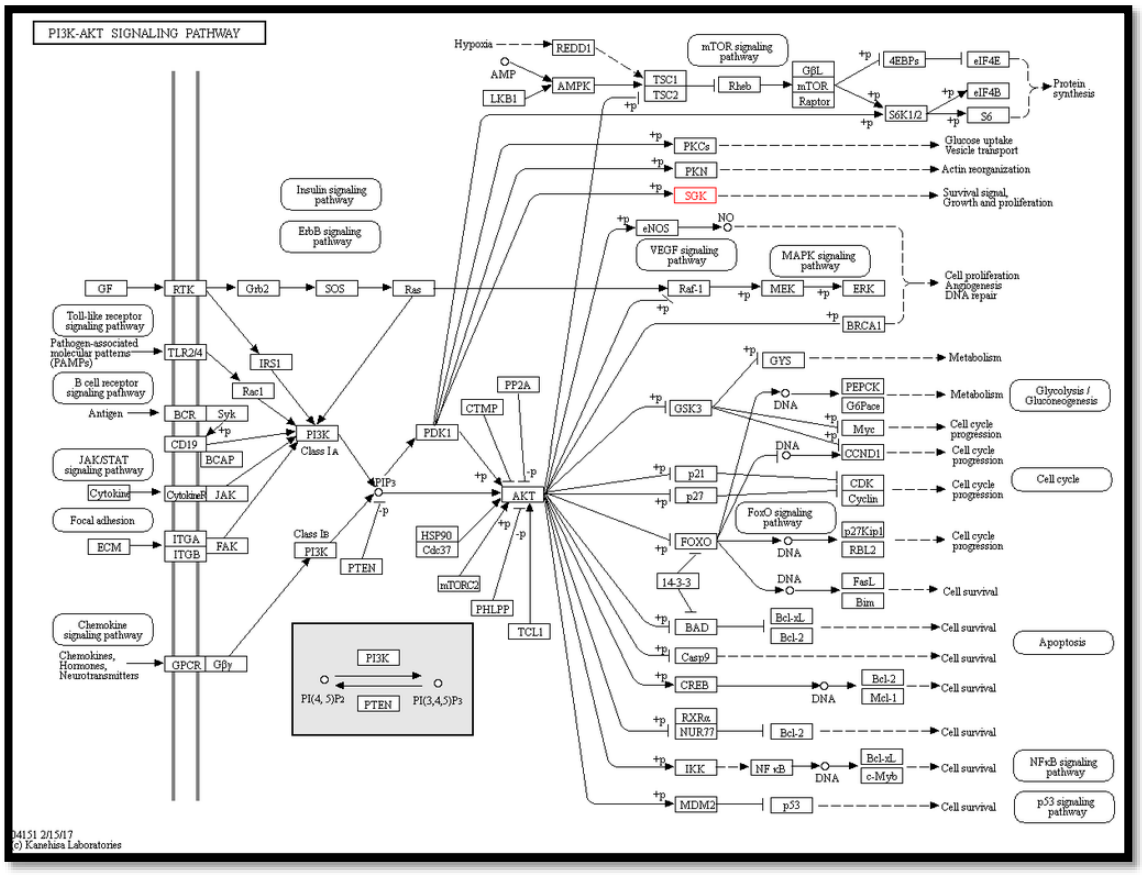

Appendix 9-13 PI3K-Akt signalling pathway. Gene included in the microarray data labelled by red. Database for Annotation, Visualisation and Integrated Discovery (DAVID), v6.7 was used to analyse large gene lists and perform comprehensive clustering to outline genes with a similar function or biological theme. KEGG pathway analysis on steroid biosynthesis was included in the DAVID output.

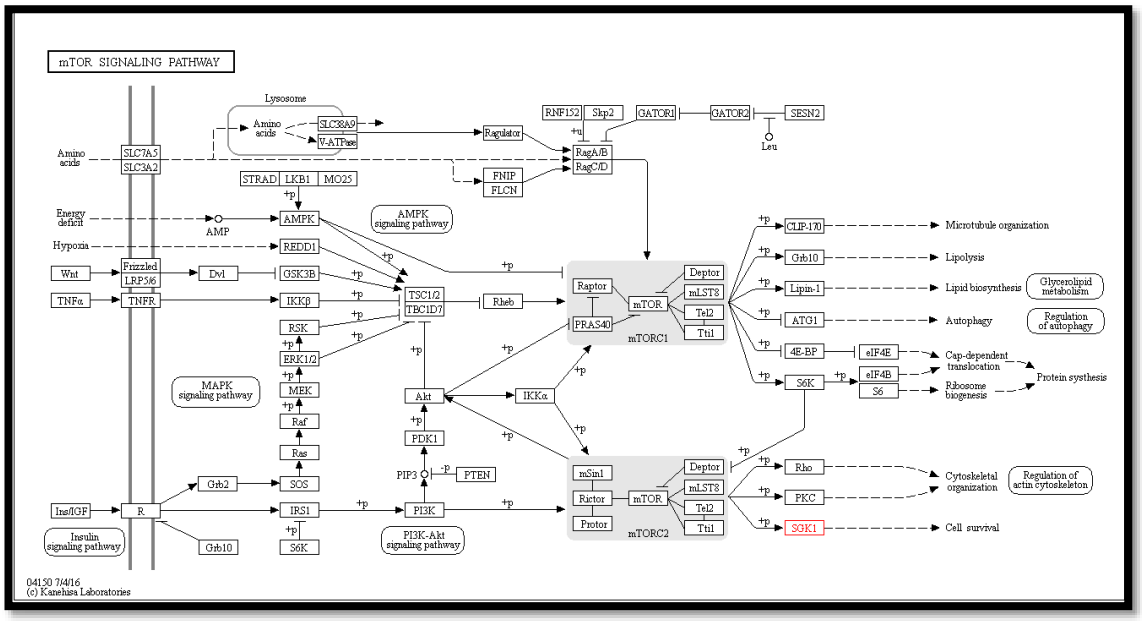

Appendix 9-14 mTOR signalling pathway. Gene included in the microarray data labelled by red. Database for Annotation, Visualisation and Integrated Discovery (DAVID), v6.7 was used to analyse large gene lists and perform comprehensive clustering to outline genes with a similar function or biological theme. KEGG pathway analysis on steroid biosynthesis was included in the DAVID output.

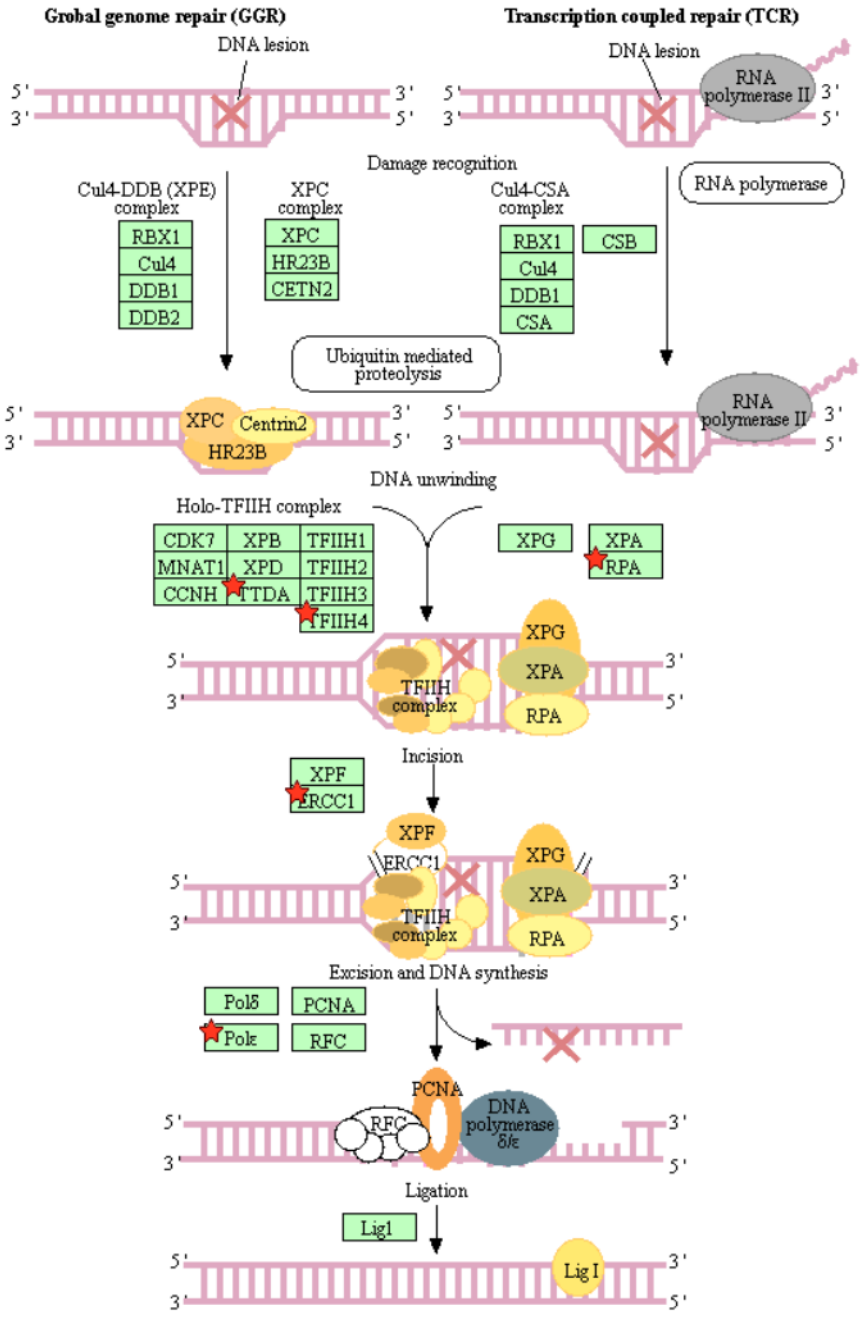

Appendix 9-15 nucleotide excision repair pathway. Genes included in the microarray data labelled by stars. Database for Annotation, Visualisation and Integrated Discovery (DAVID), v6.7 was used to analyse large gene lists and perform comprehensive clustering to outline genes with a similar function or biological theme. KEGG pathway analysis on steroid biosynthesis was included in the DAVID output.

Table 9-3 genes that have role in functional process in LNCaP-ENZ-R cell line

185 genes are involve in Acetylation	337 genes are involve in Phosphoprotein	385 genes are involve in Alternative splicing	49 genes are involve in Methylation	49 genes are involve in DNA repair	30 genes are involve in Cell cycle	30 genes are involve in Serine/threonine-protein kinase
CCZ1B, ALS2, MMS19, INTS1, BPHL, PRKX, EIF3CL, EIF4EBP1, ANKRD54, RAB28, RAVER1, RPLP1, RAPGEF6, DHX36, PTBP3, PTBP2, OGT, GNG5, AADAT, RPL35A, RSBN1L, DCTN3, MAGED2, TRERF1, TBC1D22B, JUNB, MAP4K4, PA2G4, PYCR2, PGLS, NOP2, KRT18, MAD2L1, RCC2, PSMA6, PI4K2A, RPS12,	CCZ1B, ALS2, HM13, SYT4, FAM110B, STOML1, INTS1, RNF216, KIAA0319L, PRKX, PLOD2, RAB28, SULT1A1, RAVER1, INCENP, RPLP1, MED27, RAB23, RAPGEF6, PTBP3, DHX36, GDF9, OGT, PTBP2, DHX30, GNG5, LRRC1, ANKS3, POLE, PIM1, MAGED2, REC8, PGLS, NOP2, KRT18, MAD2L1, RCC2, DHX29, RPS17, TRAPPC5, RFESD, ADD1, DEAF1, DBNDD1, SIVA1, GLG1, COASY, RALGPS2, CDV3, SRSF10, MTX3, TMX4,	ALS2, HM13, SYT4, STOML1, RNF216, KIAA0319L, MXI1, MEGF10, MED20, PLOD2, RAB28, SULT1A1, RAVER1, INCENP, RPLP1, MED27, RAPGEF6, RAPGEF5, PTBP3, DHX36, OGT, PTBP2, SAYSD1, DHX30, MRPL33, AADAT, GPR137, CRLS1, LRRC1, ANKS3, EXD2, PARP11, ACRV1, DCTN3, MAGED2, NME7, OGFOD3, REC8, NOP2, MAD2L1,	RAB7A, EID2, FOXK1, KMT2C, TXLNG, AKAP13, PRRC2A, STAU1, RNF123, ALB, RAB28, MED27, GATAD2A, RAB23, RBM47, RHOD, IMPDH1, GNG5, INPP5B, SIK3, SETDB1, DHX9, SSBP3, ACTA2, EEF1A2, SLC25A6, RAB4B, ADNP, G3BP2, PPP1R10, ILF3, RB1, HNRNPA1, HIST2H3C, HNRNPA0, RPL29, CCT7, SON, KRT18,	MMS19, SSRP1, NEIL3, MGMT, POLE, GTF2H4, PRKDC, CDK9, CHEK1, BCCIP, GTF2H5, CHEK2, SMUG1, BRCA1, RPA1, PAXIP1, PARP9, OTUB1, ERCC1	TXLNG, CHEK1, BCCIP, CHEK2, CCNG2, MLF1, CCNE2, INCENP, DDIAS, CSNK1A1, CKAP2, PDS5B, SETDB2, CKAP5, ZNF830, PIM1, SYCE2, BANP, RB1, DCTN3, BRCA1, NAE1, SPDYA, SON, MAD2L1, KRT18, RIF1, RCC2, RASSF1, RAD17	CSNK1A1, SGK1, LIMK2, PIM1, PRKDC, CDK9, CASK, CHEK1, CHEK2, PRKX, AKT1, ACVR2A, MAP4K4, MAP4K5, STK40, HIPK2, ERN1, STK19, SIK3

MRPL47, RFESD, ADD1, GPN1, RAB7A, GPN2, CDV3, GCLC, SNX1, PRRC2A, ARPC4, SNX4, SERPINH1, HADHB, PFN1, RPL3, IDH2, EIF3J, FH, DHX9, HDDC2, CKAP5, EEF1A2, MAOA, ZNF830, NDFIP1, HGD, DENR, SMAD1, TPD52L2, CPS1, HNRNPA1, HIST2H3C, BRCA1, RPS8, HNRNPA0, RPS7, CCT7, CCT5, HDAC2, SAP130, LASP1, OTUB1, PPIA, GTF2F1, CDKN2AIP, ALDH2,	ASAP2, AKAP13, RABEPK, PRRC2A, CHEK1, CHEK2, AKAP11, SERPINH1, NPRL3, RPS26, PFN1, FH, DHX9, CLCC1, KANSL3, KLF10, MAOA, ASXL1, NXF2, TPD52L2, SMAD1, HNRNPA1, RPS8, GAS6, HNRNPA0, TAX1BP1, NOP14, CBLC, CCT5, PAXIP1, SAP130, RPL18A, RNF4, LASP1, MZF1, RERE, C15ORF40, ABCF3, BCKDK, PHKB, ATP5B, TRMT10A, TRMT10C, MTFR1, RTN3, CCNE2, DIP2B, KIAA1211L, SLMAP, IL1RAP, OARD1, SLC25A1, ARHGAP11A, ATP6V0D1, IP6K1, COX17, TARSL2, SIK3, CTBP1, PEPD, EXOSC9, POLR1E,	TRAPPC4, TGIF1, STC1, MRPL47, RFESD, ADD1, DEAF1, DBNDD1, SIVA1, GLG1, IL1R2, COASY, RALGPS2, CDV3, SRSF10, MTX3, ACP6, ASAP2, AKAP13, RABEPK, PRRC2A, CHEK1, CHEK2, MYT1, HADHB, TMEM129, IDH2, TMEM183A, GPR156, DHX9, CLCC1, KANSL3, MAOA, KLF10, FOXRED2, ASXL1, NDFIP1, LGALS8, ACPT, SMAD1, TPD52L2, HNRNPA1, GAS6, TAX1BP1, NOP14, CCT7, CBLC, CCT5, PAXIP1, SAP130,	RAP1BL, SAP130, PTP4A3, ILF2, HNRNPUL2, LASP1, RASSF1, PSPC1, AVEN, HIST1H3F		

CYFIP2, GPATCH4, RWDD4, HIST1H3F, RERE, BCKDK, ABCF3, AP1B1, FOXK1, PHKB, ATP5B, EPS15L1, DPH2, SYNGR1, DSTN, RTN3, AKT1, BZW1, RANBP6, RANBP3, OARD1, SHC1, C19ORF43, TARSL2, SSBP3, PEPD, EXOSC9, SLC25A4, ACTA2, HMBS, SLC25A6, KIF15, RAB4B, ADNP, CDK9, CYB5A, IRF2BP2, BANP, RB1, RPS4X, ANXA2P2, ELMO1, EPB41L2, TARBP1, EAPP, C3ORF33,	SPECC1, RAB4B, ADNP, GTF2H5, TTF2, ANXA2P2, ELMO1, EPB41L2, EAPP, DOK6, ADK, EIF4A1, SRGAP3, AVEN, PPFIA2, NACA, ECH1, SNU13, RPL27A, BET1, TXLNG, BCCIP, EEA1, APBB1IP, MLF1, STAU1, HDGFRP3, HMMR, FAM117A, PLIN2, STRIP2, GATAD2A, ACSL3, MLLT3, MT1F, CSNK1A1, BCKDHA, SSRP1, ECI2, PDS5B, MAT2A, PDK3, PPP1R10, ILF3, NOA1, C12ORF43, ETF1, STAT3, RPL29, DNPEP, DUSP4, NUPR1, HNRNPUL2, ILF2, SLC16A6, RASSF1, C19ORF57, BLVRB, NOP58, LIN37, MMS19, MPZL1, SLC44A1, CASK, BPHL,	PARP9, RNF4, LASP1, LAMA5, MZF1, TCAF1, RWDD4, GK, RERE, C15ORF40, ABCF3, BCKDK, AP1B1, PHKB, NAAA, GAR1, ASAH1, MTFR1, N6AMT1, RTN3, CCNE2, SLMAP, IL1RAP, SEMA3C, TGFA, RBM47, ARHGAP11A, IP6K1, TARSL2, SIK3, IP6K2, CTBP1, TMCO6, PEPD, STX3, EXOSC9, POLR1E, SPECC1, RAB4B, GTF2H4, CYB5A, IL6R, TTF2, ELMO1, EPB41L2, MTMR11, ADK, EIF4A1, SRGAP3, RAPGEFL1, PPFIA2, LIMS1,				

ADK, EIF4A1, DEF8, MATR3, LIMS1, NACA, ECH1, NDUFB6, KMT2C, GDAP1, SNU13, RPL27A, PRKDC, VCPKMT, COX7A2L, RPL38, TMEM258, STAU1, RPA1, RNF123, MRPL13, PLIN2, LARS, LACTB, TNPO1, PIK3R1, ERCC1, MT1F, CSNK1A1, BCKDHA, SSRP1, ECI2, PAOX, COX7A2, PDS5B, MAT2A, AMACR, ILF3, ETF1, STAT3, DNPEP, NAE1, RPL29, ACSM3, IFIT2, SLC16A2, SON,	CACTIN, RGL1, SLC7A6, FNTB, EIF3CL, EIF4EBP1, ANKRD54, AKAP17A, HOXC9, RSBN1L, C6ORF47, NEIL3, TBC1D22B, TRERF1, JUNB, MAP4K4, MAP4K5, PYCR2, PA2G4, NDEL1, PSMA6, PI4K2A, IQCC, RAD17, PHKA2, GPN1, RAB7A, GCLC, TMEM63A, SNX1, SNX4, CXXC5, EPM2AIP1, CEPT1, EIF3G, ERO1A, BCHE, ALB, NUMB, PRKRA, RPL3, LRFN1, EIF3J, SLC35F6, NOVA1, SREBF1, CKAP2, ZGRF1, SETDB1, CKAP5, HDDC2, ZNF830, EEF1A2, DENR, CPS1, DOCK3, BRCA1, HIST2H3C,	NACA, THAP6, ABTB2, TRIM14, BET1, TRIM13, TXLNG, BCCIP, APBB1IP, MLF1, STAU1, HMMR, FAM117A, STK40, STRIP2, PLA2G12B, GATAD2A, PEX10, MLLT3, CSNK1A1, BCKDHA, ECI2, CES2, PAOX, PDS5B, PLA2G15, MAT2A, PDK3, AMACR, TMPRSS7, ILF3, ETF1, STAT3, CD1E, NAT9, NAE1, ACSM3, DUSP4, NUPR1, PTP4A3, RASSF1, C19ORF57, RBAK, APBB3, MMS19, MPZL1, SLC44A1, CASK, BPHL, CACTIN,				

MED30, IRF7, RASSF1, PSPC1, IRF2, LIN37, SH3BGRL3, SPTAN1	NMT2, NMT1, HDAC3, HDAC2, AKTIP, PPIA, OTUB1, GTF2F1, CDKN2AIP, SLC25A19, GPATCH4, ANTXR1, HIST1H3F, NOMO1, DUT, NDUFAF4, CLDN7, FOXK1, DPH2, EPS15L1, DSTN, AKT1, BZW1, PRMT1, DGCR8, PCBP2, RANBP6, RANBP3, SHC1, MKL1, KDM5A, LRWD1, IMPDH1, C14ORF93, SSBP3, SGK1, LIMK2, HMBS, KIF15, G3BP2, ARHGAP28, KTN1, LEF1, CDK9, ATP6V1H, IRF2BP2, BANP, RB1, MBNL1, TARBP1, SPDYA, SDC1, RAP1BL, RIF1, STXBP5, SBF2, DEF8, HIPK2, ERN1, MATR3, GPRC5C, KMT2C, MGMT,	ABHD17C, RGL1, FNTB, GLT8D1, KLHL5, ANKRD54, AKAP17A, RLN1, ST3GAL5, CDNF, TMEM99, RGN, SS18L1, NMNAT3, RSBN1L, SARAF, ENC1, TATDN1, GRHL2, TRERF1, TATDN3, MAP4K4, PA2G4, NDEL1, PSMA6, FAM72A, IQCC, DCUN1D4, RAD17, GPN1, GPN3, EID2, ADAMTSL3, B9D1, CDC42SE1, SNX1, ARPC4, SNX4, CXXC5, KCNRG, CCNG2, TASP1, ALB, NUMB, GMPPA, PRKRA, DRC7, EIF3J, DDIAS, STK19, NOVA1,				

	SNX16, PRKDC, VCPKMT, MINA, RPA1, CCDC120, RNF123, POM121, SLC35B2, LARS, SH2B3, GEMIN8, GPNMB, GTF3C1, TNRC6A, PIK3R1, CCP110, ARMC10, CBL, RUFY1, CD99, BCS1L, RGS17, FUCA2, WBP1L, SLBP, IFIT3, SH3BP4, SON, SLC6A9, IRF7, PSPC1, IRF2, IRF3, FAF1, SH3BP1, SPTAN1	LYSMD4, ANGPTL4, SREBF1, CKAP2, ZGRF1, SETDB1, CARD8, SETDB2, CKAP5, HDDC2, SEC11A, CPS1, TRIM62, ADGRG1, BRCA1, ZC2HC1C, NMT1, HDAC3, HDAC2, AKTIP, OTUB1, PPIA, CYFIP2, ALDH2, SLC25A19, GPATCH4, ANTXR1, DUT, CLDN7, FOXK1, DPH2, EPS15L1, SYNGR1, DSTN, AKT1, BZW1, PRMT1, ALAS1, DGCR8, PCBP2, RANBP3, POU4F1, SHC1, KDM5A, TTC39C, IMPDH1, RTN4IP1, C16ORF45, LINC01547,				

		C14ORF93, SSBP3, SGK1, LIMK2, HMBS, KIF15, G3BP2, ARHGAP28, KTN1, CDK9, LEF1, ATP6V1H, IRF2BP2, PIGS, BANP, WLS, MBNL1, PIGQ, COQ5, KRTCAP3, SPDYA, ACVR2A, RIF1, STXBP5, C3ORF33, JOSD2, SBF2, DEF8, HIPK2, ERN1, HAGHL, PPM1M, SNX13, MATR3, NDUFB6, GPRC5C, KMT2C, TPRA1, SNX16, GDAP1, PRKDC, VCPKMT, ATP5G2, SMUG1, MINA, CCDC120, RNF123, POM121, SLC35B2, TAP2, SLC35B4, LARS,				

		SNX21, BCAP29, HS6ST1, SLC25A45, SLC39A4, GPNMB, TNPO1, CXORF56, GTF3C1, TNRC6A, INPP5B, LACTB, PIK3R1, ERCC1, IPP, CCP110, DHRS12, AKIP1, PSAP, ARMC10, TSPAN14, RUFY1, CD99, FUCA2, WBP1L, GDPD1, SLBP, SH3BP4, SON, SLC6A9, MED30, SCFD2, IRF6, IFIT5, IRF7, PSPC1, IRF2, IRF3, FAF1, SH3BP1, SPTAN1				